Environmental Impact of Amines emitted to the Atmosphere

Mihayo Musabila Maguta

Dissertation for the degree of Philosophiae Doctor (PhD)

Department of Chemistry, Faculty of Mathematics and Natural Sciences,
University of Oslo, Norway

January 2014

Series of dissertations submitted to the
Faculty of Mathematics and Natural Sciences, University of Oslo
No. 1443

ISSN 1501-7710

Cover: Inger Sandved Anfinsen.
Printed in Norway: AIT Oslo AS.

Produced in co-operation with Akademika Publishing.
The thesis is produced by Akademika Publishing merely in connection with the thesis defence. Kindly direct all inquiries regarding the thesis to the copyright holder or the unit which grants the doctorate.

TABLE OF CONTENTS

ABSTRACT

Industrial development, increase in population and need for improving the living standards of people around the globe have resulted into high demand of energy worldwide. The renewable energy sources seem to be unreliable and insufficient to meet this demand; hence the continued use of fossil fuels especially coal in power generation becomes necessary. Fossil fuels are well known for their environmental detriments including global warming which leads to climate change. With this cause, the world has to use the fossil fuels in an environmentally friendly manner to ensure that the amount of pollutants released into the atmosphere is minimized.

In combating climate change, technologies have been developed whereby the prime greenhouse gas, carbon dioxide is captured and stored. One of these technologies makes use of amines which at the end of the process are released into the atmosphere where they have been proven to undergo degradation leading to the formation of other several compounds including nitramines and nitrosamines, the latter being more potent carcinogenic.

In this study the loss pathways of four nitramines through their reaction with the well-known oxidants found in the atmosphere have been thoroughly investigated. Nitrosamines have been found to undergo rapid photolysis in the presence of sunlight, thus their reaction with the most abundant oxidant at night, the nitrate radical have been investigated using two simple nitrosamines.

The rate coefficients for OH radicals, Ozone and Cl atoms reactions with 4 nitramines at 298 K and 1013 hPa have been determined using relative rate method, and the lifetimes of the 4 nitramines following their reaction with these oxidants in the atmosphere have also been determined. Likewise, the rate coefficients for the reactions of the nitrate radicals (NO_3) with two simple nitrosamines were determined at the same conditions using the same method. Moreover, the lifetimes of these nitrosamines following their reactions with the nitrate radicals in the atmosphere were calculated.

The primary products resulting from the reactions of OH radicals and Cl atoms with four nitramines have been investigated and hence identified using FT-IR detection method. Further, the OH initiated photooxidation of formamide have been studied as well and the only resulting product namely isocyanic acid was detected.

The Structure Activity Relationship (SAR) for OH reactions with nitramines was also studied and found not applicable due to the fact that, the reaction rate coefficients estimated using SAR differ significantly with the experimental results.

Infrared absorption cross-sections as well as integrated absorption intensities have been determined for a number of compounds.

PREFACE

This work has been conducted as part of the ADA (Atmospheric Degradation of Amines) project which was supported by the CLIMIT programme (grants 193438, 201604 and 208122), Masdar, Shell Technology Norway, Vattenfall AB and Statoil ASA.

ACKNOWLEDGEMENT

First and foremost, I give the glory and honour to The Almighty God, the author and finisher of everything in my life for the good health, blessings and skills, a combination which enabled me to accomplish my study programme successfully.

My sincere and heartfelt gratitude go to my supervisor Professor Claus Jørgen Nielsen for his tireless guidance both on theory and technical aspects without which nothing would have been achieved as far as this research work is concerned. Thank you very much Professor Nielsen.

I would also like to thank my co-supervisor Professor Yngve Stenstrøm from the Norwegian University of Life Sciences for the good work he did of synthesizing the nitramines and nitrosamines samples which were used in this study.

Many thanks to my collegue Arne Joakim Coldevin Bunkan for his technical and theoretical assistance including going through the manuscript. You played a big role and your contribution is highly appreciated.

I am extremely grateful to my lovely wife Mona for her tolerance of staying home alone, her encouragement, unceasing prayers as well as the good work she did of proof-reading the text. Thank you so much my love. Apologies to our little boy Mike for spending his first ten months on the planet without dad at home.

Many thanks to my Pastor Einstein P. Muro and the entire TAG Changanyikeni church for their prayers and encouragement. Thanks to the PIWC, Oslo church for their prayers and spiritual care for the whole period of my stay in Norway. May HE richly bless you all.

I also wish to extend my gratitude to my employer, the Tanzania Industrial Research and Development Organization (TIRDO) for granting me a study leave.

The Norwegian State Loan Fund (*Lånekassen*) is highly appreciated for the scholarship through the Quota Programme without which I could not get the opportunity to pursue my studies.

1 INTRODUCTION AND LITERATURE REVIEW

1.1 General introduction

Despite of many types of energy resources available for the world consumption (around $5x10^{20}$ J in 2008), the fossil fuels are still the primary energy as they contribute more than 80% of the world's energy (Sriroth *et al.*, 2010). Combustion of fossil fuels continues to dominate a global energy market that is striving to meet the ever-increasing demand for heat, electricity and transport fuels (Sims *et al.*, 2007). Among various fossil fuels, the oils are of great significance having the largest consumption (38% of the world energy consumption) followed by coal (26%) and gas (23%) being used in industrial, commercial, household and transportation sectors (Sriroth *et al.*, 2010). As an example, in the United States 300,000 MW of power capacity is generated from the existing coal-fired power plants, providing about 50% of total power generated in the country and contributing to more than 30% of carbon dioxide (CO_2) emissions (Rochelle, 2009). Approximately 25 billion metric tonnes of carbon dioxide are released annually from human activities worldwide today (Höök, 2007). About a quarter of the CO_2 emissions around the globe are exhausted from the thermal plants (Ogawa *et al.* 2009). Coal has the highest carbon content (Ogawa *et al.*, 2009), thus burning of coal particularly in power plants is the main source of CO_2 worldwide (Lepaumier *et al.*, 2009). High concentrations of carbon dioxide which is the prime green house gas together with other greenhouse gases lead to global warming, hence climate change.

1.2 Greenhouse gases

The atmospheric concentrations of key anthropogenic greenhouse gases (i.e., carbon dioxide (CO_2), methane (CH_4), nitrous oxide (N_2O), and tropospheric ozone (O_3) reached their highest recorded levels in the 1990s, primarily due to the combustion of fossil fuels, agriculture, and land-use changes (IPCC, 2001). Meanwhile, between 1970 and 2004, global emissions of CO_2, CH_4, N_2O, HFCs, PFCs and SF_6, weighted by their global warming potential (GWP), have increased by 70% (24% between 1990 and 2004), from 28.7 to 49 Gigatonnes of carbon dioxide equivalents ($GtCO_2$-eq) (IPCC, 2007). The largest growth in global greenhouse gases emissions between 1970 and 2004 has come from the energy supply sector (an increase of 145%) (IPCC, 2007). Without the near-term introduction of supportive and effective policy actions by governments, energy related greenhouse gases emissions, mainly from fossil fuel combustion, are projected to rise by

over 50% from 26.1 $GtCO_2eq$ (7.1 GtC) in 2004 to 37 – 40 $GtCO_2$ (10.1–10.9 GtC) by 2030 (Sims *et al.*, 2007). The major greenhouse gases are briefly described below.

1.2.1 Carbon dioxide (CO_2)

Carbon dioxide is emitted to the atmosphere from both natural (through the carbon cycle) and anthropogenic sources like burning of fossil fuels. Naturally, carbon is cycled between three main reservoirs: the atmosphere containing 720 Gt of carbon in the form of carbon dioxide, the terrestrial biosphere (1500 Gt) and the oceans (38,000 Gt) (Mitchell, 1989). However, humankind has altered the natural carbon cycle by burning coal, oil, natural gas and wood and since the industrial revolution began in the mid 1700s, each of these activities has increased in scale and distribution (www.ncdc.noaa.gov/oa/climate/gases.html). Carbon dioxide was the first greenhouse gas demonstrated to be increasing in atmospheric concentration with the first conclusive measurements being made in the last half of the 20th century. Prior to the industrial revolution, concentrations were fairly stable at 280 ppm. The global mean concentration of CO_2 in 2005 was 379 ppm, leading to a Radiative Forcing of +1.66 [±0.17] W m^{-2}. (Forster *et al.,* 2007). High concentration, radiative forcing and long lifetime in the atmosphere make carbon dioxide the prime greenhouse gas despite of its low global warming potential as compared to other major greenhouse gases. The current greenhouse heating due to carbon dioxide is about 50 W m^{-2}. This has increased by about 1.3 W m^{-2} since 1860 (Mitchell, 1989).

1.2.2 Methane (CH_4)

Methane is an extremely effective absorber of radiation, though its atmospheric concentration is less than CO_2 and its lifetime in the atmosphere is brief (10-12 years), compared to some other greenhouse gases (such as CO_2, N_2O, CFCs). Atmospheric concentration of methane has increased as a result of human activities such as growing rice, raising cattle, using natural gas, mining coal and landfills (Forster *et al.,* 2007). Analysis of $14_C/12_C$ ratios and $13_C/12_C$ rations by Lowe *et al.,* 1988 suggested that about 32% of atmospheric methane originates from burning of fossil fuels. The main natural sources for atmospheric methane are paddy fields, ruminants, and wetland (Mitchell, 1989). Direct atmospheric measurement of atmospheric methane has been possible since the late 1970s and its concentration rose from 1.52 ppmv in 1978 by around 1 percent per year to 1990, since then there has been little sustained increase. The current atmospheric

concentration is approximately 1.77 ppmv (www.ncdc.noaa.gov/oa/climate/gases.html). The major sink of methane in the atmosphere is the photochemical oxidation by the hydroxyl radical (OH). If methane continues to increase at the current rate concentrations will reach 2.8 ppm in the next 50 years, contributing an addition of 0.5 Wm^{-2} in radiative heating (Mitchell, 1989).

1.2.3 Nitrous oxide (N_2O)

Anthropogenic sources of atmospheric nitrous oxide include fertilizer use and fossil fuel burning (Forster *et al.,* 2007). Nylon production, nitric acid and adipic acid production and vehicle emissions also contribute to its atmospheric load (vanLoon and Duffy, 2005, www.ncdc.noaa.gov/oa/climate/gases.html,). However the major sources are the natural ones from microbial denitrification in soils, lakes and oceans (vanLoon and Duffy, 2005). Denitrification describes a group of microbiological reactions that convert nitrate to nitrous oxide along with other nitrogen species (vanLoon and Duffy, 2005). By 1981 nitrous oxide was increasing at a rate of 0.2% per year (Weiss, 1981), which, if maintained would produce a concentration of 0.332 ppm in 2035 (Mitchell, 1989). According to vanLoon and Duffy (2005), the concentration of nitrous oxide in 2002 was 318 ppbv and was increasing at a rate of 0.3 % per year. The main sink of atmospheric nitrous oxide is through reaction with light (photolysis) and excited oxygen atoms [$O(^1D)$] in the stratosphere (Mitchell, 1989). However, this reaction is too slow resulting into an average of atmospheric lifetime of around 114 years, thereby making nitrous oxide such a powerful greenhouse gas. In general, the uptake of nitrous oxide by soils is regarded to be small on a global scale, where nitrous oxide is converted to nitrogen gas through denitrification process (http://www.ghgonline.org/nitroussinks.htm).

1.2.4 Water vapour (H_2O)

Water vapour is the most abundant and important greenhouse gas in the atmosphere (Forster *et al.,* 2007). However, changes in its concentration are also considered to be a result of climate *feedbacks* related to the warming of the atmosphere rather than a direct result of industrialization. The feedback loop in which water is involved is critically important to projecting future climate change, but as yet is still fairly poorly measured and understood (www.ncdc.noaa.gov/oa/climate/gases.html). Human activities also influence water vapour through CH_4 emissions, because CH_4 undergoes chemical destruction in the stratosphere, producing a small amount of water vapour (Forster *et al.,*

2007). Oxidation of the hydrogen atoms in methane produces two molecules of water vapour for each methane molecule (Mitchell, 1989). The current concentration o f methane (1.77 ppm) appears to account for the occurrence of water vapour in excess o f 6 ppm in parts of the stratosphere (Jones *et al.*, 1986). This means that, increases in the concentration of methane may produce increases in stratospheric water vapour.

The concentration of water vapour (specific humidity) varies from as much as 15,000 ppm near the surface in the tropics to 3 ppm in the lower stratosphere and varies considerably on diurnal, synoptic, and seasonal time scales as well as with location.). The current greenhouse heating due to water vapour is about 100 Wm^{-2} (Mitchell, 1989)

As the temperature of the atmosphere rises, more water is evaporated from ground storage (rivers, oceans, reservoirs, soil). Because the air is warmer, the absolute humidity can be higher (in essence, the air is able to 'hold' more water when it's warmer), leading to more water *vapour* in the atmosphere. As a greenhouse gas, the higher concentration of water vapour is then able to absorb more thermal infrared energy radiated from the Earth, thus further warming the atmosphere www.ncdc.noaa.gov/oa/climate/gases.html). The warmer atmosphere can then hold more water vapour and this is what is referred to as a 'positive feedback loop'.

While there are good atmospheric measurements of other key greenhouse gases such as carbon dioxide and methane, the measurements of global water vapour are still poor, so it is not certain by how much atmospheric concentrations have risen in recent decades or centuries, though satellite measurements, combined with balloon data and some in-situ ground measurements indicate generally positive trends in global water vapour (www.ncdc.noaa.gov/oa/climate/gases.html).

1.2.5 Ozone (O_3)

Ozone is not only a highly reactive and toxic species, but it absorbs both infrared and ultraviolet light, contributing to the “greenhouse effect” (Finlayson-Pitts and Pitts Jr., 2000). Atmospheric Ozone is continually produced and destroyed in the atmosphere by a series of chemical reactions. In the troposphere, human activities such as exhaust emissions from automobiles and pollution from factories, fossil fuel combustion as well as burning vegetation have increased ozone through the release of gases such as carbon monoxide, hydrocarbons and nitrogen oxide, which photo-chemically react to produce ozone. (Forster *et al.,* 2007, Volz and Kley, 1988, Janach, 1989,). Existing in a broad band, commonly called the 'ozone layer', a small fraction of this ozone naturally descends

to the surface of the Earth. In the stratosphere a steady-state concentration of ozone is maintained through the "Chapman cycle," reactions (1) - (4), hypothesized in the 1930's by Sir Sydney Chapman (Finlayson-Pitts and Pitts Jr., 2000)

$$O_2 \xrightarrow{h\nu} 2O \qquad R1$$

$$O+O_2 \xrightarrow{M} O_3 \qquad R2$$

$$O+O_3 \longrightarrow 2O_2 \qquad R3$$

$$O_3 \xrightarrow{h\nu} O+O_2 \qquad R4$$

In general, ozone concentrations are higher in and around cities than in sparsely populated areas, though there is some transport of ozone downwind of major urban areas. Apart from being a greenhouse gas, ozone also plays a big role in the formation of photochemical smog. There are indications of large local increases in ozone at the surface (Bolin *et al*., 1986), mainly from sites near industrial regions in the northern hemisphere (Volz and Kley, 1988).The lifetime of ozone molecules in the troposphere is short, and the spatial variations are large, so it is difficult to estimate globally averaged trends (Mitchell, 1989).

Concentrations of ozone have risen by around 30 percent since the pre-industrial era, and the global average radiative forcing (RF) due to increases in tropospheric ozone is estimated to have enhanced the anthropogenic greenhouse gas forcing by 0.35 ± 0.2 Wm^{-2} making tropospheric ozone the third most important greenhouse gas after CO_2 and CH_4 (www.ipcc.ch/ipccreports/tar/vol4/index.php?idp=88). The overall greenhouse warming contribution of ozone is approximately 1.3 Wm^{-2} (vanLoon and Duffy, 2005).

1.2.6 Chlorinated fluorocarbons (CFCs) and other halogens

Human activities are the main source of halocarbon gases concentrations in the atmosphere. Natural processes are also a small source. The major halocarbons include the chlorofluorocarbons (e.g., CFC-11 and CFC-12), which were widely used as refrigeration agents and in other industrial processes before their presence in the atmosphere was discovered to cause ozone depletion in the stratosphere (Forster *et al.*, 2007). The abundance of chlorofluorocarbon gases is decreasing as a result of international regulations designed to protect the ozone layer (Forster *et al.,* 2007). The Montreal Protocol gases (chlorofluorocarbons (CFCs), hydrochlorofluorocarbons (HCFCs), and chlorocarbons) as a group, contributed +0.32 [±0.03] W m^{-2} to the RF in 2005. Their RF peaked in 2003 and is now beginning to decline (Forster *et al.,* 2007).

Chlorofluorocarbons (CFCs) have no natural source, but were entirely synthesized for such diverse uses as refrigerants, aerosol propellants and cleaning solvents. Their creation was in 1928 and since then their concentrations kept increasing in the atmosphere. CFCs are nontoxic, nonflammable, and highly stable, and it is these very properties that render them virtually to be nonreactive in the troposphere and hence give them sufficiently long lifetimes in the lower atmosphere to reach the stratosphere (Finlayson-Pitts and Pitts Jr., 2000). Due to the discovery that they are able to destroy stratospheric ozone, a global effort to halt their production was undertaken and was extremely successful that the levels of the major CFCs are now declining. However, their long atmospheric lifetimes determine that some concentration of the CFCs will remain in the atmosphere for over 100 years (www.ncdc.noaa.gov/oa/climate/gases.html). Apart from destroying stratospheric ozone, CFCs are important greenhouse gases. They absorb in the range 1250 - 830 cm^{-1} with each CFC having a specific absorption bands in this critical window region (vanLoon and Duffy, 2005). For instance, CFC-12 has very strong peaks centred around 1050 cm^{-1} and 900 cm^{-1} (vanLoon and Duffy, 2005). Other important greenhouse gases in this group are the long-lived synthesized gases such as CF_4 (carbontetrafuoride) and SF_6 (sulfurhexafluoride). CF_4 originates from the electrolysis of alumina (Al_2O_3) in cryolite (Na_3AlF_6) at carbon electrodes, and the release of the gas is estimated to be around 0.77 kg per tonne of aluminium produced while SF_6 is formed during magnesium production (vanLoon and Duffy, 2005). Another set of synthesized compounds called HFCs (hydrofluorcarbons) are also greenhouse gases, though they are less stable in the atmosphere and therefore have a shorter lifetime and less of an impact as a greenhouse gas www.ncdc.noaa.gov/oa/climate/gases.html).

Table 1.2.1. Pre-industrial and current concentrations of main greenhouse gases, their lifetimes, Global Warming Potentials (GWP) and Radiative Forcing

Species		Concentrations and their changes		Atmospheric life (years)	Global Warming Potential (100 year time horizon)	Increased radiative forcing Wm^{-2}
Name	Chemical formula	Pre-Industrial concentration	Concentration in 2011			
Carbon dioxide	CO_2	280 ppm	390.5 ppm	~ 100	1	1.79
Methane	CH_4	700 ppb	1774 ppb	12	25	0.5
Nitrous oxide	N_2O	275 ppb	319 ppb	114	298	0.18
CFC-11	CCl_3F	0	241 ppt	45	4750	0.06
CFC-12	CCl_2F_2	0	534 ppt	100	10900	0.17

Source: http://cdiac.ornl.gov/pns/current_ghg.html

1.3 Global warming and climate change

The planet Earth is made habitable by the presence of certain gases which trap long-wave radiation emitted from the Earth's surface, giving a global mean temperature of 15°C, as opposed to an estimated -18°C in the absence of an atmosphere (Mitchell, 1989). This phenomenon is known as “greenhouse effect”.

The concentrations of the main greenhouse gases namely, carbon dioxide, methane, and nitrous oxide are all known to be increasing and in recent years, other greenhouse gases principally chlorofluorocarbons (CFCs), have been added in significant quantities to the atmosphere as described above. Increases in such gases alter the radiation balance by trapping more of the terrestrial infrared radiation, which results in a larger amount of energy converted to thermal energy in the troposphere (Finlayson-Pitts and Pitts Jr., 2000). There are many uncertainties in deducing the consequential climatic effects. Typically, it is estimated that increased concentrations of these gases since 1860 may have raised global mean surface temperatures by 0.5°C or so, and the projected concentrations could produce a warming of about 1.5°C over the next 40 years (Mitchell, 1989). Figure 1.3.1 below shows the mechanism of the greenhouse effect.

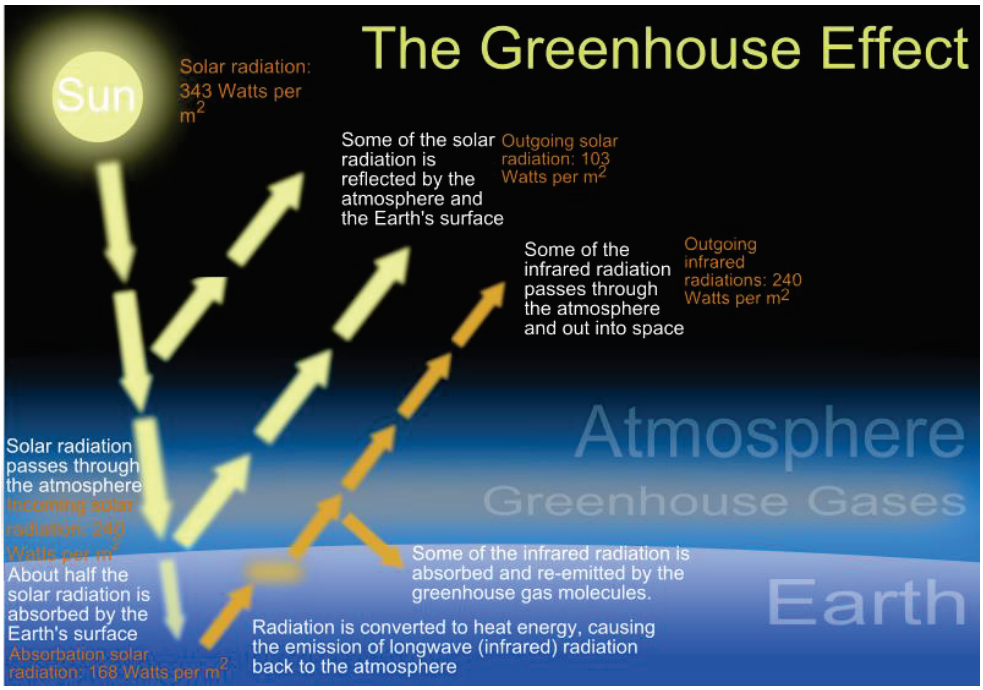

Figure 1.3.1: The greenhouse effect (sorce: Wikipedia.org)

Global warming resulting from anthropogenic carbon dioxide is one of the most important environmental issues going on all over the world today due to its consequences on climate. The projected concentration of CO_2 in the year 2100 ranges from 540 to 970 ppm, compared to about 280 ppm in the pre-industrial era and about 368 ppm in the year 2000 (IPCC, 2001).

Industrialized countries are the main source of carbon dioxide in the atmosphere (Figure 1.3.2) especially those whose large percent of their power is generated through burning of coal like US, China and India (Figure 1.3.3). The world primary energy consumption by fuel type since 1971 to 2005 is shown in figure 1.3.4.

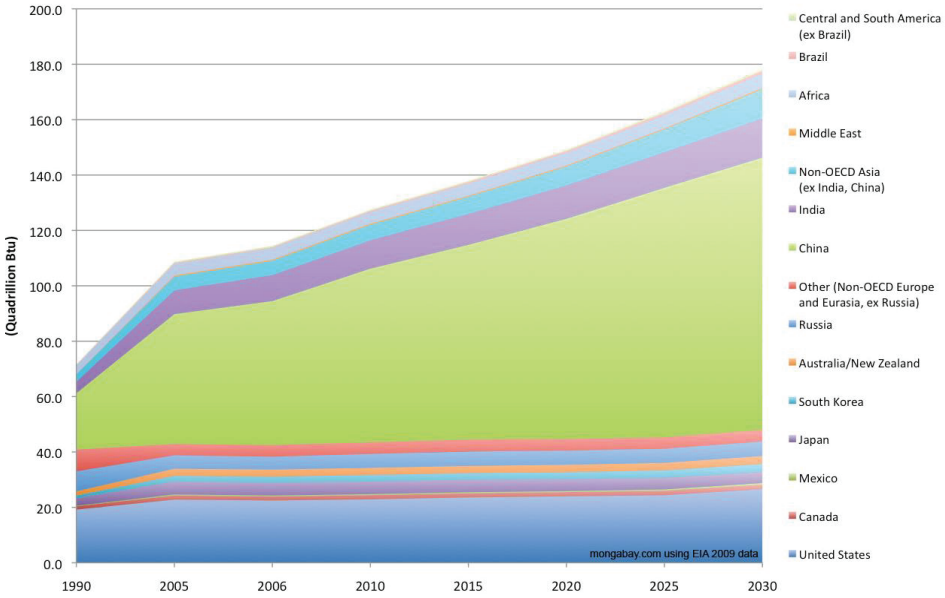

Figure 1.3.2: Past and projected world coal consumption trend by region, 1990-2030 (source: www.mongabay.com)

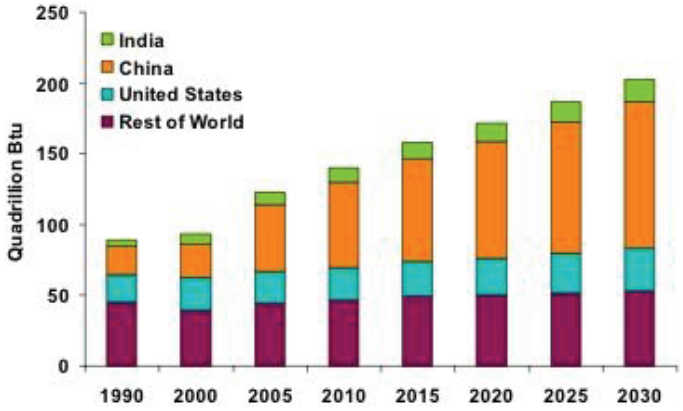

Figure 1.3.3: Past and projected world coal consumption 1990-2030 (source: EIA, IEO2008).

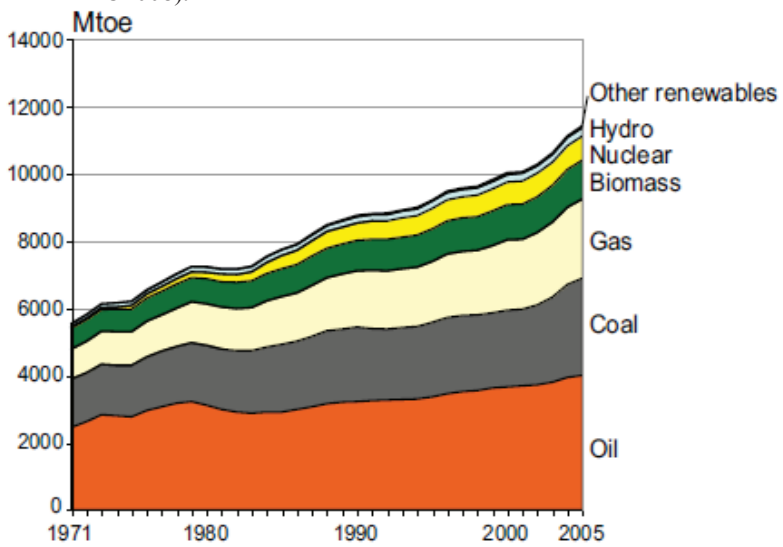

Figure 1.3.4: World primary energy consumption by fuel type (source: IPCC, 2007).

Apart from the contribution of greenhouse gases on climate change, aerosols particles also play a role in changing the climate. How ever, currently the role played by aerosols on global warming and climate change is by far less well understood compared to green house gaseses.

Aerosols have direct and indirect effects on global climate. The direct effect is based on the absorbtion of incoming solar radiation, which lead to the decrease of the radiative forcing and in turn decreases the global mean tempetarure. This gives an implication that aerosols lead to short-term regional cooling effects (Finlayson and Pitts, 2000). However, there are some aerosols like black carbon that are considered to lead to increases of the

global mean temperature. The indirect effect of aerosols is related to the formation of clouds, which in turn alter the direction of incoming solar radiation, which decreases the radiative forcing (Finlayson and Pitts, 2000).

Tropospheric particles containing carbon are often referred to as "carbonaceous aerosols" (Penner and Novakov, 1996). The form of carbon here may be organic or elemental, the latter often been referred to as graphitic or black carbon due to its strong absorption of visible light (Finlayson-Pitts and Pitts Jr., 2000). While black carbon/elemental carbon aerosol particles are the major absorbers of solar radiation, sulphate aerosols are good at solar radiation scattering leading to cooling of the planet. However, the cooling effect resulting from scattering of solar radiation by aerosol particles occurs primarily during the day and it is too minimal to counterbalance the positive radiative forcing (warming) due to greenhouse gases (Finlayson-Pitts and Pitts Jr., 2000).

1.3.1 Amines contribution in formation of aerosol particles in the atmosphere

Contribution of amines in the formation of secondary aerosols in the atmosphere has been reported (Silva *et al.*, 2008, Murphy *et al*., 2007, Qui and Zhang, 2013). Amines which are basic in nature, they react with gas-phase acids such as HNO_3 and H_2SO_4 present in the atmosphere to form particulate salts as shown in the reactions below:-

$NR_3(g) + HNO_3(g) \rightleftarrows HNR_3NO_3(s)$ …….……R5

$2NR_3(g) + H_2SO_4(g) \rightleftarrows (HNR_3)_2SO_4(s)$ ……..……..R6

Reactions (R5) and (R6) are analogous to those of ammonia leading to the formation of ammonium sulfate and ammonium nitrate. Apart from these reactions, amines have been identified as nucleation precursors to be involved in the formation of the critical nucleus under different ambient environments (Zhang *et al*., 2012, Fan *et al*., 2006). Dimethylamine for example has been found to enhance the nucleation process of sulphuric acid and water by a factor of ~ 3.5 (Yu, *et al*., 2012). In their study, Yu *et al*., (2012), made observations which provide the laboratory evidence that amines indeed can participate in aerosol nucleation and growth at the molecular cluster level. Figure 1.3.5 shows the mechanism of heterogeneous reactions of amines in the atmosphere leading to the formation of aerosol particles.

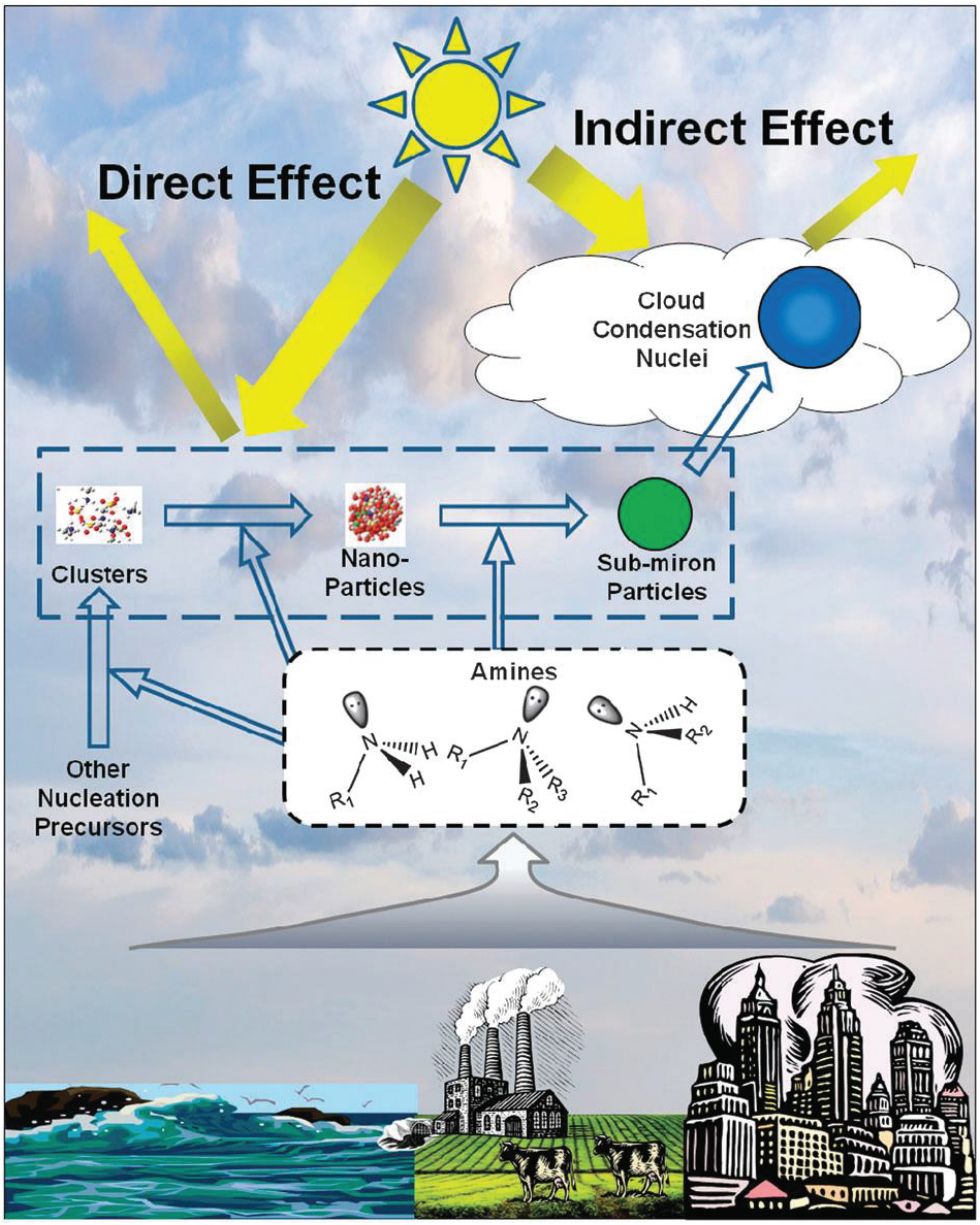

Figure 1.3.5: Schematic representation of the heterogeneous reaction of amines in the atmosphere (source: Qiu and Zhang, 2013).

While the mean global surface temperature has increased by ~0.3 - 0.6~ over the past century, the period from 1940 to the mid-1970s showed no such trend (IPCC, 1996). This period was characterized by cooler than normal temperatures, which has often been

qualitatively ascribed to the scattering of incoming solar radiation by pollution derived from aerosol particles (Finlayson and Pitts, 2000).

In addition, since heterogeneous chemistry can occur on aerosol particles, it is possible that such chemistry can alter the concentrations of other contributors to the climate system, such as the greenhouse gases. One example is the formation of N_2O from reactions of HONO on the surface of aerosol particles (Finlayson and Pitts, 2000).

Effects of global warming include; a more active hydrological cycle with more heavy precipitation events and shifts in precipitation, widespread retreat of non-polar glaciers, increases in sea level and ocean-heat content, and decreases in snow cover and sea-ice extent and thickness (IPCC, 2001).

Global warming can also result into exacerbating local and regional air pollution and delay the recovery of the stratospheric ozone layer. In addition, climate change could also affect the productivity and composition of terrestrial and aquatic ecological systems, with a potential loss in both genetic and species diversity; could accelerate the rate of land degradation; and could exacerbate problems related to freshwater quantity and quality in many areas. Conversely, local and regional air pollution, stratospheric ozone depletion, changes in ecological systems, and land degradation would affect the Earth's climate by changing the sources and sinks of greenhouse gases, radiative balance of the atmosphere, and surface albedo (IPCC, 2001).

Furthermore, climate change can affect human health directly (e.g., reduced cold stress in temperate countries but increased heat stress, loss of life in floods and storms) and indirectly through changes in the ranges of disease vectors (e.g., mosquitoes), water-borne pathogens, water quality, air quality, and food availability and quality (medium to high confidence). The actual health impacts will be strongly influenced by local environmental conditions and socio-economic circumstances, and by the range of social, institutional, technological, and behavioural adaptations taken to reduce the full range of threats to health (IPCC, 2001).

1.3.2 Climate change mitigations in the enelectricity generation sector

Mitigation of climate change can be achieved through applications of different approaches in different sectors including, energy, agriculture, industry, transport, waste

management, buildings and forestry. For the purpose of this study only the energy sector, particulary the electricity generation will be discussed.

1.3.2.1 Electricity generation sector

The electricity sector has a significant mitigation potential using a range of technologies (Table 1.3.2). The economic potential for mitigation of each individual technology is based on what might be a realistic deployment expectation of the various technologies using all efforts, but given practical constraints on rate of uptake, public acceptance, capacity building and commercialization (IPCC, 2007).

A wide range of energy-supply mitigation options are available and cost effective at carbon prices of <20US$/tCO$_2$ including fuel switching and power-plant efficiency improvements, nuclear power and renewable energy systems. Carbon Capture and Storage (CCS) will become cost effective at higher carbon prices. Several other options are still under development including advanced nuclear power, advanced renewables, second-generation biofuels and, in the longer term, the possible use of hydrogen as an energy carrier (IPCC, 2007).

Table 1.3.1: Key mitigation technologies and practices for the energy sector (IPCC, 2007)

Sector	Key mitigation technologies and practices currently commercially available	Key mitigation technologies and practices projected to be commercialized before 2030
Energy supply	Improved supply and distribution efficiency; fuel switching from coal to gas; nuclear power; renewable heat and power (hydropower, solar, wind, geothermal and bioenergy); combined heat and power; early applications of Carbon Capture and Storage (CCS, e.g. storage of removed CO2 from natural gas).	CCS for gas, biomass and coal-fired electricity generating facilities; advanced nuclear power; advanced renewable energy, including tidal and waves energy, concentrating solar, and solar PV.

Table: 1.3.2: Potential GHG emissions to be avoided by 2030 for selected electricity generation mitigation technologies (IPCC, 2007)

	Regional groupings	Mitigation potential; total emissions saved in 2030 ($GtCO_2$-eq)
Fuel switch and plant efficiency	OECD[a]	0.39
	EIT[b]	0.04
	Non-OECD	0.64
	World	1.07
Nuclear	OECD	0.93
	EIT	0.23
	Non-OECDW	0.72
	World	1.88
Hydro	OECD	0.39
	EIT	0.00
	Non-OECD	0.48
	World	0.87
Wind	OECD	0.45
	EIT	0.06
	Non-OECD	0.42
	World	0.93
Bio-energy	OECD	0.20
	EIT	0.07
	Non-OECD	0.95
	World	1.22
Geothermal	OECD	0.09
	EIT	0.03
	Non-OECD	0.31
	World	0.43
Solar PV and concentrated solar power	OECD	0.03
	EIT	0.01
	Non-OECD	0.21
	World	0.25
CCS + coal	OECD	0.28
	EIT	0.01
	Non-OECD	0.20
	World	0.49
CCS + gas	OECD	0.09
	EIT	0.04
	Non-OECD	0.19
	World	0.32

Notes:

[a] Organization for Economic Cooperation and Development

[b] Economies in Transition

1.4 The Kyoto Protocol

Following observations of some undesirable changes on the planet like increase in temperature which would trigger other catastrophic problems on health and the environment, the world had to come together to seek ways to curb the situation. Among these ways is the Kyoto protocol. This is an international agreement linked to the United Nations Framework Convention on Climate Change (UNFCCC). It (The Kyoto Protocol) was adopted in Kyoto, Japan, on 11th December 1997 and entered into force on 16th February 2005. The detailed rules for the implementation of the Protocol were adopted at COP 7 in Marrakesh in 2001, and are called the "Marrakesh Accords."

The major feature of the Kyoto Protocol is that it sets binding targets for 37 industrialized countries and the European community for reducing greenhouse gas (GHG) emissions. These amounts to an average of five per cent against 1990 levels over the five-year period 2008-2012 (http://unfccc.int/kyoto_protocol/items/2830.php).

In principal, developed countries are responsible for the current high levels of GHG emissions in the atmosphere as a result of more than 150 years of industrial activity. The Protocol places a heavier burden on developed nations under the principle of "common but differentiated responsibilities."

The Kyoto mechanisms

Under the Treaty, countries must meet their targets primarily through national measures. However, the Kyoto Protocol offers them an additional means of meeting their targets by way of three market-based mechanisms. These mechanisms are:

- Emissions trading – known as "the carbon market"
- Clean development mechanism (CDM)
- Joint implementation (JI).

The mechanisms help stimulate green investment and help Parties meet their emission targets in a cost-effective way.

The Kyoto Protocol compliance system ensures that Parties are meeting their commitments and helps them to meet their commitments if they have problems doing so (http://unfccc.int/kyoto_protocol/items/2830.php).

Adaptation

The Kyoto Protocol, like the Convention, is also designed to assist countries in adapting to the adverse effects of climate change. It facilitates the development and

deployment of techniques that can help increase resilience to the impacts of climate change. Adaptation Fund was established to finance adaptation projects and programmes in developing countries that are Parties to the Kyoto Protocol. The Fund is financed mainly with a share of proceeds from CDM project activities.

The Kyoto Protocol is generally seen as an important first step towards a truly global emission reduction regime that will stabilize GHG emissions and provides the essential architecture for any future international agreement on climate change (http://unfccc.int/kyoto_protocol/items/2830.php).

Among the requirements of the Kyoto protocol to the member countries (Parties) are stipulated in Article 2 below.

Article 2

1. Each Party included in Annex I, in achieving its quantified emission limitation and reduction commitments under Article 3, in order to promote sustainable development, shall:

(a) Implement and/or further elaborate policies and measures in accordance with its national circumstances, such as:

(i) Enhancement of energy efficiency in relevant sectors of the national economy;

(ii) Protection and enhancement of sinks and reservoirs of greenhouse gases not controlled by the Montreal Protocol, taking into account its commitments under relevant international environmental agreements; promotion of sustainable forest management practices, afforestation and reforestation;

(iii) Promotion of sustainable forms of agriculture in light of climate change considerations;

(iv) Research on, and promotion, development and increased use of, new and renewable forms of energy, of carbon dioxide sequestration technologies and of advanced and innovative environmentally sound technologies;

(v) Progressive reduction or phasing out of market imperfections, fiscal incentives, tax and duty exemptions and subsidies in all greenhouse gas emitting sectors that run counter to the objective of the Convention and application of market instruments;

(vi) Encouragement of appropriate reforms in relevant sectors aimed at promoting policies and measures which limit or reduce emissions of greenhouse gases not controlled by the Montreal Protocol;

(vii) Measures to limit and/or reduce emissions of greenhouse gases not controlled by the Montreal Protocol in the transport sector;

(viii) Limitation and/or reduction of methane emissions through recovery and use in waste management, as well as in the production, transport and distribution of energy. (http://unfccc.int/resource/docs/convkp/kpeng.pdf).

1.5 Carbon Capture and Storage (CCS)

Carbon Capture and Storage (CCS) of CO_2 has emerged as a promising technology for mitigating global warming by effectively reducing carbon dioxide emissions from large point sources, such as fossil fuel power plants. One of the more promising technologies for efficient post-combustion CO_2 capture is through the use of amines (Lepaumier *et al.*, 2009, Rochelle, 2009, Strazisar *et al.,* 2003). This technology is promoted as a "bridging"-technology to smooth the transition from today's fossil energy based system to a future sustainable energy system (Veltman *et al.*, 2010). Once the CO_2 is captured, it has to be stored and a range of potential storage options exists such as geological formations including deep saline reservoirs, depleted oil and gas wells, and unmineable coal seams (Rao *et al.*, 2002). Generally, studies indicate that geological formations are the most plentiful and attractive options (Rao *et al.*, 2002). Table 1.5 gives a summary of the estimated capacities of the Earth's major viable sink options.

Table 1.5. Estimated world sink capabilities of CO_2 disposal options (Herzog, 2001)

Sequestration option	Worldwide capacity
Ocean	1000 GtC*
Deep saline formations	100 – 1000 GtC
Depleted oil and gas reservoirs	100 GtC
Coal seams	10 – 100 GtC
Terrestrial	10 GtC
Utilisation	<1 GtC/year

* GtC = giga-tonnes carbon

The storage period should exceed the estimated peak periods of fossil fuel exploitation, so that if CO_2 re-emerges into the atmosphere, it should occur past the predicted peak in atmospheric CO_2 concentrations (Herzog *et al.,* 2004). In a CO_2 capture plant using amines, most of the amine will be recycled inside the plant, but a small fraction of amines will be released to the atmosphere together with the cleaned exhaust gas. It is estimated that one million tonnes of captured CO_2, will emit up to 160 tonnes of amines. According to the estimations made by the Norwegian Gassnova, the Kårstø 420 MW gas power plant with the capacity of capturing one million tonnes of CO_2 annually would emit amine concentrations of 1 – 4 ppm into the atmosphere, representing 40 to 160 tonnes of amine emitted to the air per year (CO_2-Kårstø, 2009). The amine emissions can be contained in water droplets, be fresh liquid droplets and in the form of gas (www.ekopolitan.se/climate/cc-and-health-amines). However, it is well known that the released amines degrade into highly toxic compounds that may cause adverse health effects and environmental damage ((www.ekopolitan.se/climate/cc-and-health-amines). A screening study by Bråten *et al.,* (2008) undertaken to understand more about atmospheric amine chemistry and to evaluate if the emissions caused by CO_2 capture using amines may pose a risk to human health and the natural environment showed that, several toxic compounds may be formed. These include toxic compounds such as nitrosamines, nitramines, and *N*-nitro amides - all of which can be formed by the reaction of amines with oxidized nitrogen compounds (Pitts *et al.*, 1978, Neurath *et al.*, 1977, Fostås *et al.,* 2011, Dauglas *et al.*, 1978, Nielsen *et al.*, 2011, Grosjean, 1991). Other degradation products of amines in the atmosphere are formamide and acetamide which has been reported to induce development toxicity and carcinogenicity respectively in experimental animals (Låg *et al.*, 2008b, Fostås *et al.,* 2011). In aqueous phase, Nitrosodimethylamine (NDMA) has been reported to be a by-product of rocket fuel production and disinfection processes at water and wastewater treatment plants (Jahan *et al.,* 2008). A research carried out by the Norwegian Institute of Public Health found that 2% of the total amount of amine emissions from a CO_2 capture plant is nitrosamines, 7% nitramines and 9% formamides. With 160 tonnes of amines emissions from a CO_2 capture plant will mean 3.2 tonnes of Nitrosamine, 11 tonnes of Nitramines and 14 tonnes of formamide (Karl *et al.*, 2009). Apart from formation of toxic compounds, other challenges which this technology faces includes, corrosion of membranes, reduced adsorption by flue gas impurities, as well as increased energy costs and needs (Ma'mun *et*

al., 2007,). The highest concentration of amines emitted and amine compounds will be found within one kilometre distance from a CO_2 capture plant. At a distance of 3 kilometres from the capture plant the concentration is almost constant and it is expected to decline gradually at distance over 10 kilometres (Karl *et al.*, 2009).

The CO_2 capture processes also produce amine waste, and a typical CO_2 capture plant with capacity of 1 million tonnes of CO_2 annually is expected to produce between 300 and 3000 tonnes of waste amine per year (Shao *et al.*, 2009).

1.6 Amines

Amines are organic derivatives of ammonia wherein one or more hydrogen atoms have been replaced by a substituent such as an alkyl or aryl group as it's the case for alcohols and ethers which are organic derivatives of water (McMury, 2008). Like Ammonia, amines contain a nitrogen atom with lone pair of electrons, making amines both basic and nucleophilic (McMury, 2008). Amines occur widely in all living organisms. Trimethylamine for instance occurs in animal tissues and is partially responsible for the distinctive odour in fish (McMury, 2008). In plants, amines were first discussed by Steiner and Stein von Kamienski (1953) and Stein von Kamiensk (1957) while Drawert in 1965 reported amines in wine. Amines liable for promoting the formation of nitrosamines have been thoroughly analysed (Neurath *et al.*, 1977). As shown below, there are three groups of amines namely primary, secondary and tertiary amines depending on the number of replaced hydrogen(s) of ammonia.

Primary amine **Secondary amine** **Tertiary amine**

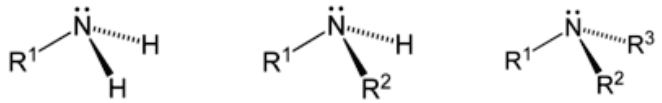

The three methylamines and ethylamine are gaseous at room temperature. Diethylamine, triethylamine and higher amines (up to about twelve carbon atoms per alkyl chain) are liquid, and long-chain amines containing still higher alkyl groups are solid. Gaseous amines possess a characteristic ammonia smell while liquid amines have a distinctive "fishy" smell (http://en.wikipedia.org/wiki/Amine).

Amines are in a group of volatile organic compounds (VOCs) emitted to the atmosphere from a number of sources including intense emissions from animal feeding operations

and industrial sources including losses from CO_2 capture in the near future (Ge *et al.,* 2011, Atkinson *et al.,* 1977). Rates of amine emissions from dairy operations have been estimated to range from 0.091 to 5 kg per head of cattle per year (Bailey *et al.*, 2005). Other sources of amines in the atmosphere include; car exhaust, biomass burning, sewage treatment plants and waste incinerators (Silva *et al.*, 2008, Westerholm *et al.*, 1993; Manahan, 1990, Schade and Crutzen, 1995, Lloyd *et al.,* 2009). In indoor air, some amines such as cyclohexylamine, morphone and 2-(diethylamino)ethanol may be present at high concentrations due to their use as corrosion inhibitors in steam boiler systems (Edgerton *et al.,* 1989). In the biosphere they result from bacterial degradation of nitrogen containing organic matter such as proteins and amino acids (Erupe *et al.*, 2008). Amines have been also measured in nonurban areas (Van Neste *et al.*, 1987; Gorzelska and Galloway, 1990; Eisele and Tanner, 1990). The most common and abundant amines in the atmosphere are the low-molecular weight aliphatic amines with carbon numbers of 1 - 6, such as methylamine (MA), dimethylamine (DMA), trimethylamine (TMA), ethylamine (EA), diethylamine (DEA), triethylamine (TEA), 1-propanamine and 1-butanamine (Ge *et al.,* 2011). Apart from degrading to toxic compounds, amines act as precursors for aerosols in the atmosphere which could have implications on health, visibility and climate change (Angelino *et al.*, 2001, Erupe *et al.*, 2008, Finlayson-Pitts and Pitts Jr., 2000, Malloy *et al.*, 2009**,** Murphy *et al*., 2007, Nadykto *et al.,* 2011, Smith *et al*., 2010, Sorooshian *et al.*, 2008;). The global emission of methylamines as per Schade and Crutzen (1995) is estimated to be 150 Gg N/year, most of which is trimethylamine.

Owing to the fact that, amines do not undergo photolysis in the atmosphere, their main removal processes are reactions with a number of reactants found in the atmosphere such as hydroxyl radical (OH), ozone (O_3) and nitrate radical (NO_3)(Tuazon *et al*., 1994, Pitts *et al*., 1978, Finlayson-Pitts and Pitts Jr., 2000, Silva *et al.*, 2008) as well as their reactions with nitric or sulphuric acid to form the corresponding nitrate salts (Seinfeld and Pandis, 1998, Murphy *et al*., 2007). The lifetimes of alkylamines in the atmosphere are in the range of a few hours to tens of hours (Erupe *et al.*, 2008). Their reaction rate constant with OH radical is in the range (1 - 7) x 10^{-11} cm^3 $molecule^{-1}$ s^{-1} (Bråten *et al.*, 2008). With an average of OH radicals concentration of 10^6 molecules cm^{-3} in the atmosphere, their lifetimes lie between 4 – 28 hours (Bråten *et al.*, 2008).

1.6.1 Why use of amines in post-combustion CO_2 capture?

Amine scrubbing has been used to separate carbon dioxide (CO_2) from natural gas and hydrogen since 1930 (Rochelle, 2009). Due to its properties (high reactivity, low solvent cost, low molecular weight and thus, high absorbing capacity on a mass basis and reasonable thermal stability and thermal degradation rate) towards CO_2 capture as compared to other alkanolamines; Monoethanolamine (MEA) has been used as a benchmark solvent for post-combustion CO_2 capture (Lepaumier *et al.*, 2009, Ma'mun, S *et al.*, 2007, Nielsen *et al.*, 2011, Puxty *et al.*, 2009). *N*-methyldiethanolamine (MDEA) and diethanolamine (DEA) are commonly used in natural gas treatment (Lepaumier *et al.*, 2009, Aronu *et al.*, 2009). Di-isopropanolamine (DIPA), triethanolamine (TEA), 2-piperidieenthanol (2-PE) and 2-amino-2-methyl-1-propanol (AMP) can also be used (Kohl and Nielsen, 1997). Apart from the above stated benefits of MEA, it also has some disadvantages which include high enthalpy of reaction with CO_2, leading to higher desorber energy consumption, the formation of a stable carbamate and also the formation of degradation products with Carbonyl Sulphide (COS) or oxygen bearing gases, inability to remove mercaptans, vapourization losses because of high vapour pressure and more corrosive than many other alkanolamines and thus, needs corrosion inhibitors when used in higher concentrations (Ma'mun *et al.*, 2007, Kapteina *et al.*, 2005).

1.6.2 The amine technology

CO_2 removal by absorption and stripping with aqueous amine is a well known and widely used technology (Rochelle, 2009). In this process, CO_2 is absorbed from a fuel gas or combustion gas near ambient temperature into an aqueous solution of amine with low volatility (Figure 1.6.2.1). The amine is regenerated by stripping with water vapour at 100 °C to 120 °C and the water is condensed from the stripper vapour leaving pure CO_2 that can be compressed to 100 to 150 bars for geological sequestration (Rochelle, 2009).

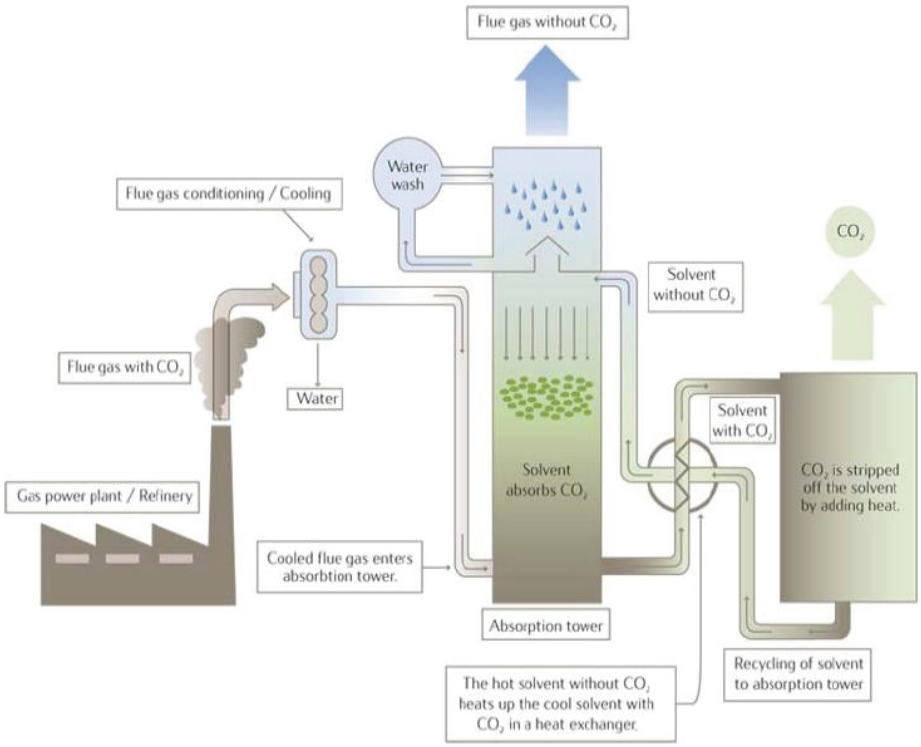

Figure 1.6.2.1: A schematic diagram showing the amine based CO_2 capture process (source: Technology Centre Mongstad, Norway).

How the technology works (as per Technology Centre Mongstad, Norway**)**

The absorber:

Exhaust gas (flue gas) containing the CO_2 is routed into a large absorption tower. The exhaust gas enters the bottom of the absorber flowing upwards where it comes into contact with the liquid amine flowing downwards allowing the CO_2 to be absorbed from the flue gas.

The water wash:

After absorbing CO_2, the remaining exhaust gas is treated in a water wash placed in the upper part of the absorber tower to remove amines before the cleaned exhaust gas is released back to the atmosphere.

The* CO_2 *desorbers

The CO_2 rich amine solvent is pumped via heat exchangers to a regenerator where the chemical reaction between the amine and CO_2 is reversed by steam flowing upwards in

the regenerator column. The separated CO_2 would then be ready for compression, transport and storage and the CO_2 lean liquid amine can be pumped back into the absorber for reuse and the cycle repeated. **(http://www.tcmda.com/en/Technology/amine-technology)**

1.6.3 Health and environmental impact of amines

1.6.3.1 Aliphatic amines and amides

The gaseous aliphatic amines, such as methylamine (MA), dimethylamine (MA) and ethylamine (EA), usually have an unpleasant smell and some of them are highly hazardous, toxic and reactive (http://www.osha.gov). Exposure to aliphatic amines (including morpholine and piperidine) can occur through inhalation, ingestion, or contact and absorption through the skin. The potential symptoms include irritation of eyes, skin, nose, throat and respiratory system; drowsiness and headache; cough, sneezing, wheezing, sore throat and dyspnea (breathing difficulty); pulmonary oedema (may be delayed); blurred vision, conjunctivitis, corneal necrosis and eye redness, pain and burns; skin redness, dermatitis, pain, and burns; mucous membrane burns; abdominal pain, nausea, vomiting, diarrhea, and shock or collapse (Ge *et al.,* 2011). The health effects include irritation of the eye, nose, throat and skin; narcosis, and cumulative liver, lung and kidney damage. The affected organs include the eyes, skin, liver, kidneys, respiratory system, cardiovascular system, and central nervous system. Most of the aliphatic amines are not carcinogenic (Ge *et al.,* 2011). Hydrazines can affect the eyes, skin, respiratory system, central nervous system, blood, liver and gas gastrointestinal tract. Additional potential symptoms include temporary blindness, malar rash, photosensitivity, antinuclear antibody, coma, and convulsions. Hydrazine and 1,1-dimethylahydrazine (Carlsen *et al*., 2007) are also possibly carcinogenic to humans. Short-chain amides, such as formamide, acetamide, dimethylacetamide, and dimethylformamide, have the similar health effects to aliphatic amines. Additional symptoms of dimethylaceamide include jaundice, depression, hallucinations, and delusions. Acetamide is classified as a carcinogen by International Agency for Research on Cancer (http://www.iarc.fr/).

1.6.3.2 Aromatic amines

Aromatic amines are of concern due to their toxicity and occupational exposure (Arya *et al.,* 2011). The amines 2-naphthylamine, benzidine, and 4-aminobiphenyl are proven human carcinogens (Pinches and Waler, 1980). They are usually associated with bladder

cancer. Some of other aromatic amines (o-, m- and p-toluidines; 2,3-, 2,4-, 2,5-, 2,6-, and 3,5-dimethylanilines; 1- naphthylamine; carbofurane; 4,40-methylenedianiline) are suspected carcinogens although their association with human tumors has not been adequately documented (Rubino *et al.*, 1982; Palmiotto *et al.*, 2001). Aromatic amines can be absorbed through the skin and by inhalation. The potential symptoms of ingestion of the most common aromatic amine, aniline, include: headache, weakness, lethargy, dizziness and drowsiness, confusion and disorientation, unconsciousness, ataxia, eye irritation, respiratory irritation (dryness of throat, coughing, wheezing), dyspnea on effort, tachycardia, cyanosis, jaundice, nausea, sometimes vomiting, ringing in health effects include hematologic disturbances methmoglobinemia and acute toxicity short-term high hazard effects. The affected organs are the blood and cardiovascular system, liver, kidneys, eyes, respiratory system, and skin. The immediately dangerous to life or health (IDLH) concentration of aniline is 100 ppm (Ge *et al.,* 2011).

1.7 Atmospheric chemistry of amines

Since amines do no absorb light in the actinic region (λ >290 nm) (Calvert and Pitts, 1966) they are not removed in the atmosphere through photolysis. Thus reactions with atmospheric oxidants such as OH and O_3 are the major removal processes for these compounds. Reaction with HNO_3 may also occur in polluted urban areas (Finlayson-Pitts and Pitts Jr., 2000).

Previous experimental studies

There are few reports of products identified in the reactions of amines with OH radicals in the atmosphere. Grosjean (1991) outlined detailed mechanisms for the atmospheric reactions of $(CH_3)_2NH$, $(CH_3)_3N$, $(CH_3CH_2)_3N$, $(CH_3CH_2)_3N$, $(CH_3)(CH_3CH_2)NH$, $(CH_3CH_2)_2NCH_3$, and $O(CH_2CH_2)_2NH$. Schade and Crutzen (1995) have presented more detailed atmospheric degradation mechanisms for CH_3NH_2, $(CH_3)_2NH$ and $(CH_3)_3N$ in a study of the emission of aliphatic amines from animal husbandry. The study on atmospheric degradation of amines by Nielsen *et al*., (2011) has updated the reaction schemes of several amines with the hydroxyl racical. The mechanistic suggestions in the following are based on the individual reports and in accordance with today's generally accepted understanding of atmospheric degradation processes. The reported *N*-nitroso- and *N*-nitro-products are highlighted in boldface type.

Methylamine (CH_3NH_2)

The study by Atkinson *et al*., (1977) on the kinetics of the OH radical reaction with CH_3NH_2 over the temperature range 299 – 426 K reported a *negative* Arrhenius activation energy, $k_{OH}(T) = 1.02\times10^{-11} \times \exp\{(230 \pm 150)K/T\}$ and $k_{OH} = (2.20 \pm 0.22) \times 10^{-11}$ cm^3 $molecule^{-1}$ s^{-1} at 298 K. Carl and Crowley20 reported later a room temperatu-re value, kOH = $(1.73 \pm 0.11) \times 10^{-11}$ cm^3 $molecule^{-1}$ s^{-1}, which is ca. 30% lower. The absolute value of Atkinson *et al*., (1977) depends on a calibrated gas whereas Carl and Crowley (1998) used the UV cross-section of the amine for calibration, and they suggest that the earlier results suffer from a calibration error. Tuazon *et al*., (1994) have determined the rate constant for reaction of methylamine with O_3 to be $k_{O3} = (7.4 \pm 2.4)$ 10^{-21} cm^3 $molecule^{-1}$ s^{-1} at 298 K.

Rudic *et al*., (2003) studied the product branching and dynamics of the reaction between methylamine and Cl atoms employing REMPI spectroscopy with TOF-MS detection. They found branching ratios for the C-H:N-H and the C-D:N-D abstractions of 0.48:0.52 and 0.58:0.42 in CH_3NH_2 and CD_3ND_2, respectively. Since OH radicals and Cl atoms often show similar selectivity in their reactions, one may expect that also hydrogen abstraction in primary amines by OH radicals will occur from both C and N.

Galano and Alvarez-Idaboy (2008) have calculated the rate constant for the methylamine reaction with OH radicals using Canonical Variational Therory employing results from CCSD(T)/6-311++G(2d,2p)//BHandHLYP/6-311++G(2d,2p) calculations. Their result are $k_{OH}(T) = 5.89\ 10^{-11} \exp(-757/RT)$ cm^3 $molecule^{-1}$ s^{-1} and $k_{OH} = 5.20 \times 10^{-12}$ at 298 K; they predicted a *positive* Arrhenius activation energy. They also predicted a branching ratio for the C-H:N-H abstractions of 0.80:0.20 at 298 K. Tian *et al*., (2009) have presented results from similar theoretical calculations at the CCSD(T)/6-311++G(2d,2p)// CCSD/6-31G(d) level of theory followed by improved canonical variational transition state theory incorporating small-curvature tunnelling. Tian *et al*., (2009) predicted a *negative* Arrhenius activation energy at atmospheric temperatures, a positive Arrhenius activation energy at higher temperatures, and $k_{OH} = 2.98\ 10^{-11}$ cm^3 $molecule^{-1}$ s^{-1} at 298 K. They further reported the theoretical branching ratio for the C-H:N-H abstractions to be 0.74:0.26 at 298 K.

Murphy *et al*., (2007) carried out 3 experiments using NO_2, H_2O_2/NO and O_3 as oxidants. The results showed that nearly 100% of the aerosol formed during a photo-oxidation

experiments with CH_3NH_2 consisted of methyl-ammonium nitrate (salt) and that less than 1% was non-salt organics. Though the formation of non-salt aerosol was small, the relative importance of non-salt organic aerosol increased through the course of the experiments.

In the recent study by Nielsen *et al.,* (2011) on the atmospheric degradation of amines, the reactiom mechanism of methylamine has been updated as shown in scheme 1.7.1.

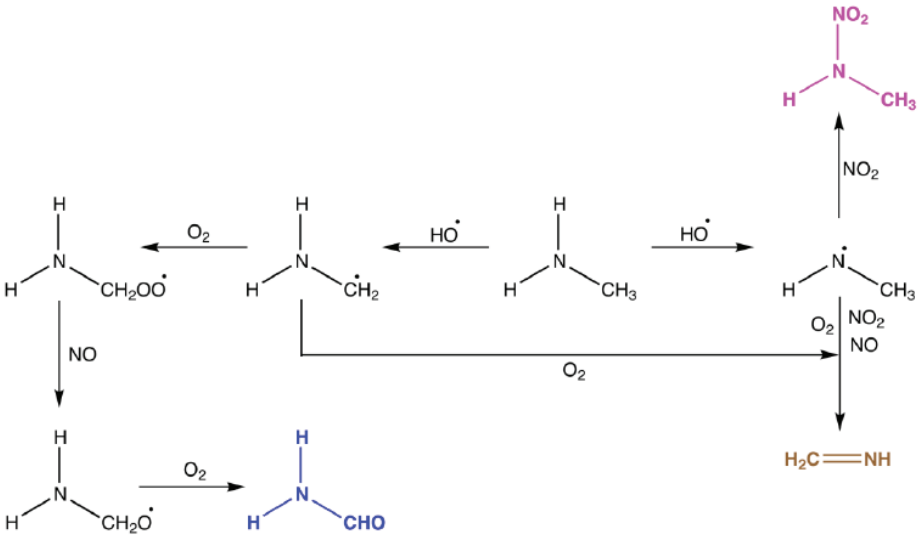

Scheme 1.7.1. Main routes of the atmospheric methylamine photo-oxidation (from Nielsen *et al.*, 2011).

Dimethylamine ($(CH_3)_2NH$)

Pitts *et al*. (1978) carried out an exploratory study of the products formed when a mixture of 500 ppb $(CH_3)_2NH$ + 80 ppb NO + 160 ppb NO_2 was subjected to natural sunlight conditions. They found $(CH_3)_2NNO_2$ (dimethyl nitramine) and $CHON(H)CH_3$ (*N*-methyl formamide) as gas phase products, but did not quantify the amounts formed. No $(CH_3)_2NNO$ (dimethyl nitrosamine) was found. No formation of HCHO (formaldehyde) was reported. Aerosol was also formed during the degradation but it was not analyzed. The product formation is in accordance with the following mechanism:

$$(CH_3)_2NH + OH \rightarrow (CH_3)_2N + H_2O \quad \text{R7a}$$

$$\rightarrow (CH_3)N(H)CH_2 + H_2O \quad \text{R7b}$$

$$(CH_3)_2N + NO_2 \rightarrow \mathbf{(CH_3)_2NNO_2} \quad \text{R8}$$

$$(CH_3)N(H)CH_2 + O_2 \rightarrow (CH_3)N(H)CH_2O_2 \quad \text{R9}$$

$$(CH_3)N(H)CH_2O_2 + NO \rightarrow (CH_3)N(H)CH_2O + NO_2 \quad \text{R10}$$

$$(CH_3)N(H)CH_2O + O_2 \rightarrow (CH_3)N(H)CHO + HO_2 \quad \text{R11}$$

Lindley *et al.,* (1979) reported the important branching ratio of the initial OH reaction with $(CH_3)_2NH$ to be $k_{R7a}/(k_{R7a} + k_{R7b}) = 0.37 \pm 0.05$. They also derived the following relative rates: $k_{R13}/k_{R14} = (1.48 \pm 0.07)\times10^{-6}$, $k_{R13}/k_{R15a} = (3.90 \pm 0.28) \times 10^{-7}$, and $k_{R15a}/k_{R15b} = 0.22 \pm 0.07$.

$$(CH_3)_2N\text{-}NO \xrightarrow{h\nu} (CH_3)_2N + NO \quad \text{R12}$$

$$(CH_3)_2N + O_2 \rightarrow CH_2{=}N\text{-}CH_3 + HO_2 \quad \text{R13}$$

$$(CH_3)_2N + NO \rightarrow \mathbf{(CH_3)_2N\text{-}NO} \quad \text{R14}$$

$$(CH_3)_2N + NO_2 \rightarrow \mathbf{(CH_3)_2N\text{-}NO_2} \quad \text{R15a}$$

$$\rightarrow CH_2{=}N\text{-}CH_3 + \mathbf{HONO} \quad \text{R15b}$$

Tuazon *et al*., (1984) did not observe $CH_2{=}NCH_3$ in their photolysis studies where O_3 was present. Instead they found 33% CH_3NO_2, 38% HCHO and 2% CO in addition to 65% $(CH_3)_2NNO_2$ and could account for ~100% of the carbon and ~95% of the nitrogen. In a later publication they studied the reactions of amines with O_3 and showed that $CH_3N{=}CH_2$ is essentially non-reactive towards O_3 (Tuazaon *et al.*, 1994). Since the experiment in which $CH_3N{=}CH_2$ was found to react quickly, was such that NO_3 may be formed (NO, NO_2 and O_3 present) it is possible that the observed products may stem from the imine versus NO_3 reaction. Lazarou *et al*., (1994) studied the reactions of the $(CH_3)_2N$ radical with NO and NO_2 by the very low pressure reactor (VLPR) technique and reported $k = (3.18 \pm 0.48) \times 10^{-13}$ and $k_R = (8.53 \pm 1.42) \times 10^{-14}$ cm^3 $molecule^{-1}$ s^{-1}. They also reported a third oxidation pathway in the $(CH_3)_2N + NO_2$ reaction:

$$(CH_3)_2N + NO_2 \rightarrow (CH_3)_2NO + NO \quad \text{R15c}$$

with a rate constant $k_{(R22c)} = (6.36 \pm 0.74) \times 10^{-13}$ cm^3 $molecule^{-1}$ s^{-1}. The rate constant for reaction (15b) could not be determined in their experiment due to overlapping signals of ions in the mass spectrometer. An evaluation of the atmospheric *N*-nitrosamine formation in the degradation of dimethylamine has been presented by Glasson (1979) and Hanst *et al.,* (1977).

Pitts *et al*., (1978) conducted an exploratory study and found that aerosol was formed during the photo-oxidation of $(CH_3)_2NH$, but it was not analyzed. Derek Price (2010) in

his master thesis analyzed the aerosol formed in the $(CH_3)_2NH/O_3/NOx$ oxidation experiments by HR-TOF-AMS. The major ion peaks observed of the aerosol included *m/z* 30.034 (CH_4N^+), *m/z* 44.050 ($C_2H_6N^+$), *m/z* 58.066 ($C_3H_8N^+$), *m/z* 86.099 ($C_5H_{12}N^+$), and *m/z* 101.114 ($C_6H_{15}N^+$), which represent the backbone amine fragments. Fragments of large hydrocarbons including *m/z* 72.094 ($C_5H_{12}^+$), *m/z* 86.11 ($C_6H_{14}^+$), and *m/z* 94.078 ($C_7H_{10}^+$) were detected, with evidence of oxidation in *m/z* 72.058 ($C_4H_8O^+$) and *m/z* 97.065 ($C_6H_9O^+$).

The present results by Nielsen *et al*., (2011) show that around 42% of the initial OH reaction with dimethylamine is N-H abstraction, which in part result in nitrosamine and nitramine formation. The amount of nitrosamine and nitramine formed depends on the NO_2 concentration. For rural areas where mixing ratios of NOx are 0.2-10 ppbV with an average ratio $NO:NO_2$ = 1:2 (National Research Council, 1991), the amount of dimethylnitramine formed will be less than 2.5% of the dimethylamine photo-oxidized. The other 58% of the initial OH reaction is C-H abstraction, of which 55% results in imine formation ($CH_2{=}NCH_3$), while the remaining 45% roughly divides into equal parts of CH_3NHCHO (*N*-methyl formamide), CH_2O (formaldehyde) and $CH_2{=}NH$ (methanimine).

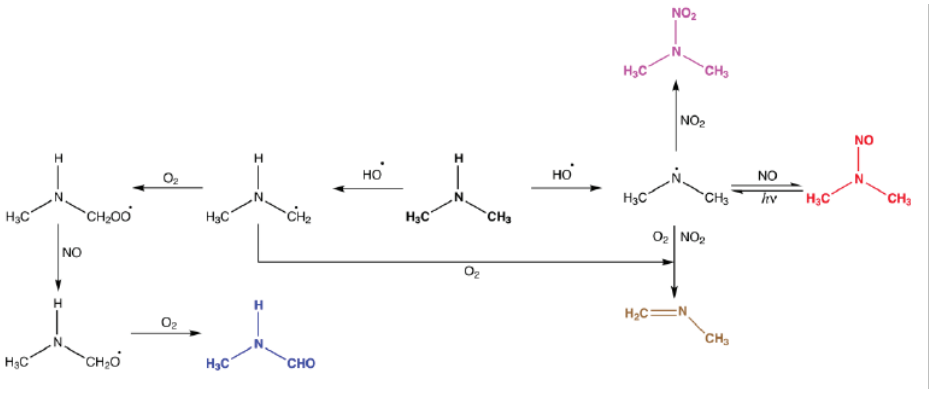

Scheme 1.7.2.: Main routes of the atmospheric dimethylamine photo-oxidation (from Nielsen *et al.*, 2011).

Trimethylamine ($(CH_3)_3N$)

Pitts *et al*., (1978) carried out an exploratory study of the products formed when a mixture of 500 ppb $(CH_3)_3N$ + 80 ppb NO + 160 ppb NO_2 was subjected to natural sunlight conditions. They found $(CH_3)_2NNO_2$ (dimethylnitramine) and $CHO\text{-}N(CH_3)_2$ (*N,N*-dimethylformamide) as gas phase products, but did not quantify the amounts

formed. Large amount (370 ppb) of HCHO (formaldehyde) was detected in the gas phase. No $(CH_3)_2NNO$ (dimethylnitrosamine) was found. The aerosol formed contained ca. 3 µg m^{-3} (1.6 ppb) $CHO\text{-}NH_2$ (formamide) and another amide-like compound with M = 87 was detected but not quantified. Schade and Crutzen (1995) suggested that this mass could correspond to $CHO\text{-}N(CH_3)\text{-}CHO$ (*N*-formyl-*N*-methyl-formamide).

The present results by Nielsen *et al*., (2011) show that around 40% of the initial OH reaction with trimethylamine results in the formation of *N,N*-dimethyl formamide. The other 60% of the initial OH reaction leads to the formation of the $(CH_3)_2N$ radical, which then, depending upon the NOx level, leads to *N*-nitroso and *N*-nitro dimethylamine formation. The major products in the OH-initiated photo-oxidation of trimethylamine are $CH_2{=}NCH_3$ (N-methylmethanimine) and $(CH_3)_2NCHO$ (*N,N*-dimethyl formamide). The atmospheric fate of *N*-methyl methanimine is uncertain. Most likely the lifetime will be very short and the compound will hydrolyze in aqueous particles to give CH_2O (formaldehyde) and CH_3NH_2 (methylamine). *N,N*-dimethyl formamide has an estimated atmospheric lifetime of more than 1 day and the major product of its reaction with OH radicals includes CH_3NCO (methylisocyanate) and $CH_2{=}NCH_3$. As methylisocyanate is a secondary product in the atmospheric photo-oxidation of dimethylamine it will be highly dispersed and it is not expected to reach any level of concern in the air masses. Methylisocyanate reacts very slowly with OH radicals and its major atmospheric fate is expected to be hydrolysis in aqueous particles forming CO and CH_3NH_2.

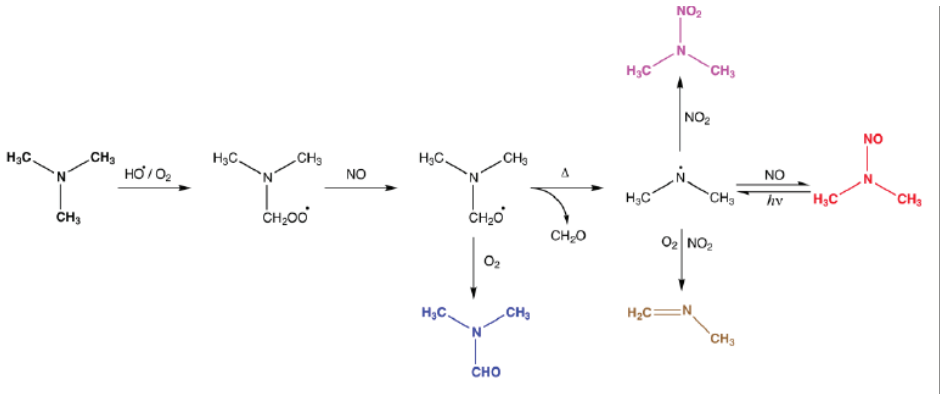

Scheme 1.7.3. Main routes of the atmospheric trimethylamine photo-oxidation (from Nielsen *et al.*, 2011

Diethylamine ($(CH_3CH_2)_2NH$)

Pitts *et al*., (1978) carried out a study of the products formed when a mixture of 500 ppb $(CH_3CH_2)_2NH$ + 80 ppb NO + 160 ppb NO_2 was subjected to natural sunlight conditions. They found the following molar conversion yields (taking into account the number of ethyl groups): 30% CH_3CHO (acetaldehyde), 4% $CH_3CO(OO)NO_2$ (PAN), 32% $(CH_3CH_2)_2NNO_2$ (diethylnitramine), 1.4% $(CH_3CH_2)_2NCHO$ (*N,N*-diethylformamide), 0.2% $(CH_3CH_2)_2NC(O)CH_3$ (*N,N*-diethylacetamide), and 2.4% $CH_3CH_2NC(O)CH_3$ (*N*-ethylacetamide) in the gas phase. In addition they found small amounts of CH_3CONH_2 (acetamide) in the aerosol phase.

Murphy *et al*., (2007) reported rapid particle formation during photo-oxidation experiments with $(CH_3CH_2)_2NH$ and, similar to the oxidation of CH_3NH_2, that the aerosol formed mainly is nitrate salt. Yields of non-salt organic aerosol were negligible. Price analyzed the aerosol formed in the $(CH_3CH_2)_2NH/O_3$/NOx oxidation experiments by HR-TOF-AMS (Price, 2010). The major ion peaks observed from the aerosol included the amine backbone m/z 30.034 (CH_4N+), m/z 44.050 (C_2H_6N+), m/z 58.066 (C_3H_8N+), m/z 86.099 ($C_5H_{12}N+$), and m/z 100.113 ($C_6H_{14}N+$). Higher mass oxidized fragments included m/z 191.084 ($C_6H_{11}N_2O_5+$).

Investigation by Price (2010) on the NO_3 radical initiated gas phase atmospheric oxidation of diethylamine, using PTR-MS detection method, he suggests the following interpretation of the major ion signals [MH]+:m/z 31, CH_2O (formaldehyde); m/z 45, CH_3CHO (acetaldehyde); m/z 47, HCOOH (formic acid and/or C_2H_5OH (ethanol); m/z 58, $CH_3CH_2NCH_2$ (ethyl methanimine); m/z 60, $(CH_3)_3N$ (trimethylamine) and/or CH_3CH_2NO (nitrosoethane); m/z 61, CH_3COOH (acetic acid) and/or $CH_3CH_2CH_2OH$ (propanol);m/z 72, $CH_3CH_2NCHCH_3$ (ethyl ethanimine); m/z 74, CH_3CH_2NHCHO (*N*-ethyl formamide); m/z 88, $CH_3CH_2NHCH_2CHO$ (*N*-ethyl acetamide); m/z 119, $(CH_3CH_2)_2NNO_2$ (*N*-nitro diethylamine).

The results from the recent study by Nielsen *et al*., (2011) employing the PTR-TOF-MS detection method show that, the major ion signals observed were m/z 74.0958 ($C_4H_{12}N+$, protonated diethylamine), m/z 72.0802 ($C_4H_{10}N+$, protonated ethylethanimine), m/z 45.0347 (C_2H_5O+, protonated acetaldehyde), m/z 119.0791 ($C_4H_{11}N_2O_2+$, protonated *N*-nitro diethylamine), m/z 31.0185 (CH_3O+, protonated formaldehyde) and m/z 88.0765

($C_4H_{10}NO+$, protonated *N*-ethyl acetamide). In addition, the m/z 103.0871 ($C_4H_{11}N_2O+$, protonated *N*-nitroso diethylamine) ion signal.

The initial H-abstraction by OH radicals may take place at three sites in diethylamine (>N-H, $–CH_2–$ and $–CH_3$), of which the methyl groups are expected tobe the least reactive. The diethylamine gas phase photo-oxidation is expected to follow the routes indicated in Scheme 1.7.4

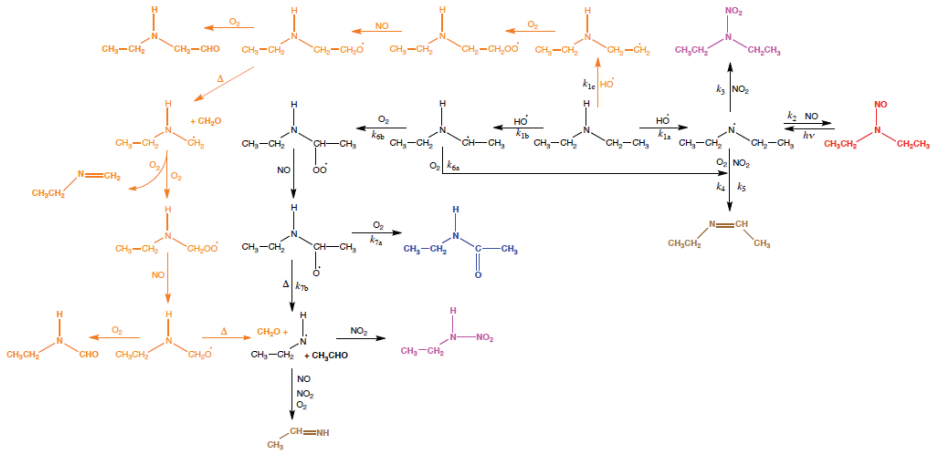

Scheme 1.7.4. Theoretical atmospheric photo-oxidation scheme for diethylamine. The orange coloured route is expected to be of less importance (from Nielsen *et al*., 2011).

2-(dimethylamino)-ethanol ($(CH_3)_2NCH_2CH_2OH$)

Harris and Pitts (1983) determined the rate constant for the reaction of OH radicals with 2-(dimethylamino)-ethanol (DMAE) to be $k_{OH} = (4.7 \pm 1.2) \times 10^{-11}$ cm^3 molecule^{-1} s^{-1} at 300 K by the flash photolysis-resonance fluorescence technique. In their experiments, OH radicals were produced by the pulsed vacuum ultraviolet photolysis of H_2O. Anderson and Stephens (1988) investigated the temperature dependence of the rate of the reaction over the temperature range 234 - 364 K by the same method and found that the reaction proceeds essentially with no temperature dependence. Their room temperature rate constant was $k_{OH} = (10.3 \pm 2.0) \times 10^{-11}$ cm^3 molecule^{-1} s^{-1}, and they suggested that a value of $k_{OH} = (9.0 \pm 2.0) \times 10^{-11}$ cm^3 molecule^{-1} s^{-1} will best describe the reaction over the entire temperature range. The two room temperature determinations, however, differ by a factor of 2. No explanation to this discrepancy is offered by the authors. Anderson and Stephens (1988) apportioned the reactivity of OH radicals with DMAE such that 55 % of

the H atom abstraction will occur from the methyl hydrogens, while about 35 % occurs from the methylene hydrogens next to the amine N. The remaining 10 % of the OH radical reactivity is expected to occur away from the amine N. They suggest the following main reactions to occur at atmospheric conditions:

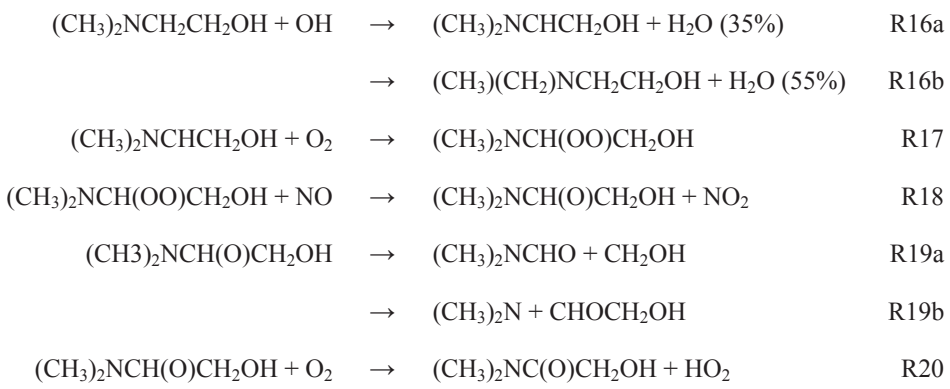

$(CH_3)_2NCH_2CH_2OH + OH$	→	$(CH_3)_2NCHCH_2OH + H_2O$ (35%)	R16a
	→	$(CH_3)(CH_2)NCH_2CH_2OH + H_2O$ (55%)	R16b
$(CH_3)_2NCHCH_2OH + O_2$	→	$(CH_3)_2NCH(OO)CH_2OH$	R17
$(CH_3)_2NCH(OO)CH_2OH + NO$	→	$(CH_3)_2NCH(O)CH_2OH + NO_2$	R18
$(CH3)_2NCH(O)CH_2OH$	→	$(CH_3)_2NCHO + CH_2OH$	R19a
	→	$(CH_3)_2N + CHOCH_2OH$	R19b
$(CH_3)_2NCH(O)CH_2OH + O_2$	→	$(CH_3)_2NC(O)CH_2OH + HO_2$	R20

The dimethyl amino radical formed in (R19b) will subsequently lead to the formation of dimethylnitrosamine and dimethylnitramine.

Tuazon *et al*., (1994) have determined the rate constant for reaction of DMAE with O_3 to be $k_{O3} = (6.76 \pm 0.83) \times 10^{-18}$ cm^3 molecule^{-1} s^{-1} at 298 K. They observed CH_2O in a yield of 30 - 45% and an unidentified amide, tentatively assigned to be $(CH_3)_2NC(O)CH_2OH$.

2-amino-2-methyl-1-propanol ($(CH_3)_2C(NH_2)CH_2OH$)

Harris and Pitts (1983) determined the rate constant for the reaction of OH radicals with 2-amino-2-methyl-1-propanol (AMP) to be $k_{OH} = (2.8 \pm 0.5) \times 10^{-11}$ cm^3 molecule^{-1} s^{-1} at 300 K by the flash photolysis-resonance fluorescence technique. OH radicals were produced by the pulsed vacuum ultraviolet photolysis of H_2O. The authors suggest that the AMP reaction with OH radicals most likely will proceed by H-abstraction from the primary amino group followed either by reaction with NO_2 to give the nitramine or, alternatively, by C-C bond scission:

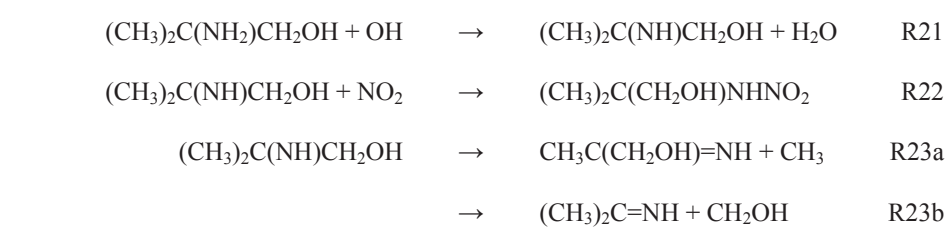

$(CH_3)_2C(NH_2)CH_2OH + OH$	→	$(CH_3)_2C(NH)CH_2OH + H_2O$	R21
$(CH_3)_2C(NH)CH_2OH + NO_2$	→	$(CH_3)_2C(CH_2OH)NHNO_2$	R22
$(CH_3)_2C(NH)CH_2OH$	→	$CH_3C(CH_2OH)=NH + CH_3$	R23a
	→	$(CH_3)_2C=NH + CH_2OH$	R23b

Bråten *et al*., (2008) derived theoretical schemes for the OH initiated photo-oxidation of AMP, Schemes 1.7.5 – 1.7.7.

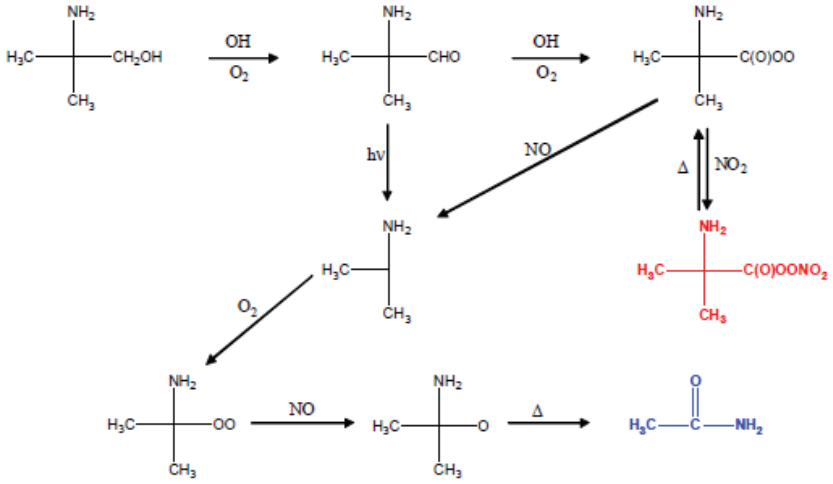

Scheme 1.7.5. The main atmospheric degradation routes of $(CH_3)_2C(NH_2)CH_2OH$ (AMP) following initial hydrogen abstraction from the CH_2-group. (From Bråten *et al*., 2008).

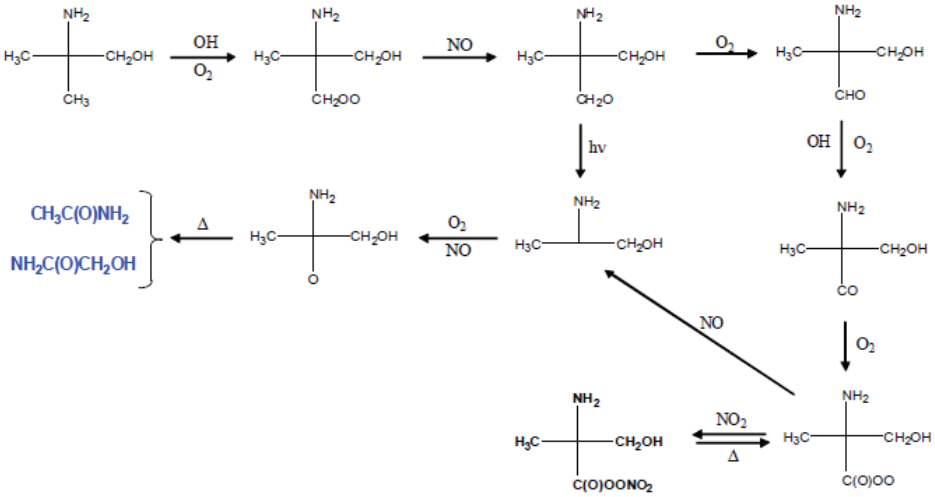

Scheme 1.7.6. The main atmospheric degradation routes of $(CH_3)_2C(NH_2)CH_2OH$ (AMP) following initial hydrogen abstraction from the CH_3-group (From Bråten *et al*., 2008).

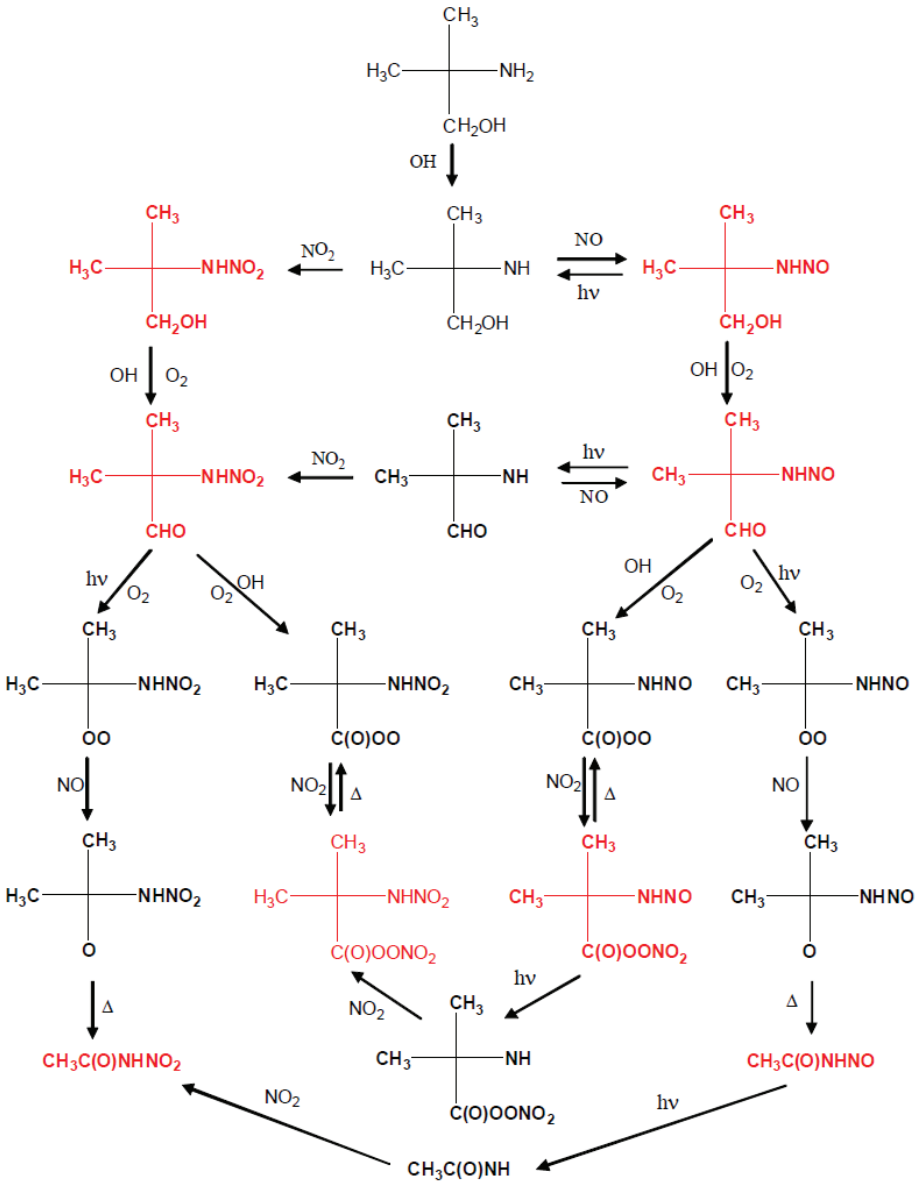

Scheme 1.7.7. The main atmospheric degradation routes of $(CH_3)_2C(NH_2)CH_2OH$ (AMP) following initial hydrogen abstraction from the NH_2-group. (From Bråten *et al*., 2008).

Monoethanolamine (MEA) ($NH_2CH_2CH_2OH$)

The results in the study by Nielsen *et al*., (2011) suggested that more than 80 % of the reaction between MEA and OH radicals takes place at $–CH_2–$, while less than 10 %

occurs at $–NH_2$ and at $–CH_2OH$, respectively. The major observed products (>80 %) in the photo-oxidation were formamide (NH_2CHO) and formaldehyde (CH_2O). Minor detected products (<10 %) were amino acetaldehyde (NH_2CH_2CHO) and 2-oxo acetamide ($NH_2C(O)CHO$). 2-nitroamino ethanol, $O_2NNHCH_2CH_2OH$, was confirmed as product in the experiments. In the same experiments it was observed, the photo-oxidation of MEA give rise to ozone and significant formation of particles. Aerosols were formed immediately after the exposure of the chamber to sunlight; simulations of the chamber experiments show that, depending on the initial conditions, between 20 and 50 % of MEA removal from the gas-phase is due to reaction with OH radicals, between 10 and 40 % is converted into particle mass (gas-to-particle conversion) during the photo-oxidation experiments, while the remaining 30 to 70 % of the initial MEA amount is lost to the walls or by dilution through replenishment flow. The theoretical photo-oxidation schemes from Bråthen *et al*., (2008) were also modified to concord with the experimental observations as shown in Schemes 1.7.8 – 1.7.9.

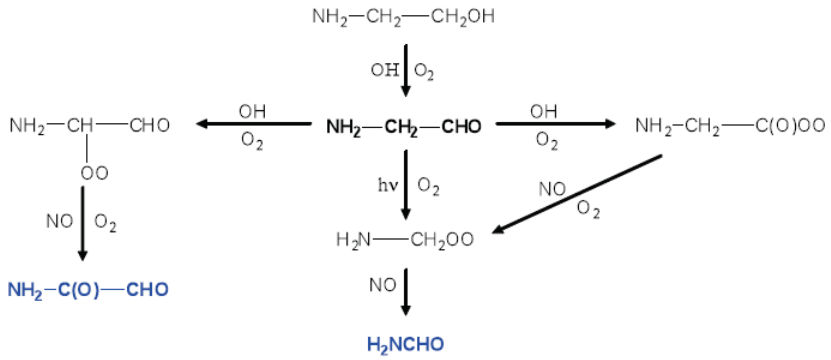

Scheme 1.7.8. Atmospheric photo-oxidation of MEA following hydrogen abstraction from the -CH_2OH group (from Nielsen *et al.*, 2011.).

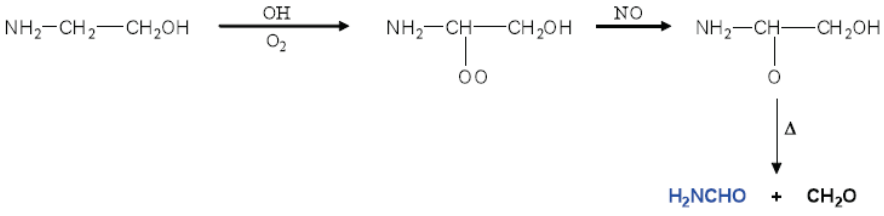

Scheme 1.7.9. Atmospheric photo-oxidation of MEA following hydrogen abstraction from the -CH_2- group (from Nielsen *et al.*, 2011).

Table 1.7.1. Summary of experimental rate constants at 296 – 300 K (/cm^{3}molecule^{-1}s^{-1}) for the reactions of OH and O_3 with amines

Compound	k_{OH}	Reference	k_{O3}	Reference
CH_3NH_2	$(2.20 \pm 0.22) \times 10^{-11}$	Atkinson *et al.*, 1977	$(7.4 \pm 2.4) \times 10^{-21}$	Tuazon *et al.*, 1994
	$(1.73 \pm 0.11) \times 10^{-11}$	Carl and Crowley, 1998		
$(CH_3)_2NH$	$(6.54 \pm 0.66) \times 10^{-11}$	Atkinson *et al.*, 1978	$(1.67 \pm 0.20) \times 10^{-18}$	Tuazon *et al.*, 1994
	$(6.49 \pm 0.64) \times 10^{-11}$	Carl and Crowley, 1998		
$(CH_3)_3N$	$(6.09 \pm 0.61) \times 10^{-11}$	Atkinson *et al.*, 1978	$(7.84 \pm 0.87) \times 10^{-18}$	Tuazon *et al.*, 1994
	$(3.58 \pm 0.22) \times 10^{-11}$	Carl and Crowley, 1998		
$(CH_3CH_2)_2NOH$	1.0×10^{-10}	Gorse *et al.*, 1977		
$(CH_3)_2NCH_2CH_2OH$	$(4.7 \pm 1.2) \times 10^{-11}$	Harris and Pitts, 1983	$(6.76 \pm 0.83) \times 10^{-18}$	Tuazon *et al.*, 1994
	$(9.0 \pm 2.0) \times 10^{-11}$	Anderson and Stephens, (1988)		
$(CH_3)_2C(NH_2)CH_2OH$	$(2.8 \pm 0.5) \times 10^{-11}$	Harris and Pitts, 1983		

1.8 Products from atmospheric degradation of amines

The main products of the atmospheric degradation of amines include a number of nitramines and nitrosamines as well as different amides, imines and aldehydes. During the day time, the atmospheric degradation of amines is dominated by the reaction with the OH radicals while the chlorine atoms play a role at the marine boundary layer. Reaction with O_3 and NO_3 could play a role in the amine oxidation during night time. Here below, a summary to each group of these compounds resulting from the degradation of amines in the atmosphere is presented.

1.8.1 Nitramines

Atmospheric nitramines are formed by photo-oxidation of amines (Lindley e*t al.*, 1979 and Pitts *et al.*, 1978). The nitrating agent NO_2 is the component of NOx of the flue gas or may be present in the ambient atmosphere from various combustion sources as well as chemical reactions taking place in the atmosphere. Nitramines can also be oxidation products of nitrosamines. Photolysis can also be a pathway of nitramine formation from nitrosamine, for instance dimethylnitramine can be formed through photolysis of dimethylnitrosamine (Pitts *et al.*, 1978).

With regard to mutagenic and carcinogenic effects, the activity of aliphatic *N*-nitramines seem in general to be much lower than those of the corresponding nitrosamines (Låg *et al.,* 2008) but the nitramines are more stable than the nitrosamines and thus the potential for exposure is likely to be higher (Låg *et al.,* 2011).

A number of aliphatic *N*-nitramines or their metabolites have been found to be mutagenic in bacterial assays (Khudoley *et al.,* 1981, Frei *et al.,* 1984; Suzuki *et al.,* 1985). Furthermore, *N*-nitromethylamine and *N*-nitroethylamine, but not *N*-nitrodimethylamine have shown to induce DNA single strand breaks in primary rat hepatocytes *in vitro* (Frei *et al.,* 1986).

Several studies have shown that, some of the nitramines are indeed carcinogenic to rats (Goodall and Kennedy, 1976; Mirvish *et al.,* 1980, Hassel *et al.,* 1987, Scherf *et al.,* 1989). Both the nitrosamine metabolite and formaldehyde are among the metabolites proposed as possible mediators of the carcinogenic effect of *N*-nitrodimethylamine, but the mechanism of *N*-nitramine carcinogenicity is still unclear (Låg *et al.,* 2011).

A lifetime study of mice and rats with *N*-nitrodimethylamine using drinking water revealed that, tumours were induced predominantly in the liver and kidney (Goodall and Kennedy, 1976). A number of rats (10 males and 10 females) were exposed to approximately 5 mg/kg bw/day via the drinking water from 35 days of age, for one year, and thereafter given drinking water only (total dose, 1.83 g/kg bw). Mice (10 males and 10 females) were exposed by repeated subcutaneous injection from birth to 7 months of age followed by administration in drinking water. Liver tumours (hepatocellular carcinomas) were observed in 85% of the rats. Mice developed predominantly hepatocellular carcinomas and renal adenocarcinomas. Statistically significant increases of other tumour types also occurred in mice. The morphology of the liver tumours after *N*-nitrodimethylamine treatment was said to contrast with that often described after treatment with the nitrosamine, NDMA (Goodall and Kennedy, 1976) suggesting that the nitramine carcinogenicity is not solely mediated through formation of the nitroso metabolite. In general less attention has been paid to nitramines and hence little information is available to this group of compounds.

1.8.2 Nitrosamines

As nitramines, nitrosamines are in a group of carcinogenic compounds (Tuazon *et al.*, 1984, Lin, 1990), the latter being more potent than the other (Padhye *et al.,* 2011, Bartsch and Montesano, 1984). It has been well documented that nitrosamines are formed through the reaction of nitric oxide (NO) with, secondary or tertiary amines. (Itoh *et al.*, 1999, Lin, 1990, Neurath *et al.,* 1977, Grosjean, 1991, Sun *et al.*, 2005). Furthermore, it is well established from condensed phase chemistry that secondary amines readily form stable nitrosamines, and that nitrosamines from primary aliphatic amines are very unstable (Challis and Challis, 1982). This has led to the general assumption that primary aliphatic amines do not form nitrosamines (Pitts *et al.*, 1978). However, recent research by Fostås *et al.,* (2011) has revealed that, primary amines can undergo degradation to secondary amines leading to the formation of stable nitrosamines.

Douglass *et al.,* (1978) reported that, *N*-nitroso compounds are formed by the interaction of a nitrogen-containing organic compound such as an amine, amide, urea, guanidine, urethane or cyanamide and a nitrosating agent, such as a nitrogen oxide. Nitrosamines are found in a number of environments for instance as contaminants in malt beverages and foods treated with nitrites, in manufacture of rubber, in cigarette smoke and in treated wastewater (Zhao *et al.*, 2007) as well as in cosmetics industries (Stefan and Bolton, 2002). Rounbehler *et al.,* (1979) detected a number of nitrosamines in the 1979 model new motorcars. Nitrosamines, particularly the tobacco-specific nitrosamines 4-(methylnitrosamino)-1-(3-pyridyl)-1-butanone (NNK) and *N*-nitrosonornicotine (NNN), are by far the most prevalent strong carcinogens in unburned tobacco (Boffetta *et al.,* 1997). The principal nitrosamines which have been detected in food are *N*-nitrosodimethylamine (NDMA), *N*-nitrosodiethylamine (NDEN) and *N*-nitoropyrrolidine (Lin, 1990). Nitrite in food is the most important precursor of the ultimate nitrosating agent (Lin, 1990). Nitrate is also present in significant amount in food, especially vegetables (Lin *et al.,* 1980) and can undergo reduction to nitrite through microbial enzymes thus it has to be considered as a nitrosating agent precursor (Lin, 1990). Nitrosamines have been detected in ambient air in Germany near a factory producing secondary amines and in the United States around industries which used dimethylamines and *N*-nitrosodimethylamine in organic synthesis (Tuazon *et al.*, 1984).

In the dark, *N*-nitrosodimethylamine (NDMA) formation has been shown to occur by the reaction of dimethylamine with nitrous acid (HNO_2) or nitrogen oxides (NOx). In the

presence of sunlight, NDMA exists in a redox equilibrium with the oxidized species, the corresponding dimethylnitramine $(CH_3)_2N\text{-}NO_2$,) (Mezyk, 2006)

$(CH_3)_2N\text{-}NO \underset{\text{redox}}{\rightleftharpoons} (CH_3)_2N\text{-}NO_2$ R24

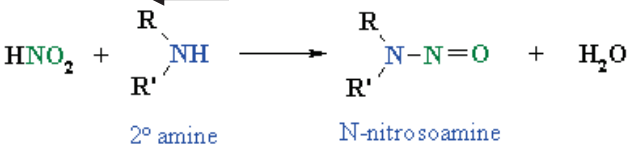

.....R25

Scheme 1.8.2.1. Reaction of nitrous acid and a secondary amine. (Adapted from: Francis A. Carey, Organic Chemistry, fourth edition, *McGraw-Hill* (2001)

1.8.3 Amides

Amides make up a large class of nitrogen containing volatile organic compounds (NVOCs) that may be found as atmospheric contaminants (El-Diba and Chakiri, 2005). They are produced on a large scale and used extensively, for example as organic solvents in the manufacture of pharmaceuticals, pesticides, fibers and adhesives (Carter, 1994, El-Diba and Chakiri, 2005, Finlayson-Pitts and Pitss Jr., 2000). Industrial uses of amides result in emissions of the compounds to the atmosphere during their commercial production, processing, storage and disposal where they can be oxidised through different chemical processes. In addition, amides are also formed in situ in the atmosphere as intermediate products in the degradation of alkylamines (Carter, 1994 Finlayson-Pitts and Pitss Jr., 2000, Tuazon *et al.*, 1994, Schade and Crutzen, 1995). Various sources of amines in the atmosphere have been stated in section 1.6. Amides have been detected in air and water (US EPA, 1986, Raja *et al.*, 2009) and also in fine particles where wood burning and cooking are the main sources (Rogge *et al.*, 1991, Cheng *et al.*, 2006).

Potential degradation processes of amides in the atmosphere include photolysis and chemical reactions with OH and NO_3 radicals and O_3 (Schade and Crutzen, 1995, Crutzen, 1983, Atkinson and Arey, 2003). Recent studies have shown that reaction with Cl atoms, which were previously only considered to be of potential importance in the marine troposphere in the early morning hours and also in heavily industrialized urban areas, may now be ubiquitous and quite significant in continental inland regions (Spicer, 1998, Thornton *et al.*, 2010).

The gas phase UV absorption cross-sections have been determined for a series of amides: *N,N*-dimethyl formamide, *N,N*-dimethyl acetamide, *N,N*-dimethyl propionamide and 1-

methyl-2-pyrrolidone (Chakir *et al.*, 2005). The spectra are structureless and show low absorption cross-sections beyond 270 nm. Consequently, tropospheric photolysis of amides will not be an important loss process.

Table 1.8.3.1. Amides reported as products in the gas phase photo-oxidation experiments of dimethylamine and trimethylamine

Parent amine	Oxidant	Amides reported		Reference
		Gas phase	Aerosol	
$(CH_3)_2NH$	OH	CH_3NHCHO		Pitts *et al.*, 1978
$(CH_3)_2NH$	O_3	CH_3NHCHO		Tuazon *et al.*, 1994
$(CH_3)_3N$	OH	$(CH_3)_2NCHO$	$CHONH_2$	Pitts *et al.*, 1978
			$CH_3N(CHO)_2$	
$(CH_3)_3N$	O_3	$(CH_3)_2NCHO$		Tuazon *et al.*, 1994
$(CH_3)_3N$	O_3/NO	$(CH_3)_2NCHO$		Erupe *et al.*, 2008
		$CH_3N(CHO)_2$		
		$CH_2OH(CH3)NCHO$		
		$(CHO)_3N$		

Koch *et al.*, (1997) studied four amides with the aim of testing/extending a commonly used Structure Activity Relationship (SAR) developed by Atkinson (1986) for prediction of OH reaction rate constants with different group of compounds. The reactions were found to show negative Arrhenius temperature dependencies and conflicted with the SAR predictions. Solignac *et al.*, (2005) studied the OH and Cl reaction kinetics of three amides and the results were not in agreement with the SAR predictions thereby supporting the findings by Koch *et al.,* (1997).

The rection kinetics of NO_3 radical with amides have been reported. Aschmann and Atkinson (1999) studied the reactions of 1-methyl-2-pyrolidone at 296 K, El Dib and Chakir (2007) studied the temperature dependence of the NO_3 reaction with 4 amides. The kinetic results relevant to the present study are summarized in Table 1.8.3.2.

Table 1.8.3.2. Rate constants at 298 - 300 K (/cm^3 molecule^{-1} s^{-1}) and activation energies (/K) for the reaction of OH radicals with selected amides

Compound	$k_{OH}/10^{-11}$	E_a/R	$k_{Cl}/10^{-11}$	$k_{NO3}/10^{-14}$	E_a/R
NH_2CHO	≈ 0.4[a]		4.5 ± 0.5[a]	< 1[a]	
CH_3NHCHO	0.86 ± 0.24[b]		9.7 ± 1.7[c]		
$(CH_3)_2NCHO$	1.4 ± 0.3[b]		19 ± 3[b]	4.5 ± 1.1[c]	1600 ± 300[c]

[a]From Barnes *et al*., (2010). [b]From Solignac *et al*., (2005). [c]From El Dib and Chakir (2007)

The amide-OH reactions are relatively fast, and the *average global lifetimes* of amides with respect to reaction with OH radicals will be of the order of a few days. Although the reactions of amides with Cl atoms are faster than the corresponding OH reactions, the average global atmospheric concentration of OH radicals is so much higher than that of Cl atoms hence the atmospheric amide loss is dominated by OH reactions.

Barnes *et al.*, (2010) have recently presented the products resulting from the photo-oxidation studies of three amide; NH_2CHO, CH_3NHCHO, and $(CH_3)_2NCHO$. Scheme 1.9.3.1 shows a summary of their findings.

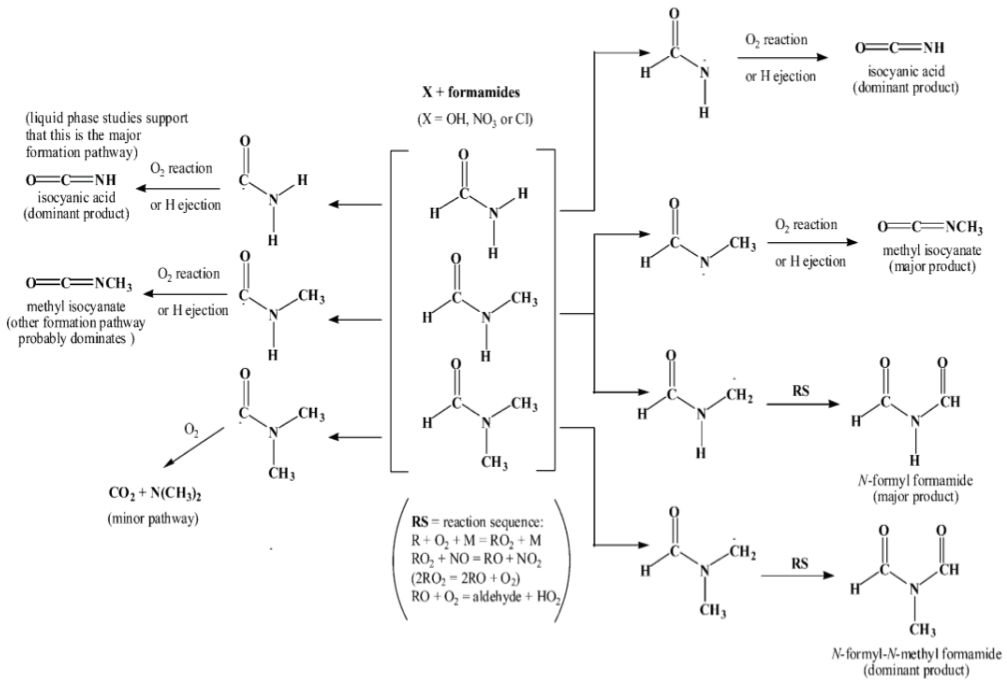

Scheme 1.8.3.1. Simplified overall reaction mechanism for the main abstraction pathways involved in the oxidation of formamide and its *N*-methylated derivates by atmospheric oxidants X, X = OH, NO_3 or Cl atoms. (Adapted from Barnes *et al.,* (2010).

1.8.4 Imines

Imines, $R_1N=CR_2R_3$, are reported as major products in amine gas phase photo-oxidation experiments. There are no experimental data available for the gas phase reactions of imines. Imines are, however, known to hydrolyse in aqueous solution resulting in amines and carbonyl compounds (Patai, 1970). Imine hydrolysis is also expected to occur on surfaces.

$R_1N=CR_2R_3 + H_2O$ (*het., l*) → $R_1NH_2 + R_2R_3CO$ R26

There is a single study of the electronic spectrum of $CH_2=NH$ in the region 235 to 260 nm showing a broad and structureless absorption with maximum near 250 nm (Teslja *et al.*, 2004). There is no information concerning the spectrum in the region of relevance to tropospheric chemistry ($\lambda > 300$ nm). It is possible, however, that the absorption band stretches into this region such that photolysis may occur in the troposphere in which case the products will be HCN and H_2 (Teslja *et al.*, 2004, Nguyen *et al.*, 1996).

Heterogeneous condensation reactions between imines and amines have been reported (Layer, 1963), *e.g.* methanimine, $CH_2=NH$, may react with methanamine, CH_3NH_2 to give methyl methanimine and ammonia:

$CH_2=NH + CH_3NH_2$ (*het.*) → $CH_2=NCH_3 + NH_3$ R27

1.8.5 Isocyanic acid and methyl isocyanate

Isocyanic acid, HNCO and methyl isocyanate, CH_3NCO, are reported as major products in amide gas phase photo-oxidation. The reaction of isocyanic acid with OH radicals was studied by Tully *et al.,* (1989) in the 624 – 875 K range and later by Glarborg *et al.*, (1994) in the 1025 – 1425 K range, and by Woolridge *et al.,* (1996) in the 620 – 1860 K range. The latter authors summarised the available experimental results to give $k_{OH}(T) = 6.03 \times 10^{-17} \times T^{1.50} \exp(-1809/T)$, from which one may extrapolate $k_{OH} \approx 7 \times 10^{-16}$ cm^3 molecule^{-1} s^{-1} at 298 K. Assuming an average global OH concentration of 10^6 cm^{-3} implies $\tau_{OH} \approx 45$ years. Isocyanic acid and aliphatic isocyanates show continuous absorption with long wavelength limits at 224, 255 and 248 nm for isocyanic acid, methylisocyanate and ethylisocyanate respectively (Woo and Liu, 1935). The dominant atmospheric loss process of HNCO will therefore be wet and dry deposition. In the aqueous phase HNCO hydrolyse to form ammonia (Nielsen *et al.*, 2011):-

$HNCO + H_2O$ (aq.) → $CO_2 + NH_3$ R28

There are no kinetic data available for methyl isocyanate. To a first approximation one may assume that the OH rate constant for reaction with CH_3NCO is of the same order of magnitude as that of CH_3CN, that is $k_{OH} \approx 2 \times 10^{-14}$ cm^3 molecule^{-1} s^{-1} at 298 K (Atkinson *et al.,* 2006). The estimated atmospheric lifetime with respect to the reaction with hydroxyl radical, $\tau_{OH} \approx 1.5$ years is too long thereby making wet and dry deposition to be the dominant atmospheric loss process for methyl isocyanate. In the aqueous phase CH_3NCO hydrolyse to form methylamine:

$$CH_3NCO + H_2O\ (aq.) \rightarrow \quad CO_2 + CH_3NH_2 \qquad \text{R29}$$

1.9 Fates of nitrosamines and nitramines in the atmosphere

The main loss pathway of nitrosamines in the atmosphere is through photolysis. Nitrosamines are unstable compounds in the presence of sunlight hence they undergo photolysis so rapidily. Jahan *et al.,* (2008) reported a rapid degradation of *N*-nitrosodimethylamine (NDMA) within half an hour after exposing it to UV light. Another rapid photodecomposition of NDMA at a rate of 3.3×10^{-3} s^{-1} with a half-life of 5 minutes in the atmosphere was reported by Tuazon *et al.,* (1984). Reactions of nitrosamines with OH can go up to 3 days (Tuazon *et al.,* 1984).

Apart from Tuazon *et al.,* (1984), the gas phase photolysis of *N*-nitrosodimethylamine (NDMA) has been studied by Bamford (1939), Lindley and Calvert (1979). Stefan and Bolton (2002) reported the photolysis of NDMA in aqueous solutions at pH = 3 and 7 and found CH_3NH_2, HCHO, HCOOH, N_2O, $(CH_3)_2NH$ and $CH_2{=}NCH_3$ as products. Tuazon *et al*., (1984) determined the photolysis rate of NDMA relative to that of NO_2 to be $j_{NDMA} / j_{NO2} = 0.53 \pm 0.03$. That is, gas phase photolysis of NDMA (and presumably also of other nitrosamines) is extremely fast with a lifetime of only minutes. The fast photolysis corresponds to a quantum yield of ~1 at wavelengths ≥290 nm, in agreement with the value of 1.03 ± 0.10 determined by Geiger and Huber (1981) at 363.5 nm. There is a single high-resolution UV spectrum of the $S_1 \leftarrow S_0$ band in NDMA (Dubs *et al.,* 1986). It exhibits a progression of diffuse subbands which are attributed to different excitations of the NO-stretching vibration in the excited electronic state.

The aqueous phase photolysis of various *N*-nitrosamines including product formation and lifetimes have been reported (Saunder and Mosier, 1980, Plumlee and Reinhard, 2007, Xu *et al.,* 2008).

Nitramines do not photolyze and are expected to accumulate in the atmosphere (Grosjean, 1991). Their reaction with OH radical can be achieved in two days (Tuazon *et al.*, 1984). Figures 1.9.1 and 1.9.2 show the UV-Vis specra for *N*-nitroso dimethylamine and *N*-nitro dimethylamine respectively. In Figure 1.9.2 it can be seen that nitramines do not absorb light in the actinic region (λ >290 nm), that is why they are not photolized in the troposphere.

In summary, the generic atmospheric reactions destroying *N*-nitroso and *N*-nitro amines are as given below:

$RR'NNO + OH \rightarrow$ Products (slow) R30

$RR'NNO + h\nu \rightarrow RR'N + NO$ (fast) R31

$RR'NNO_2 + OH \rightarrow$ Products (slow) R32

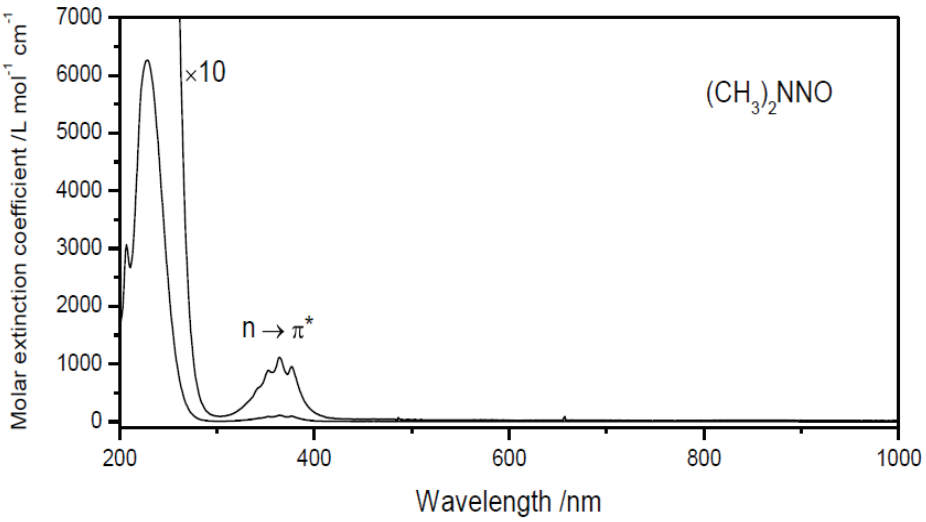

Figure 1.9.1. UV-VIS molar extinction (L mol^{-1} cm^{-1}) of *N*-nitroso dimethylamine.

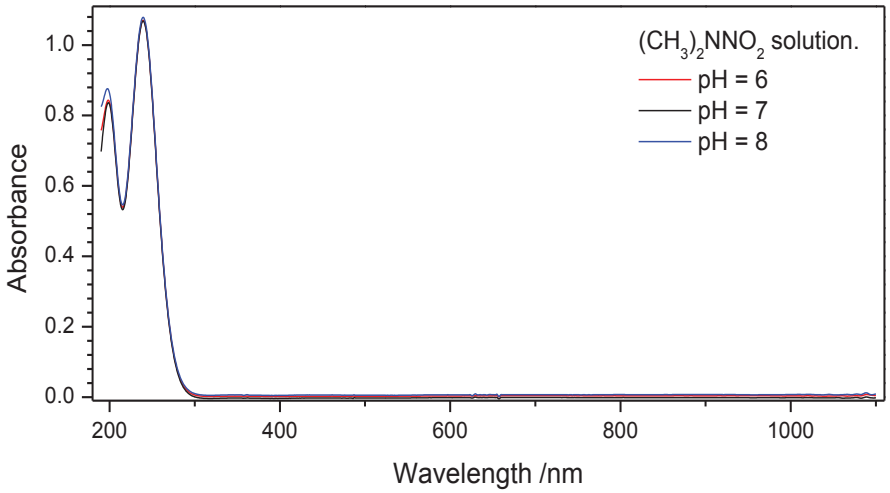

Figure 1.9.2. UV-VIS absorption spectrum of dimethylnitramine in solution.

1.10 General summary

CO_2 emissions from large scale industrial sources represent a considerable share of all anthropogenic greenhouse gases (GHG) leading to global warming and hence climate change. The warming effect of long-living GHG is partially offset by short-lived aerosols that are a by-product of fossil fuel and biomass combustion.

Carbon Capture and Storage (CCS) is one way to mitigate climate change, and one of the more mature post combustion CO_2 capture technologies is based on amine absorbents. Given the scale of implementation of post-combustion CCS, it is likely that there will be relatively small but still significant discharges of amines to the atmosphere during operation. This small amount of amines may therefore always be present in the cleaned flue gas, no matter which parent amine is used in the absorber.

The amines by themselves are not very harmful at typical ambient concentrations. However, during the course of amine emission and atmospheric transport, amine conversion and degradation reactions will take place as the emission plume dilutes. These conversion and degradation reactions will take place in both the gas phase and the atmospheric aqueous phase, which includes water-containing aerosol particles and cloud- as well as rain- and fog-droplets. Amine degradation reactions can lead to the formation of potentially carcinogenic substances such as nitrosamines and nitramines in both the gas phase and the aqueous phase. Other products from the atmospheric degradadation of amines includes amides and imines.

2 CHEMICAL KINETICS

Reaction kinetics simply refers to the measurements of rates of reactions (Pilling and Seakins, 1995). It is critical to understand the kinetics of reactions of various species in the atmosphere in order to assess their atmospheric fates (Finlayson-Pitts and Pitts Jr., 2000). In addition, it greatly simplifies the number of reactions that must be considered in assessing the atmospheric fates of a particular compound of interest. In the case of organics for example, there are in principle many potential reactions that could occur in the atmosphere. Given the thousands of organics found in air, the total number of reactions that must be considered quickly becomes intractable unless there is some means to pare the list down (Finlayson-Pitts and Pitts Jr., 2000). Knowing the kinetics of reaction of various classes of compounds with OH, O_3 and other atmospheric oxidants it becomes easier to estimate lifetimes under typical atmospheric conditions and hence to rule out those reactions that are too slow to be significant, allowing one to concentrate on the most important reactions.

2.1 Fundamental principles of gas phase kinetics

There are two types of reactions namely elementary and overall reactions. *Elementary* reactions are those that cannot be broken down into two or more simpler reactions while *Overall* reactions include two or more elementary reactions. Due to low temperatures and densities in the atmosphere, most of the atmospheric interactions are described in terms of elementary reactions (Brasseur *et al.,* 1999).

Generally, there are two types elementary reactions namely unimolecular and bimolecular reactions (processes). When a molecule or ion decomposes by itself, such an elementary step is called a unimolecular step (or process). A unimolecular step is always a first order reaction. A bimolecular process involves two reacting molecules or ions and the rates for these steps are second order.

However, there exist a number of important gas-phase processes in which three different species participate, and are termed as termolecular reactions. In the troposphere, termolecular reactions normally involve N_2 and/ or O_2 as a third body often designated as "M" whose role is generally to take up the excess energy and stabilize the reaction product(s) (Finlayson-Pitts and Pitts Jr., 2000, Wayne, 2000). Examples of these three categories of reactions are given below:

Unimolecular reaction: Thermal decomposition of ozone

$$O_3 \rightarrow O_2 + O \qquad \text{R33}$$

Bimolecular reaction: Formation of the gaseous nitrate radical

$$O_3{+}NO_2 \rightarrow NO_3 + O_2 \qquad \text{R34}$$

Termolecular reaction: The formation of ozone by reaction of a ground-state oxygen atom, $O(^3P)$, with O_2;

$$O(^3P) + O_2{+} M \rightarrow O_3 + M \qquad \text{R35}$$

The rates of reactions in this study were achieved through the use of a relative rate method. The merit of relative rate method over other techniques for determining reaction rate constants for bimolecular reactions is that there is no need for absolute concentration measurements. How ever, the method makes use of FTIR which has some pitfalls such as overlapping of bands that makes it difficult to extract precise relative concentrations. An example of the spectra with overlapping bands is the photooxidation of ethylnitramine as shown in figure 2.1.1 below.

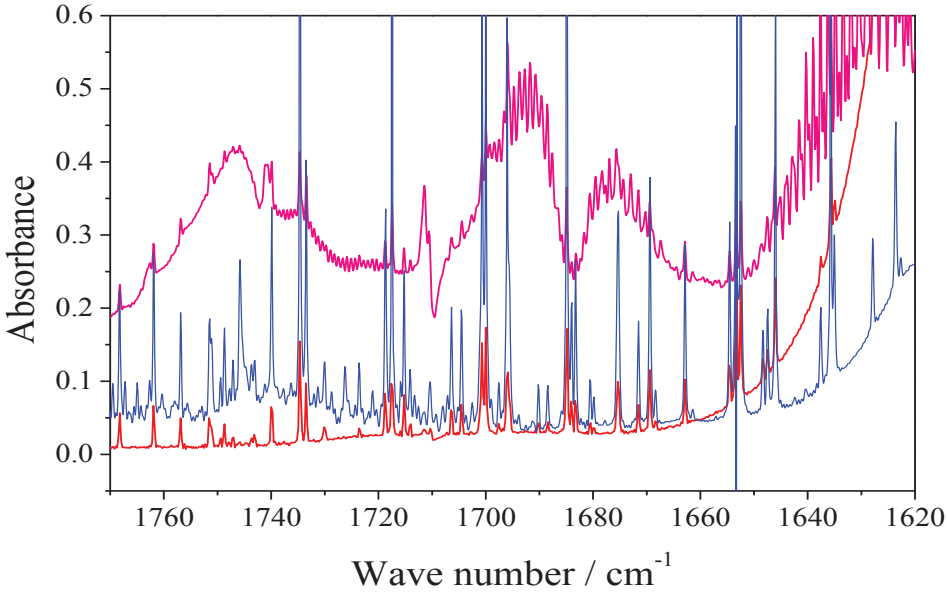

Figure 2.1.1. $CH_3CH_2NNO_2$ spectrum (Red), $CH_3CH_2NNO_2$ + OH after 45 minutes of photolysis (blue), $CH_3CH_2NNO_2$ + Cl after 74 minutes of photolysis (pink).

2.2 Rate laws, reaction orders and the rate constants for elementary reactions

The rate of reaction is defined as the change in the concentration of a reactant or product with time. For simple reactions occurring with unit stoichiometry, the rate expressed in terms of reactant disappearance is the same as the rate in terms of product formation.

Unimolecular reaction steps

The elementary reaction step,

$$A \xrightarrow{k_1} B \qquad \text{Eqn.1}$$

is unimolecular due to the fact that there is only one molecule (i.e molecule "A") reacting. The rate law for this unimolecular reaction step is given by:-

$$\frac{d[B]}{dt} = k_1[A] \qquad \text{Eqn.2}$$

or, equivalently

$$\frac{d[A]}{dt} = -k_1[A] \qquad \text{Eqn.3}$$

Rearrangement of this equation yields

$$\frac{d[A]}{[A]} = -k_1 dt$$

Let [A(0)] be the initial concentration A and let [A(t)] be the concentration at time t. Then integration of this equation yields

$$\int_{[A(0)]}^{[A(t)]} \frac{d[A]}{[A]} = -\int_0^t k_1 dt \qquad \text{Eqn. 4}$$

$$\ln \frac{[A(t)]}{[A(0)]} = -k_1 t$$

Exponentiating both sides of the equation we obtain,

$$[A(t)] = [A(0)]\exp(-k_1 t) \qquad \text{Eqn.5}$$

These elementary reaction steps indicate that the molecule A, spontaneously transforms into B at some rate k_1. The algebraic sign in front of k_1 tells whether there is gaining of the product or losing the reactant depending on whether the concentration in the

derivative is increasing or decreasing. For example, in Equation 2, [B] is increasing and in Equation 3, [A] is decreasing.

An elementary reaction step may be reversible or irreversible. Equation 1 is an irreversible unimolecular step. An example of a reversible unimolecular step is given in equation 6 below:

$$A \underset{k_{-1}}{\overset{k_1}{\rightleftharpoons}} B \qquad \text{Eqn.6}$$

This reversible unimolecular step implies the following rate laws,

$$\frac{d[B]}{dt} = +k_1[A] - k_2[B] \qquad \text{Eqn.7}$$

and/or

$$\frac{d[A]}{dt} = -k_1[A] + k_2[B] \qquad \text{Eqn.8}$$

Either one of these two equations may be used, depending on whether we are trying to account for the disappearance of reactant A or the appearance of product B in the mechanism for a particular reaction.

A unimolecular reaction step can have more than one product, for example,

$$A \xrightarrow{k_1} B + C \qquad \text{Eqn.9}$$

The unimolecular process given by equation 7 implies the same rate law as the reaction in equation 1 that is either equation 2 or equation 3.

Bimolecular reaction steps

There are several varieties of bimolecular steps. For example,

$$A + B \xrightarrow{k_2} C \qquad \text{Eqn.10}$$

implies the rate law,

$$\frac{d[C]}{dt} = +k_2[A][B] \qquad \text{Eqn.11}$$

or

$$\frac{d[A]}{dt} = -k_2[A][B] \qquad \text{Eqn.12}$$

and so on. In equation 10 only one product "C." is given. We would get the same rate laws if there had been two or more products as shown in the example below:-

$$A + B \xrightarrow{k_2} C + D \qquad \text{Eqn.13}$$

k is the *rate constant* defined as the constant of proportionality in the expression relating the rate of a reaction to the concentration of reactants and / or products, each expressed with the appropriate exponent while the *order* of a reaction is the sum of the exponents in the rate law.

Termolecular reactions involve three species

$$A + B + M \rightarrow C + D + M \qquad \text{Eqn.14}$$

Where M denotes a third body which does not enter into the reaction chemically, rather it takes out the excess energy so as to avoid the intermediate product(s) to disintegrate back to the reactants.

For a general reaction between two species where the stoichiometry parameters are not unit, i.e

$$\alpha A + \beta B \xrightarrow{k_2} C \qquad \text{Eqn.15}$$

The rate of reaction can be written in the form:-

$$\frac{d[C]}{dt} = +k_2[A]^{\alpha}[B]^{\beta} \qquad \text{Eqn.16}$$

In equation 15, the coefficient α and β are called partial orders of the reaction. The sum of α and β gives the overall reaction order. Usually the concentrations of atmospheric species are given in molecules/radicals cm^{-3} and the time in seconds, hence the reaction rates are presented in molecules cm^{-3} s^{-1}. Depending to the reaction order, the units for the rate constant can be expressed as s^{-1} for first order reactions; cm^3 $molecule^{-1}$ s^{-1} for a second order reaction and cm^6 $molecule^{-1}$ s^{-1} for a third order reaction. Concentrations of atmospheric gases are also commonly given in parts per million by volume (ppmv) with an assumption that, the atmosphere is a perfect gas for instance at standard temperature and pressure (STP). Ppmv can be easily converted to molecules cm^{-3} s^{-1} by multiplying it with 2.46×10^{13} (Finlayson-Pitts and Pitts Jr., 2000).

The lifetime (τ) of a chemical in the atmosphere is defined as the time taken for its concentration to fall to 1/e where e is the base of natural logarithms, 2.718 where as the half life ($t_{1/2}$) is the time required for the concentration of the reactant to fall to one-half of its initial value (Houston, 2001). Both the half-life and lifetime have a direct relationship with the rate constant and with the concentrations of any other reactant involved in the reactions. These relationships are summarized in Table 2.2.1 below for first-, second- and third order reactions (Finlayson-Pitts and Pitts Jr., 2000).

Table 2.2.1. Relationships between the rate constant, half-lives, and lifetimes for first-, second-, and third-order reactions

Reaction order	Reaction	Half-life of A	Lifetime of A
First	$A \xrightarrow{k_1} \text{Products}$	$t_{1/2}^{A} = 0.693 / k_1$	$\tau^{A} = 1 / k_1$
Second	$A + B \xrightarrow{k_2} \text{Products}$	$t_{1/2}^{A} = 0.693 / k_1[\text{B}]$	$\tau^{A} = 1 / k_2[\text{B}]$
Third	$A + B + C \xrightarrow{k_3} \text{Products}$	$t_{1/2}^{A} = 0.693 / k_1$	$\tau^{A} = 1 / k_3[B][C]$

The prime oxidizing agents in the troposphere are OH, O_3, NO_3 and Cl atoms. But NO_3 photolyses rapidily during the day owing to the fact that, it absorbs strongly in the visible region, thus its contribution is observed only at night. The hydroperoxyl radical (HO_2) also reacts readily with aldehydes but does not significantly impact tropospheric chemistry due to a rapid reverse reaction. It is, of course, responsible for converting NO to NO_2, ultimately leading to the production of O_3, as well as a whole host of compounds included under the umbrella of NOy. The HO_2 + NO reaction also generates OH, so understanding the sources of HO_2 is important in understanding sources of OH. The contribution from chlorine is mainly situated at the marine environment, a place where it is found in higher concentrations. OH is formed through photolytic processes thus its contribution is mainly observed during day time Typical average concentration of OH radicals is 10^6 radical cm^{-3} while that of NO_3 is 10^9 radicals cm^{-3} (Finlayson-Pitts and Pitts Jr., 2000). Concentrations of ozone and chlorines vary so there are no established average concentrations for these oxidants.

2.3 Pseudo-first order reaction conditions

In a second order reaction, it is possible to adjust the experimental conditions through making the reaction appear to be first order in one of the reactants and zero order (keep

the concentrations constant) in the other. Here the time dependence of the first order reaction can then be easily studied. Referring back to the reaction

$$A + B \xrightarrow{k} \text{Products}$$

Its differential rate law is given by;

$$-\frac{d[A]}{dt} = k[A][B] \qquad \text{Eqn.17}$$

When the initial concentration of B is very large as compared to that of A, then no matter how much A has reacted, the concentration of B will be little affected i.e. remain constant. Equation 17 can be rearranged to yield,

$$\frac{d[A]}{[A]} = -k[B]dt \qquad \text{Eqn.18}$$

Now if the concentration of B = [B(0)] is constant throughout the reaction, integration of both sides of equation 18 yields:-

$$\ln\left[\frac{A(t)}{A(0)}\right] = -k[B(0)]t \qquad \text{Eqn.19}$$

Or

$$[A(t)] = [A(0)]\exp\{-k[B(0)]t\} \qquad \text{Eqn.20}$$

Equation 20 is similar to equation 5, except that the rate constant *k* has been replaced by k[B(0)]. From equation 20, the lifetime of *A* is given by 1/*k*[B(0)]. Since only the ratio [*A*(t)]/[*A*(0)] is used, then it is not necessary to know the absolute concentration of *A*.

2.4 Temperature dependence of rate constants

Apart from depending on concentrations of the chemical reactants, the reaction rate and hence the rate coefficient both also have been found experimentally to depend on the temperature (T) and that this dependence is often very strong (Houston, 2001, Pilling and Seakins, 1995).

It has been established experimentally that the temperature dependence of many rate constants can be fit over a relatively narrow temperature range by the exponential *Arrhenius equation*

$$k = Ae^{-Ea/RT} \qquad \text{Eqn.21}$$

where R is the gas constant and the temperature T is in Kelvin (K). A, the preexponential factor, and E_a, the activation energy, are parameters characteristic of the particular reaction (Finlayson-Pitts and Pitts Jr., 2000, Laidler, 1987). From equation 21 above we see that provided E_a is positive (which is generally the case), the rate coefficient increases with increase in temperature (Pilling and Seakins, 1995).

Plot of ln k versus 1/T produces a straight line with the familiar form y = -mx + b, where
x = 1/T, y = ln k, m (slope) = - E_a/R
b (y - intercept) = ln A

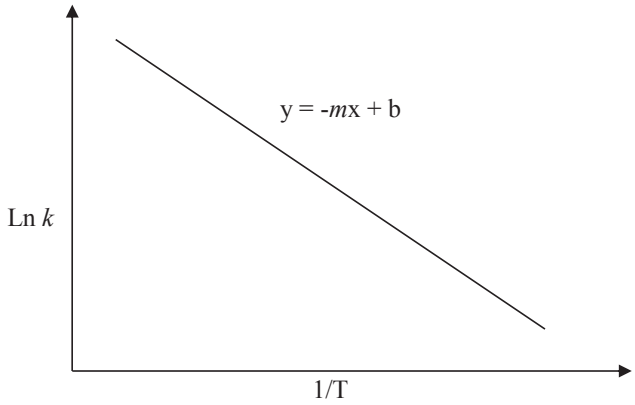

Figure 2.4.1: Arrhenius Plot

The activation energy E_a can be determined from the slope m of this line: E_a = -m.R. The value of the y-intercept corresponds to ln A.

The Arrhenius equation arises because the reactants have to overcome an energy barrier (Figure 2.4.2) when their valence electrons are rearranged as the products are formed.

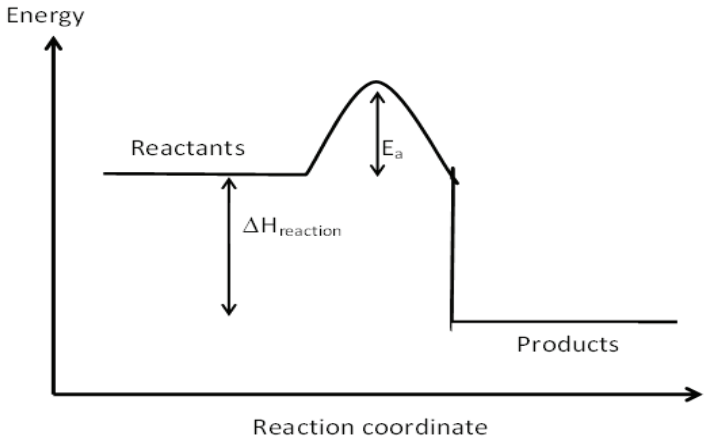

Figure 2.4.2: Activation energy and enthalpy of reaction

Nonlinear Arrhenius plots of ln *k* against 1/T have been observed for some reactions when the temperature range over which experiments could be carried out is extended (Finlayson-Pitts and Pitts Jr., 2000). This is not unexpected when the predictions of the two major kinetic theories in common use today, collision theory and transition state theory, are considered. For many reactions, the temperature dependence of *A* is small (e.g., varies with $T^{1/2}$) compared to the exponential term so that Eqn.21 is a good approximation, at least over a limited temperature range (Pilling and Seakins, 1995). For some reactions encountered in tropospheric chemistry, however, this is not the case. For example, for reactions in which the activation energy is small or zero, the temperature dependence of *A* can become significant. As a result, the Arrhenius expression (eqn. 21) is not always appropriate to describe the temperature dependence, and the form:-

$$k = BT^n e^{-Ea/RT} \qquad \text{Eqn.22}$$

is frequently used, where *B* is a temperature-independent constant characteristic of the reaction and *n* is a number adjusted to provide a best fit to the data. Although most of the reactions in atmospheric chemistry increase in rate as the temperature increases, there are several notable exceptions. The first is the case of termolecular reactions, which generally slow down as the temperature increases (Finlayson-Pitts and Pitts Jr., 2000). This can be rationalized qualitatively on the basis that the lifetime of the excited bimolecular complex formed by two of the reactants with respect to decomposition back to reactants decreases as the temperature increases, so that the probability of the excited complex being

stabilized by a collision with a third body falls with increasing temperature (Finlayson-Pitts and Pitts Jr., 2000).

2.5 Pressure dependent reactions

It has been found experimentally that, the rate constant for a thermal unimolecular reaction is independent of pressure at high pressures, but below a critical pressure, it decreases with pressure (Elliott and Frey, 1966).

Termolecular elementary reactions are among of the most important reactions in the atmosphere and their rates depend on the total pressure. Examples of termolecular reactions are given in rections 36 and 37 below,

$$O(^3P) + O_2 + M \rightarrow O_3 + M \qquad \text{R36}$$

$$OH + SO_2 + M \rightarrow HOSO_2 + M \qquad \text{R37}$$

From reaction 36, the bond formation between $O(^3P)$ and O_2 is exothermic which releases energy that must be removed in order to form a stable O_3 molecule otherwise if the energy remains as internal energy, the ozone molecule will dissociate back to reform O + O_2. As stated above, the third molecule M (normally O_2 or N_2) stabilises the excited $(O_3)^*$ intermediate by colliding with it and removing some of its excess internal energy (Finlayson-Pitts and Pitts Jr., 2000). It has been established that in such cases the effective rate expression varies pressure. At low pressure the reaction is termolecular and at higher pressure it becomes bimolecular. This is due to the fact that as the frequency of collisions increase, the stabilisation of O_3 occurs instantaneously and thus further increase in pressure will not lead to increase in rate. At the low pressure limit the frequency of collision is not enough to stabilize the product molecules before they fly apart, and the overall rate increases with pressure in a linear manner.

Considering reaction 36 as an elementary reaction, then its rate is given by,

$$Rate = k[O][O_2][M] = +\frac{d[O_3]}{dt} \qquad \text{Eqn.23}$$

From equation 23, the rate is expected to increase with concentration or pressure of M. However, some limitations exist as the rate cannot increase to infinity but only to the upper limit depending to how fast the two reactive species can combine chemically. Thus, it is expected that rates for reactions such as 36 and 37 will increase initially as the

pressure of M increases from zero and then remain constant at a certain limiting value at high pressure (Finlayson-Pitts and Pitts Jr., 2000).

2.6 Structure Activity Relationship (SAR)

In order to understand the atmospheric fate of gaseous organic pollutants and volatile organic compounds (VOCs) in general, it is necessary to know the rate with which they react with atmospheric oxidants such as hydroxyl radical (OH),ozone (O_3), etc . There are many VOCs present in the atmosphere, and the total number of identified species has been estimated at 10^4-10^5, whose lifetimes in the atmosphere span orders of magnitude (http://www.cas.manchester.ac.uk/resactivities/atmosphericchemistry/SARS/).

The dominant fate of the organic chemicals present in the troposphere is through their reaction with OH radical (Atkinson, 1988). In determining the relative importance of transport both to the remote of the globe and to the stratosphere, the tropospheric lifetime of the chemical is an important factor (Bidleman *et al.*, 1990). It is also important to understand the build-up of atmospheric concentrations of different chemicals hence their potentiality to be good absorbers of infrared radiations. Therefore there is a need to know the rate constants for the gas phase reactions of these organic compounds with the OH radical. This can be achieved through use of direct experimental measurements or reliable estimation methods. One of these estimation methods is the Structure-Activity Relationship (SAR).

According to the American Environmental Protection Agency (EPA), **Structure-Activity Relationship (SAR)** is the relationship of the molecular structure of a chemical with a physicochemical property, environmental fate attribute, and/or specific effect on human health or an environmental species. These correlations may be qualitative (simple SAR) or quantitative (QSAR) (http://www.epa.gov/hpv/pubs/general/sarfinl1.htm).

Qualitative predictions are based on a comparison of valid measured data from one or more analogues (i.e., structurally similar compounds) with the chemical of interest. For example, terms such as “similarly toxic”, “less toxic”, or “more toxic” would be used in a qualitative SAR assessment for toxicity to humans or environmental species. **Quantitative predictions**, on the other hand, are usually in the form of a regression equation and would thus predict dose-response data as part of a quantitative Structure Activity Relationship assessment (http://www.epa.gov/hpv/pubs/general/sarfinl1.htm).

King *et al.,* (1996) stated that, a structure-activity relationship (SAR) models the relationship between activities and physicochemical properties of a set of compounds and is fundamental to many aspects of chemistry. SAR modelling has been applied to a multitude of biological systems and has aided the development of many new drugs (Martin, 1978, Ramsden, 1990).

Development of estimation methods came into concern due to the fact that, there are many organic chemicals emitted into or formed in the atmosphere for which their reaction rate constants with OH radical are not experimentally available. Most of these estimation methods utilise molecular properties of the chemical which include NMR chemical shifts (Hodson, 1988), ionisation energy (Gaffney and Levine, 1979, Guesten *et al.,* 1984), bond dissociation energies (Heicklen, 1981) Infrared absorption frequencies (Jolly *et al.*, 1985) or involve transition state calculation (Cohen and Benson, 1987) as well as molecular orbital (Cooper *et al.,* 1990, Klamt, 1993)

Atkinson (1986) established a general Structure Activity Relationship (SAR) for OH radical reactions with organics that later was extended to nitrosamines and nitramines (Atkinson, 1987). This estimation has been found to provide a good agreement (generally within a factor of 2) between experimental and calculated rate constants. Nevertheless, the method has some limitations. It was found to be not applicable to ethers (Atkinson, 1986), fluoroethers (Zhang *et al.*, 1992) and certain haloalkanes including those containing $–CF_3$ groups (Atkinson 1986, Atkinson, 1987).

The estimation is based on the fact that, the reaction of the hydroxyl radical with organic compounds in gas-phase proceed by four reaction pathways which are assumed to be additive. These four pathways are; H-atom abstraction from C-H and O-H bonds; OH radical addition to double bond and triple bonds; OH radical addition to aromatic rings and OH radical interactions with N-, S- and P- atoms.

In this SAR the total OH radical reaction rate coefficient is given by:

k_{total} = k(H-atom abstraction from C-H and O-H bonds)
+k(OH radical addition to >C=C< and –C≡C-bonds)
+k(OH radical addition to aromatic rings)
+k(OH radical interaction with $–NH_2$, >NH, >N-, >NNO, SH and –S-groups)

The calculation of overall H-atom abstraction rate coefficients is based upon the estimation of CH_3-, CH_2-,>CH- and–OH group rate constants. The -CH_3, -CH_2, and >CH- group rate coefficients depend on the identity of the substituents around those groups, with

$$k(CH_3\text{-}X) = k_{prim}.F(X)$$

$$k(X\text{-}CH_2\text{-}Y) = k_{sec}.F(X).\ F(Y)$$

$$k(CH_3\text{-}X) = k_{ter}.F(X).\ F(Y).\ F(Z)$$

where k_{prim}, $k_{sec.}$, and k_{tert} are the rate coefficients per –CH_3, -CH_2, and > CH- group for a "standard" substituent and X, Y, Z are substituent groups while F(X), F(Y), and F(Z) are the corresponding substituent factors. The standard substituent group is chosen to be $X = Y = Z =$ -CH_3, F(-CH_3) = 1.00 by definition (Atkinson, 1986). Updated SAR parameters relevant to amine, nitramines and nitrosamine are given in table 2.6.1 below.

Table 2.6.1. SAR parameters for OH radical reactions with amines, nitramines and nitrosamines

Group	$k_{298}/10^{-12}$cm^{-3}molecules^{-1}	Substituent Group X	F(X)
-CH_3(k_{prim})	0.136	-NH_2, >NH, >N-, NNO, >NNO_2[a]	9.3
>CH_2(k_{sec})	0.934	-CH_3	1.0
>CH-(k_{tert})	1.94	-CH_2-, >CH, >C<	1.23
-OH	0.14	-OH	3.5
RNH_2	21	-NO_2	0
R_2NH	63		
R_3N	66		
R_2NNO_2	0		
R_2NNO	1.3		

[a]Constrained to the same value in the SAR (Kwok and Atkinson, 1995)

2.7 Research tasks

- Laboratory measurements of products formed in the gas phase reactions of OH radicals and Cl atoms with a series of nitramines and amides.

- Determination of rate coefficients for the gas phase reactions of OH radicals, Ozone, and chlorine atom with a series of nitramines and their lifetimes in the atmosphere.
- Determination of rate coefficients for the gas phase reactions of NO_3 radicals with two simple nitrosamines and their lifetimes in the atmosphere.
- Measurement of infrared absorption cross sections (base e) for a series of amines, nitramines and isocyanic acid.
- Determination of integrated absorption intensities for a series of amines, isocyanic acid and acetonitrile.

3 EXPERIMENTAL PART

3.1 Photooxidation experiments of amines

The amine photolysis by natural sunlight experiments were conducted at EUPHORE in Valencia Spain. EUPHORE consists of two large outdoor simulation chambers integrated into the Centro de Estudios Ambientales del Mediterraneo (CEAM) (Wenger *et al.*, 2004). Details on Technical information and instrumentation are given below:-

Technical data

The Installation has two twin outdoor atmospheric simulation chambers. Each one consists of a half spherical Teflon bag with a volume of about 200m^3. The chambers are made from a fluorine-ethene-propene (FPE) foil with a thickness of 0.13 mm whereby 32 individual segments are welded together to achieve the half-spherical form. This foil has a transmission of more than 80% for sunlight in the near UV and the visible range between 280 nm and 640 nm, which is the important range supplying the energy for the chemical reactions occurring in photo-oxidation processes in the troposhere. Teflon is a chemically inert material and provides the best choice to avoid uncontrolled reactions of the trace gases with the chamber walls.

The chamber is self-stabilising against wind distortions when operated with an excess pressure of 100 - 200 Pa. An internal framework made of epoxide resin tubes based on a half-spherical network construction keeps the foil in shape in the absence of excess internal pressure. The chamber floor consists of 32 symmetrically arranged aluminium panels covered with FPE (fluorinated ethylene propylene) foil, and an integrated rubber cord is used as a seal between the bag and the floor. One of the technical innovations is the refrigeration system integrated in the chamber floor, which compensates heating of the chamber air by solar radiation. Ports for input of the reactants and sampling lines for the different analytical instruments are located on the chamber floor.

Analytical instrumentation

The simulation chambers are equipped with a broad number of analytical instruments in order to analyse VOCs, O_3, NO, NO_2, PAN, organic nitrates, hydroperoxides and organic acids. For in-situ measurements highly sensitive and selective techniques such as LP-FTIR and LP-UV/VIS DOAS spectroscopy are available. For the sensitive analysis of reaction products several ozone and NOx monitors, as well as HCHO monitor, HONO-

LOPAP monitor, PTR-MS, GC-MS and GC-MS/MS systems can be employed for sampling the trace gas components directly from the gas phase, with pre-concentration techniques or solvent trapping. For the measurement of OH and OH_2 radicals a Laser Induced Fluorescence LIF is available with its excellent potential for obtaining insight into radical formation and radical cycling processes, responsible for ozone and photo-oxidant formation. To measure aerosol formation from biogenic or anthropogenic precursor VOCs during oxidation, the EUPHORE installation is equipped with a SMPS system and a continuous-operating microbalance (TEOM) providing particle numbers and mass concentration. Other off-line techniques, such HPLC and LC-MS or GC-MS for the analysis of different range of compounds, both in gas and particle phase, are also available (http://euphore.es/queeseuphore.html).

The chamber is filled to atmospheric pressure with purified dry air generated from ambient air using an air purification system. Homogeneous gas mixtures are obtained by the use of two mixing fans located inside the chamber. A White mirror system installed inside the chamber and aligned with an optical path length of 553.5 m was used for in situ measurements by Fourier transform infrared (FTIR) spectroscopy. The FTIR spectrometer (Nicolet Magna 550) was positioned on a platform beneath the chamber and operated using an MCT-B detector. Infrared spectra were derived from the co-addition of 280 scans, recorded every five minutes with a resolution of 1.0 cm^{-1}.

Figure 3.1.1 shows that PTR-TOF and FT-IR results for the three alkylamines were in excellent agreement. Both techniques detected initial amine levels of 250 ppbV which corresponds to the amount of amine that was nominally injected into the chamber. FT-IR data of methylamine and dimethylamine are reported only for the period when the chamber was kept in the dark since interferant compounds were formed under sunlight conditions. The absolute FTIR spectra obtained in this study were instrumental in the quantitative work.

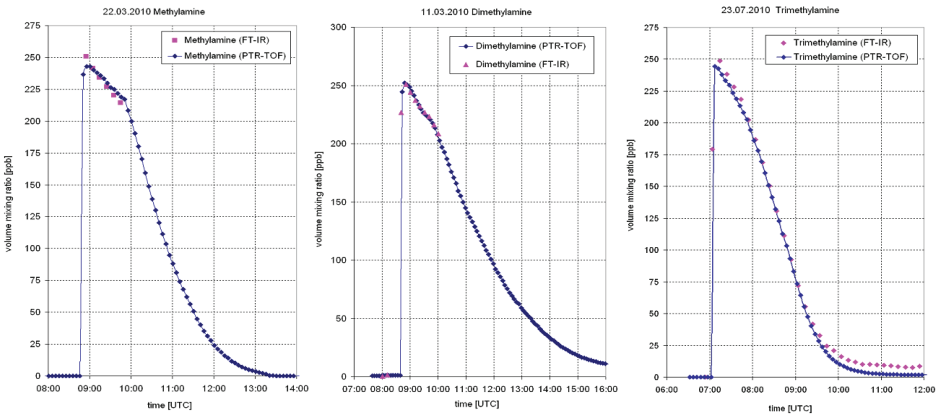

Figure 3.1.1. Comparison of FT-IR and PTR-TOF results for CH_3NH_2, $(CH_3)_2NH$ and $(CH_3)_3N$.

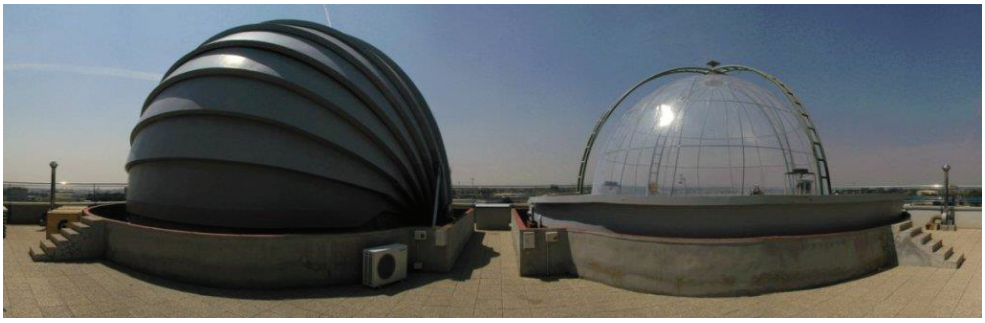

Figure 3.1.2: Two chambers of the EUPHORE one is closed (left) and the other is open (right)

Figure 3.1.3: Inside the chamber, several ports available for sampling

3.2 Reference spectra and relative rate experiments

3.2.1 Reference spectra for methylamine, di-methylamine, tri-methylamine, ethylamine, deuterated methylamine, di-deuteratedmethylamine and tri-deuteratedmethylamine

Reference spectra for the above mentioned pure gases at 293 ± 2 K were obtained using a 10.0 ± 0.1 cm long cell equipped with Cesium Iodide (CsI) windows. The infrared spectra were recorded using a Bruker IFS 66v FTIR instrument at a resolution of 1 cm^{-1}. Single channel spectra (background or sample) were recorded averaging 32 scans and applying a boxcar apodization. A Ge/KBr beam splitter was used to cover the spectral region. To ensure optical linearity a DTGS detector was used. The partial pressures of the gases filled in the cell ranged from 1 to 30 hPa and were measured using a MKS Baraton Type 122A pressure transducer with a stated accuracy of ± 0.15 %.

Additional spectra of the compounds diluted in Argon at 1013 ± 5 hPa were obtained at a resolution of 0.25 with 256 scans.

3.2.2 Reference spectra for diethylamine, triethylyamine and methanol

Reference spectra for diethylamine, triethylyamine and methanol were obtained using a 23 cm cell with Potassium bromide (KBr) windows. The cell was filled with a certain amount of the respective compound enough to generate a useful peak and then placed in the instrument. The infrared spectra were recorded using a Bruker IFS 66v FTIR instrument equipped with a DTGS detector. A total of 256 scans were co-added at a resolution of 0.25 cm^{-1} for Diethylamine and Triethylyamine while for methanol 512 scans at a resolution of 0.5 cm^{-1} were recorded using a boxcar apodization

3.2.3 Reference spectra for methylanitramine, dimethylnitramine, ethylnitramine, diethylnitramine, ethylacetate, ozone, methylformate and dimethylether,

The experiments to obtain reference spectra for the above named compounds were carried out in a 240 L electropolished stainless steel smog chamber equipped with a White type multiple reflection mirror system with a 120 meters optical path length for ro-vibrationally resolved infrared spectroscopy. The infrared spectra were recorded with a Bruker IFS 66v FTIR instrument. For each measurement a total of 128 scans were co-added at a resolution of 0.5 cm^{-1}. For good gas measurements, the nitrogen-cooled Mercury-Cadmium-Telluride (MCT) detector was used. The MCT detector has great advantages over detectors that operate at or near room temperature. For a given scanning

time, an MCT detector will produce a spectrum with a noise level 10 to 100 times lower than the noise from a DTGS detector. This low noise has two important results. First, it lowers the minimum detection limits for all compounds being measured. Second, it widens the concentration range over which valid measurements can be made (http://www.infraredanalysisinc.com/m2.htm).

The schematic representation of the reaction chamber is shown in figure 3.2.3.1 below.

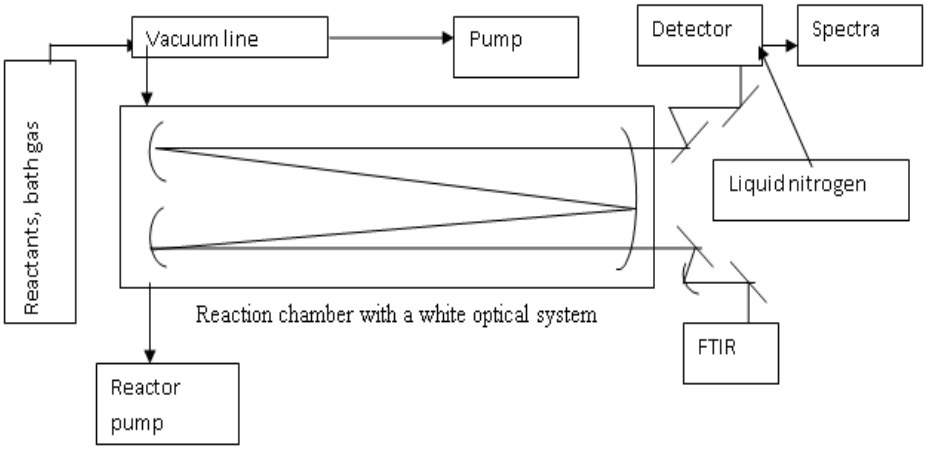

Figure 3.2.3.1: Schematic representation of the Oslo reaction chamber

The reaction chamber is equipped with UV photolysis lamps mounted in a quartz tube inside the chamber, and all experiments were carried out in synthetic air (AGA 99.99%; CH_4, CO and NO_x < 100 ppbv) at 298 ± 2 K and 1013 ± 10 hPa.

3.3 Ozone synthesis

Ozone is the strongest commercially available oxidizing agent that we can produce. How ever, the molecule is unstable and cannot be stored for future use. Therefore it must be generated close to the point of application then used immediately.

In this work, ozone was produced from oxygen (99.995%) purchased from AGA Norway using a MK II Ozone generator from BOC, UK which has a conversion efficiency of approximately 5%, and collected in a trap filled with silica beads at 195 K. Typical partial pressure of ozone was 200 Pa. In the process, oxygen gas was passed through a high energy electrical field where a portion of the oxygen is converted into ozone. In the instrument (ozone generator) electrons are accelerated across an air gap so as to give

them a sufficient energy enough to split the oxygen double bond, producing atomic oxygen. The two oxygen atoms which are produced by the collision react with other diatomic oxygen molecule to form ozone according to the reactions bellow:-

$O_2 + h\nu\ (energy) \longrightarrow 2O$ R38

$O_2 + O + M \rightarrow O_3 + M$ R39

Where "M" denotes the third body which does not enter into the reaction chemically but it carries off the excess energy of the reaction to avoid the energy-rich intermediate formed from the recombination of two species to dissociation back into the reactants.

3.4 Generation of radicals

3.4.1 Chlorine atoms

The chlorine atoms were generated by photolysis of Cl_2 using Philips TLD-08 fluorescence lamps ($\lambda_{max} \sim 370$ nm) leading to the production of ground-state chlorine atoms:

$$Cl_2 + h\nu(\lambda \approx 350\ nm) \rightarrow 2\ Cl\ (^2P_{3/2}\ exclusively)$$

The Cl_2 was a standard laboratory grade compound (AGA 2.8) and was purified by two freeze-pump-thaw cycles prior to use. Typical volume fractions were 10 – 20 ppm Cl_2.

3.4.2 The nitrate radical (NO_3)

The NO_3 radicals were generated in situ by thermal dissociation of N_2O_5. Gas streams of NO_2 and excess O_3 were mixed in glas bulb and trapped at dry ice temperature, -78 °C (excess O_3 condenses at much lower temperatures i.e. -112°C and freezes at -193°C, http://scifun.chem.wisc.edu/chemweek/ozone/ozone.html). The trapped solid containing N_2O_5, NO_2 and HNO_3 was distilled on a vauum line. NO_2 is easily removed due to the large difference in melting point temperatures; HNO_3 (mp. - 42 °C, bp. 83 °C), NO_2 (bp. 21 °C), N_2O_5 (mp. 41 °C, bp. 47 °C - sublimates).

N_2O_5 reacts with H_2O on surfaces to produce HNO_3 ($N_2O_5+H_2O \rightarrow 2HNO_3$) so to reduce HNO_3, the stream of NO_2/O_3 was trapped during the first minutes. This removes H_2O on the glass and teflon line surfaces and the trapped mixture contains very little HNO_3.
Before use, any NO_2 was pumped off keeping the $N_2O_5/NO_2/HNO_3$ mix at ice temp (0 °C). Most HNO_3 will also boil off at this temp under vacuum.

3.4.3 OH radicals

The hydroxyl radical (OH) is the major oxidizing chemical in the atmosphere, destroying about 3.7 Gt of trace gases, including CH_4 and all HFCs and HCFCs, each year (Ehhalt, 1999). In short reaction with OH radicals is the dominant gas phase loss process for a majority of tropospheric trace gases on a global scale (Finlayson-Pitts and Pitts, 1986).

In this study, hydroxyl radicals were generated by photolysis of ozone (O_3) in the presence of hydrogen gas (H_2) (99%) purchased from AGA, Norway.

Typical partial pressures of ozone and hydrogen were 50 and 200 Pa, respectively. Photolysis of ozone was carried out at intervals of 2 minutes using a Philips TL 12 lamp ($\lambda_{max} \sim 305$ nm). This OH production method produces not only OH radicals in the ground state but also in excited vibrational states (Aker and Sloan, 1986; Huang *et al.*, 1986; Streit *et al.*, 1976).

The reaction mechanism for the above stated process is summarized here below:-

$$O_3 + h\nu\ (\lambda \sim 254\ nm) \rightarrow O(^1D) + O_2 \qquad R40$$

$$O(^1D) + H_2 \rightarrow OH + H \qquad R41$$

$$H + O_3 \rightarrow OH + O_2 \qquad R42$$

The collision quenching rate coefficients of the hydroxyl radical (OH) by N_2 and O_2 is on the order of 10^{-15} and 10^{-13} cm^3 $molecule^{-1}$ s^{-1}, respectively (D'Ottone *et al.*, 2004). As the mixing ratios of O_2 and N_2 are 4 – 5 orders of magnitude larger than those of the organic reactants one may safely assume that these react exclusively with OH in the vibrational ground state.

Photolysis of the mixture of ozone and hydrogen (O_3/H_2) to produce hydroxyl radicals has been done for years in our laboratory because it conveniently produces OH concentrations of up to 10^9 cm^{-3} (Gola *et al.*, 2005). The reason for using the TL12 lamps in the photolysis is that, we do not get much radiation below 270 nm to avoid the studied molecules to undergo direct photolysis. For instance use of a lamp centred on 254 nm may result in direct photolysis such that you will observe a combined effect of OH reaction and photolysis. The spectrum for the Philips TL12 lamp is shown in figure 3.4.3.1.

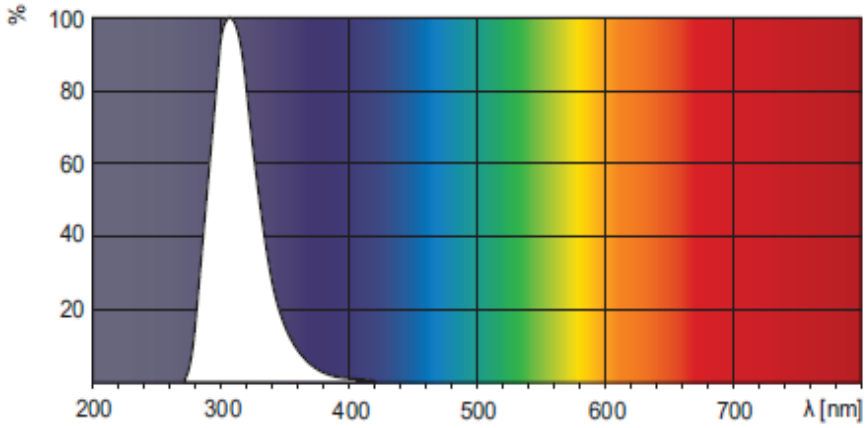

Figure **3.4.3.1**. The spectrum for the Philips TL12 lamp.

3.5 The reference compounds used in the relative experiments

The reference compounds used in this study have well established rate constants for their reaction with the respective oxidant used in each set of experiments therefore making it possible to do the relative experiments to determine the rate constants for the reactions between the substrate with the oxidant. The oxidants used in this study were, hydroxyl radicals, chlorine atoms and nitrate radicals while the substrates were nitramines and nitrosamines. Control experiments were performed to investigate the loss of reactants via photolysis, dark chemistry, and heterogeneous reactions in the reactor. The lifetimes of the reactants in the reaction chamber were studied with purified air as diluent and with the relevant radical precursor mixtures included in experiments lasting from 5 to 7 hours. The photo stability of the reactants toward the radiation used in generating the radicals was studied in separate experiments with purified air as diluent: no direct photolysis in the reactor was detected. The role of evaluating the rate coefficients is to determine the speed of the reaction which will eventually give an indication of the main removal routes of the chemicals under the study in the atmosphere.

3.5.1 Experiment with OH radicals

Methanol (CH_3OH) + OH $\rightarrow$ products

Alcohols are in a group of highly volatile organic compounds. Their presence in the atmosphere originates from both anthropogenic and natural sources. Anthropogenic sources include their use as fuel additives and as solvents (Azad and Andino, 1999), biomass burning (Jimènez *et al.*, 2003) as well as from industrial emissions (Bilde *et al.*,

1997). Hence it is important to understand their atmospheric degradation pathways. 1-Propanol, in particular, is widely used as a chemical solvent in the manufacturing of disk drives, computers, semiconductors, and various electronic components. Also it is used in the esterification of acetic acid, and it is a common ingredient found in vinegar (Azad and Andino, 1999). Alcohols such as *tert*-butyl alcohol (TBA) [Bilde *et al.*, 1997, Teton *et al.,* 1996, Japar *et al.*, 1990, Seinfield *et al.*, 1994], ethanol (Seinfield *et al.*, 1994, Picquet *et al.*, 1998), and methanol (Seinfield *et al.*, 1994,Wallington and Kurylo, 1987) have been used in oxygenated fuels to reduce automobile emissions of carbon monoxide and hydrocarbons (US EPA, 1998). Addition of alcohols to fuels allows the engine to operate at a high octane rating thereby increasing the engine combustion efficiency (Bilde *et al.*, 1997, US EPA, 1998).

Once emitted into the atmosphere, alcohols can react with oxidizing species such as hydroxyl radicals (OH), nitrate radicals (NO_3), and ozone (O_3) [Atkinson, 1997] to produce a number of radicals and products. During daytime time, reaction with the OH radical is the most dominant loss mechanism.

In this study, methanol was used as a reference compound in determination of the rate constants for the reaction between nitramines and OH radicals in the atmosphere. Results from previous studies show that the rate coefficient for the reaction of OH radicals with methanol ($k_{CH3OH+OH}$) at 298 - 300 K ranges from $(8.61 – 10.1) \times 10^{-13}$ cm^3 $molecule^{-1}$ s^{-1} (Atkinson *et al.*, 1999, Hess and Tully, 1989, Jimenez *et al.*, 2003, McClaulley, *et al*., 1989, Campbell *et al*., 1976, Picquet *et al*., 1998, Wallington *et al*., 1987).

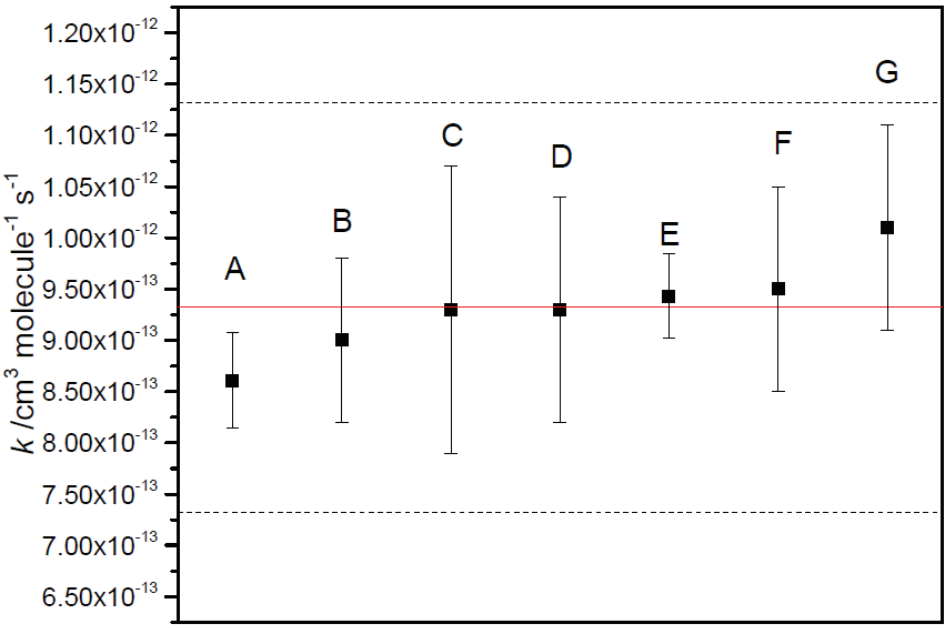

Figure 3.5.1.1. Summary of available rate coefficients for the reaction of OH raadicals with CH_3OH at 298 K. (A) Wallington *et al*., (1987); (B) Picquet *et al.,* (1998); (C) Atinkson *et al.*, (1999); (D) Jimenez *et al.*, (2003); (E) Hess & Tully, (1989); (F) Campbell *et al.*, (1976); (G) McCaullen *et al.*, (1989). IUPAC preferred value = 9.0×10^{-13} cm^3 $molecule^{-1}$ s^{-1}.

Dimethylether (CH_3OCH_3) + OH → products

As it is the case for alcohols, ethers are also used as industrial solvents and additives to unleaded gasoline to increase the octane rating. They are released to the atmosphere through evaporation and are degraded in the troposphere via their reactions with hydroxyl radicals (Mellouki *et al.,* 1995). Dimethyl ether (DME) has been proposed as an alternative diesel fuel (Sehested *et al.*, 1996, Good and Francisco, 2000). Since the emission of dimethylether to the atmosphere may be harmful to the environment, the atmospheric chemistry of dimethylether is very important due to the fact that the rate of the reaction with hydroxyl radical dictates the atmospheric lifetime of dimethylether. Previous studies have reported the rate constant for the reaction between dimethylether and hydroxyl radical to be in the range of (2.35 –2.98) x 10^{-12} cm^3 $molecule^{-1}$ s^{-1} (Arif *et al.*, 1997, Atkinson, 1994, Bonard *et al*., 2002, Mellouki *et al.*, 1995, Nelson *et al.*, 1990, Tully and Droege, 1977) with a weighted average of 2.79 x 10^{-12} cm^3 $molecule^{-1}$ s^{-1}.

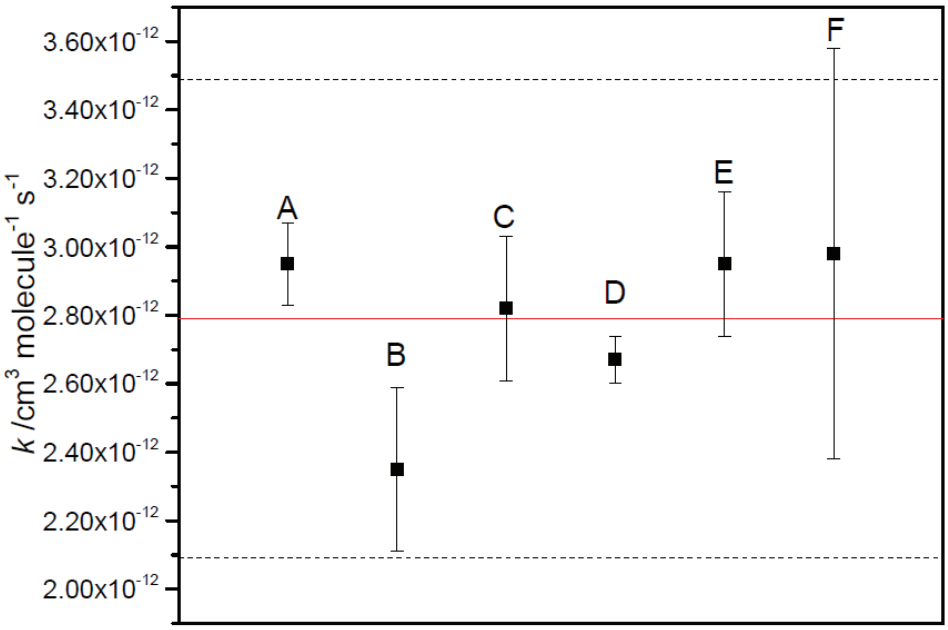

Figure 3.5.1.2. Summary of available rate coefficients for the reaction of OH radicals with $CH_3(O)CH_3$ at 298 K. (A) Tully and Droege, (1977); (B) Nelson *et al*., (1990); (C) Mellouki *et al*., (1995); (D) Bonard *et al*., (2002); (E) Arif *et al*., (1997); (F) Atkinson *et al*., (1994). IUPAC preferred value = 2.8×10^{-12} cm^3 $molecule^{-1}$ s^{-1}.

Methylformate (CH_3OCHO) + OH → products

Oxygenated compounds are widely used in paints, as solvents and degreasing agents (Le Clave *et al.*, 1997). This group of compound includes esters which are used as food flavourings and in perfumes. They are also present in some fruits, hence they can be emitted to the atmosphere naturally (Le Clave *et al.*, 1997). Tropospheric degradation of some volatile organic compounds also results into formation of esters (Szilághyi *et al.*, 2004). For example, methyl formate and ethyl formate are the most important products of the tropospheric degradation of dimethyl ether and diethyl ether, respectively (Japar *et al.,* 1990). The tropospheric fate of formates is mainly controlled by their reaction with OH radicals (Szilághyi *et al.*, 2004) and the rate coefficients for their reaction with OH radicals are well documented in literature. The rate constant for the reaction between methylformate and OH radicals are in the range of (1.73 – 2.27) x 10^{-13} cm^3 $molecule^{-1}$ s^{-1} (Le Calve *et al.*, 1997, Szilághyi *et al*, 2004, Wallington *et al.*, 1988).

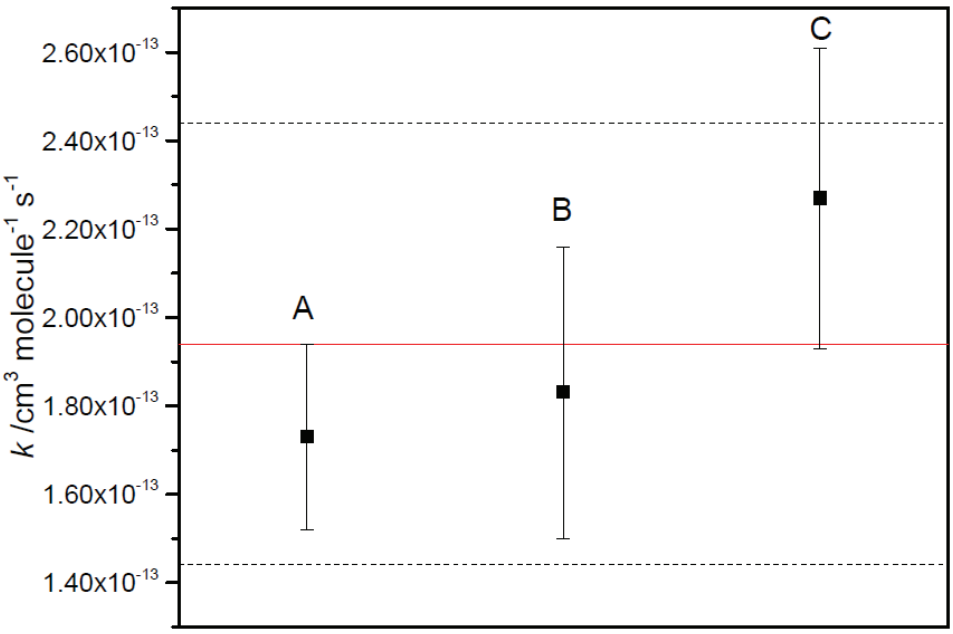

Figure 3.5.1.3. Summary of available rate coefficients for the reaction of OH radicals with CH_3OCHO at 298 K. (A) Le Calve *et al*., (1997); (B) Szilághyi *et al*., (2004); (C) Wallington *et al*., (1988). Average: $k_{CH3OCHO+OH}$ = 1.94×10^{-13} cm^3 $molecule^{-1}$ s^{-1}.

3.5.2 Experiment with Cl atoms

$CH_3OH + Cl \rightarrow$ products

Based on a critical review of all experimental data, the currently recommended rate coefficient for the reaction of Cl atoms with methanol is $k_{CH3OH+Cl}$ = (5.5 ± 0.9)× 10^{-11} cm^3 $molecule^{-1}$ s^{-1} at 298 K (http://www.iupac-kinetic.ch.cam.ac.uk). Previous studies have reported the rate constant for the reaction between methanol and chlorine atom to be in the range of (5.1 –6.21) x 10^{-11} cm^3 $molecule^{-1}$ s^{-1} (Michael *et al.*, 1979, Payne *et al*., 1988, Dóbé *et al*., 1993, Tyndall *et al*., 1999, Smith *et al*., 2002, Seakins et al., 2004, Taketani *et al*., 2005, Garzón *et al*., 2006) with a IUPAC preferred value of 5.5 x 10^{-11} cm^3 $molecule^{-1}$ s^{-1}.

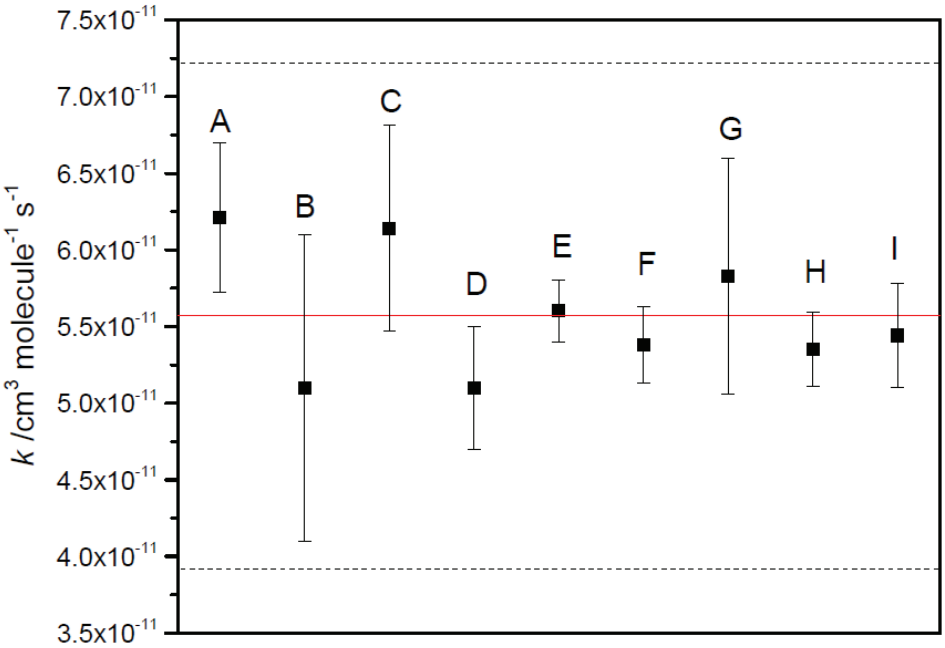

Figure 3.5.2.1. Summary of available rate coefficients for the reaction of Cl atoms with CH_3OCH_3 at 298 K. (A) Michael *et al*.,(1979); (B) Payne *et al*., (1988); (C) Dóbé *et al*., (1993); (D) Tyndall *et al*., (1999); (E) Smith *et al*., (2002); (F) Seakins *et al*., (2004);(G) Seakins *et al*., (2004) (H) Taketan *et al.,* (2005); (I) Garzón *et al*., (2006) . IUPAC preferred value: 5.5×10^{-11} cm^3 $molecule^{-1}$ s^{-1}.

$CH_3OCH_3 + Cl \rightarrow$ products.

Michael *et al.,* (1979) measured the absolute rate coefficient by the flash photolysis-resonance fluorescence technique and reported $k_{CH_3OCH_3+Cl} = (1.80 \pm 0.09)\times10^{-10}$ cm^3 $molecule^{-1}$ s^{-1} at 300 K.

Park *et al.,* (1983) measured the absolute rate coefficient in a fast-flow reactor setup using photoionization mass spectrometry detection and reported $k_{CH_3OCH_3+Cl} = (1.7\pm0.3)\times10^{-10}$ cm^3 $molecule^{-1}$ s^{-1} at 298 K.

Wallington *et al.,* (1988) measured the rate coefficient relative to those of ethane and *n*-butane. Taking the recommended values $k_{CH_3CH_3+Cl} = 5.9$ and $k_{CH_3CH_2CH_2CH_3+Cl} = 2.05 \times 10^{-10}$ cm^3 $molecule^{-1}$ s^{-1} at 298 K (uncertainty factor 1.06) (http://www.iupac-kinetic.ch.cam.ac.uk) places $k_{CH_3OCH_3+Cl} = (2.05 \pm 0.15)\times10^{-10}$ cm^3 $molecule^{-1}$ s^{-1} on an absolute scale.

Nelson *et al*. 1990 measured the rate coefficient relative to that of cyclohexane and reported k_{rel} = 0.486±0.026. Taking the recommended value for $k_{C6H12+Cl}$ = 3.3 ×10^{-10} cm^3 $molecule^{-1}$ s^{-1} at 298 K (uncertainty factor 1.15) (Calvert *et al.,* 2008) places $k_{CH3OCH3+Cl}$ = (1.60 ± 0.25)×10^{-10} cm^3 $molecule^{-1}$ s^{-1} at 298 K.

Jenkin *et al*., (1993) measured the rate coefficient relative to that of ethane and obtained k_{rel} = 2.03 ± 0.07. Taking the recommended value for $k_{CH2=CH2+Cl}$ = 1.1 × 10^{-10} cm^3 $molecule^{-1}$ s^{-1} at 1 bar and 298 K (uncertainty factor 1.35) (http://www.iupac-kinetic.ch.cam.ac.uk) places $k_{CH3OCH3+Cl}$ = (2.2 ± 0.8)×10^{-10} cm^3 $molecule^{-1}$ s^{-1} on an absolute scale at 298 K.

Notario *et al.,* (2000) determined the absolute rate coefficient using the laser photolysis-resonence fluorescence technique and reported $k_{CH3OCH3+Cl}$ = (1.3 ± 0.2) × 10^{-10} cm^3 $molecule^{-1}$ s^{-1} at 298 K.

Figure 3.5.2.2 summarizes the available experimental rate coefficient from which a best value of $k_{CH3OCH3+Cl}$ = 1.8 × 10^{-10} cm^3 $molecule^{-1}$ s^{-1} at 298 K (uncertainty factor 1.30) is extracted.

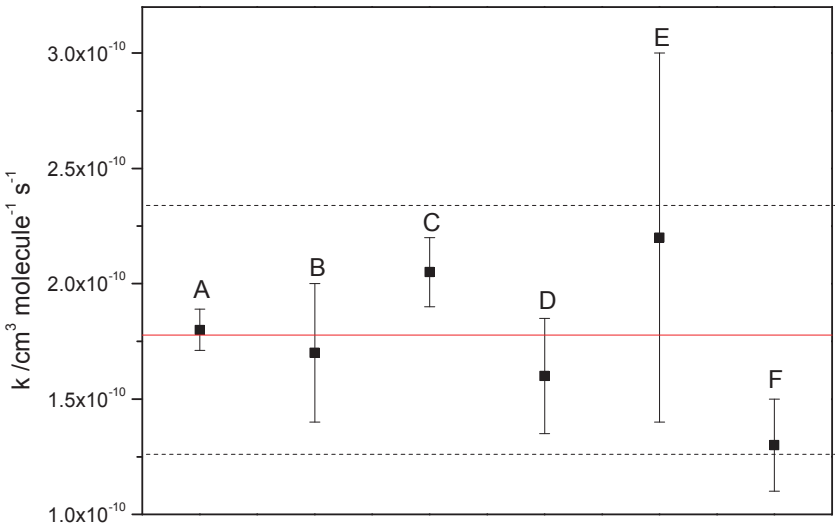

Figure 3.5.2.2. Summary of available rate coefficients for the reaction of Cl atoms with CH_3OCH_3 at 298 K. (A) Michael *et al*., (1979); (B) Park *et al*., (1983); (C) Wallington *et al*., (1988); (D) Nelson *et al*., (1990); (E) Jenkin *et al*., (1993), (F) Notario *et al*., (2000). Average: $k_{CH3OCH3+Cl}$ = 1.8×10^{-10} cm^3 $molecule^{-1}$ s^{-1}.

$CH_3OCHO + Cl \rightarrow$ products.

Wallington *et al*., (1993) measured the rate coefficient relative to that of CH_3Cl and found $k_{rel} = 2.28 \pm 0.17$. Taking the recommended value of $k_{CH_3Cl+Cl} = 4.8\times10^{-13}$ cm^3 $molecule^{-1}$ s^{-1} at 298 K (uncertainty factor 1.1) (http://www.iupac-kinetic.ch.cam.ac.uk), places $k_{CH_3OCHO+Cl} = (1.35 \pm 0.17) \times 10^{-12}$ cm^3 $molecule^{-1}$ s^{-1} at 298 K.

Notario *et al.,* (1998) determined the absolute rate coefficient by the laser photolysis resonance fluorescence technique and reported $k_{CH_3OCHO+Cl} = (1.83 \pm 0.21) \times 10^{-12}$ cm^3 $molecule^{-1}$ s^{-1} at 298 K.

Good *et al.,* (2000) measured the rate relative to CH_3F, CH_2Cl_2 and CH_2F_2 and found $1/k_{rel} = 0.22 \pm 0.1$, 0.23 ± 0.01 and 0.06 ± 0.001, respectively. Taking the recommended values $k_{CH_3F+Cl} = 3.5 \times 10^{-13}$ (uncertainty factor 1.15) (http://www.iupac-kinetic.ch.cam.ac.uk), $k_{CH_2Cl_2+Cl} = 3.4 \times 10^{-13}$ (uncertainty factor 1.1) (http://www.iupac-kinetic.ch.cam.ac.uk)and $k_{CH_2F_2+Cl} = 3.4 \times 10^{-14}$ (uncertainty factor1.6) (http://www.iupac-kinetic.ch.cam.ac.uk) cm^3 $molecule^{-1}$ s^{-1} at 298 K, places $k_{CH_3OCHO+Cl} = (1.59 \pm 0.25) \times 10^{-12}$, $(1.48 \pm 0.35) \times 10^{-12}$ and $(5.3 \pm 3.3) \times 10^{-13}$ cm^3 $molecule^{-1}$ s^{-1} respectively.

In a more recent study Wallington *et al*.(2006) measured the rate coefficient relative to those of CH_3Cl and C_2H_5Cl and reported $k_{rel} = 2.79 \pm 0.19$ and 0.157 ± 0.013, respectively. Taking the recommended value $k_{CH_3Cl+Cl} = 4.8 \times 10^{-13}$ cm^3 $molecule^{-1}$ s^{-1} (uncertainty factor 1.1) (http://www.iupac-kinetic.ch.cam.ac.uk) and $k_{C_2H_5Cl+Cl} = 8.04 \times 10^{-12}$ cm^3 $molecule^{-1}$ s^{-1} at 298 K from the study of Wine *et al*., (1983), places $k_{CH_3OCHO+Cl} = (1.34 \pm 0.09)$ and $(1.26 \pm 0.10) \times 10^{-12}$ cm^3 $molecule^{-1}$ s^{-1} respectively.

Figure 3.5.2.3 summarizes the available experimental rate coefficient from which a best value of $k_{CH_3OCHO+Cl} = 1.35 \times 10^{-12}$ cm^3 $molecule^{-1}$ s^{-1} at 298 K (uncertainty factor 1.20) is extracted. The result of Good *et al.,* (2000) from their relative rate study using CH_2F_2 as reference, $(5.3 \pm 3.3) \times 10^{-13}$ cm^3 $molecule^{-1}$ s^{-1}, has been treated as an outlier.

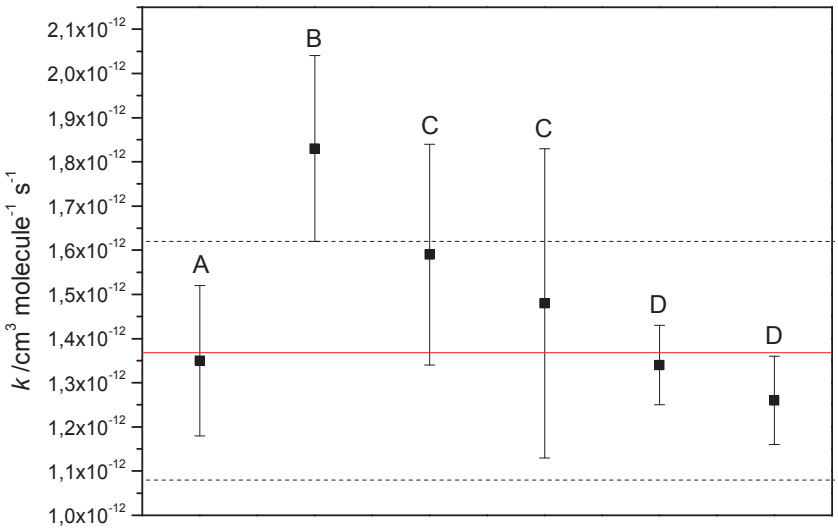

Figure 3.5.2.3. Summary of available rate coefficient for the reaction of Cl atoms with CH_3OCHO at 298 K. (A) Wallington *et al*., (1993); (B) Notario *et al*., (1998); (C) Good *et al*., (2000); (D) Wallington *et al*., (2006). Average: $k_{CH3OCHO+Cl} = 1.35\times10^{-12}$ cm^3 molecule^{-1} s^{-1}.

Ethylacetate ($CH_3CH_2OC(O)CH_3$) + Cl → products.

Acetates are emitted into the atmosphere by various anthropogenic and natural sources. They are used to a large extent in industry, particularly as solvents, and in the manufacturing of perfumes and flavourings; they are also produced in nature through vegetation (Helmig *et al.*, 1989, El Boudali *et al.,* 1996). A substantial proportion of these compounds could escape then into the atmosphere where they can undergo photochemical degradation. Another source of tropospheric acetates is the degradation of oxygenated compounds, especially ethers. For instance, *iso*-propyl acetate is produced from *iso*-propyl ether (IPE) (Wallintong *et al.*, 1993), methyl acetate from methyl *tert*-butyl ether (MTBE) (Tuazon *et al.*, 1991, Smith *et al.*, 1991) and *tert*-amyl ether (TAME) (Smith *et al.*, 1995) and ethyl acetate from ethyl *tert*-butyl ether (ETBE) (Smith *et al.*, 1992). IPE, MTBE, TAME, and ETBE are used as additives to unleaded gasoline to increase the octane rating (US EPA, 1988). As it is for many other organic chemicals, acetates are removed in the troposphere mainly through reaction with OH radicals, since photolysis (Calvert and Pitts Jr., 1966) reaction with NO_3 radicals (Langer *et al.*, 1993) and reaction with O_3 (Atkinson and Carter, 1984) have been proved to be slow processes, thus negligible in the atmospheric degradation of these VOCs. The atmospheric oxidation

of these oxygenated compounds initiated by the OH radicals could contribute to the formation of ozone and other components of the photochemical smog in urban areas (Le Calvè *et al.*, 1997). Though their main loss route in the troposphere is through oxidation by the OH radicals, their oxidation with chlorine atoms at the marine boundary layer is another significant loss process.

Notario *et al*., (1998) measured the absolute rate coefficient using the laser photolysis-resonance fluorescence technique and reported $k_{CH_3CH_2OC(O)CH_3+Cl} = (2.01 \pm 0.25) \times 10^{-11}$ cm^3 $molecule^{-1}$ s^{-1} at 298 K.

Cuevas *et al*., (2005) measured the absolute rate coefficient using the laser photolysis-resonance fluorescence technique and reported $k_{CH_3CH_2OC(O)CH_3+Cl} = (1.37 \pm 0.20) \times 10^{-11}$ cm^3 $molecule^{-1}$ s^{-1} at 298 K.

Xing *et al.,* (2009) measured the rate coefficient relative to those of HCCH and CH_2CH_2 and reported $k_{rel} = 0.336 \pm 0.040$ and 0.196 ± 0.016, respectively, at 296 K. Taking the recommended values $k_{HCCH+Cl} = 5.5 \times 10^{-11}$ (uncertainty factor 1.35) (http://www.iupac-kinetic.ch.cam.ac.uk) and $k_{CH_2CH_2+Cl} = 1.1 \times 10^{-10}$ (uncertainty factor 1.35) (http://www.iupac-kinetic.ch.cam.ac.uk) at 298 K and 1 bar of air, places $k_{CH_3CH_2OC(O)CH_3+Cl} = (1.75 \pm 0.65) \times 10^{-12}$ and $(2.16 \pm 0.80) \times 10^{-13}$ cm^3 $molecule^{-1}$ s^{-1}, respectively. Xing *et al*., (2009) also measured the absolute rate coefficient by the pulsed-laser photolysis/laser-induced fluorescence technique and reported $k_{CH_3CH_2OC(O)CH_3+Cl} = (1.76 \pm 0.11) \times 10^{-11}$ cm^3 $molecule^{-1}$ s^{-1} at 298 K.

Figure 3.5.2.4 summarizes the available experimental rate coefficient from which a best value of $k_{CH_3CH_2OC(O)CH_3+Cl} = 1.7 \times 10^{-11}$ cm^3 $molecule^{-1}$ s^{-1} at 298 K (uncertainty factor 1.25) is extracted.

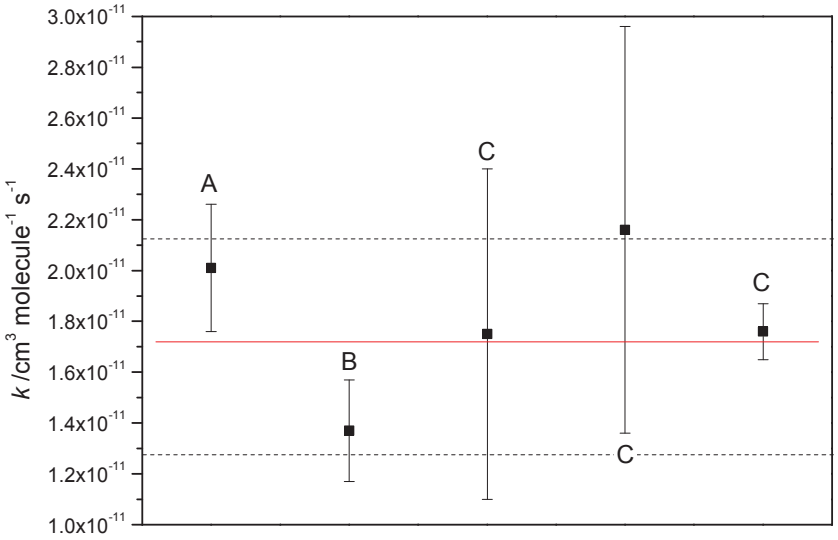

Figure 3.5.2.4. Summary of available rate coefficients for the reaction of Cl atoms with $CH_3CH_2OC(O)CH_3$ at 298 K. (A) Notario *et al*. (1979); (B) Cuevas *et al*., (2005); (C) Xing *et al*., (2009). Weighted average: $k_{CH3CH2OC(O)CH3+Cl} = 1.7\times10^{-11}$ cm^3 molecule^{-1} s^{-1}.

3.5.3 Experiment with the nitrate radical (NO_3)

$CH_2CH_2 + NO_3 \rightarrow$ products

Based on a critical review of all experimental data the currently recommended rate coefficient for the reaction of NO_3 radicals with ethene is $k_{CH2CH2+NO3} = 2.1 \times 10^{-16}$ cm^3 molecule^{-1} s^{-1} at 298 K (IUPAC). The uncertainty factor is 1.5 ($\Delta log_{10}k = \pm 0.20$).

$CH_2O + NO_3 \rightarrow$ products

Formaldehyde is one of the most prevalent carbonyl compounds in the Earth's atmosphere; it is an important component of the polluted troposphere and it is a precursor of HO*x* radicals (Iuga *et al.*, 2008). Thus, any heterogeneous interactions that formaldehyde may have with other air pollutants such as aerosols could potentially affect HO*x* levels, especially if the former is removed from the troposphere.

Aldehydes are ubiquitous key components in the chemistry of the troposphere. They are common primary pollutants from biogenic emissions and in residues of incomplete combustion (Ciccioli *et al.*, 1993). Relevant natural sources are vegetation, forest fires and microbiological processes (Kotzias *et al.,* 1997). Aldehydes are also nearly mandatory intermediates in the photo-oxidation processes of most organic compounds in the troposphere (Carlier *et al.*, 1996, Kerr and Sheppard, 1981). High concentrations are

measured in polluted urban areas as a consequence of the elevated anthropogenic emissions of aldehydes and their precursors from automobile traffic, industrial and domestic heating, and industrial activity (Carlier *et al.*, 1996, Yokouchi *et al.*, 1990). The atmospheric loss processes include photolysis, day-time reaction with OH radicals and with Cl and Br atoms in the marine boundary layer, and reaction with NO radicals during the night-time.

Based on a critical review of all experimental data the currently recommended rate coefficient for the reaction of NO_3 radicals with formaldehyde is $k_{CH2O+NO3} = 5.5 \times 10^{-16}$ cm^3 $molecule^{-1}$ s^{-1} at 298 K (http://www.iupac-kinetic.ch.cam.ac.uk/). The uncertainty factor is 1.5 ($\Delta log_{10}k = \pm 0.20$).

3.6 Preparation of samples

3.6.1 Deuterated methylamine, Di-deuteratedmethylamine and Tri-deuteratedmethylamine

Deuterated methylamine, Di-deuteratedmethylamine and Tri-deuteratedmethylamine were prepared from their analogous hyrochlorides. 1 g of the deuterated hydrochloride amine was placed in a 1 litre round-buttoned flask, fitted with a stopper holding a condenser set for downward distillation connected to a vacuum line. Then the laboratory prepared concentrated (15M) potassium hydroxide to scavenge the acid was added drop-wise while heating the mixture at 100 °C. The deuterated amine sample, free of the acid was then trapped in an ampoule at a temperature of 195 K

3.6.2 Nitramines and nitrosamines samples

Methylnitramine, dimethylnitramine, ethylnitramine, diethylnitramine, dimethylnitrosamine and diethylnitrosamine were synthesised by Prof. Stenstrøm Yngve at the Norwegian Univeristy of Life Sciences (UMB). More details on the synthesis procedures are given in appendix 9.

3.6.3 Other samples

Methylamine (assay ≥ 99 %), dimethylamine (assay ≥ 99 %), trimethylamine (assay ≥ 99 %), ethylamine (assay ≥ 99), and dimethylether (assay ≥ 99.9 %), were obtained from Fluka Analytical Germany. Methylformate (assay ≥ 97 % from Sigma Aldrich Chemie, Germany), diethylamine (assay ≥ 99.5 % from Sigma Aldrich Chemie, Germany), trimethylamine (assay ≥ 99 % from Sigma Aldrich, Belgium), formamide (assay ≥ 98 %

from Fluka chemical, Switzerland), *N*-Methylformamide (assay ≥ 99 %) and *N*-*N*-Dimethylformamide (assay ≥ 99%) from Aldrich chemistry, USA, methanol (assay ≥ 99 % from Sigma Aldrich Chemie, Germany) and ethylacetate (assay ≥ 99.5 % from Sigma Aldrich Chemie, Germany). The samples were used as received without any further treatment.

3.7 Kinetic studies

The kinetic studies were carried out by using relative rate method in a static gas mixture, in which the removals of the reacting species are measured simultaneously as a function of reaction time. Assuming that the reactants react solely with the same radical and that none of the reactants are reformed in any side reactions, the relative rate coefficient, k_{rel}, is given according to the following expression:

$$\ln\left\{\frac{[S]_0}{[S]_t}\right\} = k_{rel} \cdot \ln\left\{\frac{[R]_0}{[R]_t}\right\} \quad ; \quad k_{rel} = \frac{k_S}{k_R} \qquad \text{(Eqn. 24)}$$

where $[S]_0$, $[R]_0$, $[S]_t$ and $[R]_t$ are concentrations of the substrate and the reference compound at start and at the time t, respectively, and k_S and k_R are the corresponding rate coefficients. A plot of $\ln\{[S]_0/[S]_t\}$ vs. $\ln\{[R]_0/[R]_t\}$ will thus give the relative reaction rate coefficient $k_{rel} = k_S/k_R$ as the slope.

The experiments were carried out in a 240 L electropolished stainless steel smog chamber equipped with a White-type multiple reflection mirror system with a 120 meters optical path length for FTIR detection. All experiments were carried out in synthetic air (AGA 99.99%; CH_4, CO and NOx < 100 ppbV) at 298 ± 2 K and 1013 ± 10 hPa. The infrared spectra were recorded with a Bruker IFS 66v FTIR instrument equipped with liquid nitrogen cooled MCT detector. A total of 128 scans were co-added, each with a nominal resolution of 0.5 cm^{-1} and using boxcar apodization. Infrared spectra were recorded at regular intervals during ca. 2 hours to monitor the relative decay of the reactants. The standard experiments consisted of 8 − 20 steps of 1 − 5 minutes photolysis followed by a 1 minute waiting period and 2 minutes of data collection with the lamps turned off.

The experimental FTIR spectra were analyzed using a global non-linear least squares spectral fitting procedure (Griffith, 1996). In this method, the spectrum of the mixture of absorbing species is first simulated by calculation from initial estimates of the absorber concentrations. The calculation is then iterated to minimize the residual between the

measured and simulated spectrum using the Levenberg–Marquardt algorithm to adjust the absorber concentrations, continuum level and instrument lineshape parameters. Whenever possible, absorption coefficients are calculated from the HITRAN database (Rotham *et al.*, 2009). When HITRAN line parameter data are not available, high-resolution FTIR spectra are used to approximate the absorption coefficients. The recorded reference spectra for different compounds are presented in appendix 1. The wave number regions employed and the chemical components included in the analyses of each compound are given in Appendix 2.

The data from the independent experiments were analyzed according to eqn. 24 using a weighted least squares procedure that includes uncertainties in both reactant concentrations (York, 1966). The uncertainty in the concentration determination was taken as 1% of the initial concentration. The uncertainty in the concentration determination was taken as 1% of the initial concentration. This kind of FTIR spectra analysis has been used for years (Sellevåg *et al.*, 2004, Gola *et al.*, 2005) and proved to be robust producing reliable and trustful results.

3.8 Nitramine experiments

Each of the OH and Cl experiment was carried out several times for different mixing ratios of the nitramines and reference compounds. Initial partial pressures of the nitramines and reference compounds were in the range of 0.1 – 1.5 Pa. The stability test experiments carried out in dark in which the losses of the compounds were ascribed to their reaction with ozone were carried out only once.

3.9 Nitrosamine experiments

Kinetic studies of the NO_3 radical reactions with 2 simple nitrosamines namely; dimethylnitrosamine ($(CH_3)_2NNO$) and diethylnitrosamine ($(CH_3CH_2)_2NNO$) were carried out in the static photochemical reactor. This study aimed at providing data for a general estimation of nitrosamine reactivity towards NO_3 radical.

The experiments were repeated several times with different mixing ratios of the reactants in the range of 1 - 3 ppmV.

3.10 Measurements of infrared absorption cross-sections

The Beer-Lambert's Law defines the absorption cross section $\sigma(\tilde{\nu})$ of a compound Y at a specific wavelength $\tilde{\nu}$ as follows:-

$$\sigma(\tilde{\nu}) = {A_e(\tilde{\nu})}\Big/{n_Y l},$$ Eqn. 25

where $A_e(\tilde{\nu}) = -\ln\tau(\tilde{\nu})$ is the naperian absorbance, τ is the transmittance of a sample, n_Y is the number density of absorbers Y and l is the cell optical path length over which the absorption takes place.

The integrated absorption intensity, S_{int}, is given by:

$$S_{\text{int}} = \int_{band} \sigma(\tilde{\nu}) d\tilde{\nu} = \frac{1}{pl} \int_{band} \ln \frac{I_0}{I} dv$$ Eqn. 26

where p is the vapor pressure in the cell, l is the path length, and I_0 and I are the incident and transmitted intensities of light at frequency v.

Infrared reference spectra of samples with low vapour pressures were obtained using the reaction chamber described in section 3.2.3 above. These spectra were recorded in the 4000-600 wave number region using a Bruker IFS 66v FTIR spectrometer employing a nominal resolution of 0.25 cm^{-1}. Liquid nitrogen cooled MCT and InSb detectors were used and the light intensity was reduced to ensure linear detector response. Single channel spectra (background or sample) were recorded averaging 128 interferograms and applying a Boxcar apodization.

The absolute infrared absorption cross-section of gaseous methylamine (MA), dimethylamine (DMA) and trimethylamine (TMA) were obtained from the FT-IR spectra using the C-H stretching band region for the calibration. The integrated cross-section of the C-H stretching band region was determined by plotting the integrated absorbance intensities against the product of the number density and path length. Conservative estimates of systematic errors are: sample pressure (<5%), path length (<1%), temperature (<1%), and definition of the baseline in the integration procedure (<5%). The estimated accuracy of the absolute absorption cross- section is believed to be better than ± 7% including possible baseline offset.

The absolute cross-sections obtained are collected in Appendix 3.

4 RESULTS AND DISCUSSION

4.1 Nitramines + OH/Cl → products

All of the product and kinetic experiments were carried out in the Oslo chamber as more detailed in section 3.7. Currently there are no data in literature to compare with.

4.1.1 Methylnitramine (CH_3NHNO_2)

The reaction of CH_3NHNO_2 with OH radicals or chlorine atom principally proceeds via a hydrogen abstraction from either the -CH_3 group or the -NH group:

$$CH_3NHNO_2 + OH \rightarrow CH_2NHNO_2 + H_2O \quad \text{R43a}$$

$$\rightarrow CH_3NNO_2 + H_2O \quad \text{R43b}$$

Under the conditions in the chamber reaction (43a) is expected to proceed via the alkyl dioxy radical and the alkoxy radical to form *N*-nitro formamide, $CHONHNO_2$, or directly via hydrogen abstraction by O_2 to give *N*-nitro methanimine, $CH_2{=}NNO_2$, in analogy to the atmospheric reactions of the CH_2NH_2 and CH_3NH radicals (Nielsen *et al.*, 2011).

$$CH_2NHNO_2 + O_2 \rightarrow OOCH_2NHNO_2 \quad \text{R44a}$$

$$\rightarrow \mathbf{CH_2{=}NNO_2} + HO_2 \quad \text{R44b}$$

$$OOCH_2NHNO_2 \rightarrow CH_2{=}NNO_2 + HO_2 \quad \text{R45}$$

$$OOCH_2NHNO_2 + O_3 \rightarrow OCH_2NHNO_2 + 2O_2 \quad \text{R46}$$

$$OCH_2NHNO_2 + O_2 \rightarrow \mathbf{CHONHNO_2} + HO_2 \quad \text{R47}$$

Similarly, the CH_3NNO_2 radical is expected to lead to the *N*-nitro methanimine.

$$CH_3NNO_2 + O_2 \rightarrow CH_2{=}NNO_2 \quad \text{R48}$$

Both of these compounds are likely to have much shorter lifetimes than their parent precursor, which may explain why only weak bands attributable to organics are observed in the OH photo-oxidation experiments.

The FTIR spectra from OH initiated photo-oxidation experiments with CH_3NHNO_2 are congested (Figures 4.1.1.1 and 4.1.1.2). However, the product spectra show no indications of an N-H stretching mode but only indications of nitro-containing compound. Oxidation experiments with Cl atoms, however, reveals clear spectral features of the –$NHNO_2$ moiety, Figure 4.1.1.3. The N-H stretching mode is blue-shifted by 5 cm^{-1}, the two NO_2 stretching bands are shifted from 1611 and 1331 cm^{-1} in CH_3NHNO_2 to

1631 and 1286 cm^{-1} in the product, and a carbonyl-stretching band appears at 1763 cm^{-1}. These spectral features are consistent with *N*-nitro formamide ($CHONHNO_2$) as a major product in the photo-oxidation of methylnitramine (*N*-nitro methylamine).

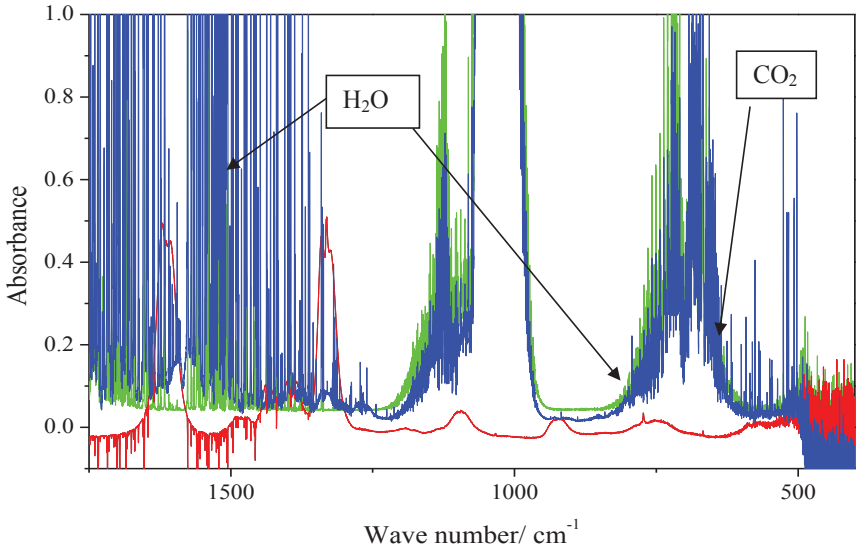

Figure 4.1.1.1. Spectrum of *N*-nitro methylamine (red), Ozone spectrum (blue), Spectrum recorded after 30 minutes of photolysis (green).

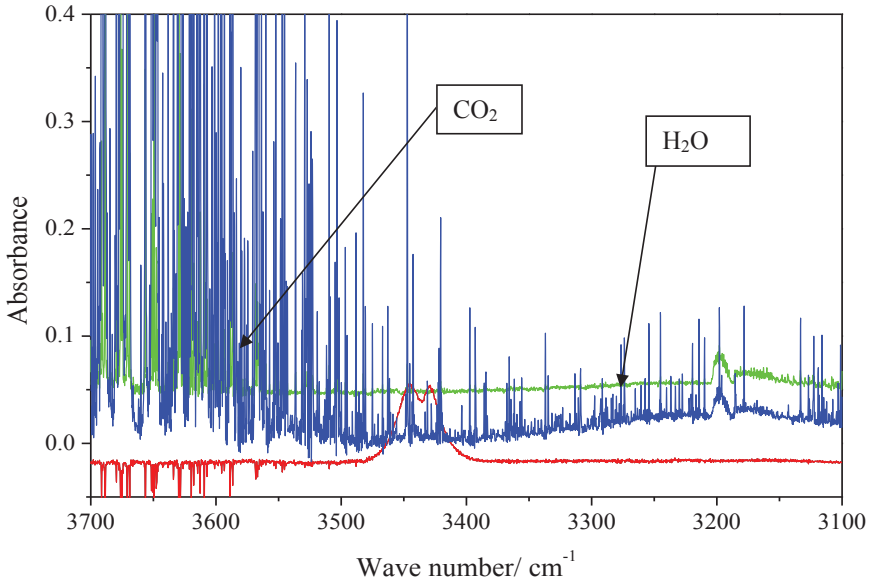

Figure 4.1.1.2. Spectrum of *N*-nitro methylamine (red), Ozone spectrum (blue), Spectrum recorded after 30 minutes of photolysis (green).

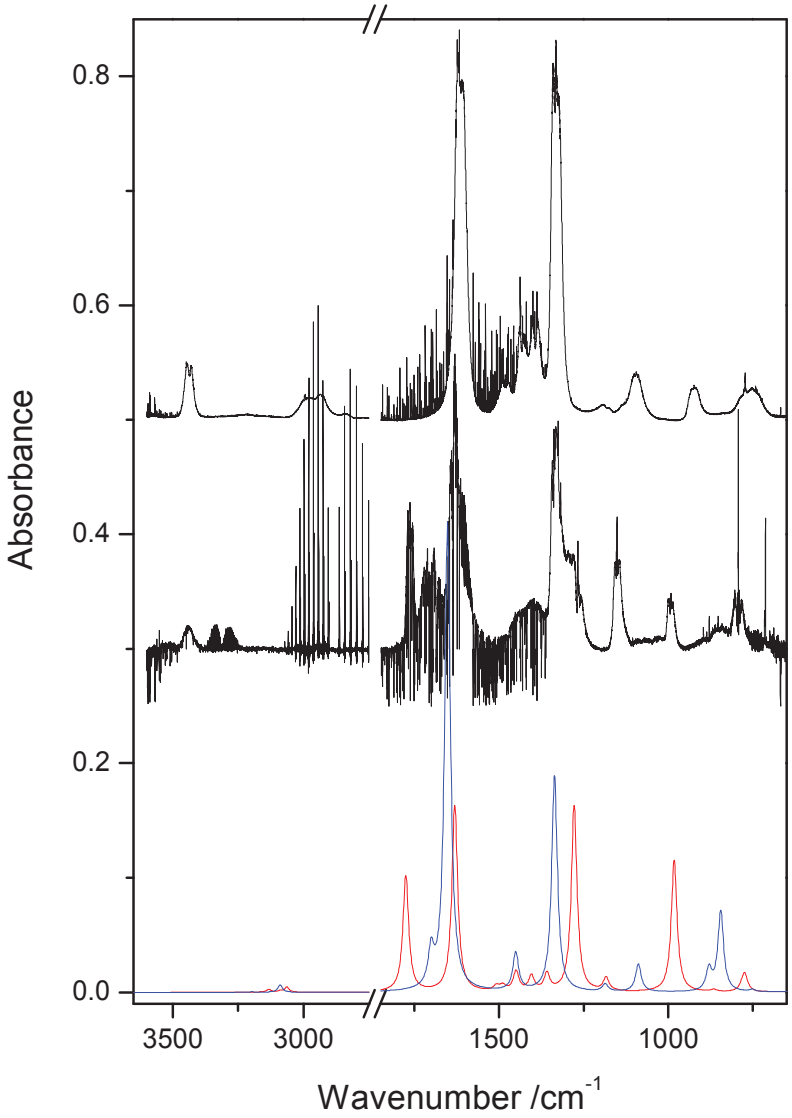

Figure 4.1.1.3. Infrared absorption spectra from Cl atom reaction with *N*-nitro methylamine. (A) Spectrum of *N*-nitro methylamine (black curve at the top). (B) Spectrum recorded after 5 min of reaction (black curve second from the top). (C) Predicted spectra of $CHONHNO_2$ (red curve) and $CH_2{=}NNO_2$ (blue curve).

4.1.2 Dimethylnitramine ($(CH_3)_2NNO_2$)

Figure 4.1.2.1 shows and example of the spectral analysis behind the kinetic results. The reaction of $(CH_3)_2NNO_2$ with OH radicals is expected to proceed via hydrogen

abstraction from the -CH_3 group eventually leading to *N*-nitro,*N*-methyl formamide, $CHO(CH_3)NNO_2$.

$(CH_3)_2NNO_2 + OH \rightarrow CH_2(CH_3)NNO_2 + H_2O$ R49

$CH_2(CH_3)NNO_2 + O_2 \rightarrow OOCH_2(CH_3)NNO_2$ R50

$OOCH_2(CH_3)NNO_2 + O_3 \rightarrow OCH_2(CH_3)NNO_2 + 2O_2$ R51

$OCH_2(CH_3)NNO_2 + O_2 \rightarrow \mathbf{CHO(CH_3)NNO_2} + HO_2$ R52

Oxidation experiments with Cl atoms confirm the spectral features that are attributed to *N*-methyl,*N*-nitro formamide, Figure 4.1.2.2.

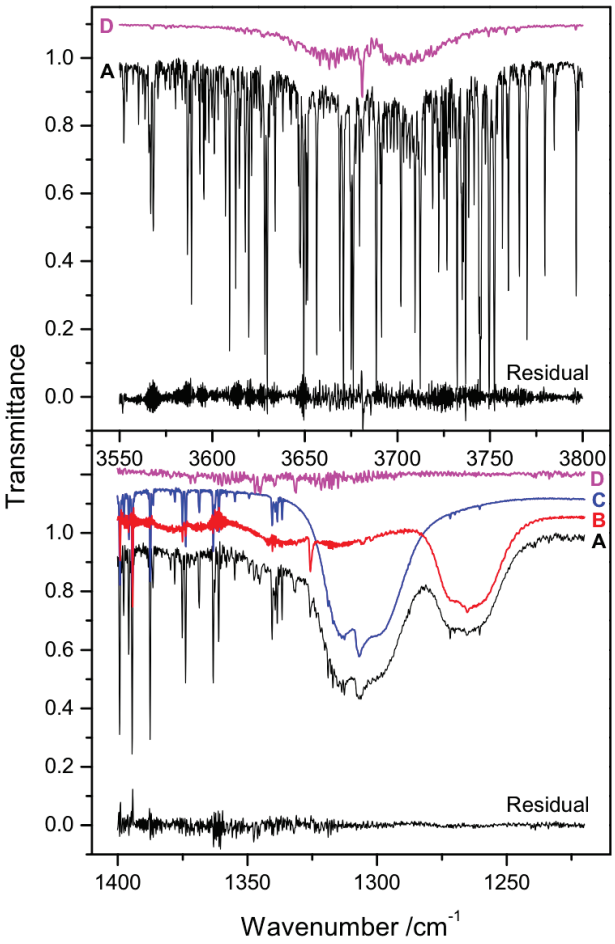

Figure 4.1.2.1. Infrared transmission spectra of (A) the *N*-nitro dimethylamine/methanol/O_3/H_2 reaction mixture after 12 minutes photolysis, (B) *N*-nitro,*N*-methyl formamide, (C) *N*-nitro

dimethylamine, (D) methanol, and the residual after spectral fitting. The spectra (B)-(D) have been shifted for the sake of clarity.

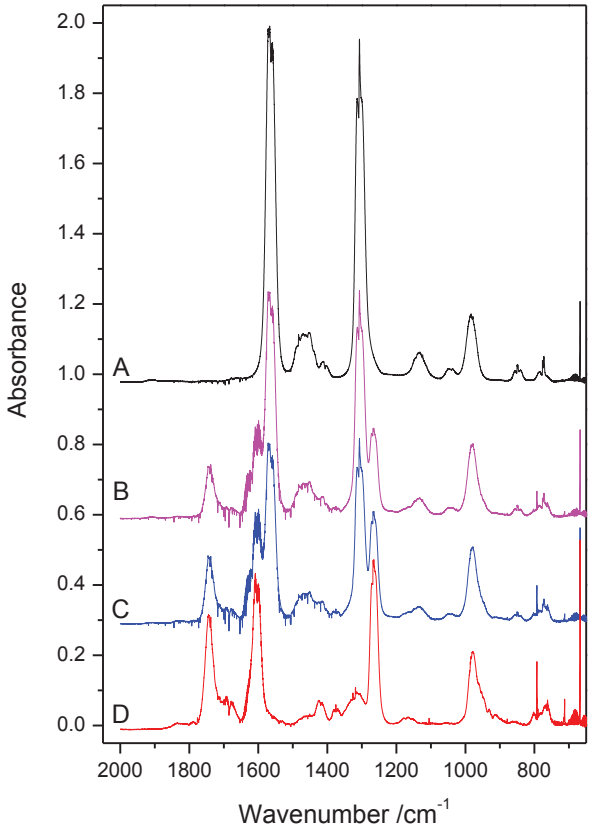

Figure 4.1.2.2. Infrared absorption spectra from Cl atom reaction with *N*-nitro dimethylamine. (A) Spectrum of *N*-nitro dimethylamine. (B)-(D) Spectra recorded after 5, 10 and 15 minutes of reaction.

4.1.3 Ethylnitramine ($CH_3CH_2NHNO_2$)

FTIR spectra from the photooxidation of ethylnitramine initiated by OH radicals/ Cl atoms are presented in Figures 4.1.3.1 and 4.1.3.2. In both experiments, a peak was observed at 2260 – 2220 cm^{-1} (Figure 4.1.3.1) which corresponds to C≡N stretching. This indicates the presence of a nitrile compound which is likely to be acetonitrile.

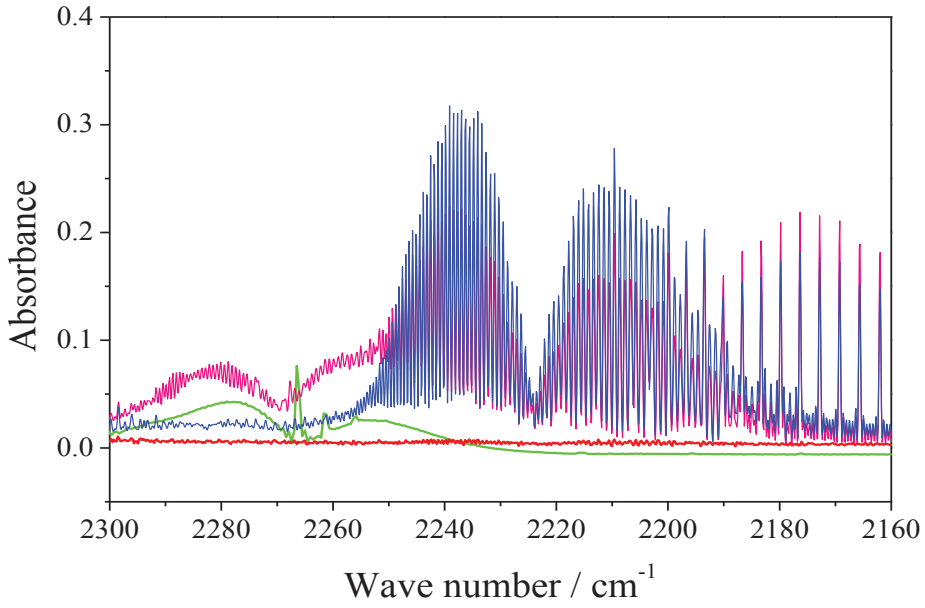

Figure 4.1.3.1. $(CH_3CH_2)_2NNO_2$ spectrum (Red), $(CH_3CH_2)_2NNO_2$ + OH after 45 minutes of photolysis (blue), $(CH_3CH_2)_2NNO_2$ + Cl after 74 minutes of photolysis (pink), Acetonitrile spectrum (green)

The photooxidation with OH generated a weak peak at 1740 cm^{-1} (Figure 4.1.3.2) while the Cl initiated photooxidation generated a visible band at the same wave number which is a C=O band characteristic for aldehydes. The suspected compound here is acetaldehyde.

The amide C=O band located at 1680 was also detected (Figure 4.1.3.2) particularly in Cl experiments while the OH experiment did not show this band. Also a band at 1690 in the Cl experiment spectrum can be ascribed to C=N stretch in imines. Thus these two bands indicate the presence of an amide and imine. The suspect compounds here are acetamide and ethanimine respectively.

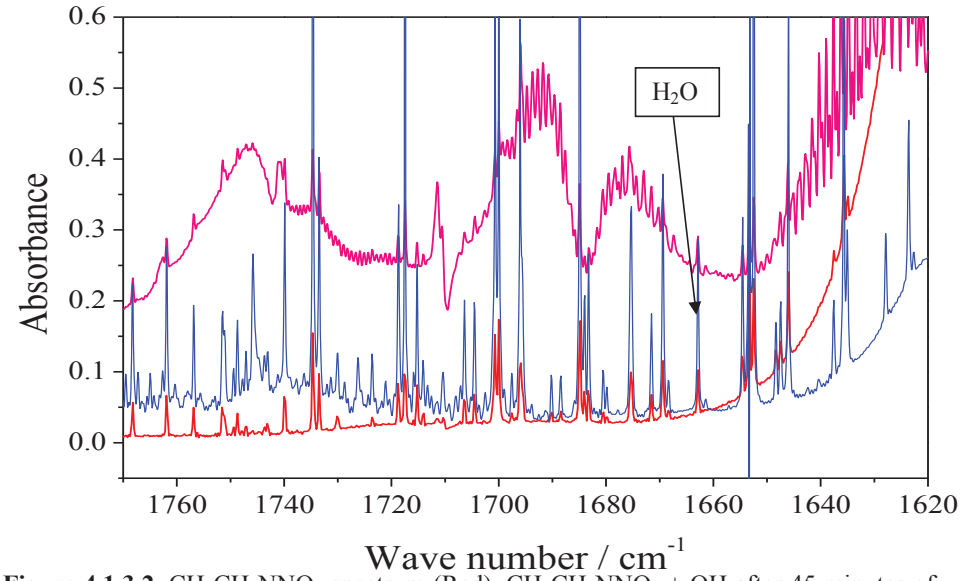

Figure 4.1.3.2. $CH_3CH_2NNO_2$ spectrum (Red), $CH_3CH_2NNO_2$ + OH after 45 minutes of photolysis (blue), $CH_3CH_2NNO_2$ + Cl after 74 minutes of photolysis (pink).

The observations in this study confirm the results obtained in the study by Nielsen *et al.,* (2011) in which the PTR-TOF-MS was used. In that study they detected a compound with m/z 42.0341 (42.0354) which seemed to correspond to the ion sum formula $C_2H_4N^+$ that most likely stemed from acetonitrile. These findings suggest a reaction mechanism in which H-abstraction from the CH_2-group takes place followed by RNH–NO_2 scission:

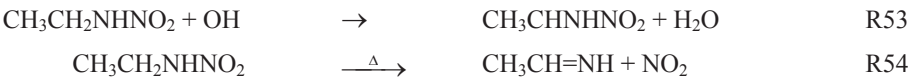

The ethanimine formed in reaction 54 (R54) will then undergo further reactions leading to the formation of acetonitrile (CH_3CN) and acetamide ($CH_3C(O)NH_2$).

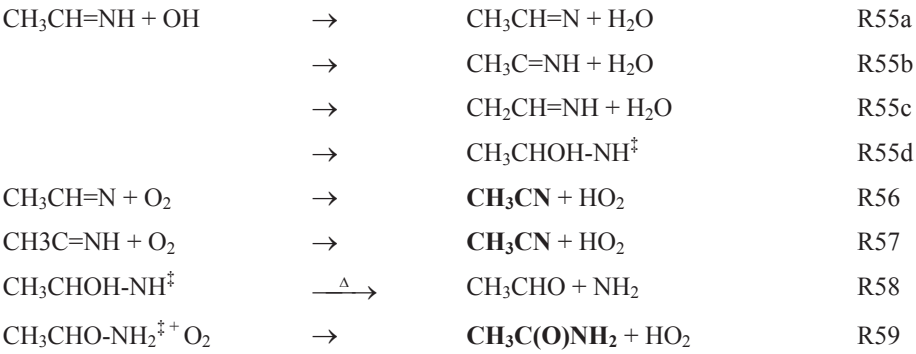

4.1.4 Diethylnitramine ($(CH_3CH_2)_2NNO_2$)

The reaction mechanism of diethylnitramine is assumed to follow the same trend as that of ethylnitramine, leading to the formation of a nitrile, aldehyde and amide with intermidiate formation of an imine.

FTIR spectra from the photooxidation of diethylnitramine initiated by OH radicals/ Cl atoms are presented in Figures 4.1.4.1 and 4.1.4.2. In both experiments, a peak was observed at 2260 – 2220 cm^{-1} (figure 4.1.4.1) which corresponds to C≡N stretching. This indicates the presence of a nitrile compound which is likely to be acetonitrile.

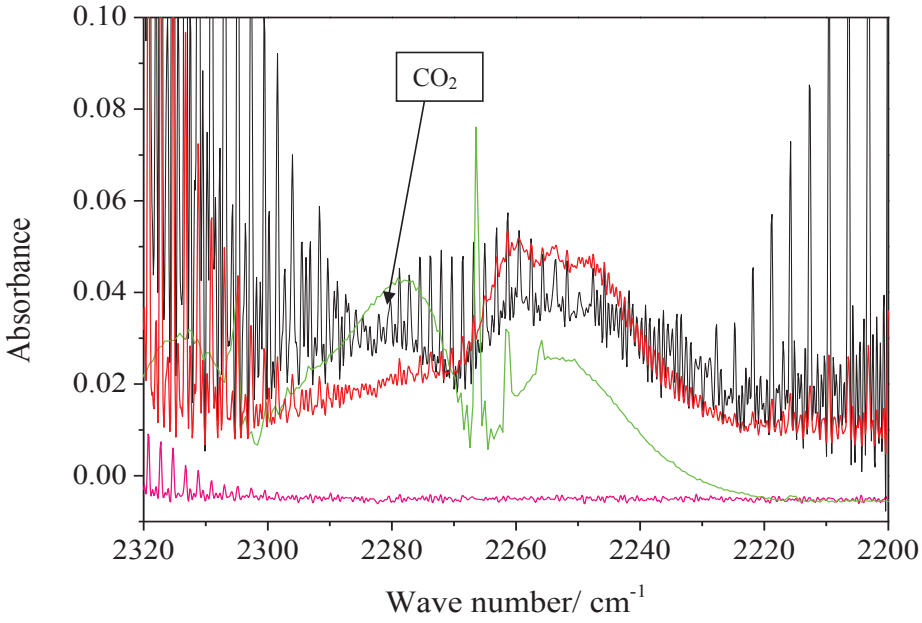

Figure 4.1.4.1. $(CH_3CH_2)_2NNO_2$ spectrum (pink), $(CH_3CH_2)_2NNO_2$ + OH spectrum recorded after 45 minutes of photolysis (black), $(CH_3CH_2)_2NNO_2$ + Cl spectrum recorded after 45 minutes of photolysis (red), Acetonitrile spectrum (green).

FTIR spectra from both OH (a bit noisy) and Cl initated photooxidation experiments showed a band at 1740 cm^{-1} (Figure 4.1.4.2) which is linked to alphatic aldehydes. The possible compound here is acetaldehyde. Spectrum from OH experiment showed a weak and noisy band at 1690 cm^{-1} while that of Cl experiment showed a clear band at the same wave number (Figure 4.1.4.3). This band is linked to C=N stretch for imines suggesting the presence of *N*-ethyl ethanimine.

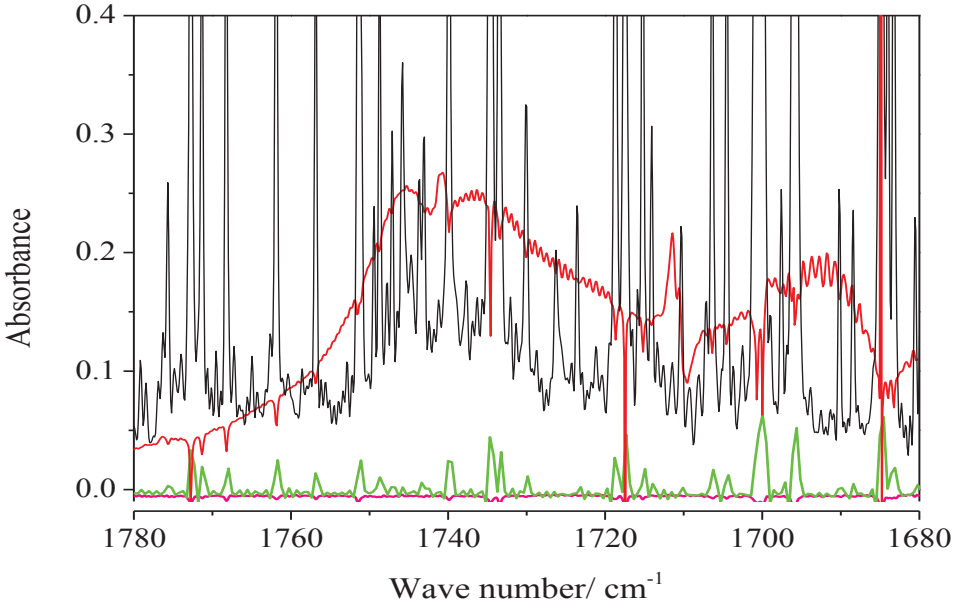

Figure 4.1.4.2. $(CH_3CH_2)_2NNO_2$ spectrum (pink), $(CH_3CH_2)_2NNO_2$ + OH spectrum recorded after 45 minutes of photolysis (black), $(CH_3CH_2)_2NNO_2$ + Cl spectrum recorded after 45 minutes of photolysis (red), Acetonitrile spectrum (green).

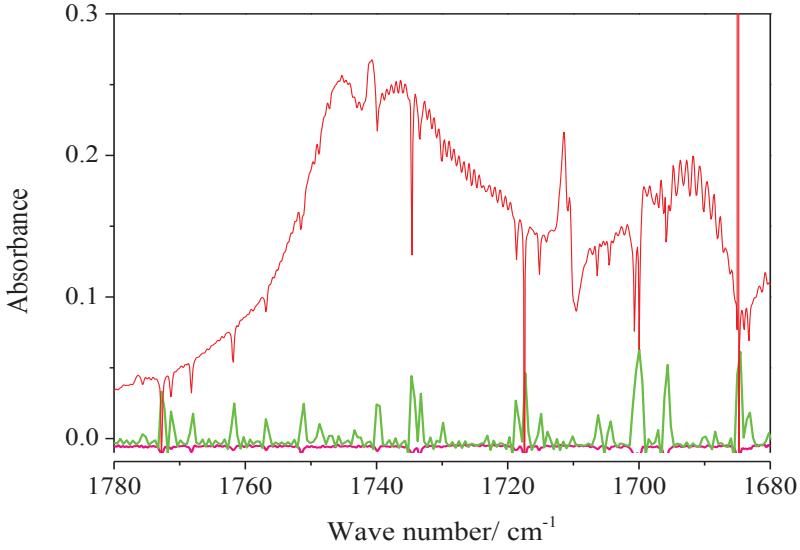

Figure 4.1.4.3. $(CH_3CH_2)_2NNO_2$ spectrum (pink), $(CH_3CH_2)_2NNO_2$ + Cl spectrum recorded after 45 minutes of photolysis (red), Acetonitrile spectrum (green).

Nielsen *et al.,* (2011) using PTR-TOF-MS detected a compound with m/z 42.0350 (42.0356) which corresponds to the ion sum formula $C_2H_4N^+$ that most likely stem from acetonitrile. The m/z 72.0831 (72.0841) corresponding to the ion $C_4H_{10}N+$, which most likely stem from *N*-ethyl ethanimine, $CH_3CH_2N{=}CHCH_3$.was also detected. This confirms the compounds observed in this study.

Table 4.1.1: Summary of the products from the OH/Cl initiated photooxidation of nitramines.

Nitramine	Products
Methylnitramine	*N*-nitro formamide ($CHONHNO_2$), *N*-nitro methanimine ($CH_2{=}NNO_2$)
Dimethylnitramine	*N*-methyl,*N*-nitro formamide ($CHON(CH_3)NO_2$
Ethylnitramine	Acetonitrile (CH_3CN), Acetaldehyde (CH_3CHO), Acetamide ($CH_3C(O)NH_2$, Ethanimine ($CH_3CH{=}NH$)
Diethylnitramine	Acetonitrile (CH_3CN), *N*-ethylethanimine ($CH_3CH_2N{=}CHCH_3$)

4.2 Formamide ($CHONH_2$) photo-oxidation studies

As it was for the nitramines, OH initiated photo-oxidation experiments for formamide were carried out in the reaction chamber employing FT-IR detection. The FT-IR spectra, Figure 4.2.1, identified the product as isocyanic acid, HNCO. Barnes *et al.,* (2010) also reported HNCO as the only product in NOx-free photo-oxidation of formamide.

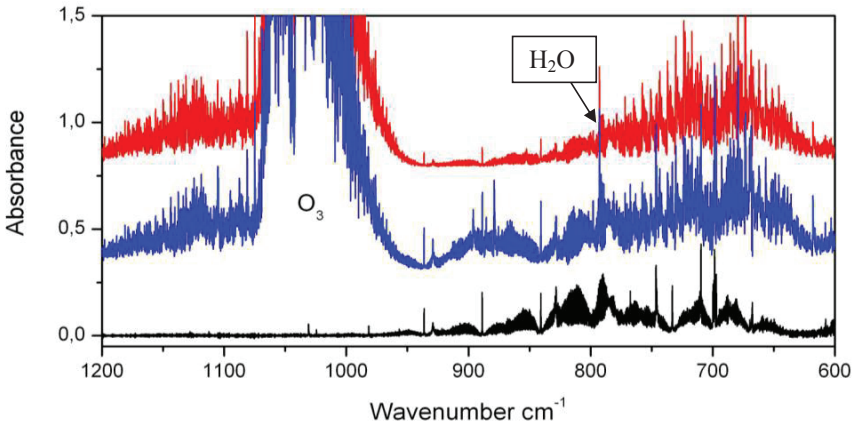

Figure 4.2.1. Infrared spectra of the 1200-600 cm^{-1} region of a formamide / O_3 /H_2 mixture during a photo-oxidation experiment. Red curve, after 1 min. photolysis; blue curve, after 5 min. photolysis; black curve, reference spectrum of isocyanic acid (HNCO).

There are two possible sites for the initial H-abstraction from formamide, **Scheme 4.2.1**, both leading to the same final product. The C-H abstraction is expected to be the dominant route in the OH reaction with formamide.

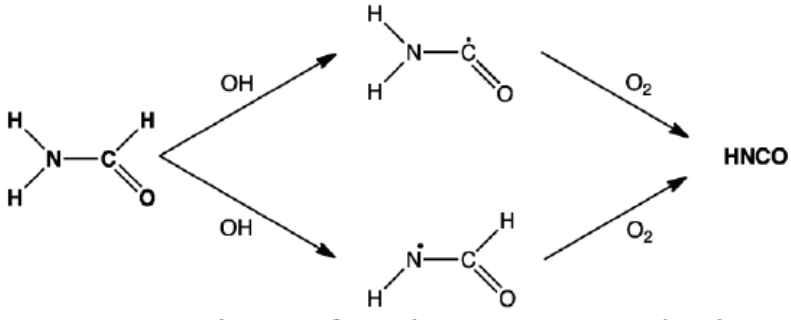

Scheme 4.2.1 Reaction scheme for the OH initiated photo-oxidation of formamide.

4.3 Kinetic experimental results and lifetime calculations for nitramines and nitrosamines

The relative rate method, in which the removal rates of the reacting species are measured simultaneously as a function of reaction, was employed in the studies of hydroxyl radicals (OH), chlorine atom (Cl) and ozone (O_3) kinetics with nitramines as well as the nitrate radical (NO_3) kinetics with nitrosamines. The kinetic analysis according to equation 24 makes an assumption that only one loss process is taking place due to the fact that, other loss processes such as gas-phase or surface reactions with the radical precursors will lead to systematic errors in the relative rates.

4.3.1 Nitramines +O_3

Before performing the relative kinetic studies of the nitramines with OH radicals, their stabilities together with those of the reference compounds in dark in the presence of hydrogen gas and ozone were investigated. Figures 4.3.1.1 to 4.3.1.7 show the observed decays for a period of two hours for the four studied nitramines and the used reference compounds.

The observed increased decays of these compounds were attributed to their reaction with O_3 and hence the following rate coefficients were determined: $k_{O3+CH3NHNO2} = 3 \times 10^{-21}$, $k_{O3+(CH3)2NNO2} = 2 \times 10^{-21}$, $k_{O3+CH3CH2NHNO2} = 4 \times 10^{-21}$, $k_{O3+(CH3CH2)2NNO2} = 2 \times 10^{-21}$, $k_{O3+CH3COOCH2CH3} = 5 \times 10^{-22}$, $k_{O3+CH3OCH3} = 3 \times 10^{-22}$ and $k_{O3+CH3OH} = 2 \times 10^{-21}$ cm^3 $molecule^-$

$^{1}s^{-1}$. In the determination of these rate coefficients, the data were fitted to an exponential decay.

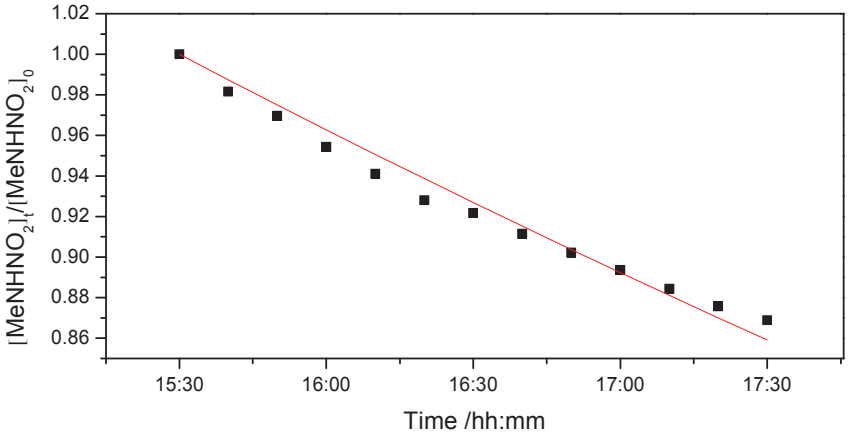

Figure 4.3.1.1. Stability of CH_3NHNO_2 in the reaction chamber under dark conditions in the presence of H_2, O_3 and synthetic air. The observed gas phase loss of CH_3NHNO_2 corresponds to a rate constant $k_{O3+CH3NHNO2} = 3 \times 10^{-21}$ cm^3 $molecule^{-1}$ s^{-1}.

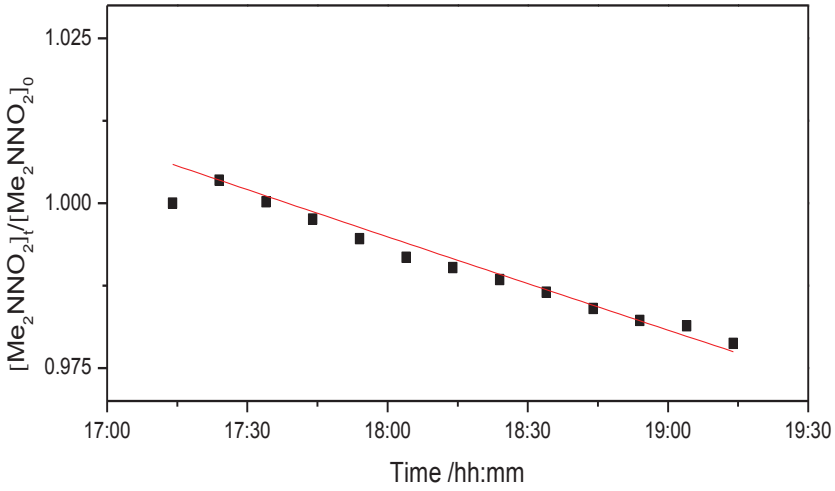

Figure 4.3.1.2. Stability of $(CH_3)_2NNO_2$ in the reaction chamber under dark conditions in the presence of H_2, O_3 and synthetic air. The observed gas phase loss of $(CH_3)_2NNO_2$ corresponds to a $k_{O3+(CH3)2NNO2} = 2 \times 10^{-21}$ cm^3 $molecule^{-1}$ s^{-1}.

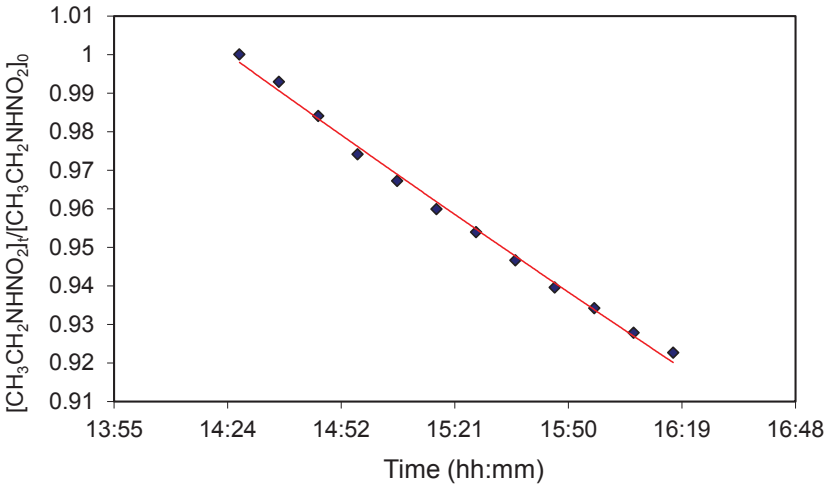

Figure 4.3.1.3. Stability of $CH_3CH_2NHNO_2$ in the reactions chamber under dark conditions in the presence of H_2, O_3 and synthetic air. The observed gas phase loss of $CH_3CH_2NHNO_2$ corresponds to a rate constant $k_{O3+CH3CH2NHNO2} = 4 \times 10^{-21}$ cm^3 molecule^{-1} s^{-1}.

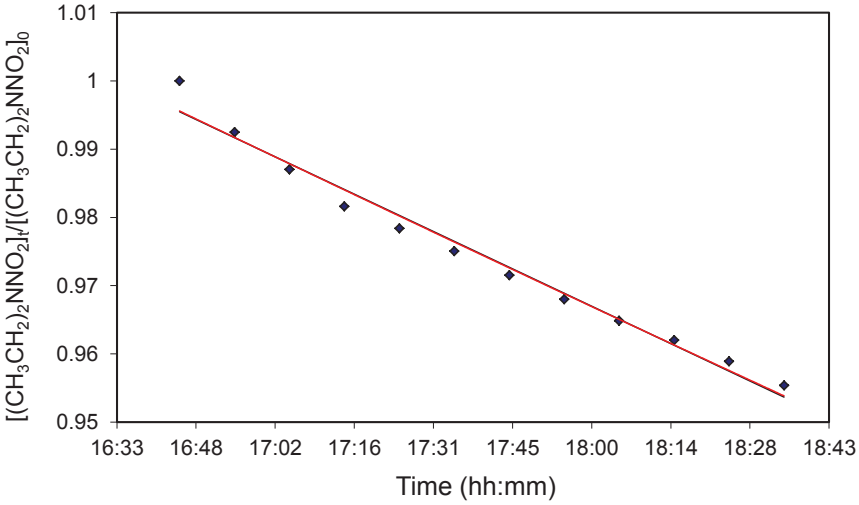

Figure 4.3.1.4. Stability of $(CH_3CH_2)_2NNO_2$ in the reactions chamber under dark conditions in the presence of H_2, O_3 and synthetic air. The observed gas phase loss of $(CH_3CH_2)_2NNO_2$ corresponds to a rate constant $k_{O3+(CH3CH2)2NNO2} = 2 \times 10^{-21}$ cm^3 molecule^{-1} s^{-1}.

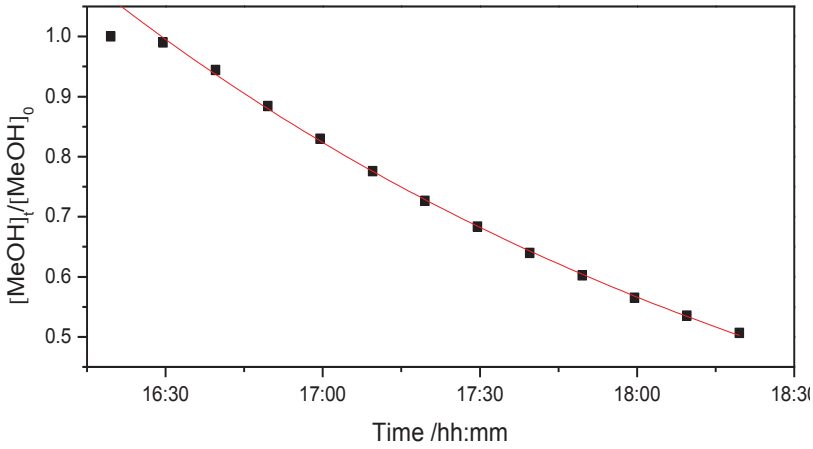

Figure 4.3.1.5. Stability of CH_3OH in the reactions chamber under dark conditions in the presence of H_2, O_3 and synthetic air. The observed gas phase loss of CH_3OH corresponds to a rate constant $k_{O3+CH3OH} = 2 \times 10^{-21}$ cm^3 $molecule^{-1}$ s^{-1}.

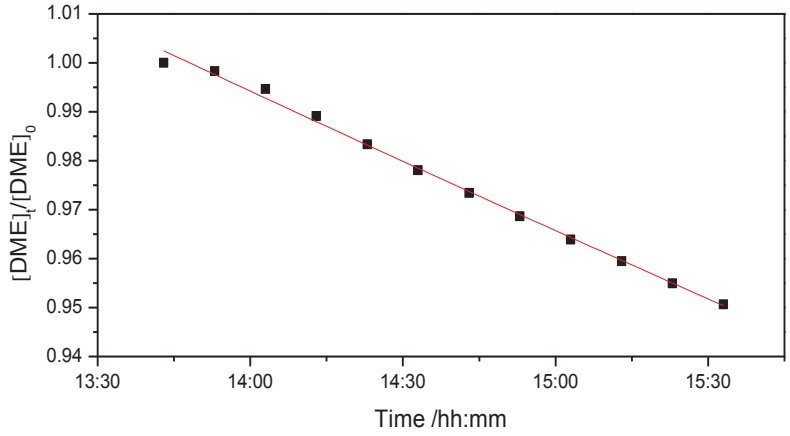

Figure 4.3.1.6. Stability of CH_3OCH_3 (DME) in the reaction chamber under dark conditions in the presence of H_2, O_3 and synthetic air. The observed gas phase loss of DME corresponds to rate constant $k_{O3+CH3OCH3} = 3 \times 10^{-22}$ cm^3 $molecule^{-1}$ s^{-1}.

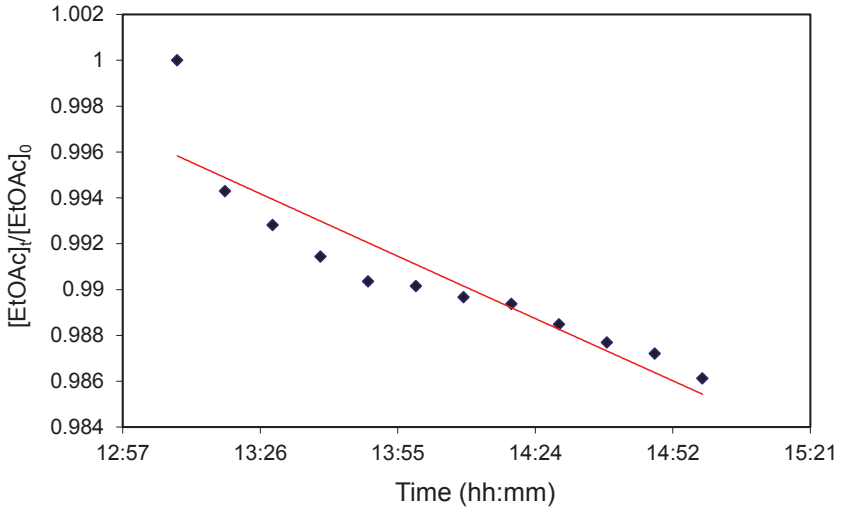

Figure 4.3.1.7. Stability of Ethylacetate ($CH_3C(O)OCH_2CH_3$) in the reactions chamber under dark conditions in the presence of H_2, O_3 and synthetic air. The observed gas phase loss of $CH_3COOCH_2CH_3$ corresponds to a rate constant $k_{O3+CH3COOCH2CH3} = 5 \times 10^{-22}$ cm^3 molecule^{-1} s^{-1}.

Table 4.3.1.1. Experimental rate constants at 298 K for the reactions of O_3 with nitramines, and the estimated lifetimes of nitramines with respect to their reaction with O_3.

Compound	k_{O3}/ cm^3 molecule^{-1} s^{-1}	Reference	Lifetime (τ_{O3})*	Lifetime (τ_{O3})**
CH_3NHNO_2	3×10^{-21}	This work	11 years	4 years
$(CH_3)_2NNO_2$	2×10^{-21}	This work	16 years	6 years
	$\leq 3 \times 10^{-21}$	Tuazon *et al.*, 1984	11 years	4 years
$CH_3CH_2NHNO_2$	4×10^{-21}	This work	8	3 years
$(CH_3CH_2)_2NNO_2$	2×10^{-21}	This work	16 years	6 years

*With a global average concentration of 40 ppb (9.84×10^{11} cm^{-3}) O_3 (Acid Deposition and Oxidant Research Centre, 2006)

**With a global average concentration of 100 ppb (2.46×10^{12} cm^{-3}) O_3 (Finlayson-Pitts and Pitts Jr. 2000).

As can be seen from table 4.3.1.1, the lifetimes of nitramines with respect to their reaction with ozone are in terms of years. Thus, reaction with ozone will not constitute an important pathway for loss of nitramines in the atmosphere.

Even in a situation with extremely high O_3 = 100 ppb (Finlayson-Pitts and Pitts Jr. 2000), the lifetime of nitramines with respect to reaction with O_3 is still of no importance.

4.3.2 Nitramines +OH

The photo-stability of the nitramines in the Oslo chamber without the presence of O_3 was investigated in separate experiments, and no significant loss of the compound was observed.

The relative experiments using OH as an oxidant lasted for 2 hours which included spectral recording and waiting time between the photolysis, during which more than 90% of the initial nitramine reacted. The losses of $CH_3CH_2NHNO_2$, $(CH_3)_2NNO_2$ $(CH_3CH_2)_2NNO_2$, CH_3OCH_3, and $CH_3COOCH_2CH_3$ with respect to reaction with O_3 in the chamber in relation to the time span of the relative rate experiments as can be seen from the plots in section 4.3.1 were minimal and hence can be neglected. For CH_3NHNO_2, and CH_3OH the additional loss due to reaction with O_3 was significant and the relative rate experiments were therefore analyzed according to equation 27. The relative importance of the O_3 correction was to substract the reaction due to the presence of ozone inorder to get the exact reaction rate coefficient due to OH reaction with the nitramines. Figure 4.3.2.1.4 shows an example of the experiment without correction with error bars on the points. The figure demonstrates that the points are further away from the regression line than the estimated errors.

$$\ln\left\{\frac{[S]_0}{[S]_t}\right\} - k_{O3+S}\cdot\int_0^t [O_3]\cdot dt = k_{rel}\cdot\left\{\ln\left\{\frac{[R]_0}{[R]_t}\right\} - k_{O3+R}\cdot\int_0^t [O_3]\cdot dt\right\} \quad ; \quad k_{rel} = \frac{k_S}{k_R} \qquad \text{Eqn. 27}$$

4.3.2.1 Methylnitramine (CH_3NHNO_2) + OH

Examples of the FTIR spectra obtained from the kinetic studies of the CH_3NHNO_2/CH_3OCH_3 and $(CH_3)_2NNO_2/CH_3OCH_3$ reactions with OH radicals and the resulting residuals from the non-linear least squares spectral analyses are shown in Figures 4.3.2.1.1 and 4.3.2.1.2 respectively. The only product band appearing in the spectra during the reaction stem is from methyl formate (CH_3OCHO) which is the product of the oxidation of dimethyl ether.

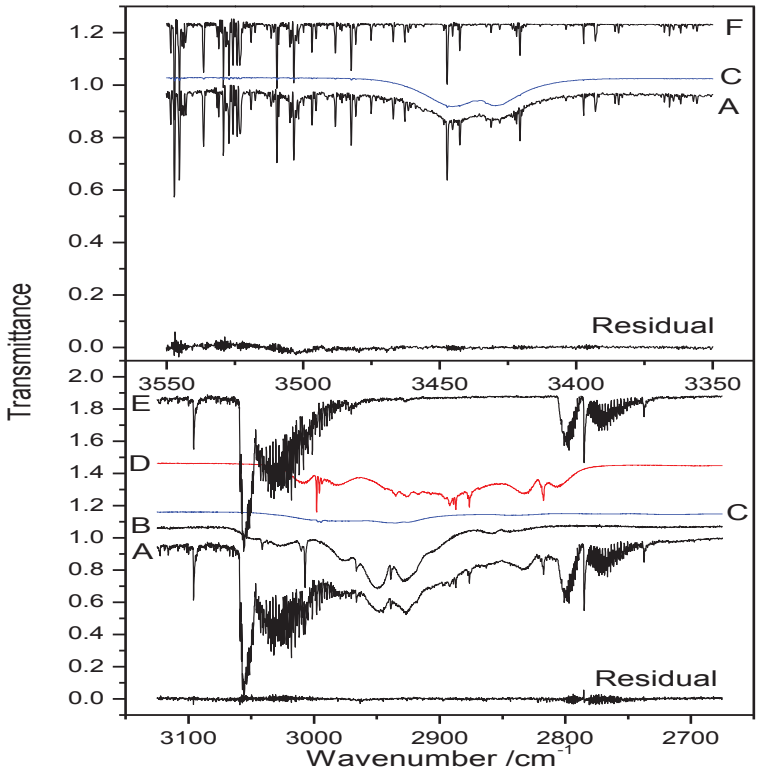

Figure 4.3.2.1.1. Infrared transmission spectra of (A) the $CH_3NHNO_2/CH_3OCH_3/H_2/O_3$ reaction mixture after 15 min photolysis, (B) CH_3OCHO, (C) CH_3NHNO_2, (D) CH_3OCH_3, (E) O_3 and (F) H_2O. The spectra (B) - (F) have been shifted for the sake of clarity.

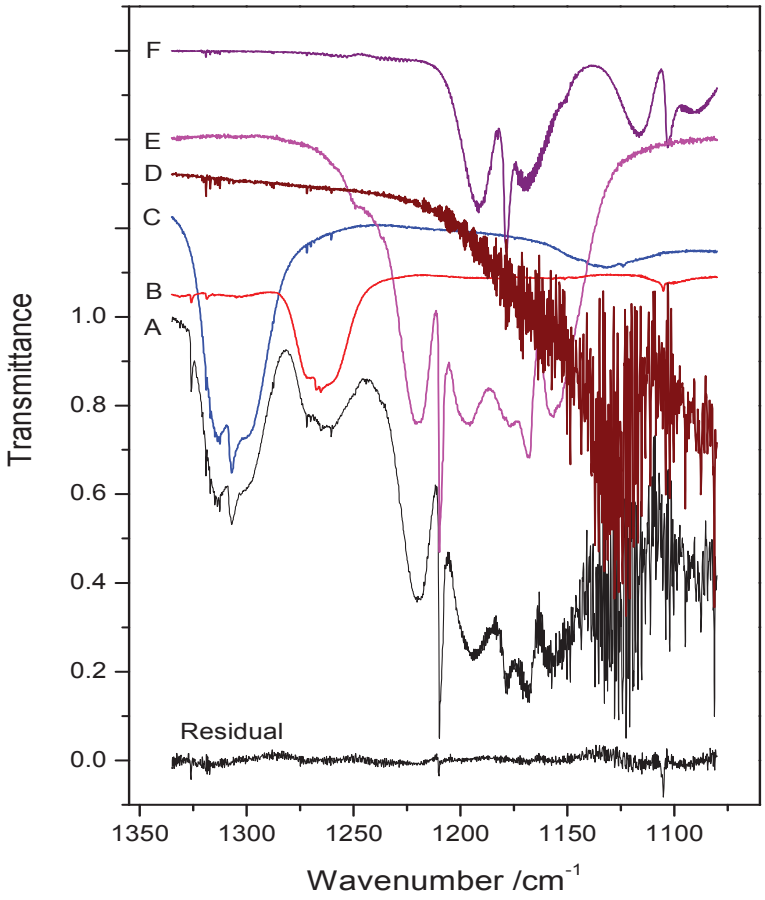

Figure 4.3.2.1.2. Examples of the FTIR spectra obtained during the kinetic studies of the $(CH_3)_2NNO_2/CH_3OCH_3$ reaction with OH radical. Infrared transmission spectra of (A) the *N*-nitro dimethylamine/dimethyl ether/O_3/H_2 reaction mixture after 12 minutes photolysis, (B) *N*-nitro,*N*-methyl formamide, (C) *N*-nitro dimethylamine, (D) ozone, (E) methyl formate, (F) dimethyl ether, and the residual after spectral fitting. The spectra (B) - (F) have been shifted for the sake of clarity.

Spectra from the CH_3NHNO_2/CH_3OH + OH experiments are shown in Figure 4.3.2.1.3. The decays of CH_3NHNO_2 and CH_3OH in the presence of OH radicals are plotted as $\ln\{[CH_3NHNO_2]_0/[CH_3NHNO_2]_t\}$ *vs*. $\ln\{[CH_3OH]_0/[CH_3OH]_t\}$ in Figures 4.3.2.1.4 (without correction for loss due to reaction with O_3) and 4.3.2.1.5 (with correction for loss due to reaction with O_3) while Figure 4.3.2.1.6 shows a similar plot of the CH_3NHNO_2 and CH_3OCH_3 decays in the presence of OH radicals. Least–squares fitting of the data resulted in the following relative rates (2σ statistical error limits): $k_{OH+CH_3NHNO_2}/k_{OH+CH_3OCH_3} = 0.304 \pm 0.014$, $k_{OH+CH_3NHNO_2}/k_{OH+CH_3OH} = 1.164 \pm 0.016$.

Taking today's recommended values for $k_{OH+CH_3OCH_3} = 2.8 \times 10^{-12}$ and $k_{OH+CH_3OH} = 9.0 \times 10^{-13}$ cm^3 molecule^{-1} s^{-1} (Atkinson *et al.*, 2006) yields $k_{OH+CH_3NHNO_2} = (0.85 \pm 0.17) \times 10^{-12}$ and $(1.05 \pm 0.21) \times 10^{-12}$ cm^3 molecule^{-1} s^{-1} respectively, at 298 K. An average of these two values obtained from the two different reference compounds gives a best value for $k_{OH+CH_3NHNO_2} = (9.5 \pm 1.9) \times 10^{-13}$ cm^3 molecule^{-1} s^{-1} at 298 K with an assumption that there were no additional molecule specific systematic errors.

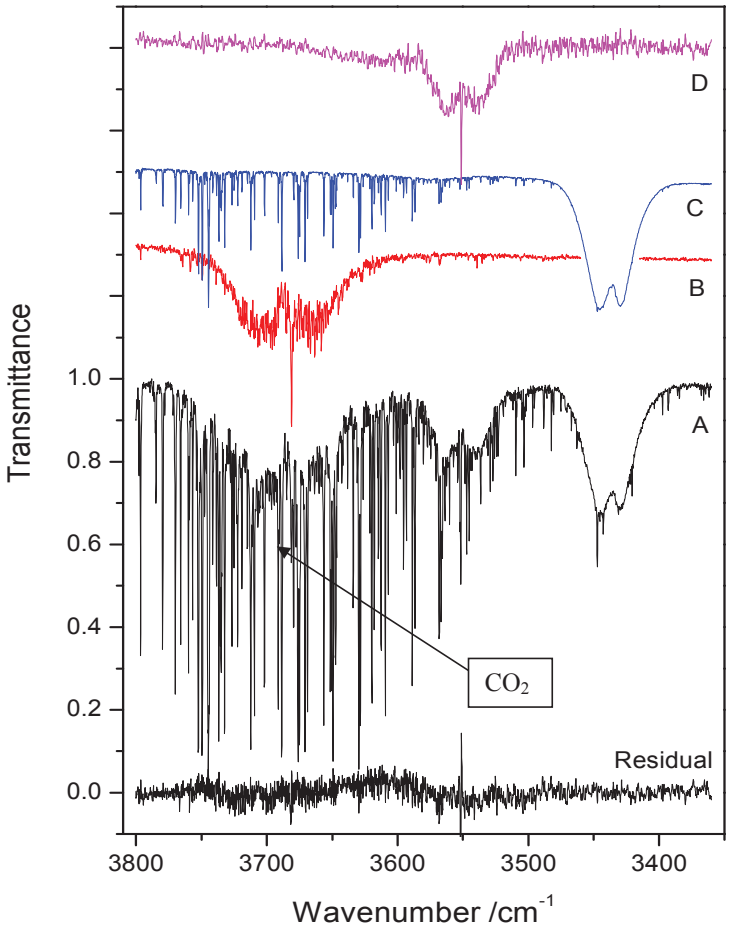

Figure 4.3.2.1.3. Examples of the FTIR spectra obtained during the kinetic studies of the CH_3NHNO_2/CH_3OH reaction with OH radicals. Infrared transmission spectra of (A) the *N*-nitro methylamine/methanol/O_3/H_2 reaction mixture after 12 minutes photolysis, (B) methanol, (C) *N*-nitro methylamine, (D) nitric acid, and the residual after spectral fitting. The spectra (B) - (D) have been shifted for the sake of clarity.

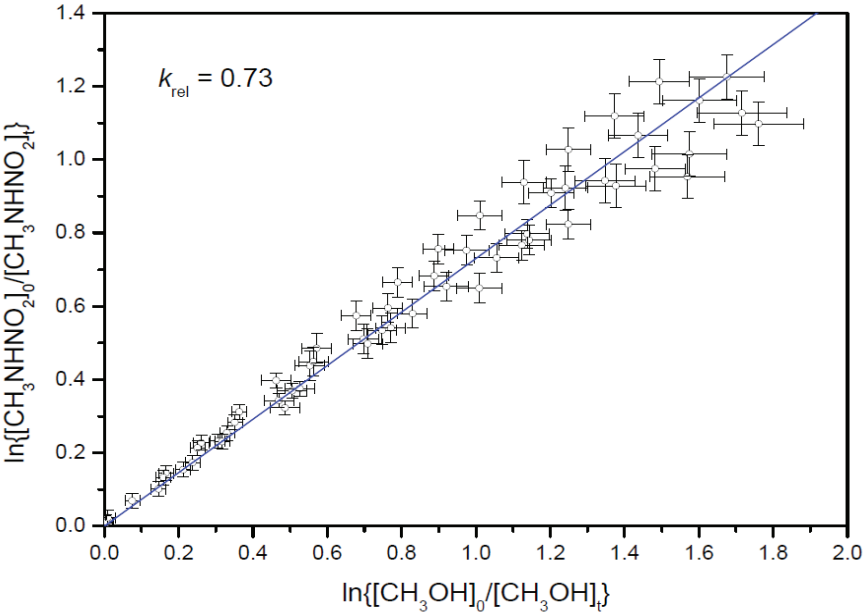

Figure 4.3.2.1.4. Relative rate plot showing the decay of CH_3NHNO_2 *vs*. CH_3OH at 1013 hPa and 298 K in the presence of OH radicals; k_{rel} = 0.73 ± 0.016 (2σ) determined from 49 data points from 9 independent experiments. The data have not been corrected for loss due to reaction with O_3.

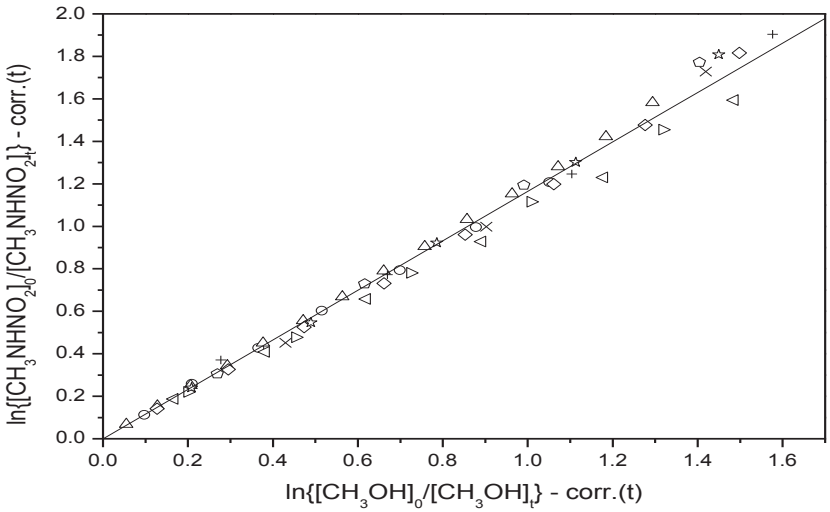

Figure 4.3.2.1.5. Relative rate plot showing the decay of CH_3NHNO_2 *vs*. CH_3OH at 1013 hPa and 298 K in the presence of OH radicals; k_{rel} = 1.164 ± 0.016 (2σ) determined from 49 data points from 9 independent experiments. The data have been corrected for loss due to reaction with O_3.

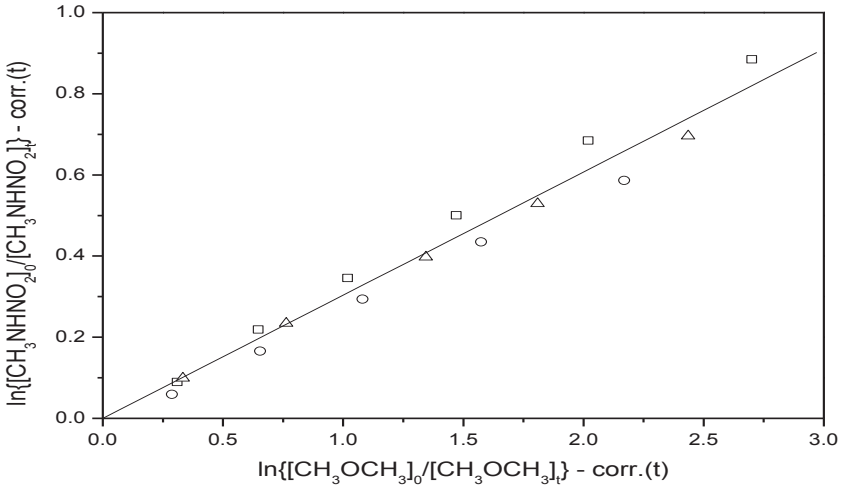

Figure 4.3.2.1.6. Relative rate plot showing the decays of CH_3NHNO_2 and CH_3OCH_3 at 1013 hPa and 298 K in the presence OH radicals; k_{rel} = 0.304 ± 0.014 (2σ) determined from 16 data points from 3 independent experiments. The data have been corrected for loss due to reaction with O_3.

4.3.2.2 Dimethylnitramine [$(CH_3)_2NNO_2$] + OH

Examples of the FTIR spectra obtained from the kinetic studies of the $(CH_3)_2NNO_2/CH_3OH$ reaction with OH radicals and the resulting residuals from the non-linear least squares spectral analyses are shown in Figure 4.1.2.1 (section 4.1.2**)**. The decays of $(CH_3)_2NNO_2$ and CH_3OCH_3 in the presence of OH radicals are plotted as $\ln\{[(CH_3)_2NNO_2]_0/[(CH_3)_2NNO_2]_t\}$ *vs*. $\ln\{[CH_3OCH_3]_0/[CH_3OCH_3]_t\}$ in Figure 4.3.2.2.1, while Figure 4.3.2.2.2 shows a similar plot for the $(CH_3)_2NNO_2$ and CH_3OH decays in the presence of OH radicals. Least–squares fitting of the data resulted in the following relative rates (2σ statistical error limits): $k_{OH+(CH_3)_2NNO_2}/k_{OH+CH_3OCH_3}$ = 1.246 ± 0.015, $k_{OH+(CH_3)_2NNO_2}/k_{OH+CH_3OH}$ = 3.83 ± 0.04. This places $k_{OH+(CH_3)_2NNO_2}$ at (3.85 ± 0.7) × 10^{-12} and (3.45 ± 0.7) × 10^{-12} cm^3 $molecule^{-1}$ s^{-1} respectively at 298 K. Assuming no other molecule specific systematic errors and including the uncertainty factors in the reference rate constant values, then the average of these two rate constants obtained in the present experiments using two different reference compounds gives the best value for $k_{OH+(CH_3)_2NNO_2}$= (3.65 ± 0.7) × 10^{-12} cm^3 $molecule^{-1}$ s^{-1} at 298 K which is in an excellent agreement with the previous result of Tuazon *et al*., (1984), (3.6 ± 0.7) × 10^{-12} cm^3 $molecule^{-1}$ s^{-1} at 296 K.

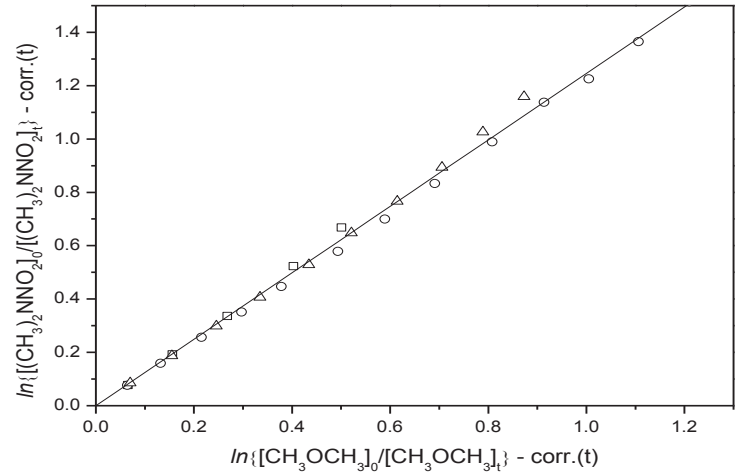

Figure 4.3.2.2.1. Relative rate plot showing the decay of $(CH_3)_2NNO_2$ *vs*. CH_3OCH_3 at 1013 hPa and 298 K in the presence of OH radicals; $k_{rel} = 1.246 \pm 0.015$ (2σ) determined from 29 data points from 3 independent experiments. The data have been corrected for loss due to reaction with O_3.

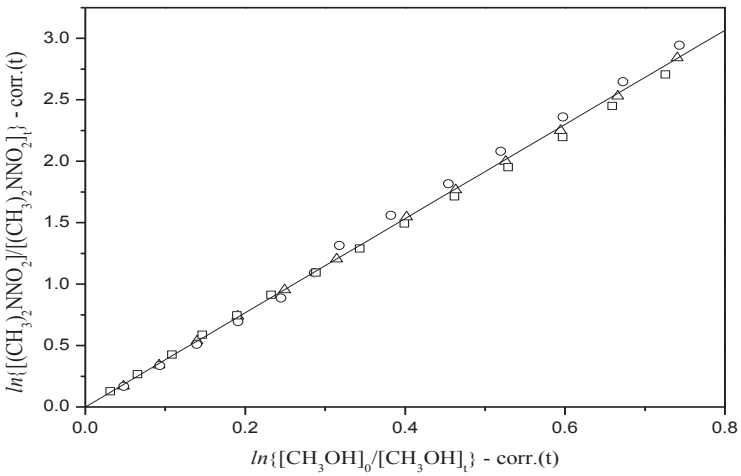

Figure 4.3.2.2.2. Relative rate plot showing the decay of $(CH_3)_2NNO_2$ *vs*. CH_3OH at 1013 hPa and 298 K in the presence of OH radicals; $k_{rel} = 3.83 \pm 0.04$ (2σ) determined from 39 data points from 3 independent experiments. The data have been corrected for loss due to reaction with O_3.

4.3.2.3 Ethylnitramine ($CH_3CH_2NHNO_2$) and Diethylnitramine [$(CH_3CH_2)_2NNO_2$] + OH

The rate coefficients for the OH radicals reactions with ethylnitramine ($CH_3CH_2NHNO_2$) and diethylnitramine ($(CH_3CH_2)_2NNO_2$) were also determined using relative rate experiments employing ethylacetate ($CH_3C(O)OCH_2CH_3$) as a reference compound. The

rate coefficient of OH radicals reaction with ethylacetate has been previously reported by Picquet *et al*., (1998) as (1.73 ± 0.2) × 10^{-12} cm^3 $molecule^{-1}$ s^{-1}, Campbell *et al*., (1978) as (1.84 ± 0.37) × 10^{-12} cm^3 $molecule^{-1}$ s^{-1}, Wallington *et al*., (1988) as (1.51 ± 0.14) × 10^{-12} cm^3 $molecule^{-1}$ s^{-1} and by El Boudali *et al*., (1996) as (1.67 ± 0.22) × 10^{-12} cm^3 $molecule^{-1}$ s^{-1} at 298 K. The relative decay plots for these two nitramines in the presence of OH radicals are shown in Figure 4.3.2.3.1 and Figure 4.3.2.3.2 respectively and the derived relative rate coefficients are summarized in Table 4.3.2.1.

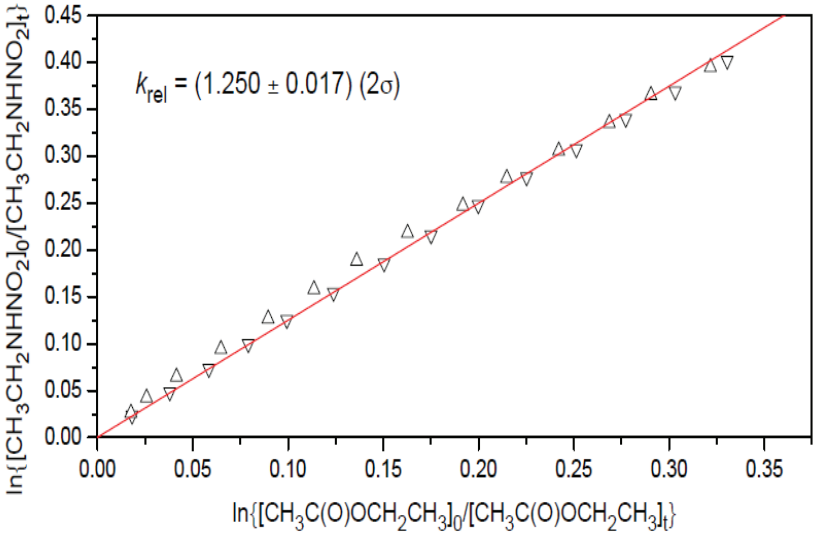

Figure 4.3.2.3.1. Relative rate plot showing decays of $CH_3CH_2NHNO_2$ and $CH_3C(O)OCH_2CH_3$ in the presence of OH radicals plotted as $ln\{[CH_3CH_2NHNO_2]_0/[CH_3CH_2NHNO_2]_t\}$ *vs*. $ln\{[CH_3C(O)OCH_2CH_3]_0/[CH_3C(O)OCH_2CH_3]_t\}$.

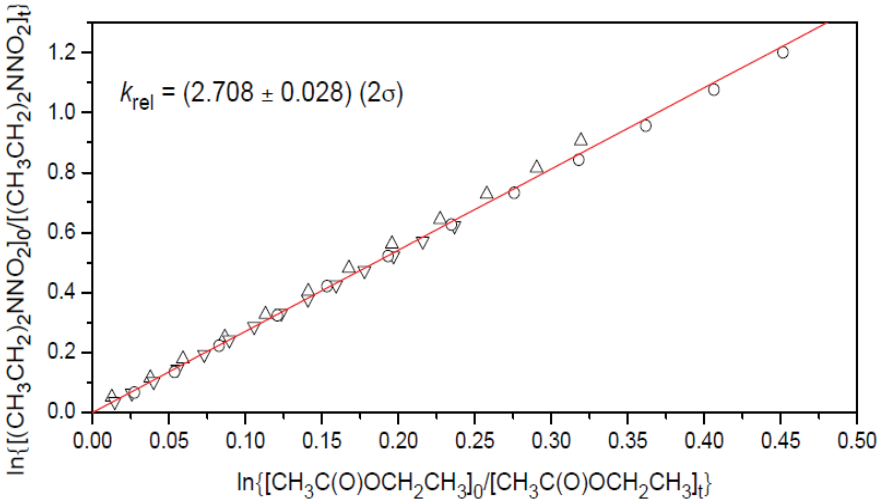

Figure 4.3.2.3.2. Relative rate plot showing decays of $(CH_3CH_2)_2NNO_2$ and $CH_3C(O)OCH_2CH_3$ in the presence of OH radicals plotted as $ln\{[(CH_3CH_2)_2NNO_2]_0/(CH_3CH_2)_2NNO_2]_t\}$ *vs.* $ln\{[CH_3C(O)OCH_2CH_3]_0/[CH_3C(O)OCH_2CH_3]_t\}$.

Table 4.3.2.1. Experimental rate constants at 295-300 K for the reactions of OH radicals with nitramines, and the estimated lifetimes of nitramines with respect to their reaction with OH.

Compound	k_{rel}	$k_{OH}/10^{-12}$ cm^3 molecule^{-1} s^{-1}		Reference	Lifetime (τ_{OH})
CH_3NHNO_2	0.304 ± 0.014[a]	0.85 ± 0.17			
	1.126 ± 0.016[b]	1.01 ± 0.21	0.93 ± 0.19	This work	12 days
$(CH_3)_2NNO_2$	1.246 ± 0.015[a]	3.49 ± 0.70			
	3.71 ± 0.04[b]	3.34 ± 0.70	3.42 ± 0.7	This work	3 days
			3.6 ± 0.7	Tuazon *et al.*, 1984	
$CH_3CH_2NHNO_2$	1.250 ± 0.017[c]		2.1 ± 0.4	This work	6 days
$(CH_3CH_2)_2NNO_2$	2.708 ± 0.028[c]		4.6 ± 0.8	This work	3 days

[a]Reference compound dimethylether (CH_3OCH_3), $k_{OH+CH3OCH3} = 2.8 \times 10^{-12}$ cm^3 molecule^{-1} s^{-1} (IUPAC, 2007). [b]Reference compound methanol (CH_3OH), $k_{OH+CH3OH} = 9.0\times10^{-13}$ cm^3 molecule^{-1}s^{-1} (IUPAC, 2007). [c]Reference compound ethylacetate ($CH_3C(O)OCH_2CH_3$), $k_{OH+CH3C(O)OCH2CH3} = 1.7\times10^{-12}$ cm^3 molecule^{-1}s^{-1} (rounded average of previous studies). The lifetimes are estimated on a global average OH concentration of 10^6 cm^{-3} (Lawrence *et al.*, 2001)

As can be seen from the results in Table 4.3.2.1, the atmospheric lifetimes of nitramines with respect to their reaction with OH radicals are expected to be in the order of days.

Thus the reaction of OH radicals with nitramines will constitute an important loss pathway of nitramines in the atmosphere.

4.3.3 Nitramines + Cl

The chlorine atom is one of the powerful oxiding agents playing a big role in removing pollutants from the atmosphere particularly at the Marine Boundary layer (MBL) where it is found in significant amount. Thus, its rate of reaction with nitramines was investigated to evaluate its contribution on removing this group of compounds from the atmosphere.

Recent measurements of Thornton *et al*., (2010), suggests that Chlorine chemistry may be more important in continental air.

The photo-stability of the nitramines in the Oslo chamber without the presence of Cl_2 was investigated in separate experiments, and that no significant photolysis was registered

A series of kinetic experiments were carried out employing the relative rate method to determine the rate coefficients of Cl atom reactions with four nitramines. The obtained relative rates and the derived absolute rates for all experiments are compiled in Table 4.3.3.1.

4.3.3.1 CH_3NHNO_2 + Cl

Three experiments were carried out using CH_3OH as a reference compound from which k_{rel} = 0.234 ± 0.004 (2σ) was derived (Figure 4.3.3.1.1). Also 3 experiments were done with CH_3OCHO as reference compound from which k_{rel} = 4.07 ± 0.31 (2σ) was derived (Figure 4.3.3.1.2).

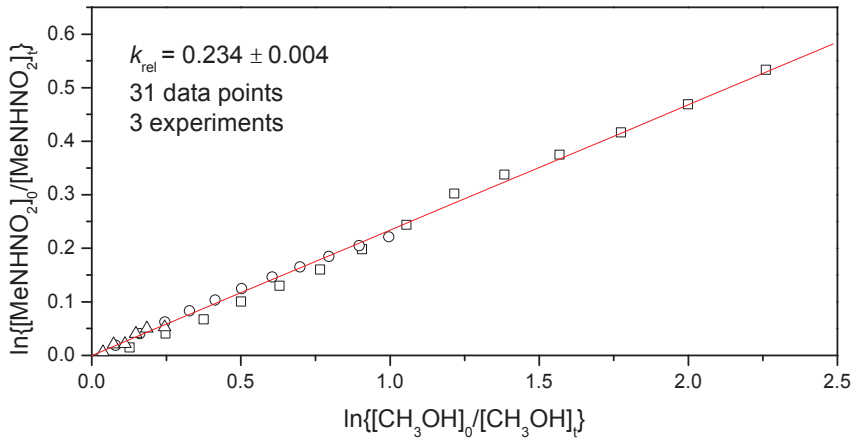

Figure 4.3.3.1.1. Relative rate plot showing decays of CH_3NHNO_2 and CH_3OH in the presence of Cl atoms plotted as $ln\{[CH_3NHNO_2]_0/[CH_3NHNO_2]_t\}$ *vs.* $ln\{[CH_3OH]_0/[CH_3OH]_t\}$.

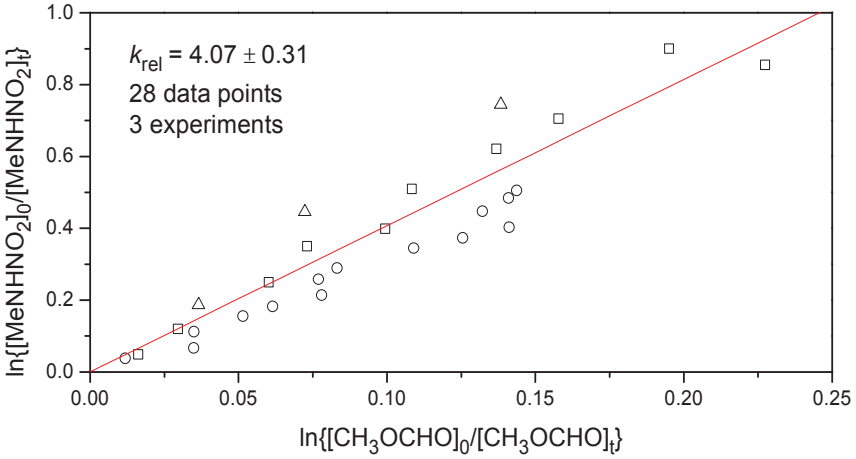

Figure 4.3.3.1.2. Relative rate plot showing decays of CH_3NHNO_2 and CH_3OCHO in the presence of Cl atoms plotted as $ln\{[CH_3NHNO_2]_0/[CH_3NHNO_2]_t\}$ *vs.* $ln\{[CH_3OCHO]_0/[CH_3OCHO]_t\}$.

The statistical errors in the relative rates are smaller than the uncertainty factors in the rate coefficients of the reference compounds. The latter therefore dominate the uncertainty in the absolute rate coefficients. The present results suggest a weighted average for the rate coefficient for the CH_3NHNO_2 + Cl reaction to be $k_{CH3NHNO2+Cl}$ = (9.3 ± 1.1) × 10^{-12} molecule cm^{-3} s^{-1} at 298 K.

4.3.3.2 $(CH_3)_2NNO_2$ + Cl

Three experiments were carried out with CH_3OH as reference compound from which k_{rel} = 0.907 ± 0.010 (2σ) was derived (Figure 4.3.3.2.1), and 3 experiments with CH_3OCH_3 as reference compound from which k_{rel} = 0.402 ± 0.011 (2σ) was derived (Figure 4.3.3.2.2). Because these two experiments suggest that the absolute rate constant for the $(CH_3)_2NNO_2$+Cl reaction is almost the same as that of $(CH_3CH_2)_2NNO_2$+Cl (see later), a third series of experiments was carried out employing ethylacetate ($CH_3CH_2OC(O)CH_3$) as reference compound. The results from these experiments gave k_{rel} = 4.35 ± 0.03 (2σ) (Figure 4.3.3.2.3). The statistical errors in the relative rates are much smaller than the uncertainty factors in the rate coefficients of the reference compounds. The latter therefore dominate the uncertainty in the absolute rate coefficients. The present results suggest a weighted average for the rate coefficient for the $(CH_3)_2NNO_2$ + Cl reaction to be $k_{(CH3)2NNO2+Cl}$ = (6.5 ± 0.7) × 10^{-11} molecule cm^{-3} s^{-1} at 298 K.

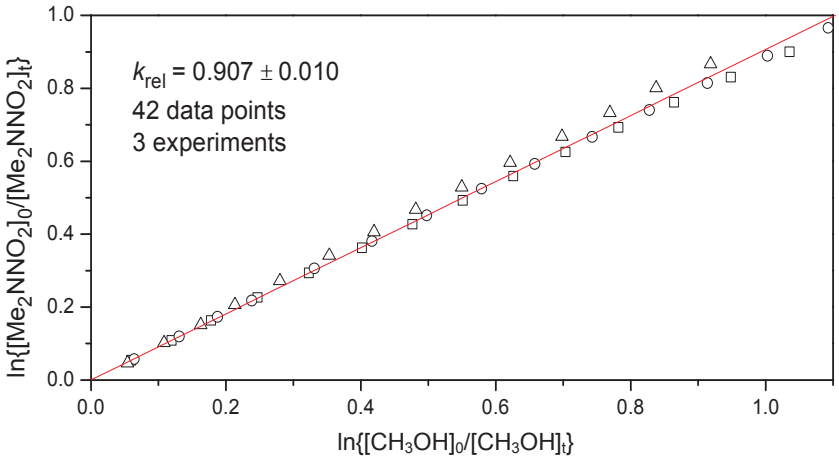

Figure 4.3.3.2.1. Relative rate plot showing decays of $(CH_3)_2NNO_2$ and CH_3OH in the presence of Cl atoms plotted as $ln\{[(CH_3)_2NNO_2]_0/[(CH_3)_2NNO_2]_t\}$ *vs.* $ln\{[CH_3OH]_0/[CH_3OH]_t\}$.

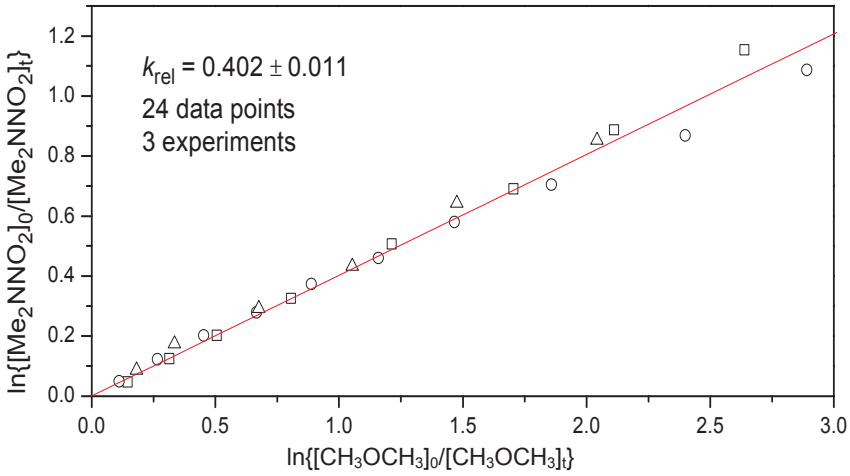

Figure 4.3.3.2.2. Relative rate plot showing decays of $(CH_3)_2NNO_2$ and CH_3OCH_3 in the presence of Cl atoms plotted as $ln\{[(CH_3)_2NNO_2]_0/[(CH_3)_2NNO_2]_t\}$ *vs.* $ln\{[CH_3OCH_3]_0/[CH_3OCH_3]_t\}$.

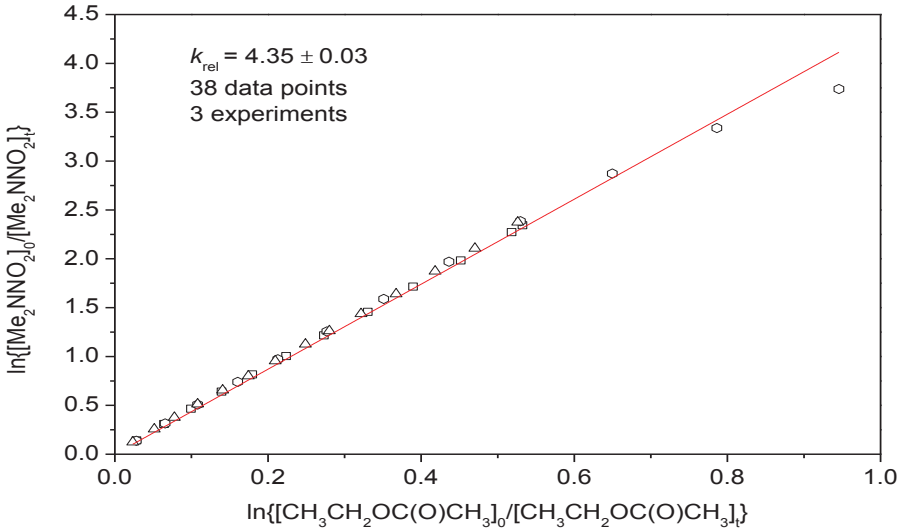

Figure 4.3.3.2.3. Relative rate plot showing decays of $(CH_3)_2NNO_2$ and $CH_3CH_2OC(O)CH_3$ in the presence of Cl atoms plotted as $ln\{[(CH_3)_2NNO_2]_0/[(CH_3)_2NNO_2]_t\}$ *vs.* $ln\{[CH_3CH_2OC(O)CH_3]_0/[CH_3CH_2OC(O)CH_3]_t\}$.

4.3.3.3 $CH_3CH_2NHNO_2$ + Cl

Methylformate (CH_3OCHO) was used as reference compound in an initial experiment from which k_{rel} = 10.24 ± 0.4 (1σ) was derived, Figure 4.3.3.3.1. When rates differ by an order of magnitude the relative rate method becomes sensitive to systematic errors and hence CH_3OCHO was not used in additional experiments. CH_3OH was used as reference compound in 4 experiments from which k_{rel} = 0.3027 ± 0.0024 (1σ) was derived, Figure 4.3.3.3.2. Another set of 3 experiments with ethylacetate ($CH_3CH_2OC(O)CH_3$) as reference compound was done from which k_{rel} = 1.233 ± 0.007 (1σ) was derived, Figure 4.3.3.3.3.

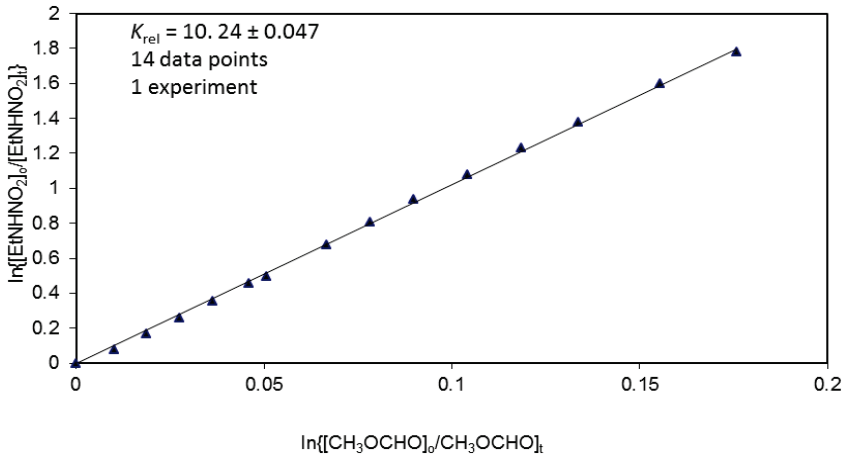

Figure 4.3.3.3.1. Relative rate plot showing decays of $CH_3CH_2NHNO_2$ and CH_3OCHO in the presence of Cl atoms plotted as $ln\{[(CH_3CH_2NHNO_2]_0/[(CH_3CH_2NHNO_2]_t\}$ *vs*. $ln\{[CH_3OCHO]_0/[CH_3OCHO]_t\}$.

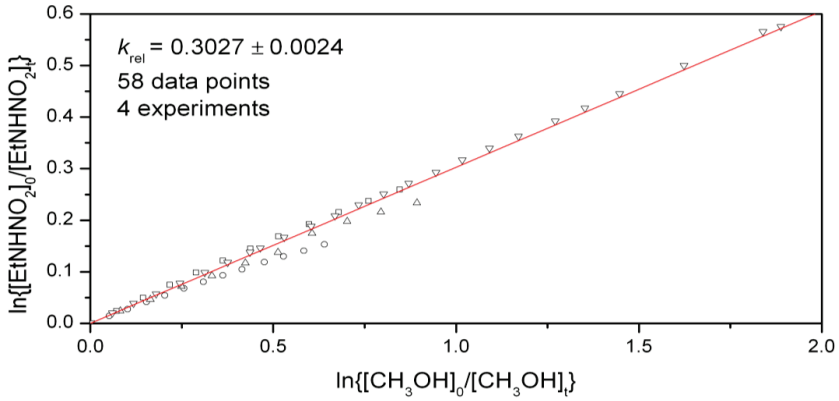

Figure 4.3.3.3.2. Relative rate plot showing decays of $CH_3CH_2NHNO_2$ and CH_3OH in the presence of Cl atoms plotted as $ln\{[(CH_3CH_2NHNO_2]_0/[(CH_3CH_2NHNO_2]_t\}$ *vs*. $ln\{[CH_3OH]_0/[CH_3OH]_t\}$.

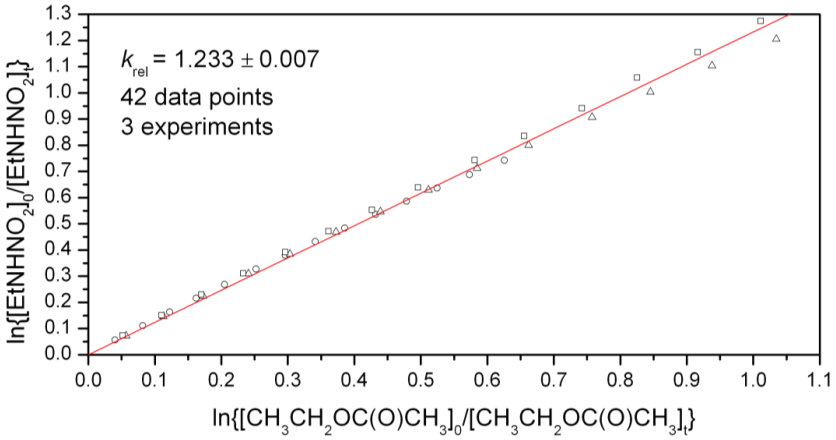

Figure 4.3.3.3.3. Relative rate plot showing decays of $CH_3CH_2NHNO_2$ and $CH_3CH_2OC(O)CH_3$ in the presence of Cl atoms plotted as $ln\{[(CH_3CH_2NHNO_2]_0/[(CH_3CH_2NHNO_2]_t\}$ *vs*. $ln\{[CH_3CH_2OC(O)CH_3]_0/[CH_3CH_2OC(O)CH_3]_t\}$.

The statistical errors in the relative rates are much smaller than the uncertainty factors in the rate coefficients of the reference compounds. The latter therefore dominate the uncertainty in the absolute rate coefficients. The present results suggest a weighted average for the rate coefficient for the $CH_3CH_2NHNO_2$ + Cl reaction to be $k_{CH3CH2NHNO2+Cl} = (1.88 \pm 0.22) \times 10^{-11}$ molecule cm^{-3} s^{-1} at 298 K.

4.3.3.4 $(CH_3CH_2)_2NNO_2$ + Cl

Four experiments were carried out with CH_3OH as reference compound from which k_{rel} = 0.892 ± 0.007 (1σ) was derived (Figure 4.3.3.4.1), and 3 experiments with $CH_3CH_2OC(O)CH_3$ as reference compound from which k_{rel} = 3.56 ± 0.05 (1σ) was derived (Figure 4.3.3.4.2). The statistical errors in the relative rates are much smaller than the uncertainty factors in the rate coefficients of the reference compounds. The latter therefore dominate the uncertainty in the absolute rate coefficients. The present results suggest a weighted average for the rate coefficient for the $(CH_3CH_2)_2NNO_2$ + Cl reaction to be $k_{(CH3CH2)2NNO2+Cl} = (5.5 \pm 0.7) \times 10^{-11}$ molecule cm^{-3} s^{-1} at 298 K.

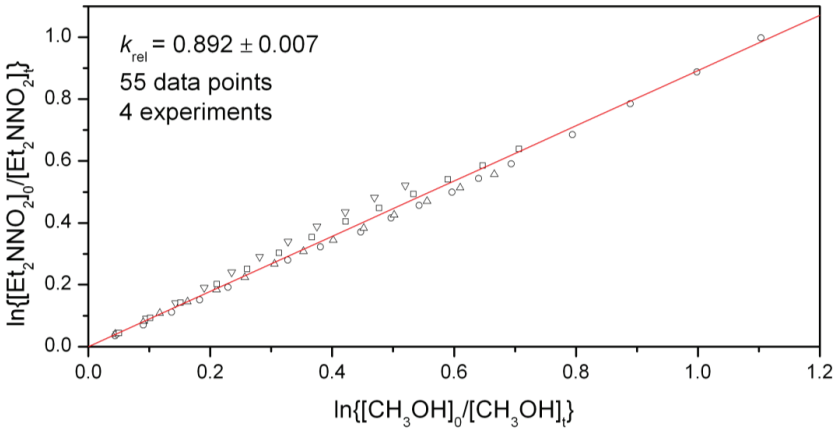

Figure 4.3.3.4.1. Relative rate plot showing decays of $(CH_3CH_2)_2NNO_2$ and CH_3OH in the presence of Cl atoms plotted as $ln\{[(CH_3CH_2)_2NNO_2]_0/[(CH_3CH_2)_2NNO_2]_t\}$ *vs.* $ln\{[CH_3OH]_0/[CH_3OH]_t\}$.

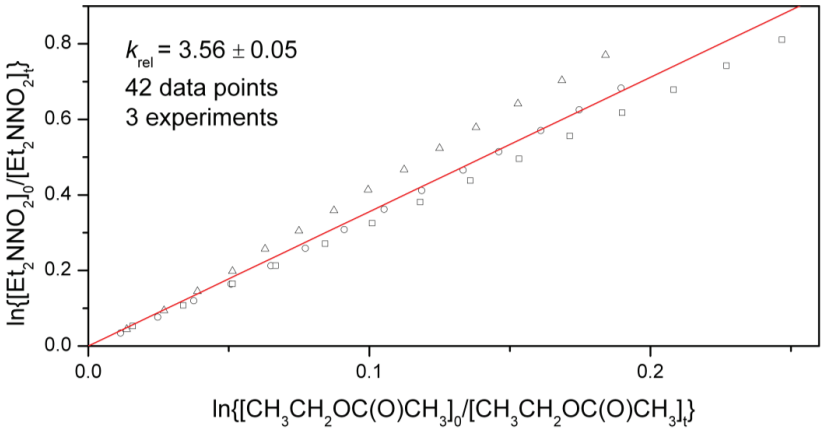

Figure 4.3.3.4.2. Relative rate plot showing decays of $(CH_3CH_2)_2NNO_2$ and $CH_3CH_2OC(O)CH_3$ in the presence of Cl atoms plotted as $ln\{[(CH_3CH_2)_2NNO_2]_0/[(CH_3CH_2)_2NNO_2]_t\}$ *vs.* $ln\{[CH_3CH_2OC(O)CH_3]_0/[CH_3CH_2OC(O)CH_3]_t\}$.

Table 4.3.3.1. Experimental relative rate coefficients and derived absolute rate coefficients (/cm^3 molecule^{-1} s^{-1}) for the reactions of nitramines with Cl atoms.

Nitramine	Reference compound	k_{rel}	k_{ref} [a]	$k_{Nitramine+Cl}$
CH_3NHNO_2	CH_3OH	0.234 ± 0.004	5.5×10^{-11}	$(1.3 \pm 0.2) \times 10^{-11}$
$(CH_3)_2NNO_2$	CH_3OH	0.907± 0.010	5.5×10^{-11}	$(5.0 \pm 0.9) \times 10^{-11}$
	CH_3OCH_3	0.402 ± 0.011	1.8×10^{-10}	$(7.2 \pm 0.6) \times 10^{-11}$
	$CH_3CH_2OC(O)CH_3$	4.35 ± 0.03	1.7×10^{-11}	$(7.4 \pm 0.5) \times 10^{-11}$
			Average	$(6.5 \pm 0.7) \times 10^{-11}$
$CH_3CH_2NHNO_2$	CH_3OH	0.3027 ± 0.0024	5.5×10^{-11}	$(1.66 \pm 0.28) \times 10^{-11}$
	$CH_3CH_2OC(O)CH_3$	1.233 ± 0.007	1.7×10^{-11}	$(2.10 \pm 0.15) \times 10^{-11}$
			Average	$(1.88 \pm 0.22) \times 10^{-11}$
$(CH_3CH_2)_2NNO_2$	CH_3OH	0.892 ± 0.007	5.5×10^{-11}	$(4.91 \pm 0.84) \times 10^{-11}$
	$CH_3CH_2OC(O)CH_3$	3.56 ±0.05	1.7×10^{-11}	$(6.1 \pm 0.48) \times 10^{-11}$
			Average	$(5.5 \pm 0.7) \times 10^{-11}$

Reference compound methanol (CH_3OH), $k_{Cl+CH3OH} = 5.5\times10^{-11}$ cm^3 molecule^{-1}s^{-1} (IUPAC, 2011). Reference compound dimethylether (CH_3OCH_3), $k_{Cl+CH3OCH3} = 1.8 \times10^{-10}$ cm^3 molecule^{-1} s^{-1} (Extracted best value from previous studies). [c]Reference compound ethylacetate ($CH_3C(O)OCH_2CH_3$), $k_{OH+CH3C(O)OCH2CH3} = 1.7\times10^{-11}$ cm^3 molecule^{-1}s^{-1} (extracted best value from previous studies).

Table 4.3.3.2. Lifetimes for the nitramines with respect to their reaction with cl atom in the atmosphere

Nitramine	Rate constant (/cm^3 molecule^{-1} s^{-1})	Lifetime (τ_{Cl})
CH_3NHNO_2	$(1.3 \pm 0.2) \times 10^{-11}$	3 months
$(CH_3)_2NNO_2$	$(6.5 \pm 0.7) \times 10^{-11}$	18 days
$CH_3CH_2NHNO_2$	$(1.88 \pm 0.22) \times 10^{-11}$	2 months
$(CH_3CH_2)_2NNO_2$	$(5.5 \pm 0.7) \times 10^{-11}$	21 days

The lifetimes are estimated based on a global average concentration of Cl atom at the Marine Boundary Layer of 10^4 cm^{-3} (Finlayson and Pitts, 2000, Pszenny, *et al.*, 1993, Singh *et al.*, 1996a).

From Table 4.3.3.2 above we see that, the atmospheric lifetime of nitramines with respect to reaction with Cl atoms will be around half a month and above. Hence it can be concluded that Cl atom chemistry will not constitute an important loss process for nitramines in the atmosphere.

4.3.4 Nitrosamines + NO_3 radical

Initial studies of the NO_3 radical reaction with *N*-nitroso diethylamine indicated the reaction to be very slow and only two reference compounds were found to be suitable: formaldehyde and ethene. After optimizing the reaction conditions in the chamber, two series of relative rate studies were carried out with these reference compounds to determine the rate coefficients of NO_3 radical reactions with two nitrosamines namely *N*-nitroso dimethylamine [$(CH_3)_2NNO_2$] and *N*-nitroso diethylamine [$(CH_3CH_2)_2NNO_2$]. The obtained relative rates and the derived absolute rate coefficients are collected in Table 4.3.4.1. The errors in the relative rates coefficients are much smaller than the recommended uncertainty factors in the absolute rate coefficients ($\Delta log_{10}k_{ref} = \pm 0.20$). The latter uncertainty is therefore dominant. Furthermore, the lifetimes of the two nitrosamines with respect to their reaction with the nitrate radical in the atmosphere were calculated and the results are summarised in Table 4.3.4.2.

4.3.4.1 Dimethylnitrosamine [$(CH_3)_2NNO$] + NO_3

The $(CH_3)_2NNO + NO_3$ reaction is very slow, near the lower limit for reactions that can be studied in the reaction chamber and the results are consequently sensitive to systematic errors. Figure 4.3.4.1.1 summarises the results from 3 independent experiments with CH_2CH_2 as reference compound from which $k_{(CH_3)2NNO+NO_3}/k_{CH2CH2+NO_3} = 0.760 \pm 0.016$ was derived. Taking $k_{CH2CH2+NO_3} = 2.1\times10^{-16}$ cm^3 $molecule^{-1}$ s^{-1}, places $k_{(CH_3)2NNO+NO_3} =$ 1.60 x 10^{-16} cm^3 $molecule^{-1}$ s^{-1} on an absolute scale. Figure 4.3.4.1.2 summarises the results from 2 independent experiments with CH_2O as reference compound from which $k_{(CH_3)2NNO+NO_3}/k_{CH2O+NO_3} = 0.223 \pm 0.005$ was derived. Taking $k_{CH2O+NO_3} = 5.5\times10^{-16}$ cm^3 $molecule^{-1}$ s^{-1}, places $k_{(CH_3)2NNO+NO_3} = 1.22$ x 10^{-16} cm^3 $molecule^{-1}$ s^{-1} on an absolute scale.

The present results suggest a weighted average for the rate coefficient for the $(CH_3)_2NNO + NO_3$ reaction to be $k_{(CH_3)2NNO+NO_3} = (1.41 \pm 0.13) \times 10^{-16}$ molecule cm^{-3} s^{-1} at 298 K.

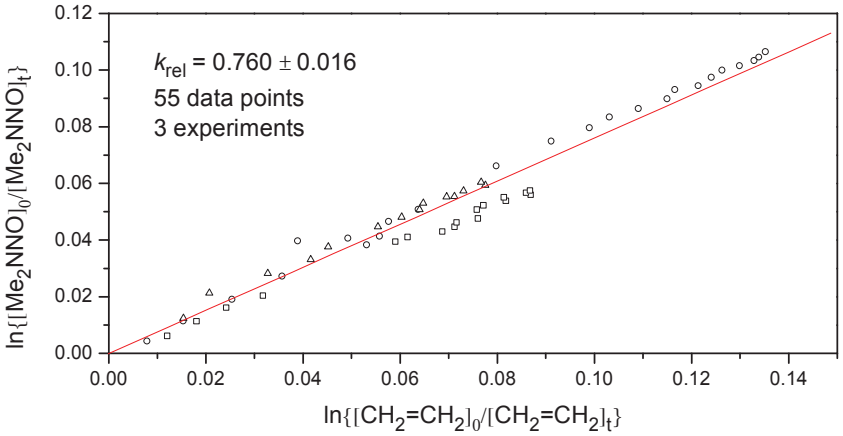

Figure 4.3.4.1.1. Relative rate plot showing decays of $(CH_3)_2NNO$ and CH_2CH_2 in the presence of NO_3 radicals plotted as $ln\{[(CH_3)_2NNO]_0/[(CH_3)_2NNO]_t\}$ *vs*. $ln\{[CH_2CH_2]_0/[CH_2CH_2]_t\}$.

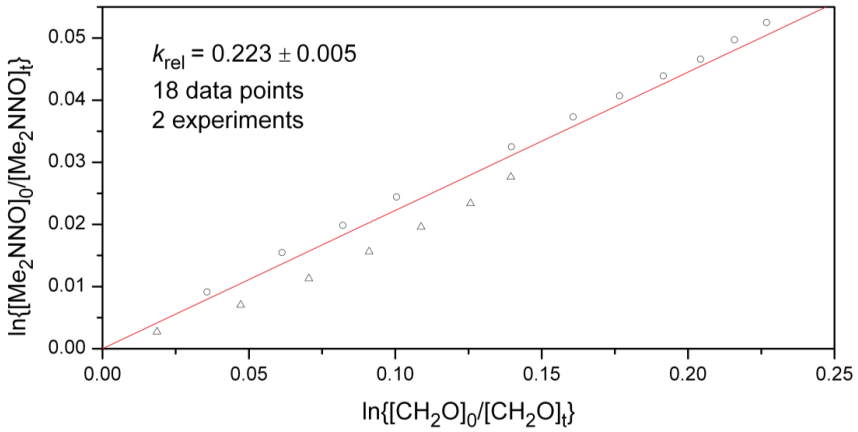

Figure 4.3.4.1.2. Relative rate plot showing decays of $(CH_3)_2NNO$ and CH_2O in the presence of NO_3 radicals plotted as $ln\{[(CH_3)_2NNO]_0/[(CH_3)_2NNO]_t\}$ *vs*. $ln\{[CH_2O]_0/[CH_2O]_t\}$.

4.3.4.2 Diethylnitrosamine [$(CH_3CH_2)_2NNO$] + NO_3

For $(CH_3CH_2)_2NNO$, the following relative rates were determined: $k_{(CH3CH2)2NNO+NO3}/k_{CH2O+NO3}$ = 0.8760 ± 0.0026 (Figure 4.3.4.2.1), $k_{(CH3CH2)2NNO+NO3}/k_{CH2CH2+NO3}$ = 2.618 ± 0.011 (Figure 4.3.4.2.2). Taking today's recommended values for $k_{CH2CH2+NO3}$ = 2.1 × 10^{-16} and $k_{CH2O+NO3}$ = 5.5 × 10^{-16} cm^3 $molecule^{-1}$ s^{-1}, places $k_{(CH3CH2)2NNO+NO3}$ at respectively 4.8 × 10^{-16} and 5.5 × 10^{-16} cm^3 $molecule^{-1}$ s^{-1} on an absolute scale.

The present results suggest a weighted average for the rate coefficient for the $(CH_3)_2NNO$ + NO_3 reaction to be $k_{(CH3CH2)2NNO+NO3} = (5.16 \pm 0.37) \times 10^{-16}$ molecule cm^{-3} s^{-1} at 298 K.

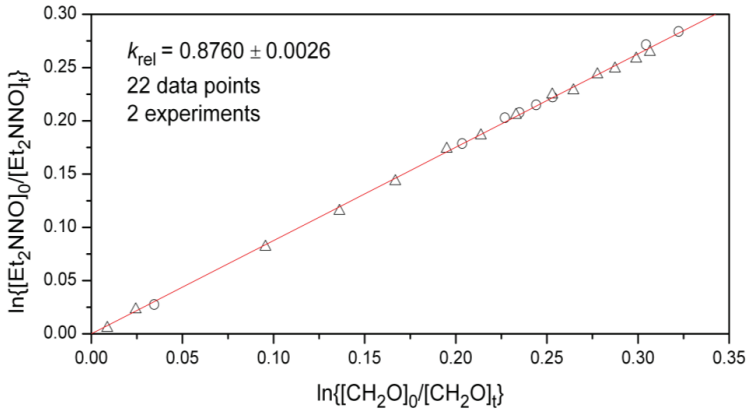

Figure 4.3.4.2.1. Relative rate plot showing decays of $(CH_3CH_2)_2NNO$ and CH_2O in the presence of NO_3 radicals plotted as $\ln\{[(CH_3CH_2)_2NNO]_0/[(CH_3CH_2)_2NNO]_t\}$ vs. $\ln\{[CH_2O]_0/[CH_2O]_t\}$.

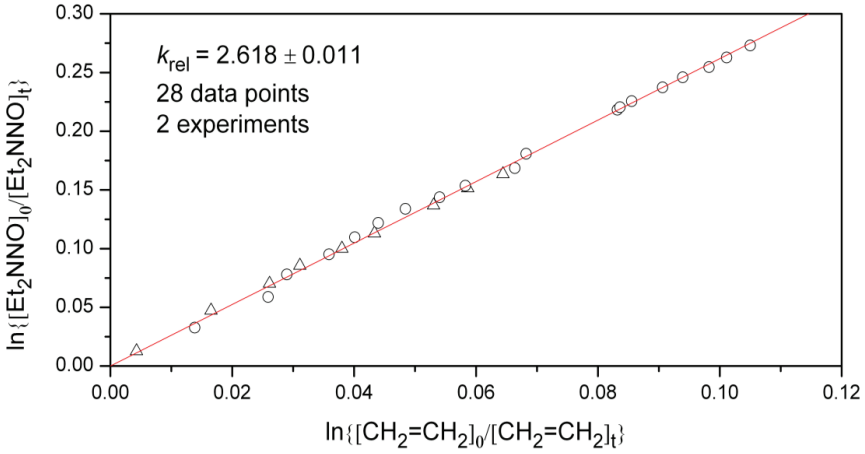

Figure 4.3.4.2.2. Relative rate plot showing decays of $(CH_3CH_2)_2NNO$ and CH_2CH_2 in the presence of NO_3 radicals plotted as $ln\{[(CH_3CH_2)_2NNO]_0/[(CH_3CH_2)_2NNO]_t\}$ *vs.* $ln\{[CH_2CH_2]_0/[CH_2CH_2]_t\}$.

Table 4.3.4.1. Experimental relative rate coefficients and derived absolute rate coefficients (/cm^3 molecule^{-1} s^{-1}) for the reactions of nitrosamines with NO_3 radicals.

Nitramine	Reference compound	k_{rel}	k_{ref}	$k_{Nitrosamine+NO3}$
$(CH_3)_2NNO$	CH_2O	0.223 ± 0.005	5.5×10^{-16}	$(1.227 \pm 0.071) \times 10^{-16}$
	CH_2CH_2	0.760 ± 0.016	2.1×10^{-16}	$1.596 \pm 0.190) \times 10^{-16}$
			Average	$(1.41 \pm 0.13) \times 10^{-16}$
$(CH_3CH_2)_2NNO$	CH_2O	0.8760±0.0026	5.5×10^{-16}	$(4.818 \pm 0.190) \times 10^{-16}$
	CH_2CH_2	2.618±0.011	2.1×10^{-16}	$(5.498 \pm 0.547) \times 10^{-16}$
			Average	$(5.16 \pm 0.37) \times 10^{-16}$

Table 4.3.4.2. Lifetimes of nitrosamines with respect to their reaction with NO_3 radicals in the atmosphere.

Nitrosamine	Rate constant (/cm^3 molecule^{-1} s^{-1})	Lifetime (τ_{NO3})
$(CH_3)_2NNO$	$(1.41 \pm 0.13) \times 10^{-16}$	2 months
$(CH_3CH_2)_2NNO$	$(5.16 \pm 0.37) \times 10^{-16}$	18 days

With a global average concentration of 50 ppt ($1.23x10^9$ cm^{-3}) NO_3.

The results in Table 4.3.4.2 show that, the removal of nitrosamines from the atmosphere through their reaction with nitrate radicals ranges from days to months. Thus there is a likelihood of these highly carcinogenic compounds to accumulate in the atmosphere during the night.

4.4 Structure Activity Relationship (SAR) for OH reactions with nitramines

The OH-SAR of Kwok and Atkinson (1995) includes parameters for estimation of the reactivity of nitrosamines and nitramines (see Table 2.6.1). The relevant parameters, group rate constants $k(R_2NNO)$ and $k(R_2NNO_2)$, and a common substituent factor $F(R_2NNO) = F(R_2NNO_2)$, are based on kinetic data for one nitrosamine, $(CH_3)_2NNO$, and one nitramine, $(CH_3)_2NNO_2$.

Assuming a common substituent factor for primary and secondary nitramines, $F(RNHNO_2) = F(R_2NNO_2)$, the rate coefficients (in units of 10^{-12} cm^3 molecule^{-1} s^{-1} at

298K) for OH reactions with CH_3NHNO_2 $(CH_3)_2NNO_2$, $CH_3CH_2NHNO_2$ and $(CH_3CH_2)_2NNO_2$ can then, according to the OH-SAR, be written as:

Nitramine			k_{obs}
CH_3NHNO_2	k_{OH}	$= k_{prim}$ x $F(RNHNO_2) + k(RNHNO_2)$	
		$= 0.136$ x $9.3 + k(RNHNO_2) = 1.3 + k(RNHNO_2)$	0.95
$(CH_3)_2NNO_2$	k_{OH}	$= 2$ x $(k_{prim}$ x $F(RNNO_2)) + k(R_2NNO_2)$	
		$= 2$ x $(0.136$ x $9.3) + 1.3 = 3.8$	3.55
$CH_3CH_2NHNO_2$	k_{OH}	$= k_{prim}$ x $F(-CH_2-) + k_{sec}$ x $F(-CH_3)$ x $F(RNHNO_2) + k(RNHNO_2)$	
		$= 0.136$ x $1.23 + 0.934$ x 1 x $9.3 + k(RNHNO_2) = 8.9 + k(RNHNO_2)$	2.1
$(CH_3CH_2)_2NNO_2$	k_{OH}	$= 2$ x $(k_{prim}$ x $F(-CH_2-) + k_{sec}$ x $F(-CH_3)$ x $F(R_2NNO_2)) + k(R_2NNO_2)$	
		$= 2$ x $(0.136$ x $1.23 + 0.934$ x 1.0 x $9.3) + 1.3 = 19.0$	4.6

It is obvious from above that the existing SAR parameters for nitramines first of all do not predict the observed OH reactivity of $(CH_3CH_2)_2NNO_2$, and second, that $F(RNHNO_2)$ cannot be equal to $F(R_2NNO_2)$. The $-NO_2$ group is electron withdrawing to the extent that the substituent factor $F(-NO_2)$ has been found to be zero for other organics, *i.e.* there is essentially no reactivity towards OH radicals of a substituted CH_2- group ($R–CH_2–NO_2$). It is therefore unrealistic to constrain the substituent factors of $–CNHNO_2$, $–R_2NNO_2$ to be the same as those of $–NH_2$, >NH and >N– as implemented in the OH-SAR of Kwok and Atkinson (1995) (see Table 2.6.1). It is therefore suggested that, the OH-SAR for nitramines should be modified such that the reactivity of this class of compounds be described in terms of 4 parameters: $F(RNHNO_2)$, k(RNHNO2), $F(R_2NNO_2)$ and $k(R_2NNO_2)$; the substituent factors express the electron donating/withdrawing properties of the substituents, the group rate constants express the effect of pre-reaction adduct formation in the reaction ($k(RNHNO_2)$ also includes the contribution from direct H-abstraction from the >NH group).

The available data suggest the following values ($/10^{-12}$ cm^3 $molecule^{-1}$ s^{-1} at 298 K): $F(RNHNO_2) = 1.2$, $F(R_2NNO_2) = 0.4$; $k(RNHNO_2) = 0.8$ and $k(R_2NNO_2) = 3.4$. Although the values appear sensible one should not put too much trust in them (4 parameters extracted from the 4 linear equations) (Nielsen *et al.*, 2011). In summary, the existing data is insufficient to determine a unique set of SAR parameters describing the nitramine

reactivity towards OH radicals; more data are needed to develop a reliable SAR for this class of compounds.

4.5 Infrared Absorption Cross-sections and Integrated absorption intensities (S_{int})

4.5.1 Infrared Absorption Cross-sections

The absolute infrared absorption cross-section (base e) of gaseous isocyanic acid, Methylamine, Dimethylamine, Trimethylamine, Deuteratedmethylamine, Dideuteratedmethylamine, Trideuteratedmethylamine, ethylalamine, diethylamine, triethylamine, dimethylnitramine, and diethylnitrosamine were obtained from the FT-IR spectra using the CH/CD stretching band region for the calibration. The integrated cross-section of the CH/CD stretching band region was determined by plotting the ratio of integrated absorbance intensities with the path length against the product of the number density and path length. Conservative estimates of systematic errors are: sample pressure (<5%), path length (<1%), temperature (<1%), and definition of the baseline in the integration procedure (<5%). The estimated accuracy of the absolute absorption cross section is believed to be better than ± 7% including possible baseline offset. The reference spectra are collected in Appendix 1.

The absorption cross-sections (base e) of dimethylamine, ethylamine, *N*-nitroso diethylamine and diethylanitramine are shown on figure 4.5.1.1, 4.5.1.2, 4.5.1.3 and 4.5.1.4 respectively. The absorption cross-sections of the remaining compounds are collected in Appendix 3.

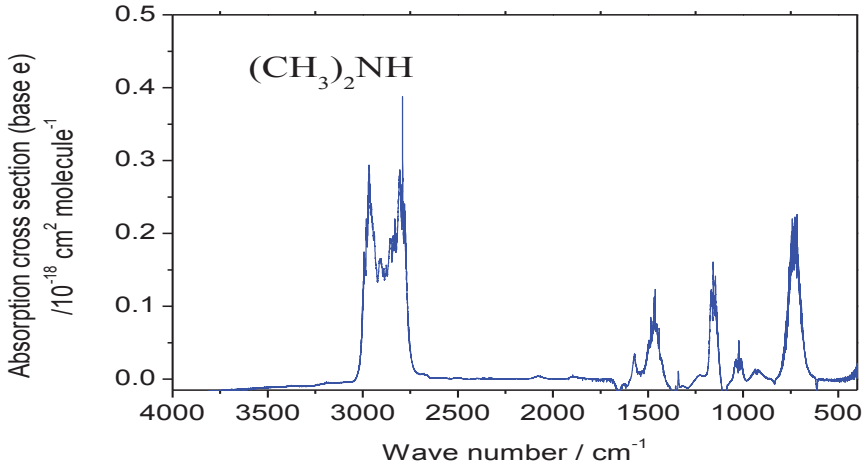

Figure 4.5.1.1. Infrared absorption cross-section (base e) of dimethylamine.

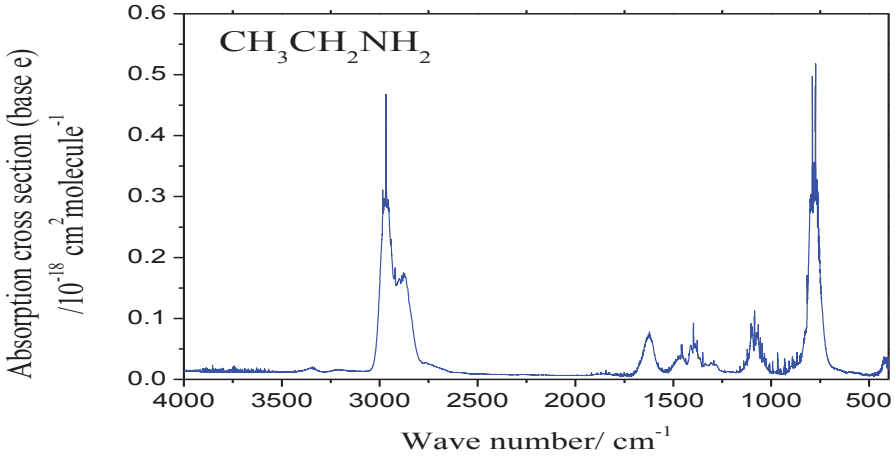

Figure 4.5.1.2. Infrared absorption cross-section (base e) of ethylamine.

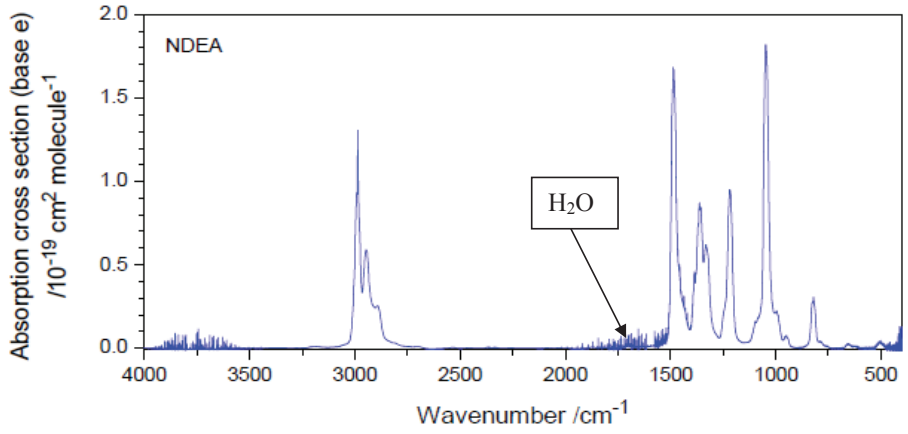

Figure 4.5.1.3. Infrared absorption cross-section (base e)of *N*-nitroso diethylamine.

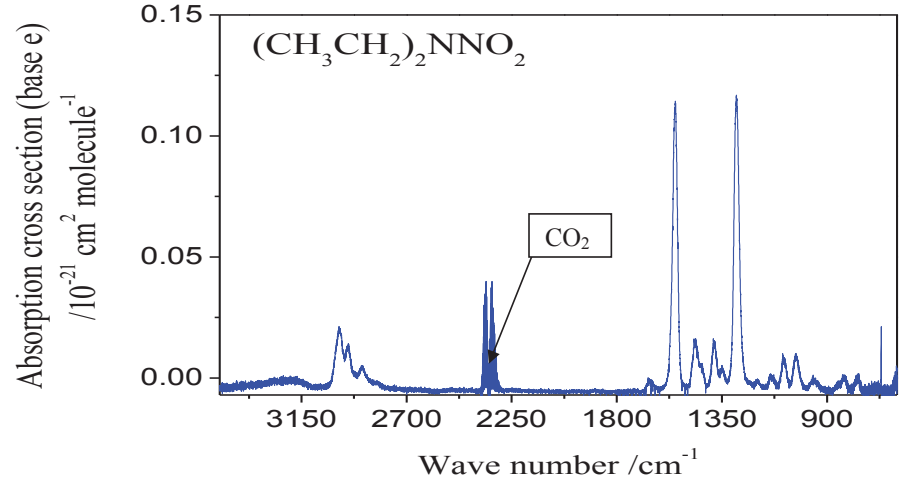

Figure 4.5.1.4. Infrared absorption cross-section (base e) of diethylnitramine.

4.5.2 Integrated absorption intensities (S_{int})

The integrated absorption intensities of nine amines, isocyanic acid and acetonitrile were determined using equation 26 given as:-

$$S_{\text{int}} = \int_{band} \sigma(\tilde{\nu}) d\tilde{\nu} = \frac{1}{pl} \int_{band} \ln \frac{I_0}{I} dv$$

To find $\int_{\text{band}} \ln(I_0/I)dv$, the absorbance area of the C-H/C-D/N-H/C-N band in the responsible compound spectrum was determined for different pressures. The ratio of the integrated absorbance intensity to the path length (cm^{-2}) was plotted against the number density (molecules cm^{-3}) and the integrated absorption intensities S_{int} in cm $molecule^{-1}$ were determined from the gradient of each plot. The experimental gas path lengths (l) used in the calculations were 10 cm and 23 cm. Where the C-H band did not give a straight line (no linearity) or it was absent, then other bands such as C-N, N-H etc were used. Examples of the graphs used in the determination of the integrated absorption intensities are given below and the rest are collected in appendix 4. The obtained results are summarised in Table 4.5.2.1 below.

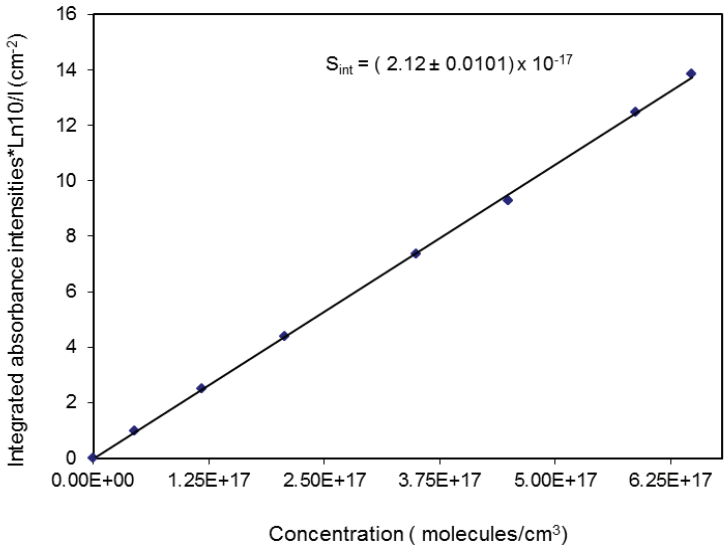

Figure 4.5.2.1. Beer-Lambert's law plot of CH_3NH_2 bands that were measured in the 3150 - 2650 cm^{-1} region.

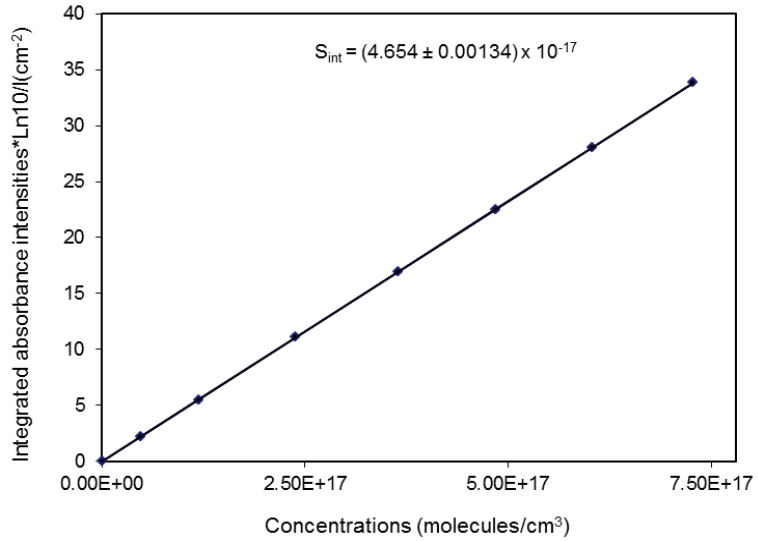

Figure 4.5.2.2. Beer-Lambert's law plot of $(CH_3)_2NH$ bands that were measured in the 3050 - 2650 cm^{-1} region.

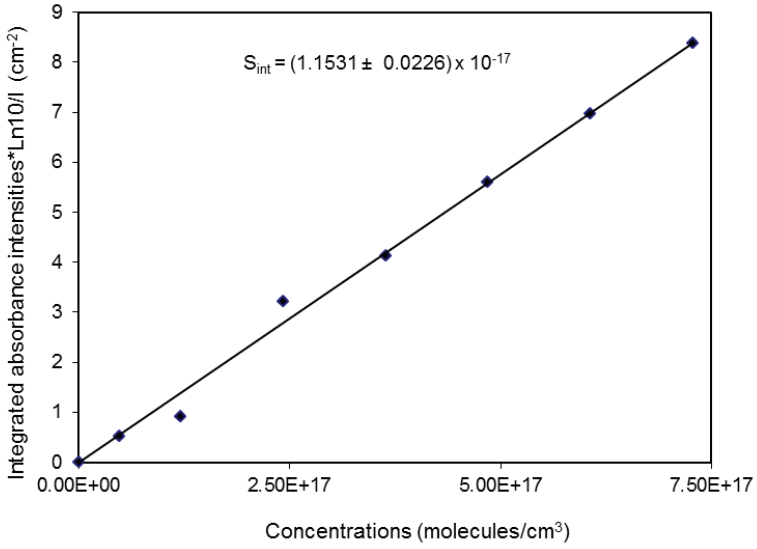

Figure 4.5.2.3. Beer-Lambert's law plot of CD_3NH_2 bands that were measured in the 2350 – 1950 cm^{-1} region

Table 4.5.2.1. The integrated absorption intensities, S_{int} /10^{-18} cm molecule^{-1}

Compound	Spectral region / cm^{-1}	S_{int} /10^{-18} cm molecule^{-1}
CH_3NH_2	3150 - 2650	21.2 ± 0.1
$(CH_3)_2NH$	3050 - 2650	46.54 ± 0.01
$(CH_3)_3N$ (C-N Stretch)	900 - 760	3.169 ± 0.006
CD_3NH_2	2350 - 1950	11.531 ± 0.226
$(CD_3)_2NH$	2375 - 1925	31.844 ± 0.17
$(CD_3)_3N$	2270 - 1980	44.942 ± 1.248
$CH_3CH_2NH_2$	3150 - 2650	34.8 ± 0.01
$(CH_3CH_2)_2NH$	3150 - 2600	79.93 ± 0.07
$(CH_3CH_2)_3N$	3200 - 2550	11.13 ± 0.03
HNCO (N-H Stretch)	3800 - 3200	21.287 ± 1.113
CH_3CN (C-N Stretch)	2350 – 2200	43.176 ± 0.137

5 CONCLUSION

The aim of this study was to provide information on the secondary product compounds formed from the photooxidation of amines emitted into the atmosphere as well as on the atmospheric fates of the primary products particularly the nitramines and nitrosamines. To achieve this, the study assessed the products resulting from the reactions of nitramines with the hydroxyl radicals and chlorine atoms and also investigated the atmospheric fates of nitramines and nitrosamines.

The study has provided information on the kinetics for the reaction of OH radicals, chlorine atoms and ozone with methylanitramine, dimethylnitramine, ethylanitramine and diethylanitramine as well as for the reaction of diethylnitrosamine and dimethylnitrosamine with the nitrate radicals. In conjunction to this, the lifetimes of the studied nitramines with respect to their reaction with the above named oxidants were determined. Lifetimes of nitrosamines following their reaction with the nitrate radical were also determined. We have established that, the nitramines which do not undergo photolysis in the troposphere can be removed through their reaction with OH radicals after 3 – 12 days. Their removal by chlorine atom and ozone ranges from 18 days to 3 months and 3 to 6 years respectively. Hence it can be concluded that the reaction of nitramines with Cl atom and ozone will not constitute an important loss processes for nitramines in the atmosphere. The most carcinogenic compounds, the nitrosamines do undergo fast photolysis during daytime, but they may possibly accumulate at night since their removal by the most abundant oxidant at that time, the nitrate radicals ranges from 18 days to 2 months which is too slow.

The rate coefficients for the reaction between nitramines with chlorine atoms and with ozone as well as for the reaction between the hydroxyl radical and and CH_3NHNO_2, $CH_3CH_2NHNO_2$ and $(CH_3CH_2)_2NNO_2$ has been measured for the first time. Which means this work has provided new data on the reaction rate coefficients between nitramines with chlorine atoms as well as with ozone which has given a better understanding on the atmospheric fates of this group of compounds. New data also have been obtained for the reaction between hydroxyl radical and methylnitramine, ethylnitramine, diethylnitramine. The measured rate coefficient for the reaction between the hydroxyl radicals and dimethylnitramine was in perfect agreement with that of Tuazon *et al*., (1984) which gives more confidence on these two results.

As per Karl *et al.,* (2009), nitrosamines can travel up to 1 km from the source, which means that, some measures need to be incorporated in the Carbon Capture and Storage (CCS) technology to avoid release of amines into the atmosphere so as to limit the formation of these deadly compounds in order to safeguard the people working in the plant and those living in the nearby vicinity.

The Structure Activity Relationship (SAR) for OH reactions with nitramines has been studied and found that, the existing data is insufficient to determine a unique set of SAR parameters describing the nitramine reactivity towards OH radicals; hence more data are needed to develop a reliable SAR for this class of compounds. It is suggested that the OH-SAR for nitramines be modified such that the reactivity of this class of compounds be described in terms of four parameters: $F(RNHNO_2)$, $k(RNHNO_2)$, $F(R_2NNO_2)$ and $k(R_2NNO_2)$ instead of applying the assumption made by Kwok and Atkinson (1995) that, the substituent factors of $–CNHNO_2$, $–R_2NNO_2$ are the same as those of $–NH_2$, >NH and >N– (see Table 2.6.1) which seem to be unrealistic.

Despite of the fact that this study has provided new experimental data and insight to the atmospheric chemistry of amines, still further studies are needed for a better understanding of the atmospheric chemistry of amines. The following further studies are recommended:-

i) More investigation on the reactions of other nitrosamines with NO_3
ii) More kinetic studies on the reaction between nitramines and the hydroxyl radicals to determine the Structure Activity Relationship (SAR)
iii) More product studies from the reaction between nitramines and the hydroxyl radicals
iv) More mechanistic studies for the reaction between amines and the hydroxyl radicals

6 REFERENCES

Acid Deposition and Oxidant Research Centre, "Tropospheric ozone: A growing threat", *Prime Station Corp*., Niigata Japan (2006).

Aker, P. M., Sloan, J. J. "The initial product vibrational energy distribution in the reaction between $O(^1D_2)$ and H_2", *Journal of Chemical Physics* 85 (1986) 1412 - 1417.

Anderson, L. G., Stephens, R. D., "Kinetics of the Reaction of Hydroxyl Radicals with 2-(Dimethylamino) Ethanol from 234-364 K", *International Journal of Chemical Kinetics*, 20 (1988) 103 - 110.

Angelino, S., Suess, D. T., and Prather, K. A., "Formation of aerosol particles from reactions of secondary and tertiary alkylamines: Characterization by aerosol Time-Of-Flight mass spectrometry", *Environmental Science & Technology*, 40 (2001) 3130 – 3138.

Arif, M., Dellinger, B., and Taylor, P. H., "Rate coefficients of hydroxyl radicals reaction with dimethyl ether and methyl *tert*-butyl ether over an extended temperature range", *Journal of Physical Chemistry A*, 101 (1997) 2436 – 2441.

Aronu, U. E., Hallvard F. Svendsen, H. F., Hoff, K. A., Juliussen, O, "Solvent selection for carbon dioxide absorption", *Energy Procedia,* 1 (2009) 1051 – 1057.

Arya, A., Arya, S and Arya, M, "Chemical carcinogen and cancer risk: An overview", *Journal of Chemical and Pharmaceutical Research,* 5 (2011) 621 - 631.

Aschmann, S. M., Atkinson, R., "Atmospheric chemistry of 1-methyl-2-pyrrolidinone", *Atmospheric Environment,* 33 (1999) 591 - 599.

Atkinson, R., Perry, R. A. and Pitts, J. N, Jr., "Rate constants for the reaction of the OH radicals with CH_3SH and CH_3NH_2 over the temperature range 299 - 426 K", *Journal of Chemical Physics,* 66 (1977) 1578 – 1581.

Atkinson, R., Perry, R. A., Pitts, J. N., Jr., "Rate constants for the reactions of the hydroxyl radicals with dimethylamine, trimethylamine, and ethylamine over the temperature range 298-426 K", *Journal of Chemical Physics,* 68 (1978) 1850 - 1853.

Atkinson, R and. Carter, W. P. L, "Kinetics and mechanisms of the gas phase reactions of ozone with organic compounds under atmospheric conditions", *Chemical Review*s, 84 (1984) 437 – 470.

Atkinson, R., "Kinetics and mechanisms of the gas-phase reactions of the hydroxyl radicals with organic compounds under atmospheric conditions", *Chemical Reviews*, 86 (1986), 69 - 201.

Atkinson, R., "A Structure Activity Relationship for the estimation of rate constants for the gas-phase reactions of OH radicals with organic compounds", *International Journal of Chemical Kinetics*, 19 (1987) 799 - 828.

Atkinson, R. "Gas-phase tropospheric chemistry of organic compounds", *Journal of Physical and Chemical Reference Data* Monograph, 2 (1994), p. 132

Atkinson, R., "Atmospheric Transformations of automotive emissions in air pollution, the automotive and public health", *National Academy Press*, Washington, DC, (1988).

Atkinson, R. "Atmospheric reactions of alkoxy and β-hydroxyalkoxy radicals", *International Journal of Chemical Kinetics*, 29 (1997) 99 – 111.

Atkinson, R., "Product studies of gas-phase reactions of organic compounds", *Pure and Applied Chemistry,* 70 (1998) 1335 – 1343.

Atkinson, R., Baulch, D. L., Cox, R. A., Hampson, R. F Jr., Kerr, J. A., Rossi, M. J., and Troe, J., "Evaluated kinetic and photochemical data for atmospheric chemistry: Supplement VII, Organic species – IUPAC subcommittee on gas kinetic data evaluation for atmospheric chemistry", *Journal of Physical and Chemical reference Data*, 28 (1999) 191 – 393.

Atkinson, R., Arey, J., "Atmospheric degradation of volatile organic compounds", *Chemical Review*, 103 (2003) 4605 – 4638.

Atkinson, R., Baulch, D. L., Cox, R. A., Crowley, J. N., Hampson, R. F., Hynes, R. G., Jenkin, M. E., Rossi, M. J., Troe, J. "Evaluated kinetic and photochemical data for atmospheric chemistry: Volume II - gas phase reactions of organic species", *Atmospheric Chemistry and Physics*, 6 (2006) 3625 - 4055.

Azad, K and Andino, J. M., "Products of the gas-phase photooxidation reactions of 1-propanol with OH radicals", *John Wiley & Sons*, *Inc*. (1999).

Bailey, D., Cativiela, J. P., Descary, B., Grantz, D., Hamilton, K., D., Martin, P. E., Meyer, D., Mullinax, D., Simunovic, C. A., Sweet, J., Warner, D., and Watson, J., "Dairy emissions factors for volatile organic compounds", *San Joaquin Valley Air Pollution Control District*, Fresno, CA, (2005).

Bamford, C. H., "A study of the photolysis of organic nitrogen compounds - Part I dimethyl- and diethyl-nitrosamines", *Journal of the Chemical Society*, 12 (1939) 12 - 17.

Barnes, I., Becker, K. H., Fink, E. H., Reimer, A., Zabel, F. and Niki, H., "FTIR spectroscopic study of the gas-phase reaction of HO_2 with H_2CO, *Chemical Physics Letters*, 115 (1985) 1 - 8.

Barnes, I., Solignac, G., Mellouki, A., Becker, K. "Aspects of the atmospheric chemistry of amides", *Journal of Chemical Physics and Physical Chemistry,* 11 (2010) 3844 – 3857.

Bartsch, H. and Montesano, R., "Relevance of nitrosamines to human cancer", *Carcinogenesis,* 5 (1984) 1381 - 1393.

Bidleman, T., Atlas, E. L., Atkinson, R., Bonsang, B., Burns, K., Keene, W. C., Knap, A. H., Miller, J., Rudolph, J., and Tanabe, S., "The Long-range atmospheric transport of natural and contaminant substances", *Kluwer Academy*, (1990).

Bilde, M., Mogelberg, T. E., Sehested, J., Nielsen, O. J., Wallington, T. J., Hurley, M. D., Japar, S. M., Dill, M., Orkin, V. L., Buckley, T. J., Huie, R. E., Kurylo, M. J., "Atmospheric chemistry of dimethyl carbonate: reaction with OH radicals, UV spectra of $CH_3OC(O)OCH_2$ and $CH_3OC(O)OCH_2O_2$ radicals, reactions of $CH_3OC(O)OCH_2O_2$ with NO and NO_2, and fate of $CH_3OC(O)OCH_2O$ radicals", *Journal of Physical Chemistry* A, 101 (1997) 3514 – 3525.

Boffetta, P., Jourenkova; N., and Gustavsson, P., "Cancer risk from occupational and environmental exposure to polycyclic aromatic hydrocarbons", *Cancer Causes Control,* 8 (1997) 444 - 472.

Bolin, B., Doos, B. R., Jaeger, J., and Warrick, R. A. (Eds.), "The greenhouse effect, climatic change and ecosystems", *SCOPE Rep*., 29 (1986) 1 - 541.

Bonard, A., V. Daële, J.L. Delfau, and C. Vovelle, "Kinetics of OH radical reactions with methane in the temperature range 295–660 K and with dimethyl ether and methyl-tert-butyl ether in the temperature range 295–618 K", *Journal of Physical Chemistry A* 106 (2002) 4384 – 4389.

Brasseur, G. P., Orlando, J. J. and Tyndall, G. S., "Atmospheric and Global Change", *Oxford University Press*, (1999).

Bråten H. B, Bunkan, A. J., Bache-Andreassen, L., Solimannejad, L., Nielsen, C. J., "Final report on a theoretical study on the atmospheric degradation of selected amines", NILU (2008).

Burrows, J. P., Moortgat, G. K., Tyndall, G. S., Cox, R. A., Jenkin, M. E., Hayman, G. D., Veyret, B., "Kinetics and mechanism of the photooxidation of formaldehyde. 2. Molecular modulation studies". *Journal of Physical Chemistry A*, 93 (1989) 2375 - 2382.

Cabañas Galan, B., "kinetic studies of methylamine, dimethylamine and trimethylamine reaction with NO_3 radicals"., Universidad de Castilla-La Mancha, Spain, *unpublished results.*

Calvert, J. G.; Derwent, R. G.; Orlando, J. J.; Tyndall, G. S.; Wallington, T. J., "Mechanisms of atmospheric oxidation of the alkanes", *Oxford University Press*, (2008).

Calvert, J. G. and Pitts, J. N. Jr., "Photochemistry"*, Wiley*, New York, (1966).

Campbell, I.M., McLaughlin, D.F., Handy, B.J., "Rate constants for reactions of hydroxyl radicals with alcohol vapours at 292 K", *Chemical Physics Letters*, 39 (1976) 362–364.

Campbell, I. M. and Parkinson, P. E., "Rate constants for reactions of hydroxyl radicals with ester vapours at 292 K", *Chemical Physics Letters*, 53 (1978) 385 - 387.

Carey, F. A., "Organic Chemistry, fourth edition", *McGraw-Hill* (2001) pp 888 - 890.

Carl, S. A. and Crowley, J. N., "Sequential two (blue) photon absorption by NO_2 in the presence of H_2 as a source of OH in pulsed photolysis kinetic studies: Rate constants for reaction of OH with CH_3NH_2, $(CH_3)_2NH$, $(CH_3)_3N$, and $C_2H_5NH_2$ at 295K", *Journal of Physical Chemistry A,* 102 (1998) 8131 - 8141.

Carlier, P., Hannachi, H. and Mouvier, G., "The Chemistry of carnony Compounds in the atmosphere – a review", *Atmospheric Environment*, 20 (1986) 2079 - 2099.

Carlsen, L., Kenesova, O. A., Batyrekova, S. E, "A preliminary assessment of the potential environmental and human health impact of unsymmetrical dimethylhydrazine as a result of space activities", *Chemosphere,* 67 (2007) 1108 - 1116.

Carter, W. P. L., "Development of ozone reactivity scales for volatile organic compounds", *Journal of Air and Waste Management Association*, 44 (1994) 881 – 899.

Chakir, A., Solignac, B., Mellouki, A., Daumont, D., "Gas phase UV absorption cross-sections for a series of amides", *Chemical Physics Letters*, 404 (2005) 74 - 78.

Challis, B. C., Challis, J. A. "*N*-nitrosamines and *N*-nitrosimies", In: The chemistry of amino, nitroso, and nitro compounds and their derivatives. Supplement F. Ed. by: Patai, S. Chichester, *Wiley*, (1982) pp 1151 - 1223.

Cheng, Y., Li, S-M., Leithead, A.,"Chemical characteristics and origins of nitrogen-containing organic compounds in PM2.5 aerosols in the Lower Fraser Valley", *Environmental Science & Technology*, 40 (2006) 5846 – 5852.

Chow, Y. L., Wu, Z. Z., Lau, M. P., Yip, R. W., "On the singlet and triplet excited-states of nitrosamines", *Journal of the American Chemical Society*, 107 (1985) 8196 - 8201.

Ciccioli, P., Brancaleoni, E., Frattoni, M., Cecinato, A. and Brachetti, A., "Ubiquitous occurrence of semi-volatile carbonyl compounds in tropospheric samples and their possible sources", *Atmospheric Environment Part A*, 27 (1993) 1891 - 1901.

Cohen, N., and Benson, S. W., "Transition-state theory calculations for reactions of hydroxyl radicals with haloalkanes", *Journal of Physical Chemistry A*, 91 (1987) 162 – 170

Cooper, D. S., Allan, N. L., and McCulloch, A., "Reactions of hydrofluorocarbons and hydrochlorofluorocarbons with the hydroxyl radicals", *Atmospheric Environment Part A, General topics*, 24A (1990) 2417 – 2419.

CO_2-Kårstø – KU- "Fagrapport konsekvenser av utslipp til luft", 2009 (unpublished report).

Crutzen, J. P., "The major biochemical cycles", *Scope 21* (Eds.: B. Bolin and R. Cook), *Wiley*, Chichester, (1983) pp. 67 – 112.

Cuevas, C. A.; Notario, A.; MartÌnez, E.; Albaladejo, J., "Influence of temperature in the kinetics of the gas-phase reactions of a series of acetates with Cl atoms", *Atmospheric Environment,* 39 (2005) 5091 - 5099.

Curtiss, L. A., Raghavachari, K., Redfern, P. C., Rassolov, V., Pople, J. A. "Gaussian-3 (G3) theory for molecules containing first and second-row atoms", *Journal of Chemical Physics*, 109 (1998) 7764 - 7776.

D'Anna, B., Andresen, W., Gefen, Z., Nielsen, C. J., "Kinetic study of OH and NO_3 radical reactions with 14 aliphatic aldehydes", *Journal of Physical Chemistry Chemical Physics,* 3 (2001) 3057-3063.

DeMore, W. B., and Bayes, K. D., "Rate constants for the reactions of hydroxyl radicals with several alkanes, cycloalkanes and dimethyl ether", *Journal of Physical Chemistry A,* 103 (1999) 2649 – 2654.

Dóbé, S., Otting, M., Temps, F., Wagner, H. Gg. and Ziemer, H., "Fast flow kinetic studies of the reaction $CH_2OH + HCl \leftrightharpoons CH_3OH + Cl$. The Heat of Formation of Hydroxymethyl", *Physical Chemistry* 97 (1993) 877 – 883.

D'Ottone, L.; Bauer, D.; Campuzano-Jost, P.; Fardy, M.; Hynes, A. J., "Vibrational deactivation studies of OH X $^2\Pi$ (v = 1–5) by N_2 and O_2", *Journal of Physical Chemistry and Chemical Physics*, 6 (2004) 4276 – 4282.

Douglass, M. L.; Kabacoff, B. L.; Anderson, G. A.; Cheng, M. C., "The Chemistry of nitrosamine formation, inhibition and destruction", *Journal of the Society of Cosmetic Chemists*, 29 (1978) 581 - 606.

Drawert, F. "Fliichtige Basen des Weines", Vitis 5 (1965) 127.

Dubs, M., Bruhlmann, U., Huber, J. R., "Sub Doppler laser induced fluorescence measurements of the velocity distribution and rotational alignment of NO photofragments", *Journal of Chemical Physics,* 84 (1986) 3106 - 3119.

DuPart M.S., Bacon T.R., and Edwards D.J., "Understanding corrosion in alkanolamine gas treating plants; Parts 1&2", *Hydrocarbon Processing,* 72 (1993) 75 - 80.

Edgerton, S. A., Kenny, D.V., and Joseph, D. W., "Determination of amines in indoor air from steam humidification", *Environmental Science & Technology,* 23 (1989) 484 – 488.

Eisele, F. L., and Tanner, D. J., "Identification of ions in continental air", *Journal of Geophysical Research,* 95 (1990) 20539 - 20550.

Ehhalt, D. H., "Gas phase chemistry of the troposphere. In: Global aspects of atmospheric chemistry", Vol. 6 [Baumgaertel, H., W. Gruenbein, and F. Hensel (eds.)]. *Springer Verlag,* Darmstadt, (1999) pp. 21 – 110.

El Boudali, A., LeCalve, S., LeBras, G., Mellouki, A., "Kinetic studies of OH reactions with a series of acetates". *Journal of Physical Chemistry A,* 100 (1996) 12364 - 12368.

El Dib, G., Chakir, A and Daumont, D., "Gas phase reactions of NO_3 radicals with amides", *Geophysical Research Abstracts*, 7 (2005) 02365.

El Dib, G. and Chakir, A., "Temperature-dependence study of the gas-phase reactions of atmospheric NO_3 radicals with a series of amides", *Atmospheric Environment*, 41 (2007) 5887 - 5896.

Elliott, C. S., Frey, H. M., "Theoretical Treatment of the Pressure Dependence of the Unimolecular Rate Constant Part 1. Cyclobutene, 1-Methylcyclobutene and 3-Methylcyclobutene", *Transactions of the Faraday Society*, 62 (1966) 895 – 909.

Energy Information Administration, Office of Integrated Analysis and Forecasting, U.S. Department of Energy Washington, DC 20585, International Energy Outlook, (2008) DOE/EIA-0484 (www.eia.doe.gov/oiaf/ieo/index.html).

Erupe, M. E., Proce, D. J., Silva, P. J., Malloy, Q. G. J., Warren, L. Q. B., and Cocker, D. R III; "Secondary organic aerosol formation from reaction of tertiary amines with nitrate radical", *Atmospheric Chemistry and Physics Discussions,* 8 (2008) 16585 – 16608.

Fan, J., R. Zhang, D. Collins, and G. Li, "Contribution of secondary condensable organics to new particle formation: A case study in Houston, Texas", *Geophysics Research Letters* 33 (2006), L15802, DOI:10.1029/2006GL026295.

Feilberg, K. L., Johnson, M. S., Nielsen, C. J., "Relative reaction rates of HCHO, HCDO, DCDO, $H^{13}CHO$ and $HCH^{18}O$ with OH, Cl, Br, and NO_3 radicals", *Journal of Physical Chemistry A,* 108 (2004) 7393 – 7398.

Finlayson-Pitts, B. J., and Pitts, Jr., J. N, "Atmospheric Chemistry: Fundamentals and Experimental Techniques", *John Wiley & Sons Ltd*, New York, (1986).

Finlayson-Pitts, B. J., and Pitts, Jr., J. N., "Chemistry of the Upper and Lower Atmosphere: Theory, Experiments, and Applications"; *Academic Press*, (2000).

Fostås, B., Gangstad, A., Nenseter, B., Pedersen, S., Sjøvoll, M., Sørensen, A. L., "Effects of NOx in the Flue Gas Degradation of MEA", *Energy Procedia,* 4 (2011) 1566 – 1573.

Forster, P., V. Ramaswamy, P. Artaxo, T. Berntsen, R. Betts, D.W. Fahey, J. Haywood, J. Lean, D.C. Lowe, G. Myhre, J. Nganga, R. Prinn, G. Raga, M. Schulz and R. Van Dorland: Changes in Atmospheric Constituents and in Radiative Forcing. In: Climate Change 2007: The Physical Science Basis. Contribution of Working Group I to the Fourth Assessment Report of the Intergovernmental Panel on Climate Change [Solomon, S., D. Qin, M. Manning, Z. Chen, M. Marquis, K. B. Averyt, M. Tignor and H.L. Miller (eds.)]. Cambridge University Press, Cambridge, United Kingdom and New York, NY, USA, (2007).

Frei E, Pool, B. L., Plesch, W., and Wiessler, M., "Biochemical and biological properties of prospective *N*-nitrodialkylamine metabolites and their derivatives", *IARC Scientific Publications* 57, (1984) 491 - 497.

Gaffney, J. S., and Levine, S. Z., "Predicting gas phase organic molecule reaction rates using linear free-energy correlation I. Oxygen (O^3P) and hydroxyl addition and abstraction reactions", *International Journal of Chemical Kinetics*, 11 (1979) 1197 - 1209.

Galano, A., Alvarez-Idaboy, J. R. "Branching ratios of aliphatic amines + OH gas-phase reactions: A variational transition-state theory study", *Journal of Chemical Theory and Computation,* 4 (2008) 322 - 327.

Garzón, A. G., Cuevas, C. A., Ceacero, A. A., Notario, A., Albaladejo, J. and Fernández-Gómez, M. "Atmospheric reactions $Cl+CH_3–(CH_2)_n–OH$ (n =0 – 4): A kinetic and theoretical study" *Journal of Chemical Physics*, 125 (2006) 104305.

Ge, X., Wexler, A. S., and Clegg, S. L., "Atmospheric amine - Part I. A review", *Atmospheric Environment,* 45 (2011) 524 – 546.

Geiger, G.; Huber, J. R., "Photolysis of Dimethylnitrosamine in the Gas-Phase", *Helvetica Chimica Acta*, 64 (1981) 989 - 995.

Geiger, G., Stafast, H., Bruehlmann, U., Huber, J. R., "Photodissociation of dimethylnitrosamine", *Chemical Physics Letters*, 79 (1981) 521 - 524.

Gierczak, T., Talukdar, R. K., Herndon, S., Vaghjiani, G. L., and Ravishankara, A. R., "Rate Coefficients for the Reactions of Hydroxyl Radicals with Methane and Deuterated Methanes", *Journal of Physical Chemistry A*, 101 (1997) 3125 – 3134.

Glarborg, P., Kristensen, P. G., Jensen, S. H., Damjohansen, K, "A flow reactor study of HNCO oxidation chemistry", *Combustion and Flame*, 98 (1994) 241 - 258.

Glasson, W. A., "An experimental evaluation of atmospheric nitrosamine formation", *Environmental Science & Technology,* 13 (1979) 1145 - 1146.

Gola, A, A., D'Anna, B., Feilberg, K, L., Sellevåg, S, R., Bache-Andreassen, L., and Nielsen, C, J., "Kinetic isotope effects in the gas phase reactions of OH and Cl with

CH_3Cl, CD_3Cl, and $^{13}CH_3Cl$", *Atmospheric Chemistry and Physics Discussions*, 5 (2005) 3873 – 3898.

Good, D, A. and Francisco, J. S., "Tropospheric oxidation mechanism of dimethyl ether and methyl formate", *Journal of Physical Chemistry A*, 104 (2000) 1171 - 1185.

Good, D. A.; Hansen, J.; Kamoboures, M.; Santiono, R.; Francisco, J. S., "An Experimental and Computational Study of the Kinetics and Mechanism of the Reaction of Methyl Formate with Cl Atoms", *Journal of Physical Chemistry A,* 104 (2000) 1505 - 1511.

Goodall, C. M., Kennedy, T. H., "Carcinogenicity of dimethylnitramine in NZR rats and NZO mice", *Cancer Letters,* 1 (1976) 295 – 298.

Gorse, R. A., Jr.; Lii, R. R.; Saunders, B. B. Hydroxyl radical reactivity with diethylhydroxylamine. *Science (Washington, DC, United States)*, 197 (1977), 1365-7.

Gorzelska, K., and Galloway J. N., "Amine Nitrogen in the Atmospheric Environment over the North Atlantic Ocean", *Global Biogeochemical Cycle,* 4 (1990) 309 - 333.

Gowenlock, B. G., Pfab, J., Williams, G. C., "Quantum yields for the photolysis of some nitrosamines in solution". *Journal of Chemical Research (S)*, 9 (1978) 362 - 363.

Graedel, T. E. and Crutzen, P. J., "Atmospheric Change: An Earth System Perspective", W. *H. Freeman and Company*, (1993) pp 41.

Greenhill, P. G. and O'Grady, V. B., "The Rate Constant of Hydroxyl Radicals with Methanol and (D_3)Methanol", *Australian journal of Chemistry,* 39 (1986), 1775 – 1787.

Griffith, D. W. T., "Synthentic calibation and quantitative analysis of gas-phase FTIR spectra" *Applied Spectroscopy,* 50 (1996) 59 - 70.

Grosjean, D., "Atmospheric Chemistry of Toxic Contaminants. 6. Nitrosamines: Dialkyl Nitrosamines and Nitrosomorpholine", *Journal of the Air & Waste Management Association,* 41 (1991) 306 - 311.

Güesten, H., Klansic, L. and Maric, D., "Prediction of the abiotic degradebaility of organic compounds in the troposphere", *Journal of Atmospheric Chemistry*, 2 (1984) 83 - 93

Guidance on Estimating Motor Vehicle Emission Reductions from the Use of Alternative Fuels and Fuel Blends; U.S.E.P.A.; Report No. 1 EPA-AA-TSS-PA-87-4; Ann Arbour, Michigan, (1998).

Harris, G. W., Pitts, J. N., "Rates of Reaction of Hydroxyl Radicals with 2-(Dimethylamino)Ethanol and 2-Amino-2-Methyl-1-Propanol in the Gas-Phase at 300 ± 2 K". *Environmental Science & Technology*, 17 (1983) 50 - 51.

Hanst, P. L., Spence, J. W. and Miller, M., "Atmospheric Chemistry of *N*-Nitroso Dimethylamine", *Environmental Science & Technology*, 11 (1977) 403 - 405.

Hassel, M., Frei, E., Scherf, H. R., and Wiessler, M., "Investigation into the pharmacodynamics of the carcinogen *N*-nitrodimethylamine". *IARC Science Publications,* 84 (1987)150 - 152.

Haszeldine, R. N. and Jander, J., "Studies in spectroscopy. Part VI. Ultra-violet and infra-red spectra of nitrosamines, nitrites, and related compounds", *Journal of Chemical Society*, (1954) 691 - 695.

Heicklen, J., "The correlation of rate coefficients for hydrogen-atom abstraction by hydroxyl radicals with carbon-hydrogen bond dissociation enthalpies", *International Journal of Chemical Kinetics*, 13 (1981) 651 – 665.

Helmig, D., Muller, J., and Klein, W., "Volatile organic substances in a forest atmosphere", *Chemosphere*, 19 (1989) 1399 – 1412.

Herzog, H., "What future for carbon capture and sequestration?" *Environmental Science & Technology* (2001), 35:148A–153A.

Herzog, H. and Golomb, D., "Carbon capture and storage from fossil fuel use", (2004) **(pdf).**

Hess, W.P., Tully, F.P., "Hydrogen-atom abstraction from methanol by OH radicals", *Journal of Physical Chemistry A* 93 (1989) 1944–1947.

Hodson, J., "The estimation of the photo degradation of organic compounds by hydroxyl radical reaction rate constants obtained from nuclear magnetic resonance spectroscopy chemical shift data", *Chemosphere,* 13 (1988) 2339 – 2348.

Höök, M., Carbon capture and storage", UHDSG report, (2007).

Houston, P. L., "Chemical kinetics and reaction dynamics", *McGraw-Hill*, New York, (2001).

Huang, Y., Gu, Y., Liu, C., Yang, X., Tao, Y., "The nascent product vibrational energy distribution of the reaction $O(^1D) + H_2$ by the grating selection chemical laser technique", *Chemical Physics Letters,* 127 (1986) 432 - 437.

Iijima, M. CO_2 Recovery from flue gas using hindered amines (http://www.co2management.org/proceedings/Masaki_Iijima.pdf)

IPCC: Climate Change (2001): Synthesis Report.

Itoh, T., Matsuya, Y., Maeta, H., Miyakazi, M., Nagata, K., and Ohsawa, A., "Reaction of secondary and tertiary amines with nitric oxide in the presence of oxygen", *Chemical and Pharmaceutical Bulletin,* 47 (1999) 819 - 823.

Iuga, C., Olea, R. E., and Vivier-Bunge, A., "Mechanism and kinetics of the OH radicals reaction with formaldehyde bound to an $Si(OH)_4$ monomer", *Journal of the Mexican Chemical Society,* 51 (2008) 36 - 46.

IUPAC Subcommittee on gas kinetic data evaluation. http://www.iupac-kinetic.ch.cam.ac.uk/

Janach, W. E., "Surface ozone: Trend details, seasonal variations, and interpretation", *Journal of Geophysics Research,* 94 (1989) 18289 - 18295.

Jahan, K., Smith, R., Scrivani, D., Giacobbe, D., McDonough, J. and Addu, A., "Fate of nitrosodimethylamine (NDMA)", *Waste Management and the Environment,* 4 (2008) 665 - 674.

Japar, S. M., Wallington, T. J., Richert, J. F., Ball, J. C., "The atmospheric chemistry of oxygenated fuel additives: t-Butyl alcohol, dimethyl ether, and methyl t-Butyl ether" *International Journal of Chemical Kinetics*, 22 (1990) 1257 – 1269.

Jenkin, M. E.; Hayman, G. D.; Wallington, T. J.; Hurley, M. D.; Ball, J. C.; Nielsen, O. J.; Ellermann, T., "Kinetic and mechanistic study of the self-reaction of methoxymethylperoxy radicals at room temperature". *Journal of Physical Chemistry A,* 97 (1993) 11712 - 11723.

Jimènez, E., Gilles, M. K., and Ravishankara, A. R., "Kinetics of the reactions of hydroxyl radical with CH_3OH and C_2H_5OH between 235 and 360 K", *Journal of Photochemistry and Photobiology A: Chemistry*, 157 (2003) 237 – 245.

Jones, R. L., Pyle, J. A., Hardes, J. E., Zavody, A .M., RusseII III, J . M. and Gille, J . C., "The water vapour budget of the stratosphere studied using LIMS and SAMS satellite data", *Quarterly Journal of the Royal Meteorological Society*, 112 (1986) 1127 - 1144.

Johnson, M. S., Feilberg, K. L., von Hessberg, P and Nielsen, O. J., "Isotopic processes in atmospheric chemistry", *Chemical Society Reviews*, 31, (2002)313–323.

Kapteina, S., Slowik, K., Verevkin, S. P., and Heintz, A.: "Vapor pressures and vaporization enthalpies of a series of ethanolamines", *Journal of Chemical Engineering Data*, 50 (2005) 398 – 402.

Karl, M., Brooks, M., Wright, R. and Knudsen, S: "Amines worst case studies: Worst case studies on amine emissions from CO_2 capture plants (Task 6)", (2009) (Norwegian Institute of Public Health report).

Karl, M., Dye, C., Schmidbauer, N., Wisthaler, A., Mikoviny, T., D′Anna, B., Müller, M., Borrás, E., Clemente, E., Munoz, A., Porras, R., Ródenas, M., Vázquez, M., Brauers, T., "Study of OH-initiated degradation of 2-aminoethanol", *Atmospheric Chemistry and Physics*, 12 (2012) 1881 – 1901.

Kerr, J. A. and Sheppard, D. W., "Kinetics of the reactions of hydroxyl radicals with aldehydes studied under atmospheric conditions" *Environmental Science & Technology,* 15 (1981) 960 - 963.

Khudoley, V., Malaveille, C., and Bartsch H., "Mutagenicity studies in Salmonella typhimurium on some carcinogenic *N*-Nitramines *in vitro* and in the host-mediated assay in rats" *Cancer Research,* 41 (1981) 3205 – 3210.

King, R. D., Mungglетont, S. H., Srinivasani, A., and Sternberg, M. J. E., "Structure-activity relationships derived by machine learning: The use of atoms and their bond connectivities to predict mutagenicity by inductive logic programming, *Proceedings of the National Academy of Sciences*, 93, (1996) 438-442.

Klamt, A., "Estimation of gas phase hydroxyl radical rate constants of organic compounds from molecular orbital calculations", *Chemosphere*, 26 (1993) 1273 – 1289.

Koch, R., Kruger, H. U., Elend, M., Palm, W. U., Zetzsch, C., "Rate constants for the gas-phase reaction of OH with amines: tert-Butyl amine, 2,2,2-trifluoroethyl amine and 1,4-diazabicyclo[2.2.2]octane", *International Journal of Chemical Kinetics,* 28 (1996), 807 - 815.

Koch, R., Palm, W. U., Zetzsch, C. "First rate constants for reactions of OH radicals with amides", *International Journal of Chemical Kinetics*, 29 (1997) 81 - 87.

Kohl, A, L., and Nielsen, R. B., "Gas Purification", fifth edition, Golf, Houston, 1997.

Kotzias, D., Konidara, C. and Spartá, C., in Biogenic Volatile Organic Compounds in the atmosphere: Summary of Present Knowledge*,* eds. G. Helas, S. Slanina and R. Steinbrecher, *SPB Academic Publishers*, Amsterdam, (1997), p. 67.

Kramp, F and Paulson, S. E., "On the uncertainties in the rate coefficients for OH reactions with hydrocarbons, and the rate coefficients of the 1,3,5-trimethylbenzene and m-xylene reactions with OH radicals in the gas phase". *Journal of Physical Chemistry A*, 102 (1998) 2685 - 2690.

Kwok, E. S. C, Atkinson, R., "Estimation of hydroxyl radical reaction rate constants for gas-phase organic compounds using a Structure Reactivity Relationship; an update", *Atmospheric Environment,* 29 (1995) 1685 - 1695.

Låg, M., Instanes, C., Lindemann, B. and Andreassen, Å. "Health effects of possible degradation products of different amines relevant for CO_2 capture", *Norsk institutt for luftforskning*, (2008b).

Låg, M., Lindeman, B., Instanes, C., Brunborg, G., and Schwarze, P, "Health effects of amines and derivatives associated with CO_2 capture", *Norwegian Public Health Institute* Report, (2011).

Laidler, J. K. "Chemical Kinetics",3rd edition, *Harper & Row, Publishers*, New York (1987).

Langer, S., Ljungström, E., and I. Wängberg, I., "Rates of reaction between the nitrate radical and some aliphatic esters"*Journal of Chemical Society, Faraday Transactions,* 89 (1993) 425 - 431.

Lawrence1, M. G., Jöckel1, P., and von Kuhlmann, R., "What does the global mean OH concentration tell us?" *Atmospheric Chemistry and Physics*, 1, (2001) 37 – 49.

Layer, R. W. "Chemistry of imines", *Chemical Reviews*, *63* (1963) 489 - 510.

Lazarou, Y.G., Kambanis, K.G., Papagiannakopoulos, P., "Gas-Phase Reactions of $(CH_3)_2N$ Radicals with NO and NO_2", *Journal of Physical Chemistry A,* 98 (1994) 2110 - 2115.

Le Calve´, S. P., Le Bras, G., and Mellouki, A, "Temperature dependence of the rate coefficients of the reaction of the OH radicals with a series of Formates", *Journal of Physical Chemistry A,* 101 (1997) 5489 – 5493.

Le Calve´, S. P., Le Bras, G., and Mellouki, A, "Kinetic studies of OH reactions with *iso*-propyl, *iso*-butyl, *sec*-butyl, and *tert*-butyl acetate", *International Journal of Chemical Kinetics*, 29 (1997) 683 – 688.

Lepaumier, H., Picq, D., and Carrette, P., "New amines for CO_2 capture. II. oxidative degradation mechanisms", *Industrial and Engineering Chemistry Research,* 48 (2009) 9068 – 9075.

Lloyd, J. A., Heaton, K. J., Johnston, M. V., "Reactive uptake of trimethylamine into ammonium nitrate particles"*Journal of Physical Chemistry A*, 113 (2009) 4840 – 4843.

Lin, J. K., "Nitrosamines as potent environmental carcinogens in man", *Clinical Biochemistry,* 23 (1990) 67 – 71.

Lin, J. K., Yen, J. Y., "Changes in the nitrate and nitrite contents of fesh vegetables during cultivation and post-harvest storage", *Food and Cosmets Toxicology,* 18 (1980) 597 – 603.

Lindley, C. R. C.; Calvert, J. G.; Shaw, J. H., "Rate studies of the reactions of the $(CH_3)_2N$ radical with O_2, NO, and NO_2", *Chemical Physics Letters*, 67 (1979) 57 - 62.

Lowe, D. C., Brenninkmeijer, C. A. M., Manning, M. R., Sparks, S. and Wallace, G., "Radiocarbon determination of atmospheric methane at Baring Head, New Zealand", *Nature*, 332 (1988), 522 - 525.

Malloy, Q. G. J., Qi1, L., Warren1, B., Cocker, D.R III., Erupe, M. E., and Silva, P. J; "Secondary organic aerosol formation from primary aliphatic amines with NO_3 radical", *Atmospheric Chemistry and Physics Discussions,* 8 (2008) 12695 – 12720.

Ma'mun, S., Svendsen, H. F., Hoff, K. A., Juliussen, O, "Selection of new absorbents for carbon dioxide capture", *Energy Conversion and Management,* 48 (2007) 251 – 258.

Manahan, S. E.: "Environmental Chemistry", 4th Ed., *Lewis*, (1990).

Martin, Y. C., "Quantitative Drug Design: A Critical Introduction", *Dekker*, New York, (1978).

McCaulley, J.A. Kelly, N. Golde, .M.F Kaufman, F. "Kinetic studies of the reactions of F and OH with CH_3OH", *Journal of Physical Chemistry A*, 93 (1989) 1014–1018.

McMurry, J., Organic Chemistry, *Thomson Brooks\ Cole* (2008) pages 916 – 961.

Mellouki, A., Teton, S., and Le Gras, G., "Kinetics of OH radical reactions with a series of ethers", *International Journal of Chemical kinetics*, 27 (1995) 791 - 805.

Mezyk, S. P., Ewing, D. B., Kiddle, J. J., and Madden; K. P., "Kinetics and mechanisms of the reactions of hydroxyl radicals and hydrated electrons with nitrosamines and nitramines in water", *Journal of. Physical Chemistry A,* 110 (2006) 4732 - 4737.

Michael, J. V.; Nava, D. F.; Payne, W. A.; Stief, L. J., "Rate constants for the reaction of atomic chlorine with methanol and dimethyl ether from 200 to 500 K", *Journal of Chemical Physics,* 70 (1979) 3652-3656.

Mirvish, S. S., Bulay, O., Runge, R. G., and Patil, K., "Study of the carcinogenicity of large doses of dimethylnitramine, *N*-nitroso-1-proline and sodium nitrite administered in drinking water to rats", *Journal of National Cancer Institute*, 64 (1980) 1435 - 1442.

Mitchell, J. F. B., "The greenhouse effect and climate change", *Reviews of Geophysics,* 27 (1989) 115 - 139.

Müller, C., Iinuma, Y., Karstensen, J., van Pinxteren, D., Lehmann, S., Gnauk, T. and , Herrmann , H., "Seasonal variation of aliphatic amines in marine sub-micrometer particles at the Cape Verde islands", *Atmospheric Chemistry and Physics*, 9 (2009) 9587 – 9597.

Murphy, S. M., Sorooshian, A., Kroll, J. H., Ng, N. L., Chhabra, P., Tong, C., Surratt, J. D., Knipping, E., Flagan, R. C., and Seinfeld, J. H., "Secondary aerosol formation from atmospheric reactions of aliphatic amines", *Atmospheric Chemistry and Physics*, 7 (2007) 2313 – 2337.

Nadykto, A. B., Yu, F., Jakovleva, M. V., Her, J. and Xu, Y., "Amines in the atmosphere: A Density Fuction Theory study of the thermochemistry of pre-nucleation clusters", *Entropy,* 13 (2011) 554 – 569.

National Research Council. Committee on tropospheric ozone formation and measurement rethinking the ozone problem in urban and regional air pollution. *National Academy Press,* Washington, D.C., (1991).

Neftel, A., Moor, E., Oeschger, H. and Stauffer, B., "Evidence from polar ice cores for the increase in atmospheric CO_2 in the past two centuries", *Nature,* 315 (1985) 45 - 47.

Nelson, L., Rattigan, O., Neavyn, R., Sidebottom, H., Treacy, J. and Nielsen, O. J., "Absolute and relative rate constants for the reactions of hydroxyl radicals and chlorine atoms with a series of aliphatic alcohols and ethers at 298 K", *International Journal of Chemical Kinetics,* 22 (1990) 1111 - 1126.

Neurath, G. B., Dünger, M., Pein, F. G., Ambrosius, D. and Schreiber, O., "Primary and Secondary amines in the human environment", *Food and Cosmetics Toxicology*, 15 (1977) 275 – 282.

Nguyen Minh, T., Sengupta, D., Ha, T.-K., "Another look at the decomposition of methyl azide and methanimine: How is HCN formed?" *Journal of Physical Chemistry A*, 100 (1996) 6499 - 6503.

Nielsen, C. J., D'Anna, B., Dye, C., George, C., Graus, M., Hansel, A., Karl, M., King, S., Musabila, M., Müller, M., Schmiedbauer, N., Stenstrøm, Y., Wisthaler, A., "Atmospheric Degradation of Amines (ADA). Summary Report: Gas phase photoPoxidation of 2-aminoethanol (MEA)"- NILU (2010).

Nielsen, C. J., D'Anna, B., Dye, C., Graus, M., Karl, M., King, S., Maguta, M. M., Muller, M., Schmidbauer, N., Stenstrom, Y., Wisthaler, A. and Pedersen, S., "Atmospheric chemistry of 2-aminoethanol (MEA)", *Energy Procedia,* 4 (2011) 2245 – 2252.

Nielsen, C. J.; D'Anna, B.; Karl, M.; Aursnes, M.; Boreave, A.; Bossi, R.; Bunkan, A. J. C.; Glasius, M.; Hansen, A.-M. K.; Hallquist, M.; Kristensen, K.; Mikoviny, T.; Maguta, M. M.; Müller, M.; Nguyen, Q.; Westerlund, J.; Salo, K.; Skov, H.; Stenstrøm, Y.; Wisthaler, A., "Summary Report: Photo-oxidation of Methylamine, Dimethylamine and Trimetahylamine". *Climit project no. 201604* - NILU (2011).

Notario, A.; Mellouki, A.; Le Bras, G., "Rate constants for the gas-phase reactions of Cl atoms with a series of ethers", *Internation Journal of Chemical Kinetics,* 32 (2000) 105 - 110.

Notario, A.; Le Bras, G.; Mellouki, A., "Absolute Rate Constants for the reactions of Cl atoms with a series of esters", *Journal of Physical Chemistry A,* 102 (1998) 3112 - 3117.

Ogawa, T., Ohashi, Y., Yamanaka, S., Miyaike; K, "Development of carbon dioxide removal system from the flue gas of coal fired power plants", *Energy Procedia,* 1 (2009) 721 - 724.

Padhye, L. P., Hertzberg, B., Yushin, G. and Huang, Ching-Hua, "*N*-Nitrosamines formation from secondary amines by nitrogen fixation on the surface of activated carbon", *Environmental Science & Technology,* 45 (2011) 8368 – 8376.

Palmiotto, G., Pieraccini, G., Moneti, G., Dolara, P., "Determination of the levels of aromatic amines in indoor and outdoor air in Italy", *Chemosphere,* 43 (2001) 355 - 361.

Park, J. Y.; Slagle, I. R.; Gutman, D., "Kinetics of the reaction of chlorine atoms with vinyl bromide and its use for measuring chlorine-atom concentrations", *Journal of Physical Chemistry A,* 87 (1983) 1812 - 1818.

Patai, S. "The chemistry of the carbon-nitrogen double bond", London, *Interscience*, (1970).

Penner, J, E., and T. Novakov, "Carbonaceous Particles in the Atmosphere: A Historical Perspective to the Fifth International conference on carbonaceous particles in the atmosphere", *Journal of Geophysics Research,* 101 (1996) 19373 - 19378.

Perry, R, A., R. Atkinson, R., and Pitts, J. N., "Rate constants for the reaction of OH radicals with dimethyl ether and vinyl methyl ether over the temperature range 299–427 °K", Journal of Chemical Physics 67, (1977); 611 – 614.

Picquet, B., Heroux, S., Chebbi, A., Doussin, J., Durand-Jolibois, R., Monod, A., Loirat, H. and Carlier, P., "Kinetics of the reactions of OH radicals with some oxygenated volatile organic compounds under simulated atmospheric conditions" *International Journal of Chemical Kinetics*, 30 (1998) 839 – 847.

Pinches, M.A., Waler, R. F., "Determination of atmospheric contaminants using a continuous paper-tape person personal monitor-I. Analysis of aromatic amines", *The Annals of Occupation Hygiene,* 23 (1980) 335 - 352.

Pilling, M. J. and Seakins, P. W., "Reaction kinetics", *Oxford University Press* (1995).

Pitts, Jr J. N., Grosjean, D., Vancauwenberghe, K. V., Schimid, J. P., and Fitz, D. R., "Photooxidation of alphatic amines under simulated atmospheric conditions: Formation of nitrosamines, nitramines, amides and photochemical oxidant", *Environmental Science & Technology,* 12 (1978) 946 – 953.

Plumlee, M. H.; Reinhard, M., "Photochemical attenuation of *N*-nitrosodimethylamine (NDMA) and other nitrosamines in surface water", *Environmental Science & Technology*, 41 (2007) 6170 - 6176.

Price, D. J., "Field and smog chamber studies of agricultural emissions and reaction products", *Utah State University*, (2010).

Pszenny, A. A. P., W. C. Keene, D. J. Jacob, S. Fan, J. R. Maben, M. P. Zetwo, M. Springer-Young, and J. N. Galloway, "Evidence of inorganic chlorine gases other than hydrogen chloride in marine surface air, *Geophysics Research Letters,* 20 (1993) 699 – 702.

Puxty, G., Rowland, R., Allport, A., Yang, Q., Bown, M., Burns, R., Maeder, M., and Attalla, M., "Carbon dioxide post-combustion capture: a novel screening study of the carbon dioxide absorption performance of 76 amines", *Environmental Science & Technology*, 43 (2009) 6427 – 6433.

Payne, W. A., Brunning, J., Mitchell, M. B. and Stief, L. J., "Kinetics of the reactions of atomic chlorine with methanol and the hydroxymethyl radical with molecular oxygen at 298 K" *International Journal of Chemical Kinetics,* 20 (1988) 63 – 74.

Qiuw, C and Zhang, R., "Multiphase chemistry of atmospheric amines", *Physical chemistry, chemical physics*, 15 (2013), 5738 - 5752

Rademacher, P. and Lüttke, W., "Schwingungsspektren isotoper dimethylnitrosamine", *Spectrochimica Acta Part A: Molecular Spectroscopy*, 27 (1971) 715 – 738

Raja, S., Raghunathan, R., Kommalapati, R. R., Shen, X., Collett, J. L. Jr., Valsaraj, K. T., "Organic composition of fogwater in the Texas–Louisiana gulf coast corridor", *Atmospheric Environment*, 43 (2009) 4214 – 4222.

Ramsden, C., "Comprehensive Medicinal Chemistry 4", *Pergamon*, Oxford (1990).

Rao, A. B., and Rubin, E. S., "A technical, economica, and environmental assessment of amine-based CO_2 capture technology for power plants green house gas control", *Environmental Science & Technology,* 36 (2002) 4467 – 4475.

Rochelle, G. T., "Amine scrubbing for CO_2 capture", *Science*, 325 (2009) 1652 – 1654.

Rogge, W. F., Hildemann, L. M., Mazurek, M. A., Cass, G. R., "Sources of fine organic aerosol. 1. Charbroilers and meat cooking operations", *Environmental Science & Technolology*, 25 (1991) 1112– 1125.

Rothman, L. S.; Gordon, I. E.; Barbe, A.; ChrisBenner, D.; Bernath, P. F.; Birk, M.; Boudon, V.; Brown, L. R.; Campargue, A.; Champion, J.-P.; Chance, K.; Coudert, L. H.; Danaj, V.; Devi, V. M.; Fally, S.; Flaud, J.-M.; Gamache, R. R.; Goldmanm, A.; Jacquemart, D.; Kleiner, I.; Lacome, N.; Lafferty, W. J.; Mandin, J.-Y.; Massie, S. T.; Mikhailenko, S. N.; Miller, C. E.; Moazzen-Ahmadi, N.; Naumenko, O. V.; Nikitin, A. V.; Orphal, J.; Perevalov, V. I.; Perrin, A.; Predoi-Cross, A.; Rinsland, C. P.; Rotger, M.; Simeckova, M.; Smith, M. A. H.; Sung, K.; Tashkun, S. A.; Tennyson, J.; Toth, R. A.; Vandaele, A. C.; VanderAuwera, J., "The HITRAN 2008 molecular spectroscopic database", *Journal of Quantitative Spectroscopy & RadiativeTransfer,* 110 (2009) 533 -572.

Rostkowska, K., Zwierz, K., Różański, A., Moniuszko-Jakoniuk, J., Roszczenko, A., "Formation and metabolism of *N*-Nitrosamines", *Polish Journal of Environmental Studies,* 7 (1998) 321 - 325.

Rounbehler, D. P., Reisch, J., and Fine, D. H., "Nitrosamines in new motorcars", *Food and Cosmetics Toxicology,* 18 (1979) 147 – 151.

Rubino, G.F., Scansetti, G., Piollatto, G., Pira, E., "The carcinogenic effect of aromatic amines: an epidemiological study on the role of o-toluidine and 4,4′-methylene bis (2-methylaniline) in inducing bladder cancer in Man", *Environmental Research,* 27 (1982) 241-254.

Rudic, S., Murray, C., Harvey, J. N., Orr-Ewing, A. J., "The product branching and dynamics of the reaction of chlorine atoms with methylamine" *Physical Chemistry Chemical Physics*, *5* (2003) 1205-1212.

Saueressig, G., Crowley, J. N., Bergamaschi, P., Bruhl, C., Brenninkmeijer, C. A. M., and Fischer, H., "Carbon 13 and D kinetic isotope effects in the reactions of CH_4 with $O(^1D)$ and OH: New laboratory measurements and their implications for the isotopic composition of stratospheric methane", *Journal of Geophysics Research*, 106(D19), (2001) 23127 – 23138.

Saunders, D. G.; Mosier, J. W., "Photolysis of *N*-nitrosodi-n-propylamine in water", *Journal of Agricultural and Food Chemistry*, 28 (1980) 315 - 319.

Schade, G. W.; Crutzen, P. J., "Emission of aliphatic-amines from animal husbandry and their reactions - potential source of N_2O and HCN", *Journal of Atmospheric Chemistry*, 22 (1995) 319 - 346.

Scherf, H. R., Frei, E., and Wiessler, M., "Carcinogenic properties of *N*-nitrodimethylamine and *N*-nitromethylamine in the rat", *Carcinogenesis*, 10 (1989) 1977 - 1981.

Seakins, P. W., Orlando, J. J. and Tyndall, G. S., "Rate coefficients and production of vibrationally excited HCl from the reactions of chlorine atoms with methanol, ethanol, acetaldehyde and formaldehyde", *Physical Chemistry Chemical Physics*, 6 (2004) 2224 - 2229.

Sehested, J., Mogelberg, T., Wallington, T. J., Kaiser, E. W., and Nielsen, O. J., "Dimethyl ether oxidation: Kinetics and mechanism of the $CH_3OCH_2 + O_2$ reaction at 296 K and 0.38−940 Torr total pressure", *Journal of Physical Chemistry A*, 100 (1996), 17218 -17225.

Seinfeld J. H., Andino, J. M., Bowman, F. M., Foster, H. J. L. and Pandis, S. N. "Tropospheric Chemistry", *Advanced Chemical Engineering*, 19 (1994) 325 - 407

Seinfeld, J. H. and Pandis, S. N., "Atmospheric chemistry and physics: From air pollution to climate change", *John Wiley and Sons, Inc*., (1998).

Shao, R. And Stangeland, A., "Amines used in CO_2 capture- Health and environmental impacts", (The Bellona Foundation Report, (2009).

Singh, H. B., G. L. Gregory, A. Anderson, E. Browell, G. W. Sachse, D. D. Davis, J. Crawford, J. D. Bradshaw, R. Talbot, D. R. Blake, D. Thornton, R. Newell, and J. Merrill, "Low ozone in the Marine Boundary Layer of the Tropical Pacific Ocean: photochemical loss, chlorine atoms, and entrainment", *Journal of Geophysics Research.,* 101 (1996a) 1907 - 1917.

Silva, P. J., Erupe, M. E., Price, D and Elias, J., "Trimethylamine as precursor to secondary organic aerosol formation via nitrate radical reaction in the atmosphere", *Environmental Science & Technology,* 42 (2008) 4689 – 4696.

Sims, R. E. H., Schock, R. N., Adegbululgbe, A., Fenhann, J., Konstantinaviciute, I., Moomaw, W., Nimir, H. B., Schlamadinger, B., Torres-Martínez, J., Turner, C., Uchiyama, Y., Vuori, S.J.V., Wamukonya, N., Zhang, X., 2007: Energy supply. "In Climate Change (2007): Mitigation. Contribution of Working Group III to the Fourth Assessment Report of the Intergovernmental Panel on Climate Change" [B. Metz, O.R. Davidson, P.R. Bosch, R. Dave, L.A. Meyer (eds)], Cambridge University Press, Cambridge, United Kingdom and New York.

Slagle, I.R., Dudich, J. F., Gutman, D., "Identification of reactive routes in the reactions of oxygen atoms with methylamine, dimethylamine, trimethylamine, ethylamine, diethylamine, and triethylamine", *Journal of Physical Chemistry A*, 83 (1979) 3065 - 3070.

Smith, J. N., Barsanti, K. C., Friedli, H. R., Ehn, M., Kulmala, M., Collins, D. R., Scheckman, J. H., Williams, B. J., and McMurry, P. H., "Observations of aminium salts in atmospheric nanoparticles and possible climatic implications", *Proceedings of the National Academy of Sciences,* 107 (2010) 66434 – 66439.

Smith, J. D., DeSain, J. D. and Taatjes, C. A., "Infrared laser absorption measurements of HCl(v=1) production in reactions of Cl atoms with isobutane, methanol, acetaldehyde, and toluene at 295 K", Chemical Physics Letters, 366 (2002), 417 - 425.

Smith, D. F.; Kleindienst, Hudgens, T. E., McIver, E. E., Bufalini, C. D., "The photooxidation of methyl *tertiary* butyl ether", *International Journal of Chemical Kinetics,* 23 (1991), 907 - 924.

Smith, D. F.; Kleindienst, T. E.; Hudgens, E. E.; McIver, C. D.;Bufalini, J. J., "Kinetics and mechanism of the atmospheric oxidation of Ethyl *tertiary* butyl ether", *International Journal of Chemical Kinetics,* 24 (1992) 199 - 2154.

Smith, D. F.; McIver, C. D.; Kleindienst, T. E., "Kinetics and mechanism of the atmospheric oxidation of tertiary amyl methyl ether", *International Journal of Chemical Kinetics,* 27 (1995) 453 - 472.

Solignac, G., Mellouki, A., Le Bras, G., Barnes, I., Benter, T. "Kinetics of the OH and Cl reactions with *N*-methylformaraide, *N,N*-dimethylformaraide and *N,N*-dimethylacetamide", *Journal of Photochemistry and Photobiology Chemistry*, 176, (2005) 136 - 142.

Sorooshian, A., Murphy, S. M., Hersey, S., Gates, H., Padro, L. T., Nenes, A., Brechtel, F. J., Jonsson, H., Flagan, R. C., and Seinfeld, J. H., "Comprehensive airborne characterization of aerosol from a major bovine source", *Atmospheric Chemistry and Physics,* 8 (2008) 5489 – 5520.

Spicer, C. W., Chapman, E. G., Finlayson-Pitts, B. J., Plastidge, R. A., Hubbe, J. M., Fast, J. D. and Berkowitz, C. M. "Unexpectedly high concentrations of molecular chlorine in coastal air", *Nature* 394 (1998) 353 – 356.

Sriroth, Klanarong, Piyachomkwan, Kuakoon, Wanlapatit, Sittichoke, Nivitchanyong, Siriluck; "The promise of a technology revolution in cassava bioethanol: From Thai practice to the world practice", *Fuel,* 89 (2010) 1333 – 1338.

Stefan, M. I.; Bolton, J. R., "UV direct photolysis of *N*-nitrosodimethylamine (NDMA): kinetic and product study", *Helvetica Chimica Acta*, 85 (2002) 1416 - 1426.

Steiner, M. & Stein von Kamienski, E., "Der papierchromatographische Nachweis primlrer, sekundlrer und tertilrer Alkylamine in Pflanzen", *Die Nacurwissenschaften* 40 (1953) 483.

Stein von Kamienski, E., "Untersuchungen iiber die fliichtigen Amine der Pflanzen", *Planta* 50 (1957) 315 – 330.

Strazisar, B, R., Anderson, R. R., and White; C. M., "Degradation for Monoethanolamine in a CO_2 Capture Facility", *Energy and Fuel,* 17 (2003) 1034 – 1039.

Streit, G. E.; Whitten, G. Z.; Johnston, H. S., "The fate of vibrationally excited hydroxyl radicals, HO (v < 9), in the stratosphere", *Geophysical Research Letters,* 3 (1976) 521 - 523.

Su, F., Calvert, J. G., Shaw, J. H., "Mechanism of the photo-oxidation of gaseous formaldehyde", *Journal of Physical Chemistry A*, 83 (1979) 3185 - 3191.

Su, F., Calvert, J. G., Shaw, J. H., Niki, H., Maker, P. D., Savage, C. M., Breitenbach, L. D. "Spectroscopic and kinetic studies of a new metastable species in the photo-oxidation of gaseous formaldehyde" *Chemistry Physics Letters*, 65 (1979) 221 - 225.

Sun, W. C., Yong, C. B., and Li, M. H., "Kinetics of the absorption of carbon dioxide into mixed aqueous solutions of 2-amino-2-methyl-1-propanol and piperazine", *Chemical Enginnering Science*, 60 (2005) 503 - 516.

Suzuki, E., Mochizuki, M., Osabe, N. S. M., and Okada, M., "*In vitro* metabolism of *N*-nitrodialkylamines", *Japanese Journal of Cancer Research* (GANN), 76 (1985) 28 – 36.

Szilághyi, I., Dóbé, S., Bérces, T., Márta, F., and Viskolcz, B., "Direct kinetic study of reactions of hydroxyl radicals with alkyl formates", *Journal of Physical Chemistry A*, 218 (2004) 479 - 492

Taketani, F., Takahashi, K., Matsumi, Y. and Wallington, T. J., "Kinetics of the reactions of Cl*($^2P_{1/2}$) and Cl($^2P_{3/2}$) atoms with CH_3OH, C_2H_5OH, n-C_3H_7OH, and i-C_3H_7OH at 295 K": *Journal of Physical Chemistry A*, 109 (200) 3935 - 3940, 2005.

Teslja, A., Nizamov, B., Dagdigian, P. J., "The electronic spectrum of methyleneimine", *Journal of Physical Chemistry A*, 108 (2004), 4433 - 4439.

Teton, S., Mellouki, A., Le Bras, G. “Rate constants for reactions of OH radicals with a series of asymmetrical ethers and *tert*-butyl alcohol” *International Journal of Chemical Kinetics* 28 (1996) 291 – 297.

Thornton, J. A., Kercher, J. P., Riedel, T. P., Wagner, N. L., Cozic,J., Holloway, J. S., Dubé, W. P., Wolfe, G. M., Quinn, P. K., Middlebrook ,A. M., Alexander, B. and Brown, S. S.,“A large atomic chlorine source inferred from mid-continental reactive nitrogen chemistry”, *Nature*, 464 (2010) 271 – 274.

Tian, W., Wang, W., Zhang, Y., Wang, W., “Direct dynamics study on the mechanism and the kinetics of the reaction of CH_3NH_2 with OH”, *International Journal of Quantum Chemistry*, *109*, (2009) 1566 - 1575.

Tuazon, E. C, Winer, A. M., Graham, R. A., Schmid, J. P., and Pitts, Jr. J, N., “Fourier Transform Infrared detection of nitramines in irradiated amine-NO systems”, *Environmental Science & Technology*, 12 (1978) 954 – 958.

Tuazon, E. C., Atkinson, R. Aschmann, S. M., and Arey, J., “Kinetics and products of the gas-phase reactions of O_3 with amines and related compounds”, *Research on Chemical Intermediates,* 20 (1994) 303 - 320.

Tuazon, E. C., Carter, W. P. L., Atkson, R., Winer, A. M., and Pits Jr., J. N., “Atmospheric reactions of *N*-Nitrosodimethylamine and dimethylnitramine”, *Environmental Science & Technology,* 18 (1984) 49 – 54.

Tuazon, E. C.; Carter, W. P. L.; Aschmann, S. M.; Atkinson, R. “Products of the gas-phase reaction of methyl *tert*-butyl ether with the OH radical in the presence of NO_x” *International Journal of Chemical Kinetics* 23 (1991) 1003 - 1015.

Tully, F. P. and Droege, A. T., “Kinetics of the reactions of the hydroxyl radical with dimethyl ether and diethyl ether”, *International Journal of chemical kinetics*, 19 (1987), 251–259

Tully, F. P., Perry, R. A., Thorne, L. R., Allendorf, M. D. “Free-radical oxidation of isocyanic acid”, *Symposium (International) on Combustion*, 22 (1989), 1101-1106.

Tyndall, G. S.; Orlando, J. J.; Wallington, T.; Hurley, M. D.; Goto, M.; Kawasaki, M. "Mechanism of the reaction of OH radicals with acetone and acetaldehyde at 251 and 296 K", Journal of *Physical Chemistry Chemical Physics,* 4 (2002) 2189 - 2193.

Tyndall, G. S., Orlando, J. J., Kegley-Owen, C. S., Wallington, T. J. and Hurley, M. D., "Rate coefficients for the reactions of chlorine atoms with methanol and acetaldehyde: *International Journal of Chemical Kinetics*, 31 (1999) 776 - 784.

U. S. Environmental Protection Agency, *Health and Environmental Effects Profile for N,N-dimethylformamide*, Environmental Criteria and assessment office, Office of Health and Environmental Assessment, Office of Research and Development, Cincinnati, OH, (1986).

vanLoon, G. W and Duffy, S. J., "Environmental Chemistry", second edition *Oxford University Press* (2005).

Van Neste, A., and R. A. Duce, "Methylamines in the marine atmosphere", *Geophysics Research Letters,* 14 (1987) 711 - 714.

Veltman, K., Singh B., and Hertwich, E. G., "Human and Environmental Impact Assessment of post-combustion CO_2 capture focusing on emissions from amine-based scrubbing solvents to air", *Environmental Science & Technology*, 44 (2010) 1496 – 1502.

Veyret, B., Rayez, J. C., Lesclaux, R., "Mechanism of the photo-oxidation of formaldehyde studied by flash-photolysis of CH_2O-O_2 mixtures", *Journal of Physical Chemistry A*, 86 (1982) 3424 - 3430.

Veyret, B., Lesclaux, R., Rayez, M. T., Rayez, J. C., Cox, R. A., Moortgat, G. K., "Kinetics and mechanism of the photooxidation of formaldehyde. 1. Flash-photolysis study", *Journal of Physical Chemistry A*, 93 (1989) 2368 - 2374.

Volz, A., and Kley, D., "Evaluation of the Montsouris series of ozone measurements made in the nineteenth century", *Nature,* 332 (1988) 240 - 242.

Wallington, T. J., and Kurylo, M. J., "The gas phase reactions of hydroxyl radicals with a series of aliphatic alcohols over the temperature range 240–440 K" *International Journal of Chemical Kinetics*, 19 (1987) 1015 – 1023

Wallington, T. J., Dagaut, P., Liu, R. H., Kurylo, M. J., "The gas-phase reactions of hydroxyl radicals with a series of esters over the temperature- range 240 – 440 K", *International Journal of Chemical Kinetics,* 20 (1988) 177 - 186.

Wallington, T. J.; Skewes, L. M.; Siegl, W. O.; Wu, C. H.; Japar, S. M., "Gas phase reaction of Cl atoms with a series of oxygenated organic species at 295 K". *International Journal of Chemical Kinetics* 20 (1988) 867 - 875

Wallington, T. J., Andino, J. M., Skewes, L. M.; Siegl, W. O., and Japar, S. M "Kinetics of the reaction of OH radicals with a series of ethers under simulated atmospheric conditions at 295 K", *International Journal of Chemical Kinetics* 21 (1989) 993 - 1001

Wallington, T.J., Andino, J.M., Potts, A.R., Rudy, S.J., Siegl, W.O., Zhang, Z.Y., Kurylo, M.J., Huie, R.E., "Atmospheric chemistry of automotive fuel additives-diisopropyl ether", *Environmental Science & Technology,* 27 (1993) 98 – 104.

Wallington, T. J.; Hurley, M. D.; Ball, J. C.; Jenkin, M. E., "FTIR product study of the reaction of $CH_3OCH_2O_2$+HO_2". *Chemical Physics Letters* 211 (1993) 41 - 47.

Wayne, R. P., "Chemistry of Atmospheres", third edition, *Oxford University Press*, (2000).

Weiss, R. F., "The temporal and spatial distribution of tropospheric nitrous oxide", *Journal of Geophysics Research*, 86 (1981) 7185 - 7195.

Wenger, J. C., Calve, S. L., Sidebottom, H. W., Wirtz, K., Reviejo. M. M. and Franklin, J. A., "Photolysis of chloral under atmospheric conditions", *Environmental Science & Technology*, 38 (2004) 831 - 837.

Westerholm, R., Li, H., and Almen, J., "Estimation of aliphatic amine emissions in automobile exhausts", *Chemosphere*, 27 (1993) 1381 – 1384.

Wine, P. H.; Semmes, D. H., "Kinetics of atomic chlorine (2PJ) reactions with the chloroethanes EtCl, MeCHCl2, $ClCH_2CH_2Cl$ and $ClCH_2CHCl_2$", *Journal of Physical Chemistry A*, 87 (1983) 3572 - 3578.

Xu, B.; Chen, Z.; Qi, F.; Yang, L., "Photodegradation of *N*-nitrosodiethylamine in water with UV irradiation", *Chinese Science Bulletin*, 53 (2008) 3395 - 3401.

Yokouchi, Y., Mukai, H., Nakajima, K. and Ambe, Y., "Semi-volatile aldehydes as predominant organic gases in remote areas", *Atmospheric Environment, Part A*, 24 (1990) 439 - 442.

Yu, H., McGraw, R and. Lee, S.-H., "Effects of amines on formation of atmospheric sub-3 nm particles and their subsequent growth", *Geophysics Research Letters*., 39 (2012), L02807, doi: 10.1021/2011GL050099.

Zhang, Z., Sain, R. D., Kuryl, M. J., and Huie, R, E. "Rate constants for reactions of the hydroxyl radical with several partially fluorinated ethers", *Journal of Physical Chemistry A*, 96 (1992) 9301 – 9304.

Zhang, R., A.F. Khalizov, L. Wang, M. Hu, X. Wen, Nucleation and growth of nanoparticles in the atmosphere, *Chemical Review*. 112 (2012), 1957-2011.

Zhao, Y., Garrison, S. L., Gonzalez, C., Thweatt, W. D., and Marquez, M., "*N*-Nitrosation of Amine by NO_2 and NO: A Theoretical study", *Journal of Physical Chemistry A* 111 (2007) 2200 - 2205.

7 APPENDICES

7.1 Appendix 1: Reference Infrared Spectra for the compounds used in this study.

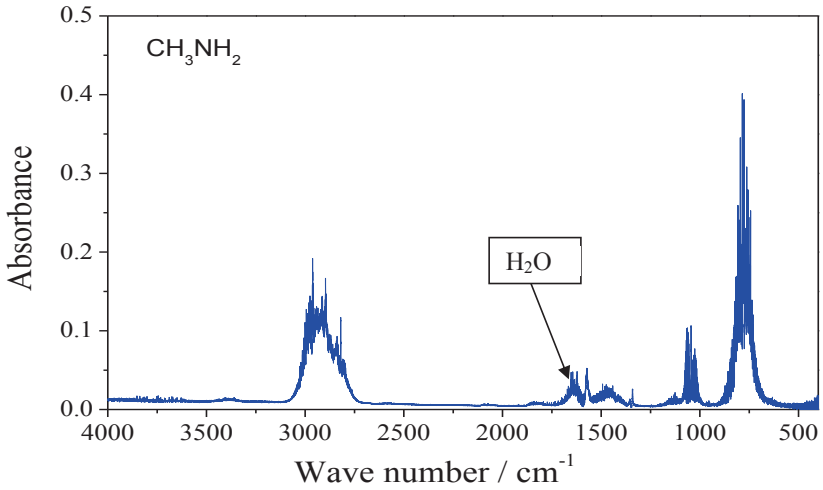

Figure 7.1.1. Infrared spectrum of CH_3NH_2 obtained of 8.65 mbar in a 10 cm cell at room temperature. Spectral resolution 0.25 cm^{-1}.

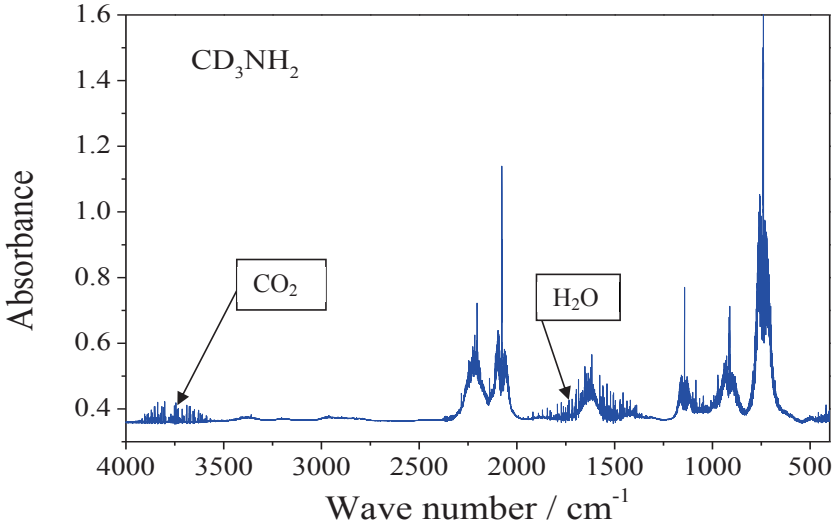

Figure 7.1.2. Infrared spectrum of CD_3HN_2 obtained of 19.8 mbar in a 10 cm cell at room temperature. Spectral resolution 0.25 cm^{-1}.

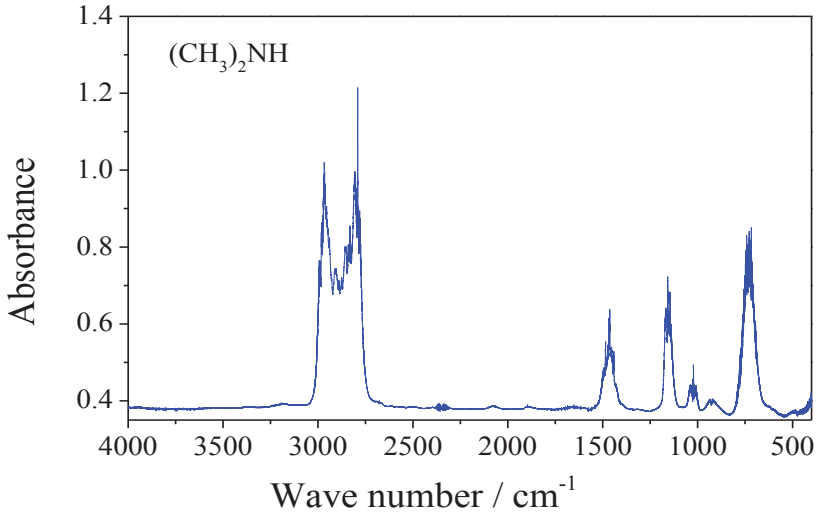

Figure 7.1.3. Infrared spectrum of $(CH_3)_2NH$ obtained of 20 mbar in a 10 cm cell at room temperature. Spectral resolution 0.25 cm^{-1}.

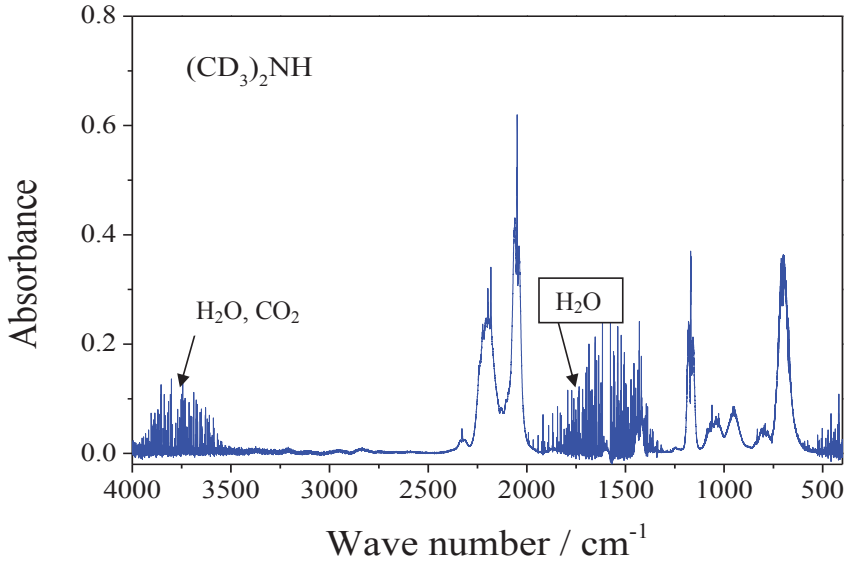

Figure 7.1.4. Infrared spectrum of $(CD_3)_2NH$ obtained of 20 mbar in a 10 cm cell at room temperature. Spectral resolution 0.25 cm^{-1}.

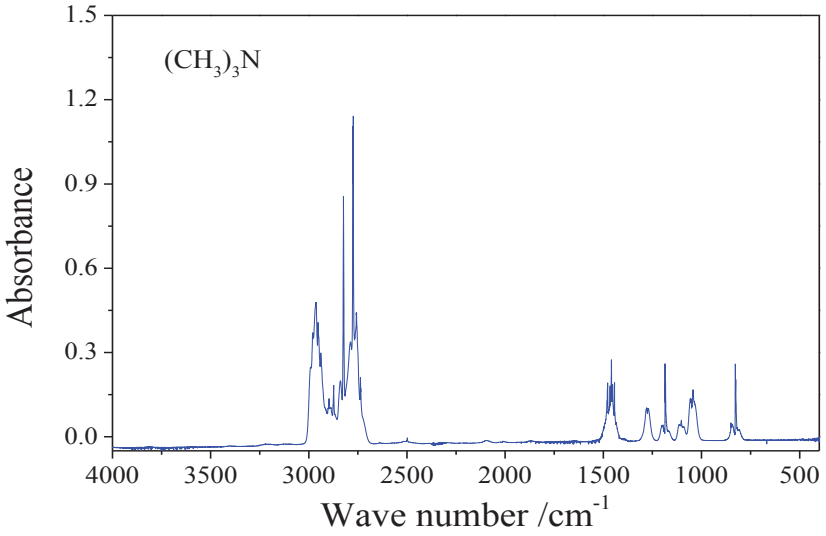

Figure 7.1.5. Infrared spectrum of $(CH_3)_3N$ obtained of 20 mbar in a 10 cm cell at room temperature. Spectral resolution 0.25 cm^{-1}.

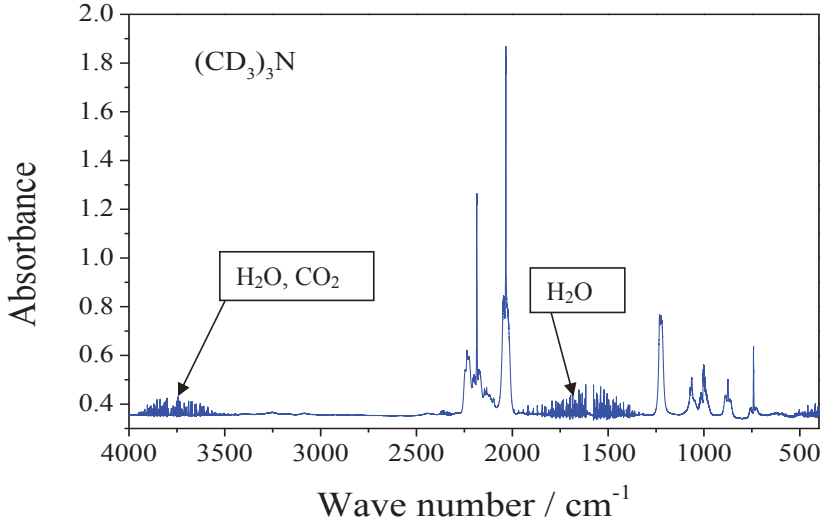

Figure 7.1.6. Infrared spectrum of $(CD_3)_3N$ obtained of 20 mbar in a 10 cm cell at room temperature. Spectral resolution 0.25 cm^{-1}.

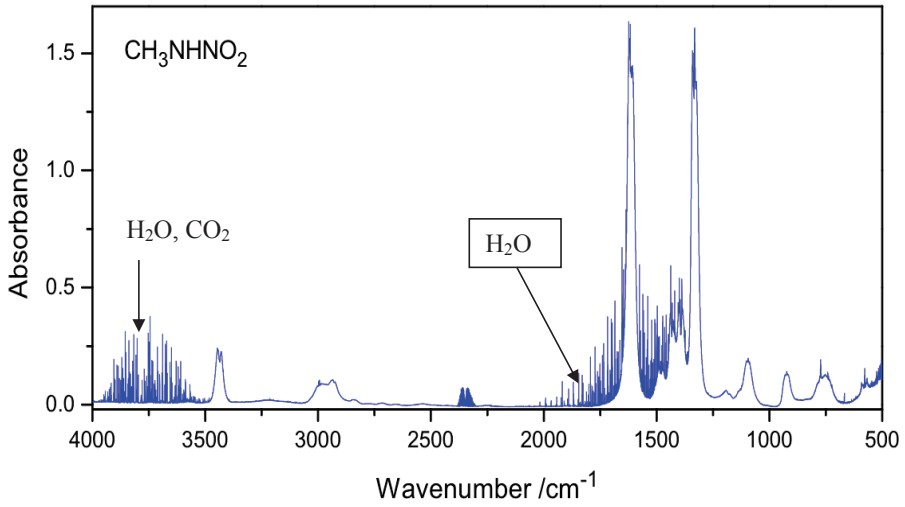

Figure 7.1.7. Infrared spectrum of CH_3NHNO_2 obtained of 4.7 mg in a 240 L reaction chamber at room temperature. Path length 120 m, spectral resolution 0.25 cm^{-1}.

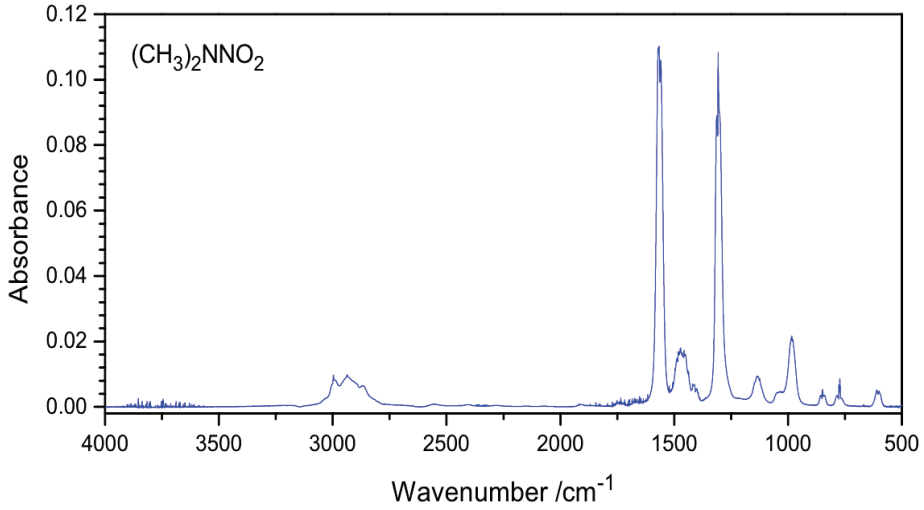

Figure 7.1.8. Infrared spectrum of $(CH_3)_2NNO_2$ obtained of 0.340 mbar in a 23 cm cell at room temperature. Spectral resolution 1 cm^{-1}.

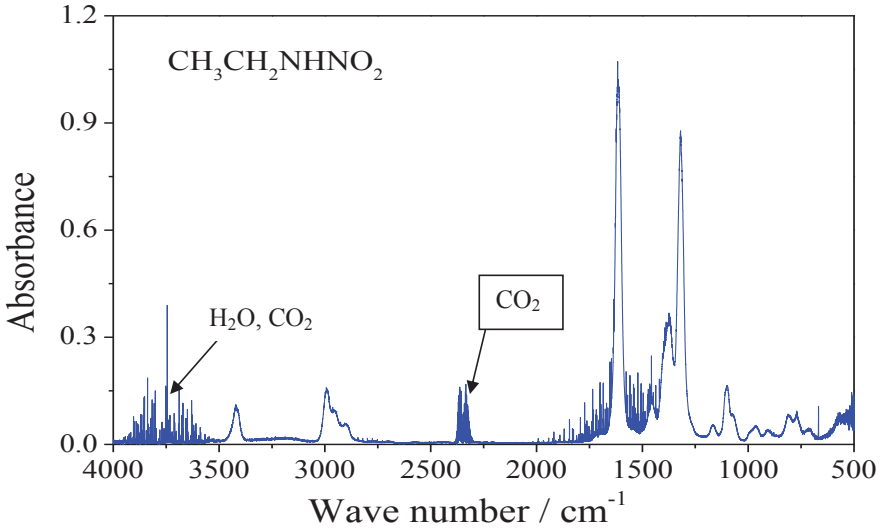

Figure 7.1.9. Infrared spectrum of $CH_3CH_2NHNO_2$ obtained in a 240 L reaction chamber at room temperature. Path length 120 m, spectral resolution 0.5 cm^{-1}.

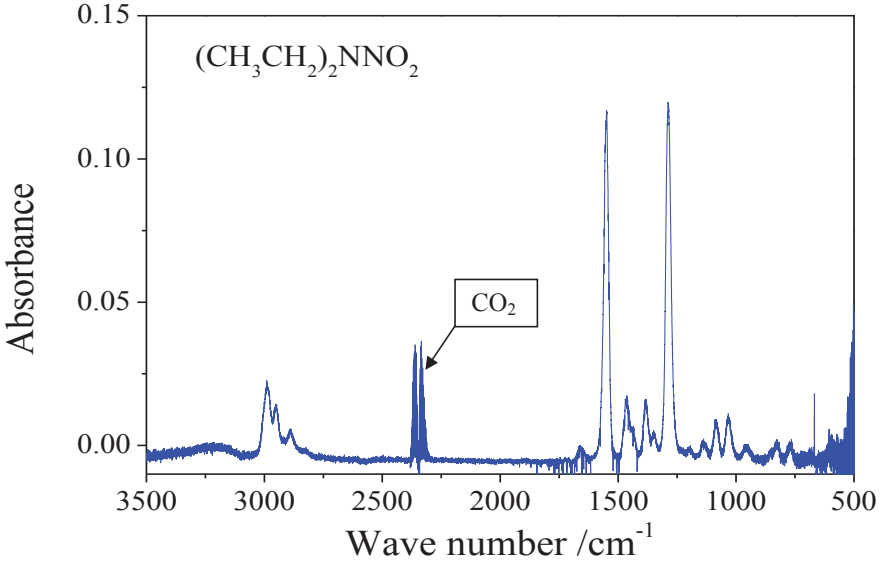

Figure 7.1.10. Infrared spectrum of $(CH_3CH_2)_2NNO_2$ obtained of 0.82 in a 240 L reaction chamber at room temperature. Path length 120 m, spectral resolution 0.5 cm^{-1}.

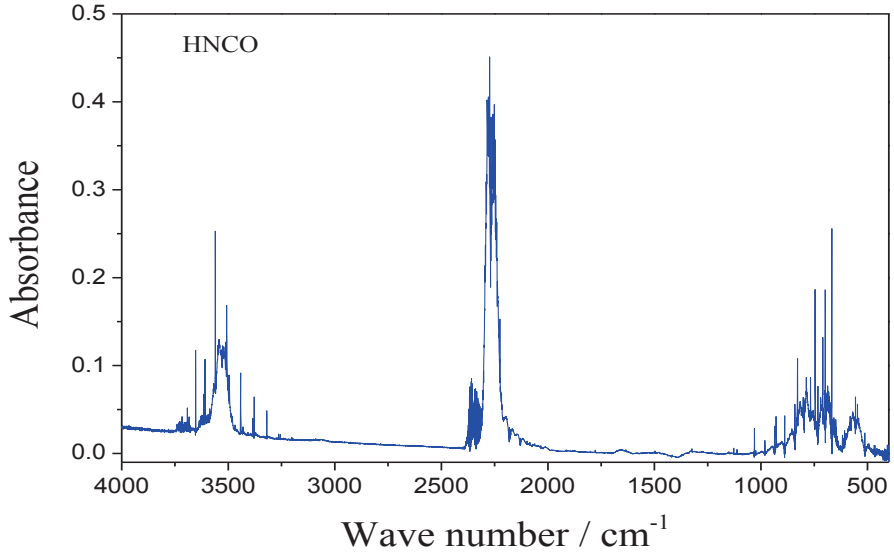

Figure 7.1.11. Infrared spectrum of HNCO obtained of 10 mbar in a 10 cm cell at room temperature. Spectral resolution 1 cm^{-1}.

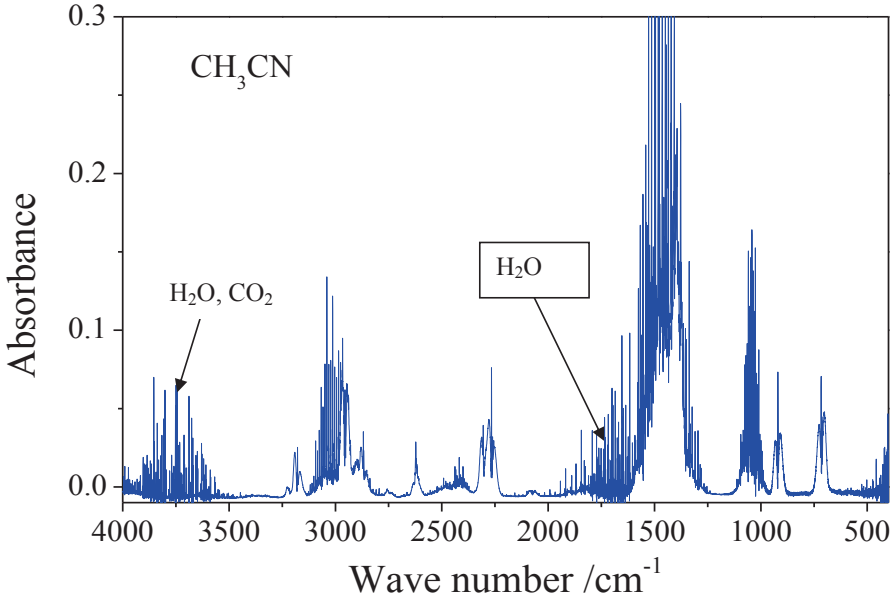

Figure 7.1.12. Infrared spectrum of Acetonitrile obtained of 20 mbar in a 23 cm cell at room temperature. Spectral resolution 1 cm^{-1}.

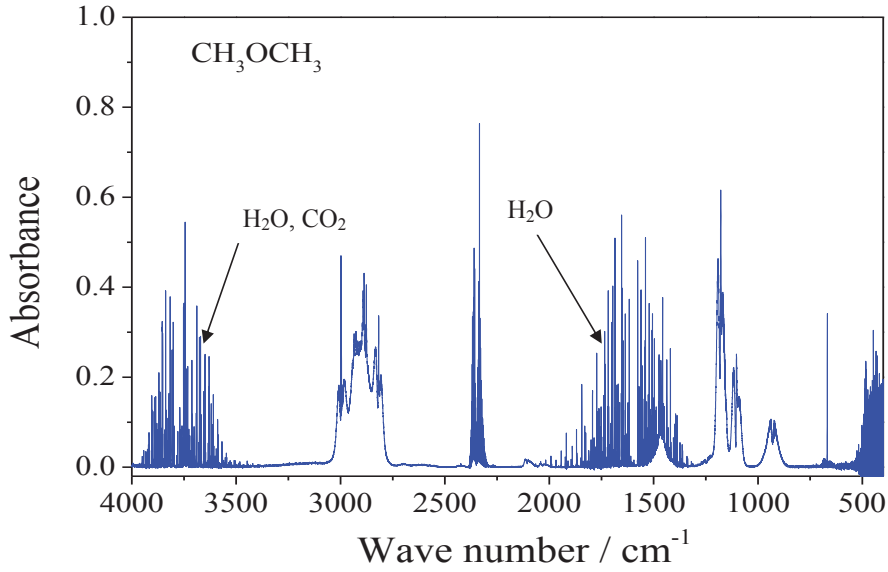

Figure 7.1.13. Infrared spectrum of Dimethylether obtained of 2 mbar in a 240 L reaction chamber at room temperature. Path length 120 m, spectral resolution 1 cm^{-1}.

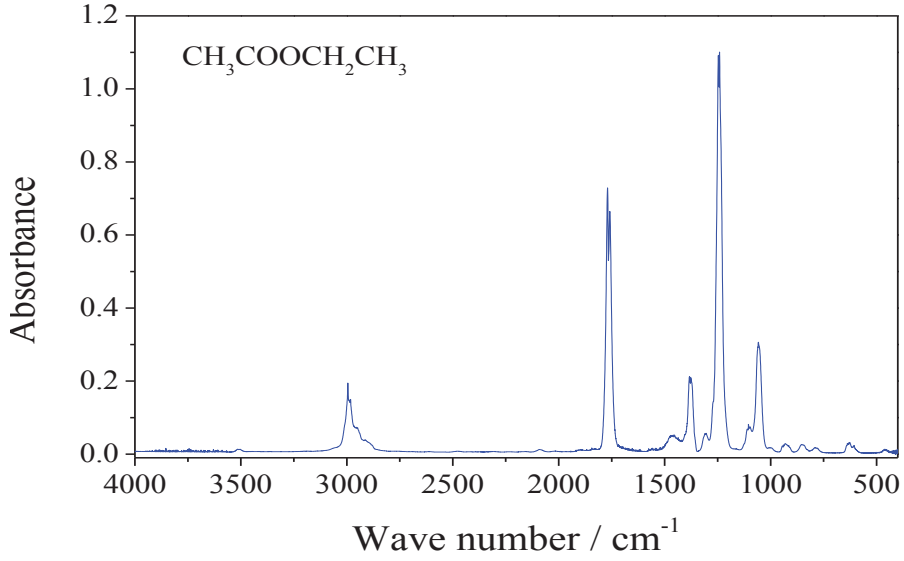

Figure 7.1.14. Infrared spectrum of Ethyl acetate obtained of 2 mbar in a 23 cm cell at room temperature. Spectral resolution 1 cm^{-1}.

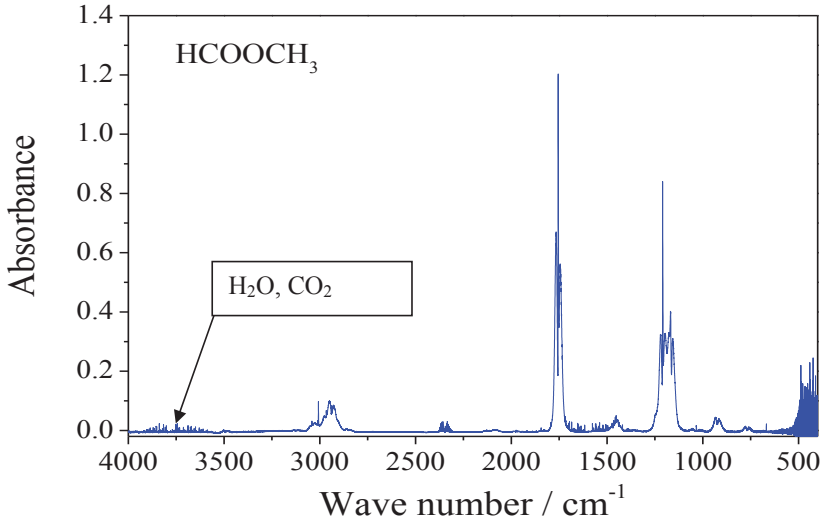

Figure 7.1.15. Infrared spectrum of Methylformate obtained of 1 mbar in a 240 L reaction chamber at room temperature. Path length 120 m, spectral resolution 0.5 cm^{-1}.

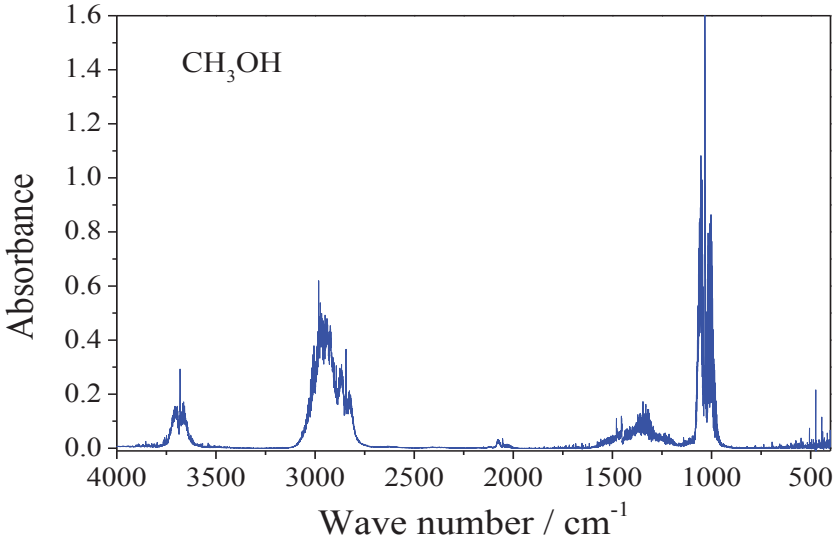

Figure 7.1.16. Infrared spectrum of Methanol obtained of 10 mbar in a 23 cm cell at room temperature. Spectral resolution 0.5 cm^{-1}.

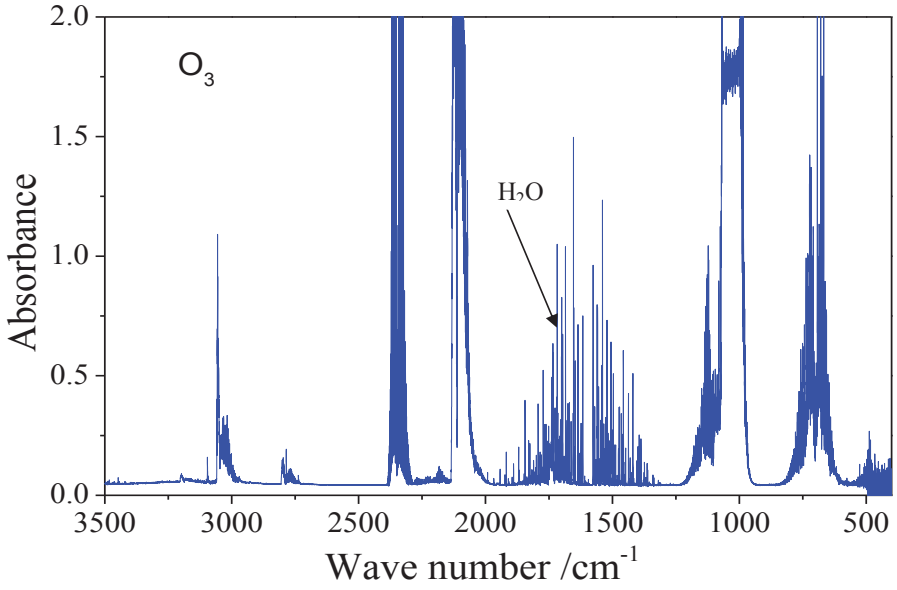

Figure 7.1.17. Infrared spectrum of Ozone obtained in a 240 L reaction chamber at room temperature. Path length 120 m, spectral resolution 0.5 cm-1.

7.2 Appendix 2: Infrared spectral regions employed and chemical species included in the quantification of reactants

Species	Wavenumber region	Spectra included in analysis
CH_3NH_2	2725 - 3075	H_2O, CH_4, CH_3NH_2
$(CH_3)_2NH$	2650 - 3050	H_2O, NO_2, $(CH_3)_2NH$
$(CH_3)_3N$	2680 - 3015	H_2O, NO_2, $(CH_3)_3N$
CD_3NH_2	2000 - 2150	H_2O, $(CD_3)_2NH_2$
$(CD_3)_2NH$	1950 - 2250	H_2O, $(CD_3)_2NH$
$(CD_3)_3N$	1990 - 2075	H_2O, $(CH_3)_3N$
CH_3NHNO_2	3350 – 3550	CH_3NHNO_2, $CHONHNO_2$, H_2O
$(CH_3)_2NNO_2$	1220 – 1335	$(CH_3)_2NNO_2$, $CH_3N(CHO)NO_2$, CH_3OH, H_2O, HNO_3
$CH_3CH_2NHNO_2$	1240 - 1429	H_2O NO_2 $CH_3CH_2NHNO_2$
$(CH_3CH_2)_2NNO_2$	1240 - 1327	H_2O NO_2 $(CH_3CH_2)_2NNO_2$
CH_3OH	3580 – 3800	CH_3OH, H_2O, O_3, CO_2
CH_3OCH_3	2676 – 3125	CH_3NHNO_2, CH_3OCH_3, CH_3OCHO, O_3, H_2O
$CH_3COOCH_2CH_3$	1220 – 1335	$(CH_3)_2NNO_2$, $CH_3N(CHO)NO_2$, CH_4, N_2O, HNO_3
O_3	1940 – 2240	O_3, CO, H_2O
CH_3OCHO	1100 - 1277	CH_3OCHO, CH_4, N_2O, HNO_3

7.3 Appendix 3: Infrared absorption cross sections base e

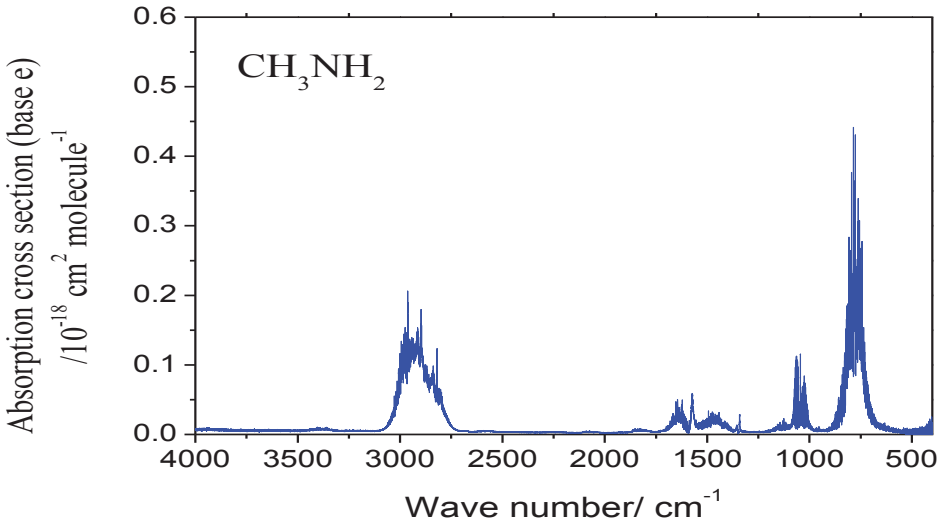

Figure 7.3.1. Infrared absorption cross-section of methylamine.

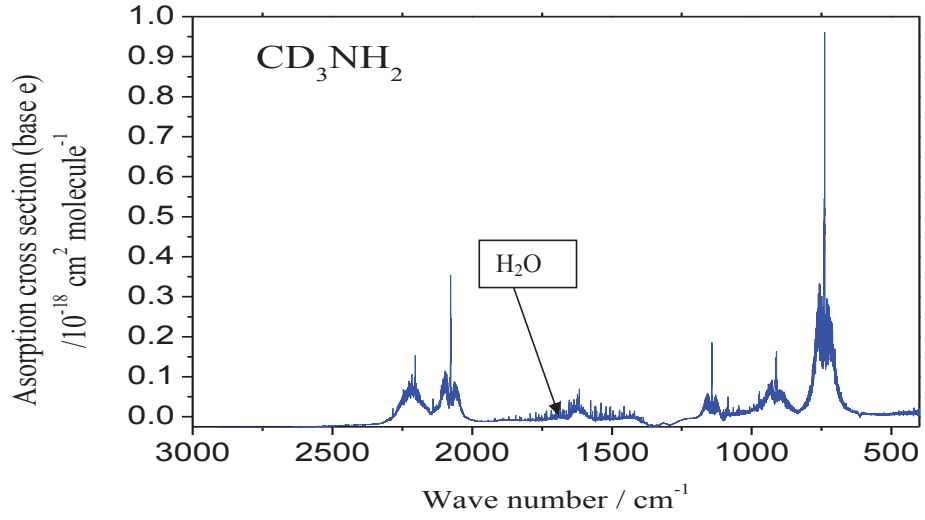

Figure 7.3.2. Infrared absorption cross-section of deuterated methylamine

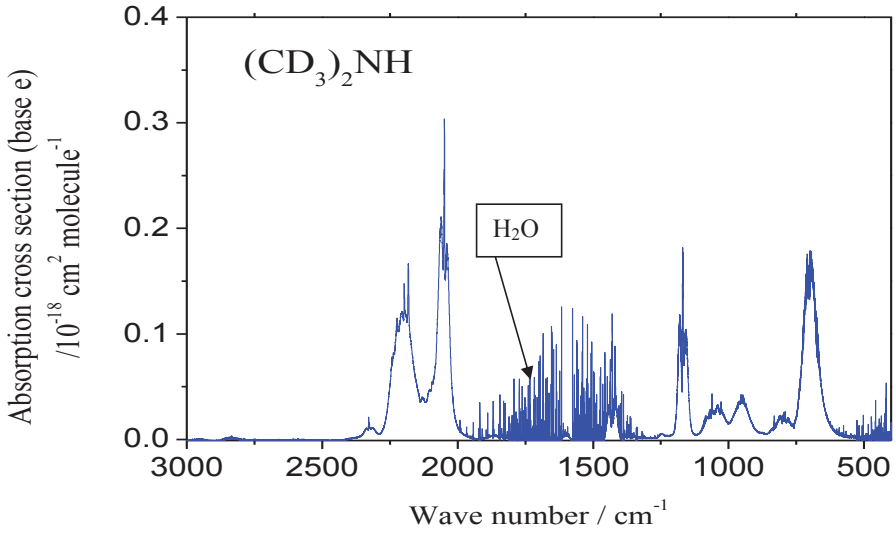

Figure 7.3.3. Infrared absorption cross-section of deuterated dimethylamine.

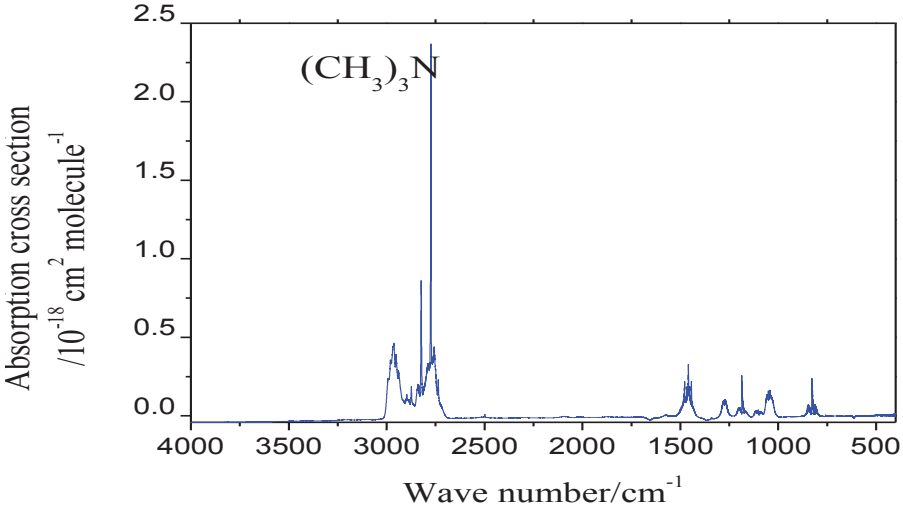

Figure 7.3.4. Infrared absorption cross-section of trimethylamine.

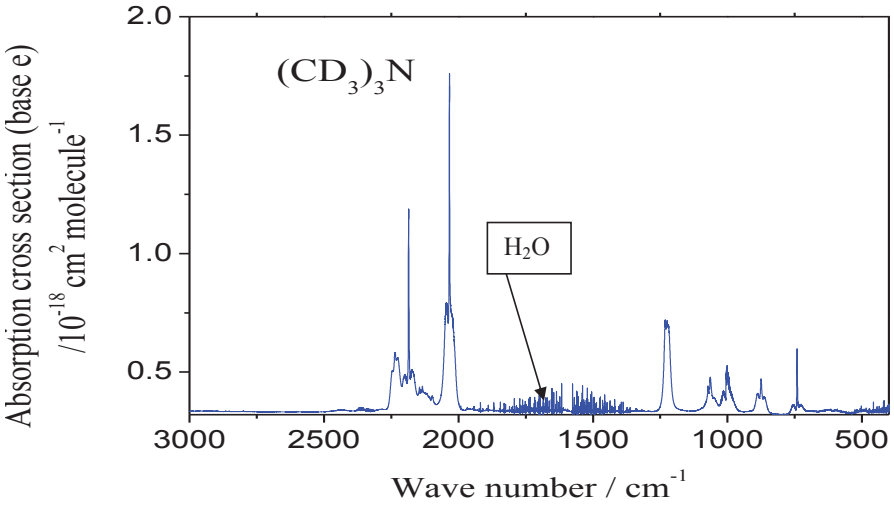

Figure 7.3.5. Infrared absorption cross-section of deuterated trimethylamine.

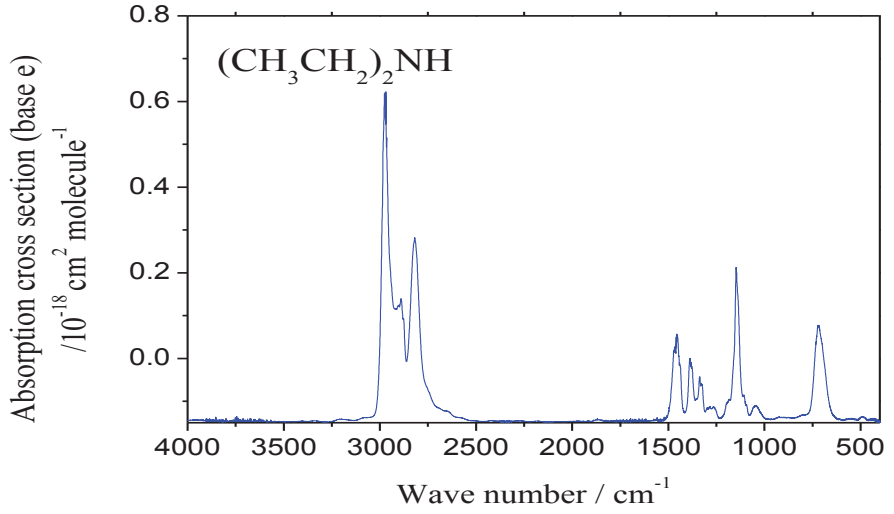

Figure 7.3.6. Infrared absorption cross-section of diethylamine.

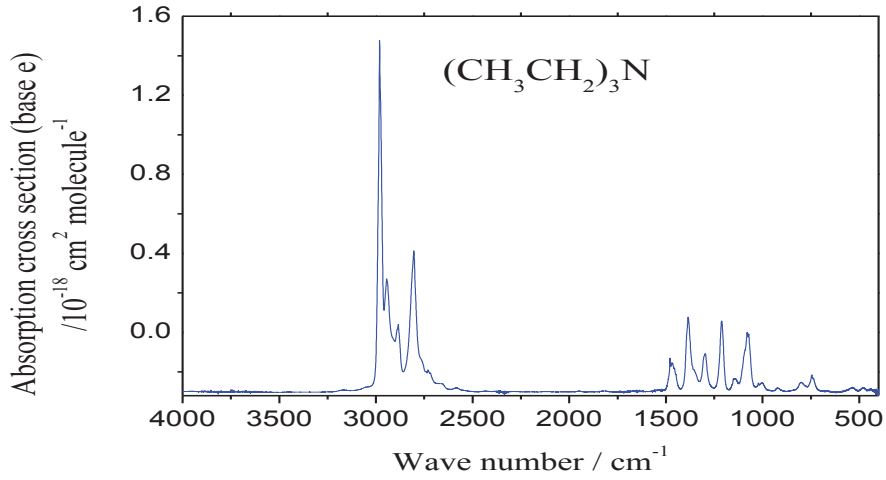

Figure 7.3.7. Infrared absorption cross-section of triethylamine.

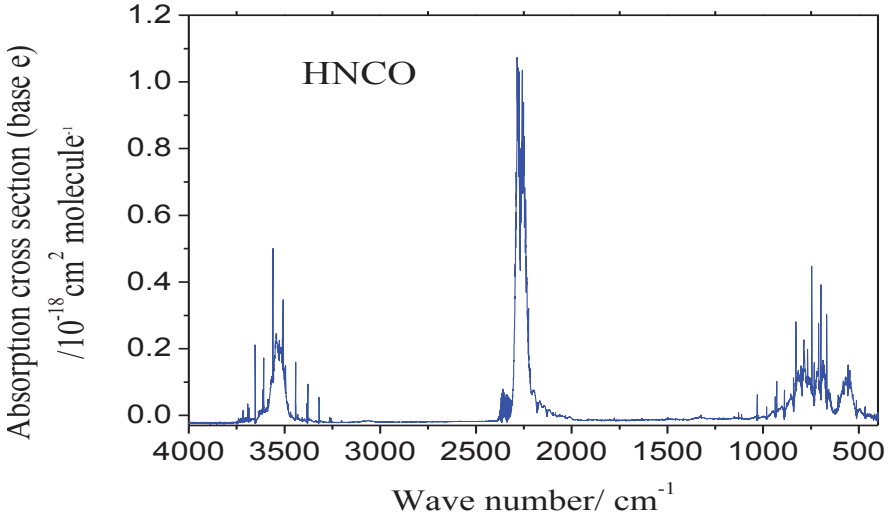

Figure 7.3.8. Infrared absorption cross-section of isocyanic acid.

7.4 Appendix 4: Integrated absorption intensities determination graphs

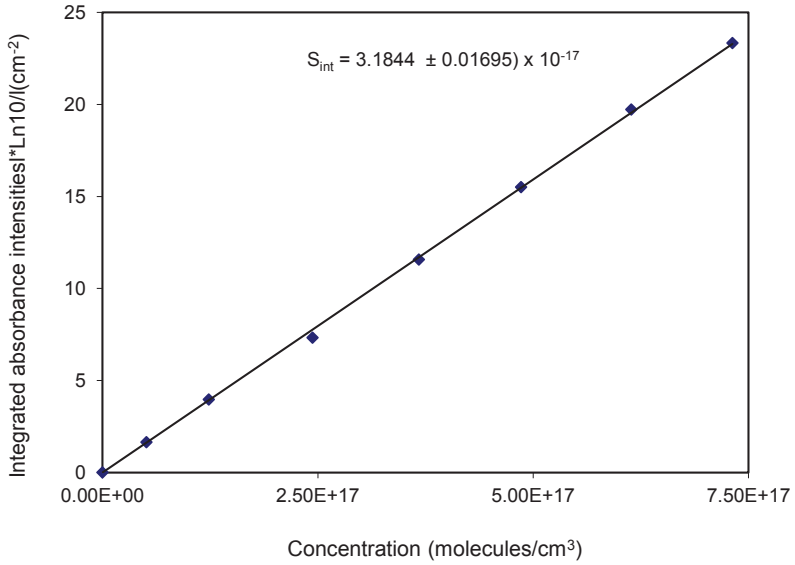

Figure 7.4.1. Beer-Lambert's law plot of $(CD_3)_2NH$ bands that were measured in the 2375 – 1925 cm^{-1} region

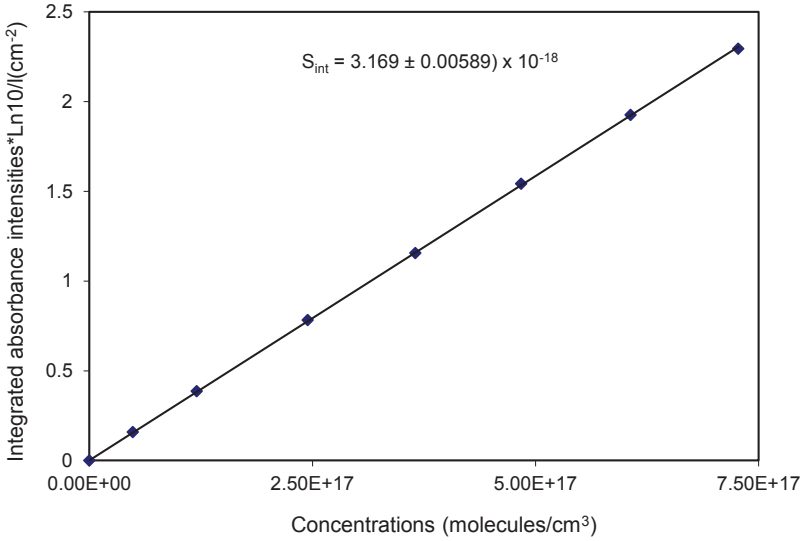

Figure 7.4.2. Beer-Lambert's law plot of $(CH_3)_3N$ bands that were measured in the 900 – 760 cm^{-1} region.

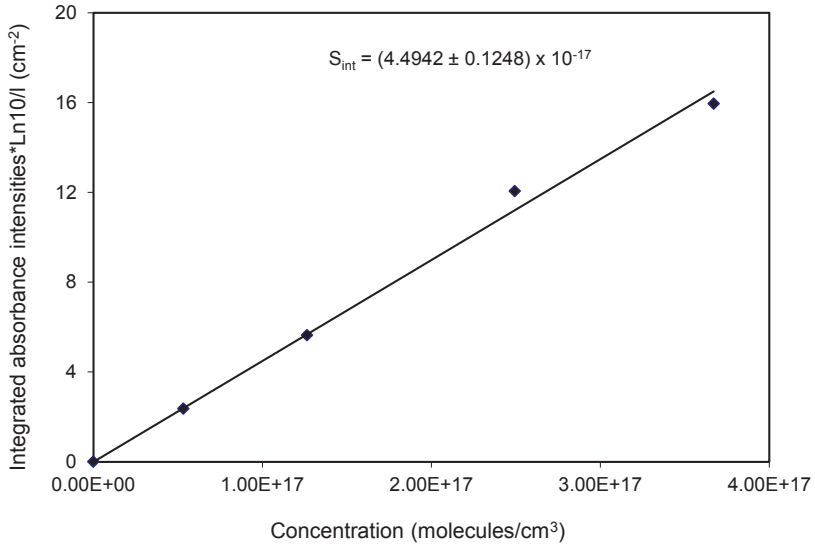

Figure 7.4.3. Beer-Lambert's law plot of $(CD_3)_3N$ bands that were measured in the 2270 – 1980 cm^{-1} region.

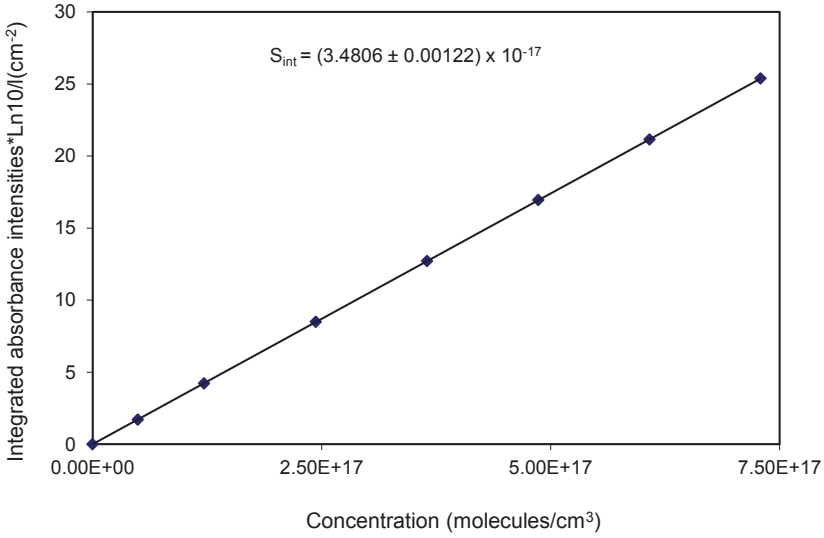

Figure 7.4.4. Beer-Lambert's law plot of $CH_3CH_2NH_2$ bands that were measured in the 3150 - 2650 cm^{-1} region.

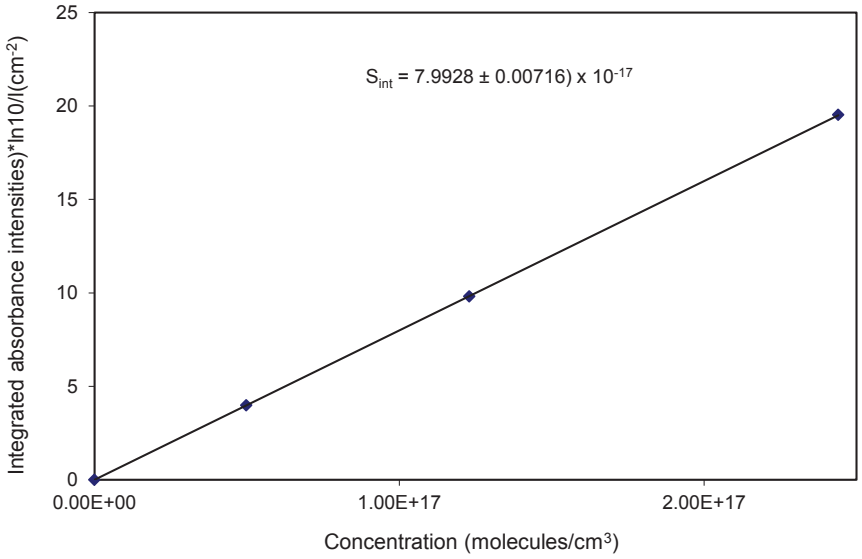

Figure 7.4.5. Beer-Lambert's law plot of $(CH_3CH_2)_2NH$ bands that were measured in the 3150 - 2600 cm^{-1} region.

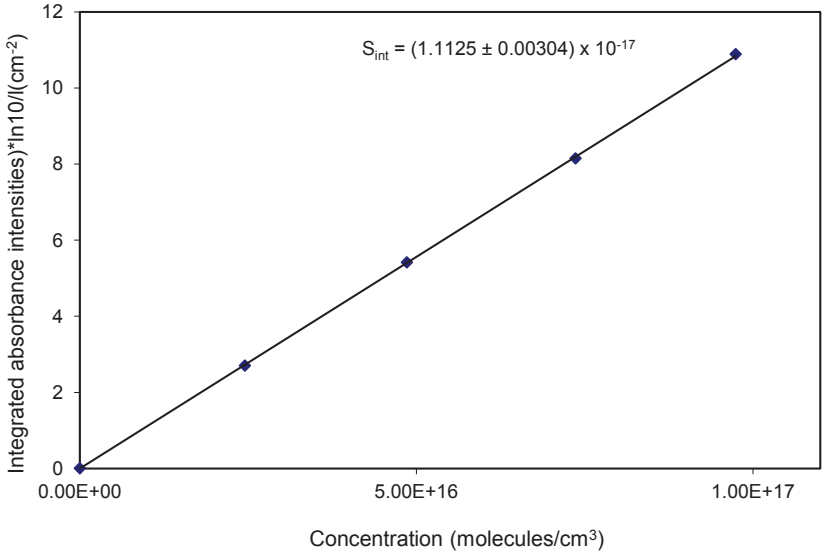

Figure 7.4.6. Beer-Lambert's law plot of $(CH_3CH_2)_3N$ bands that were measured in the 3200 - 2550 cm^{-1} region.

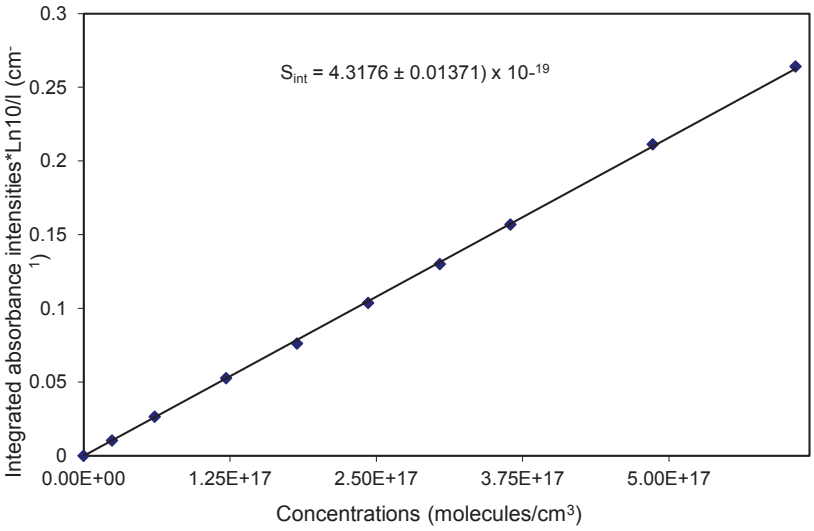

Figure 7.4.7. Beer-Lambert's law plot of CH_3CN bands that were measured in the 2350 - 2200 cm^{-1} region.

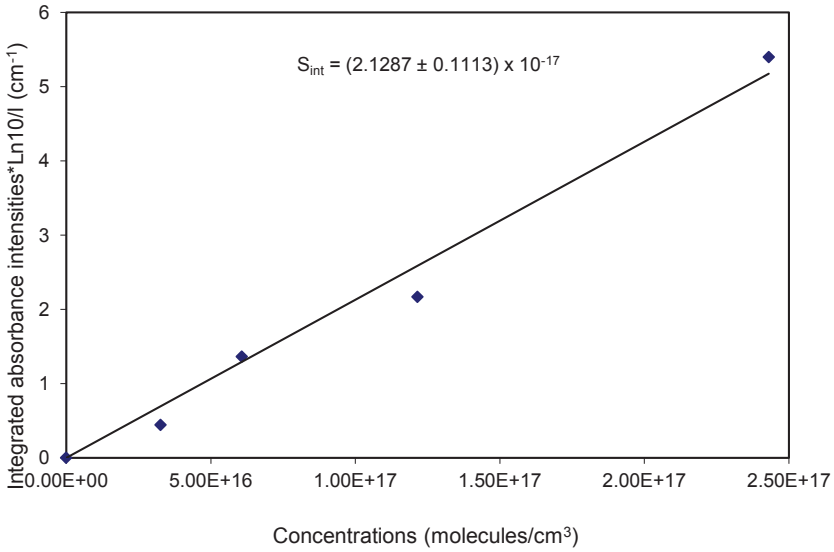

Figure 7.4.8. Beer-Lambert's law plot of HNCO bands that were measured in the 3800 - 3200 cm^{-1} region.

7.5 Appendix 5: Relative rate experiment graphs for individual experiments

A. Relative rate plots showing the decays of Methylnitramine and Methanol at 1013 hPa and 298 K in the presence of OH radicals.

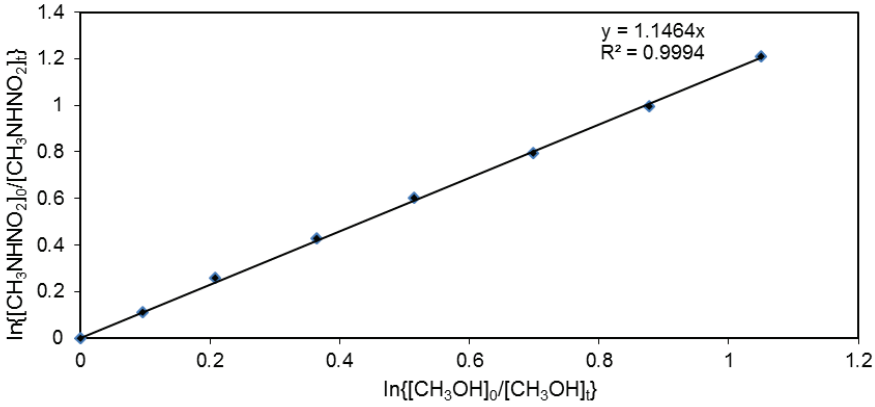

Experiment 1.

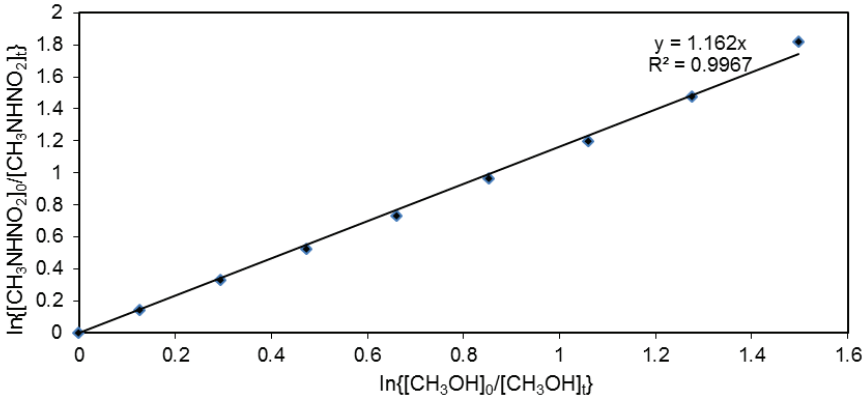

Experiment 2.

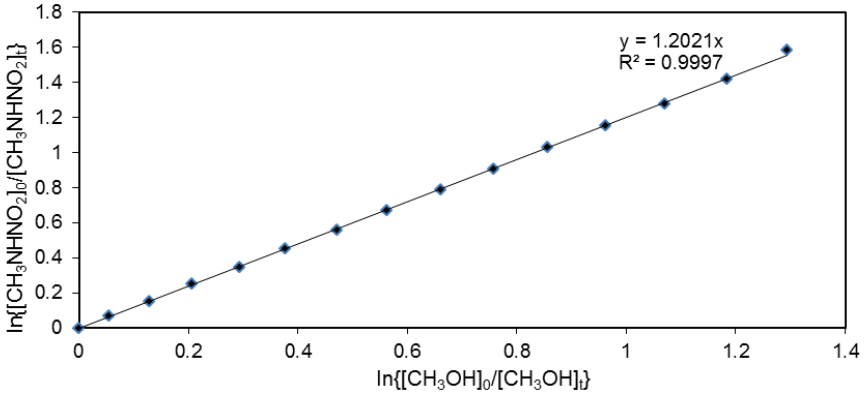

Experiment 3.

B. Relative rate plots showing the decays of Methylnitramine and Dimethylether at 1013 hPa and 298 K in the presence of OH radicals.

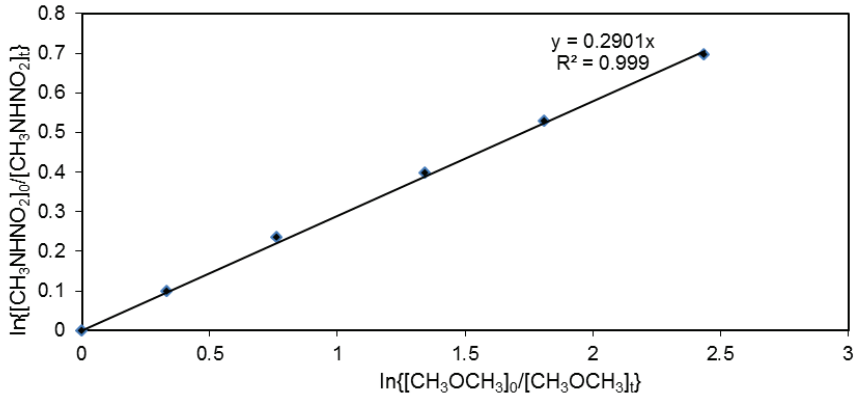

Experiment 1.

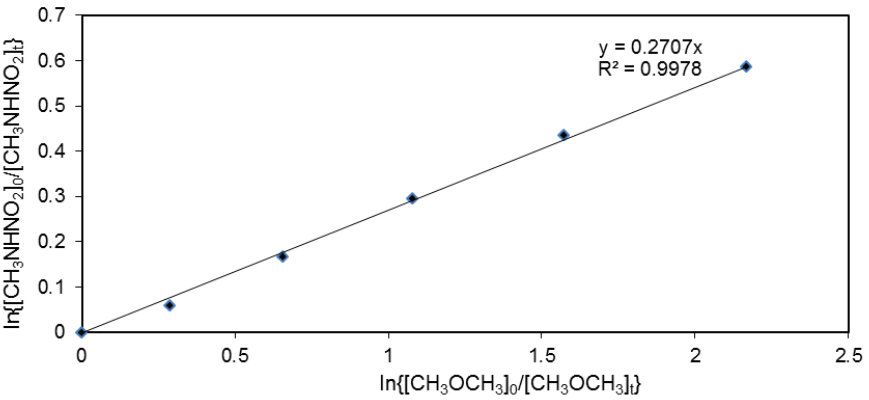

Experiment 2.

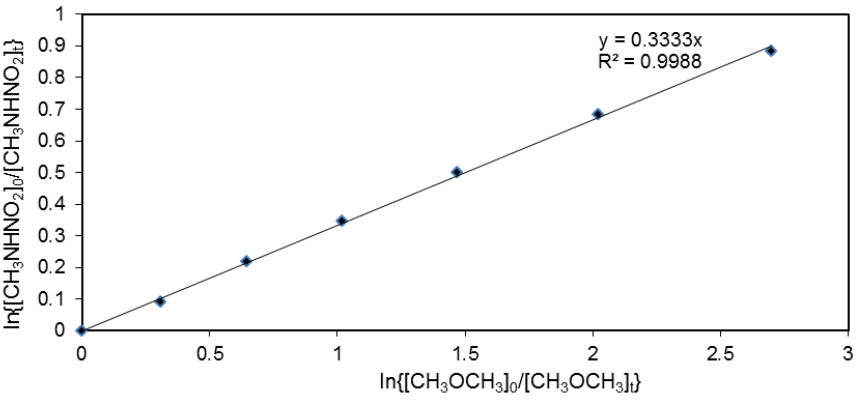

Experiment 3.

C. Relative rate plots showing the decays of Dimethylnitramine (DMNA) and Methanol (MeOH) at 1013 hPa and 298 K in the presence of OH radicals.

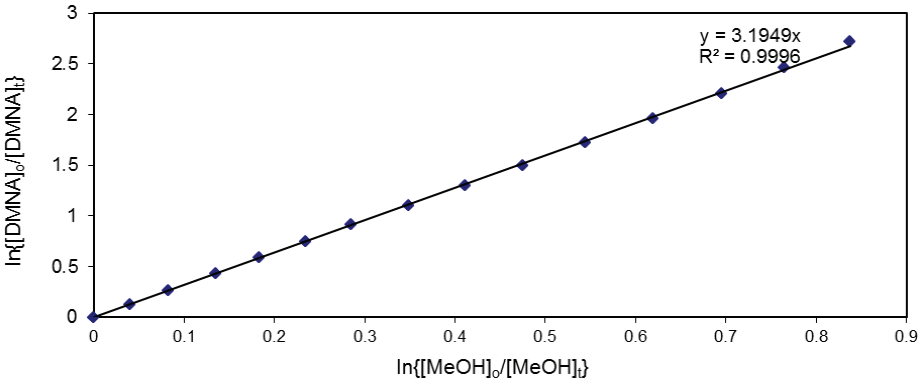

Experiment 1.

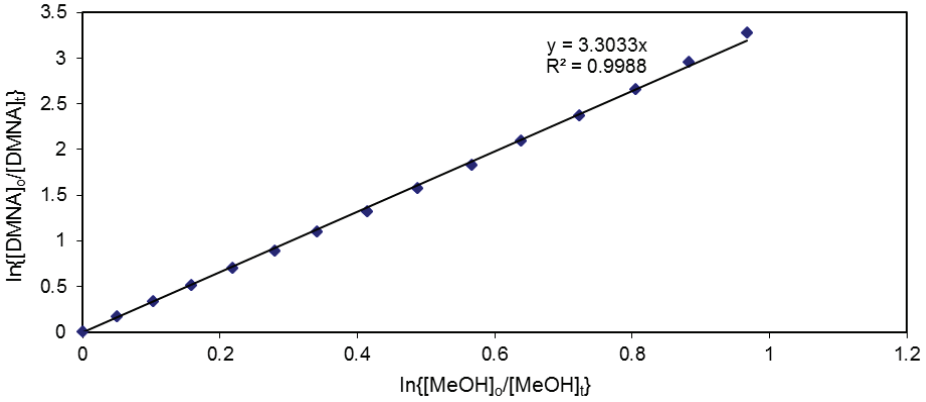

Experiment 2.

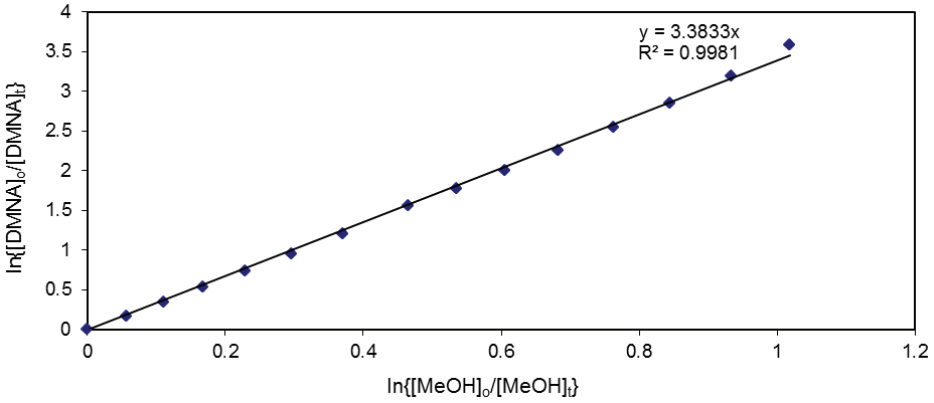

Experiment 3.

D. Relative rate plots showing the decays of Dimethylnitramine (DMNA) and Dimethylether (DME) at 1013 hPa and 298 K in the presence of OH radicals.

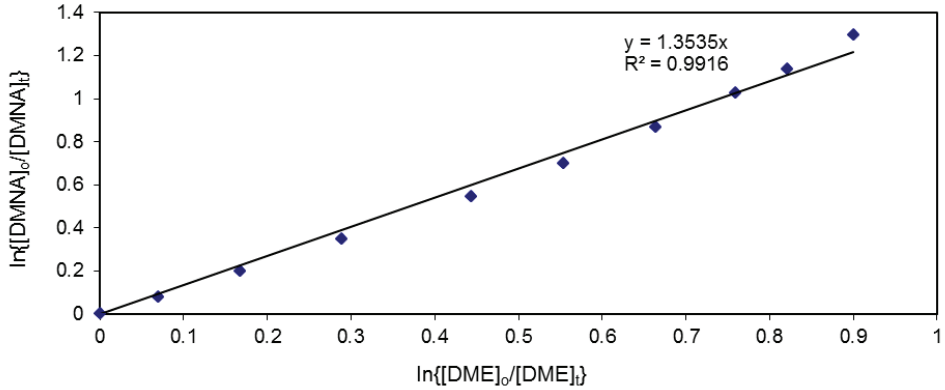

Experiment 1.

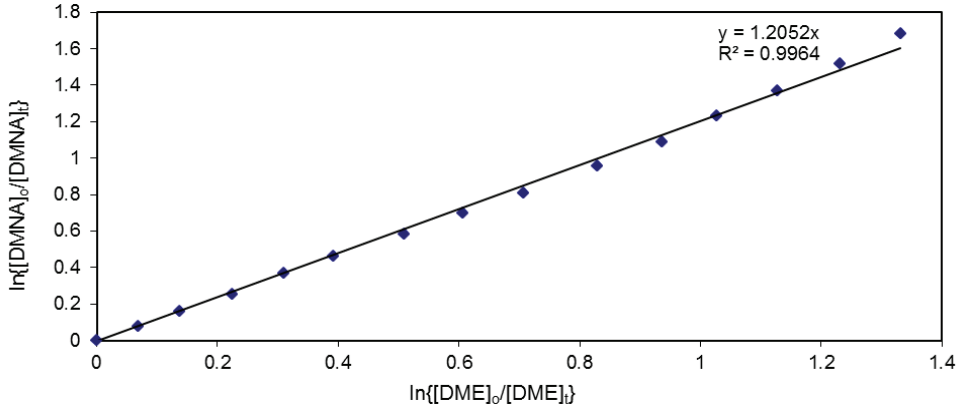

Experiment 2.

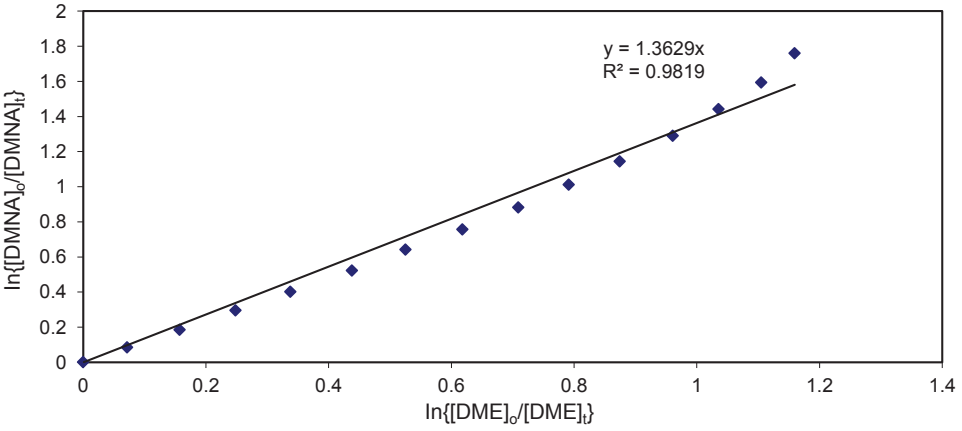

Experiment 3.

E. Relative rate plots showing the decays of Ethylnitramine and Ethylacetate (EtOAc) at 1013 hPa and 298 K in the presence of OH radicals.

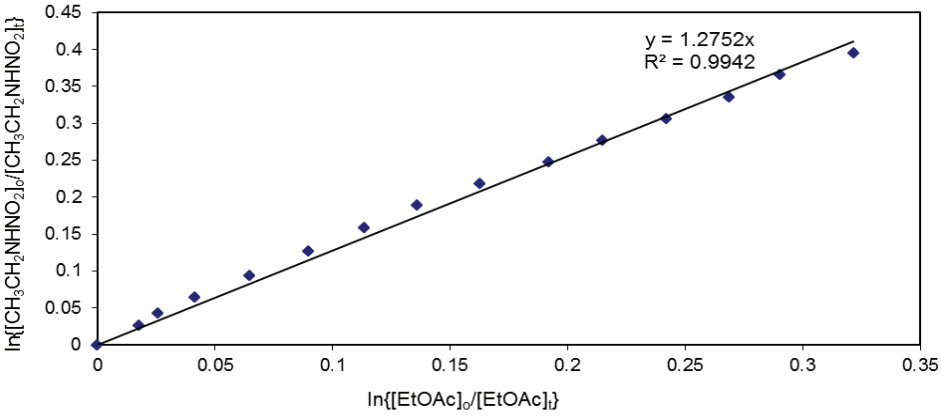

Experiment 1.

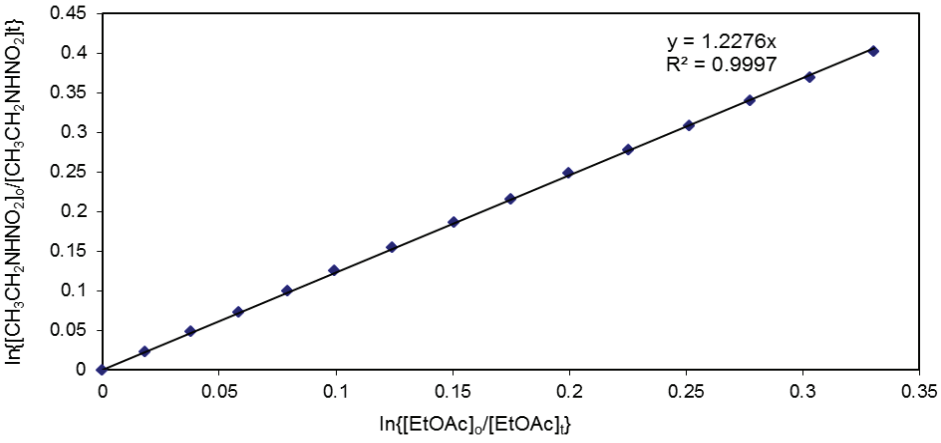

Experiment 2.

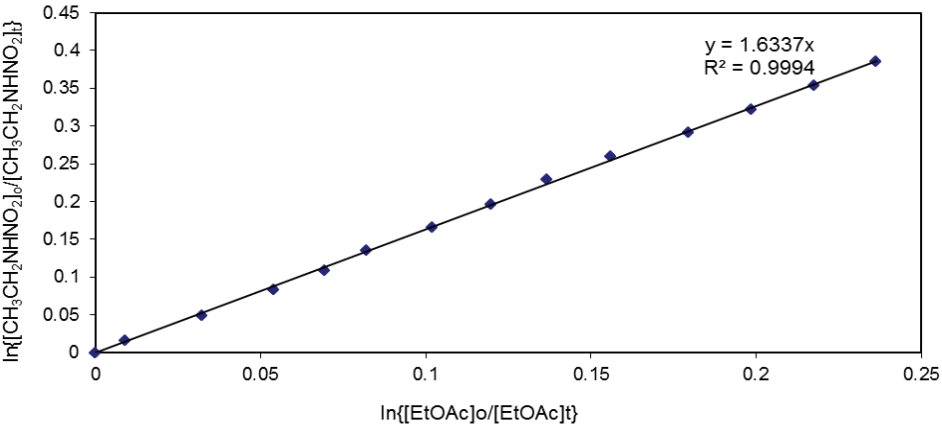

Experiment 3.

F. Relative rate plots showing the decays of Diethylnitramine and Ethylacetate (EtOAc) at 1013 hPa and 298 K in the presence of OH radicals.

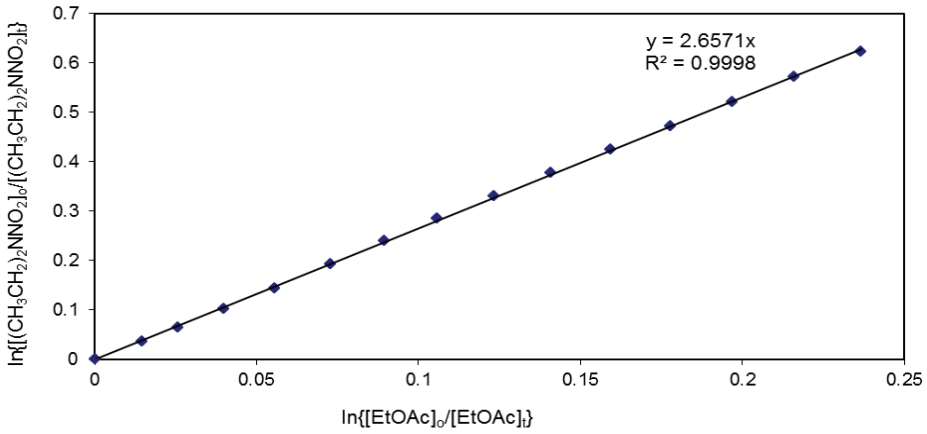

Experiment 1.

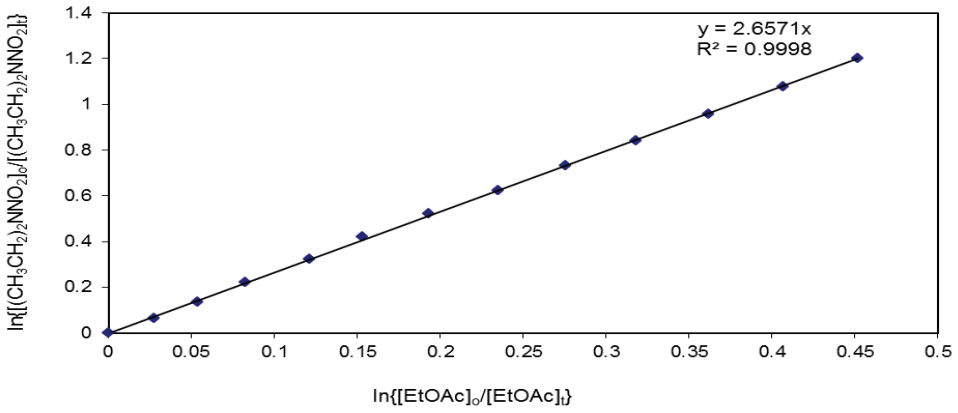

Experiment 2.

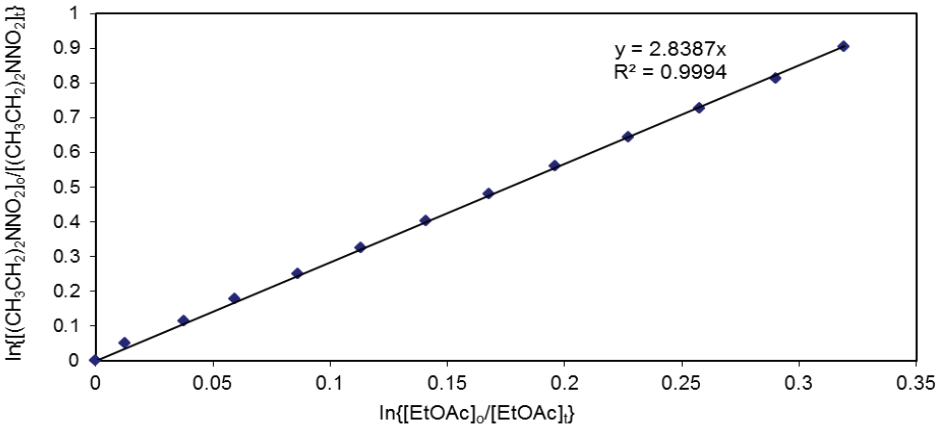

Experiement 3.

G. Relative rate plots showing the decays of CH_3NHNO_2 and CH_3OH at 1013 hPa and 298 K in the presence of Cl atoms.

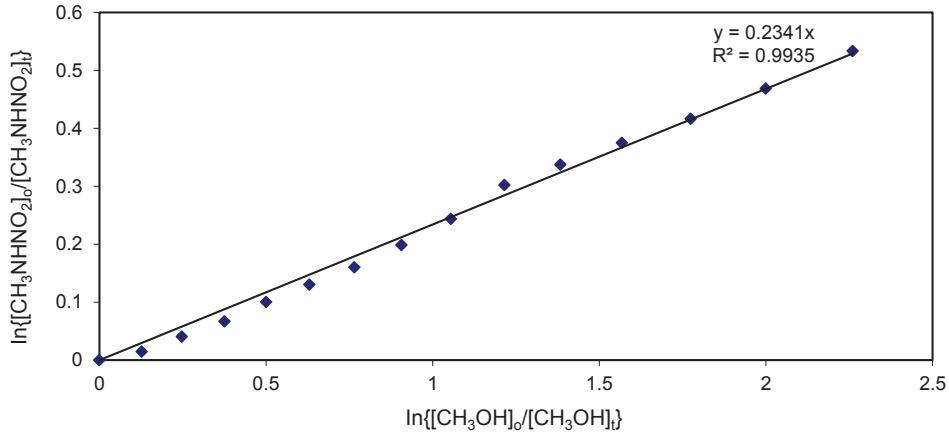

Experiment 1.

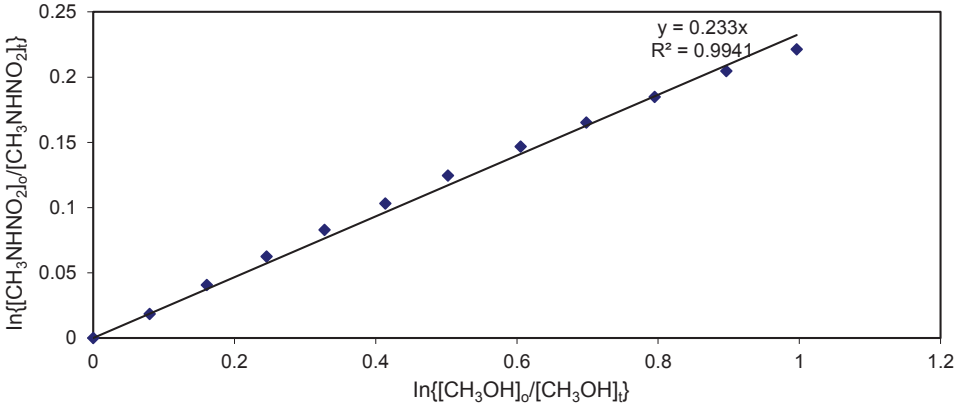

Experiment 2.

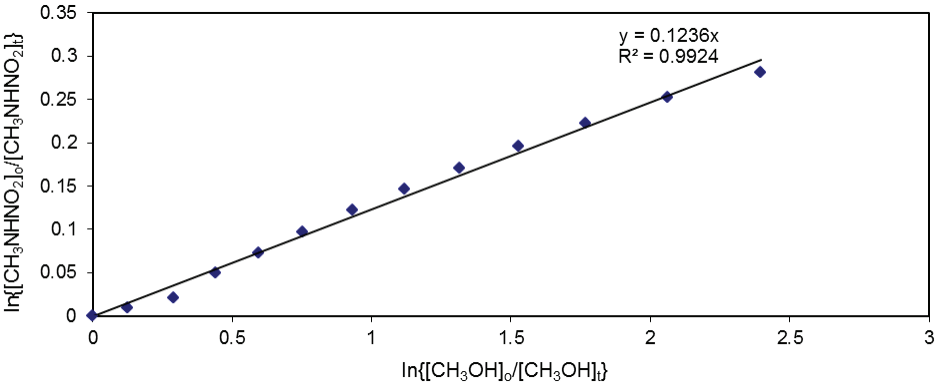

Experiment 3.

H. Relative rate plots showing the decays of CH_3NHNO_2 and Methylformate (CH_3OCHO) at 1013 hPa and 298 K in the presence of Cl atoms.

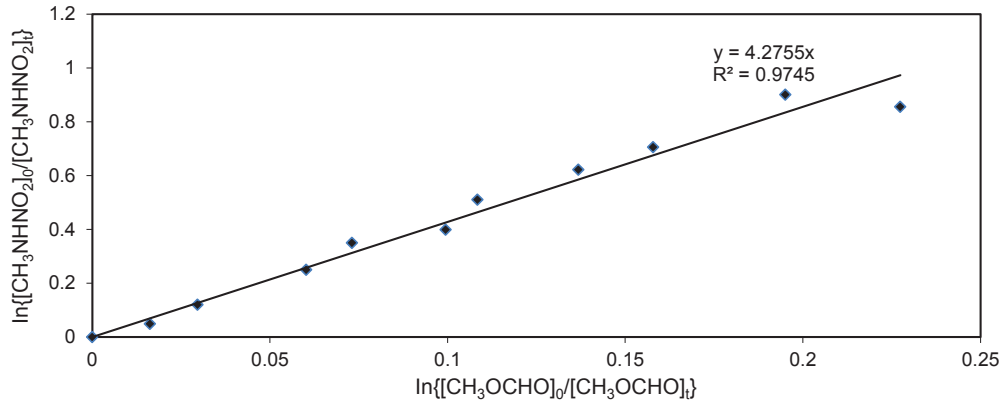

Experiment 1.

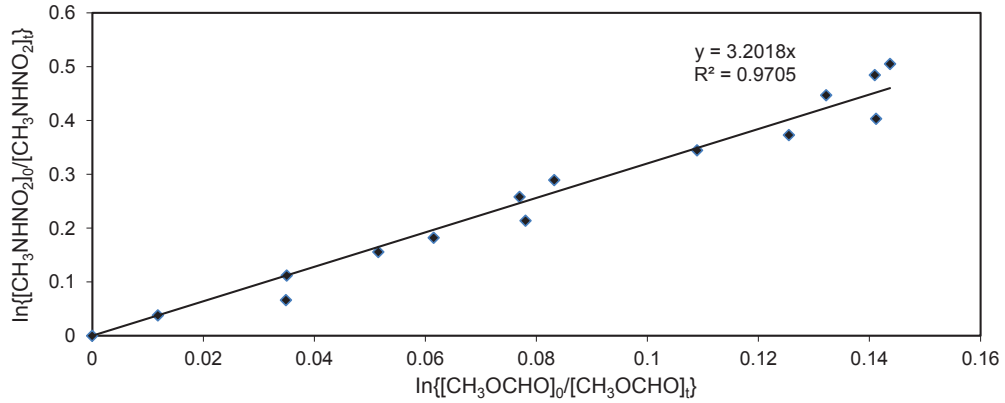

Experiment 2.

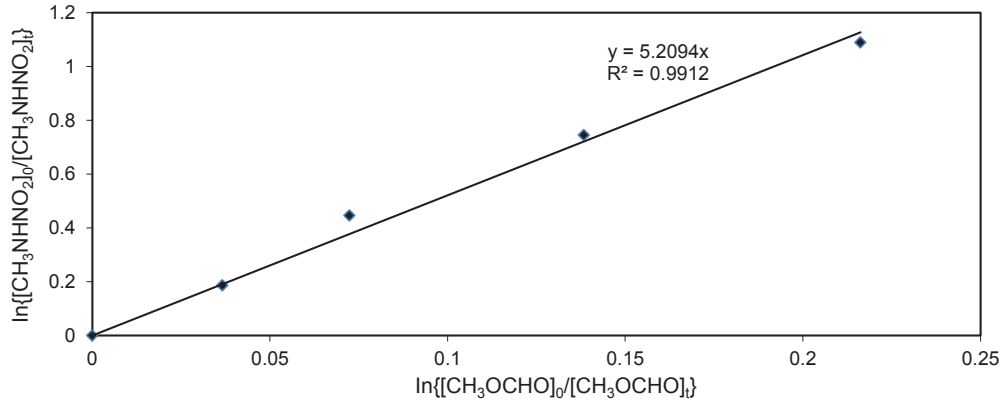

Experiment 3.

I. Relative rate plots showing the decays of Dimethylnitramine (DMNA) and Methanol (MeOH) at 1013 hPa and 298 K in the presence of Cl atoms.

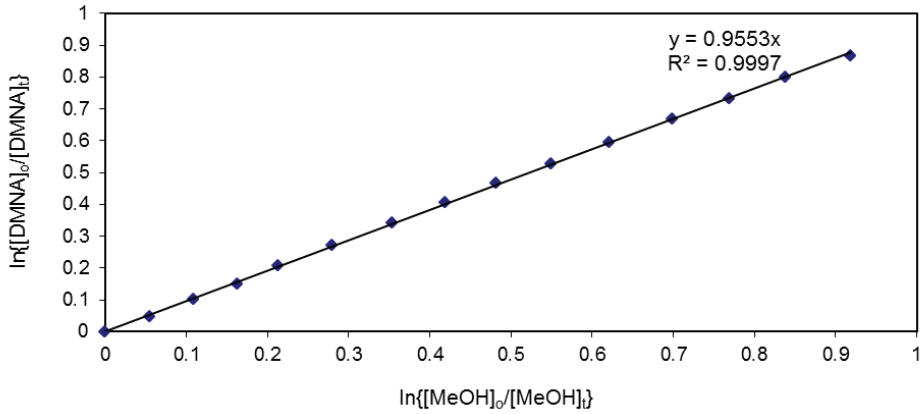

Experiment 1.

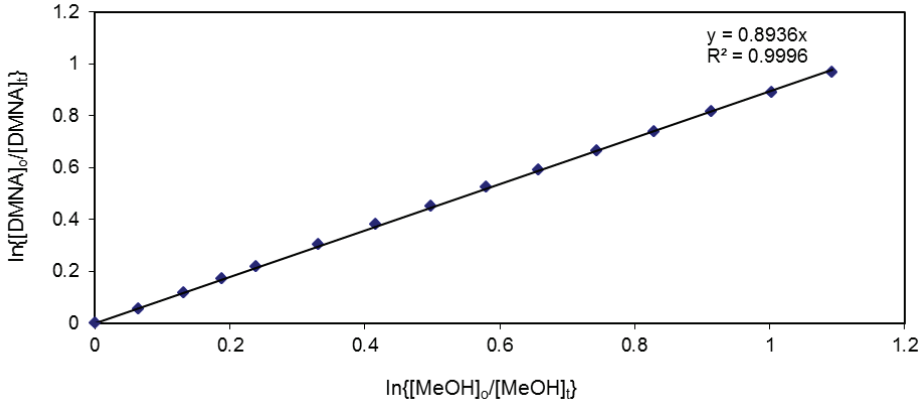

Experiment 2.

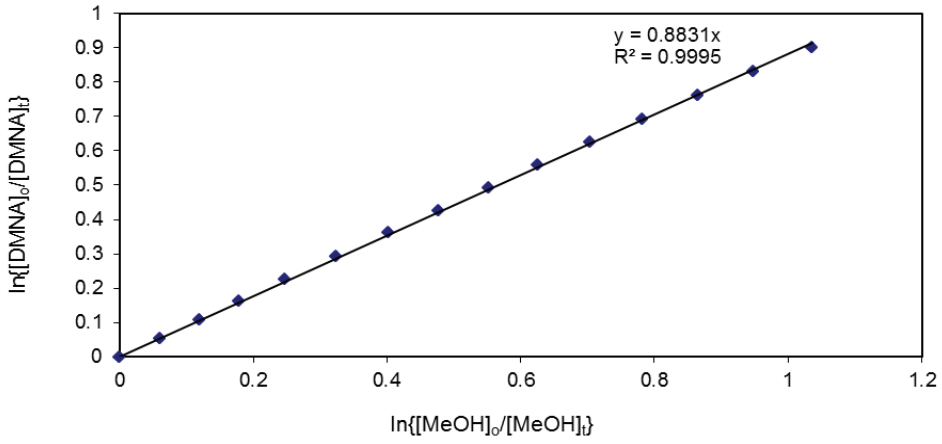

Experiment 3.

J. Relative rate plots showing the decays of Dimethylamine (DMNA) and Dimethylether (DME) at 1013 hPa and 298 K in the presence of Cl atoms.

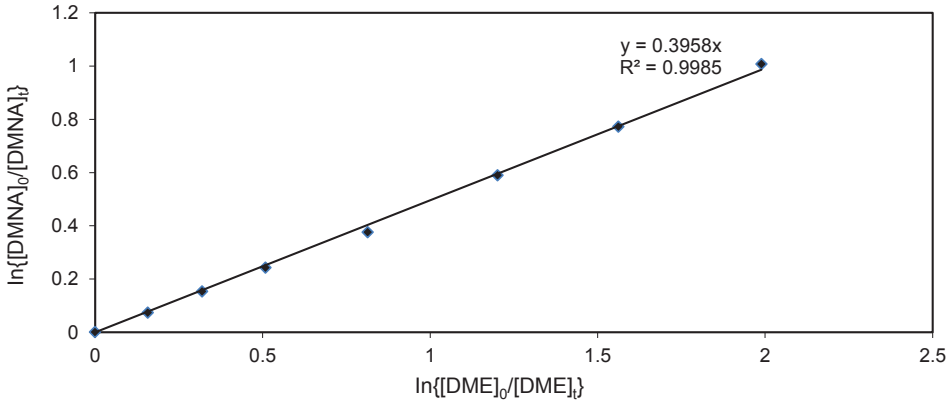

Experiment 1.

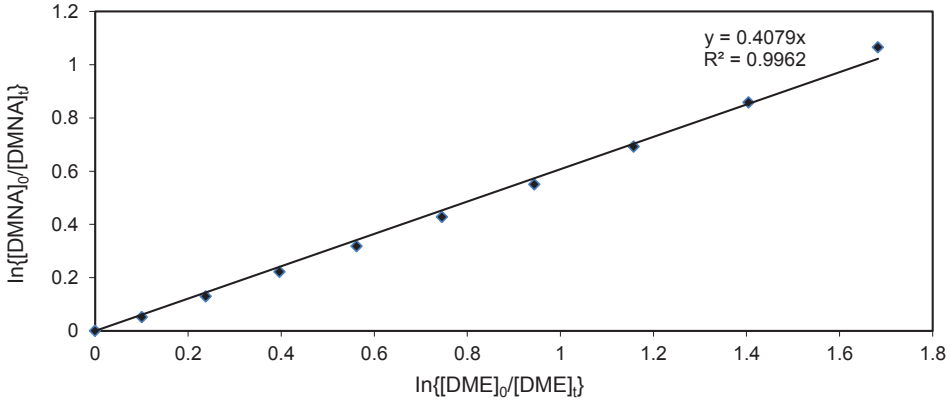

Experiment 2.

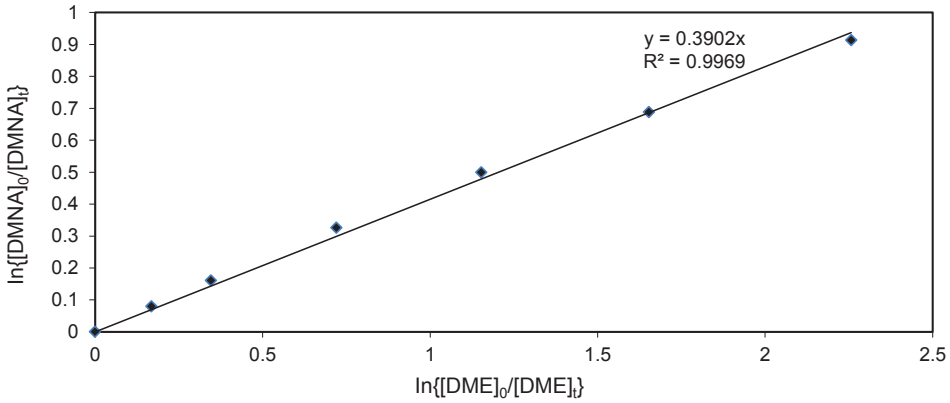

Experiment 3.

K. Relative rate plots showing the decays of Dimethylamine (DMNA) and Ethylacetate (EtOAc) at 1013 hPa and 298 K in the presence of Cl atoms.

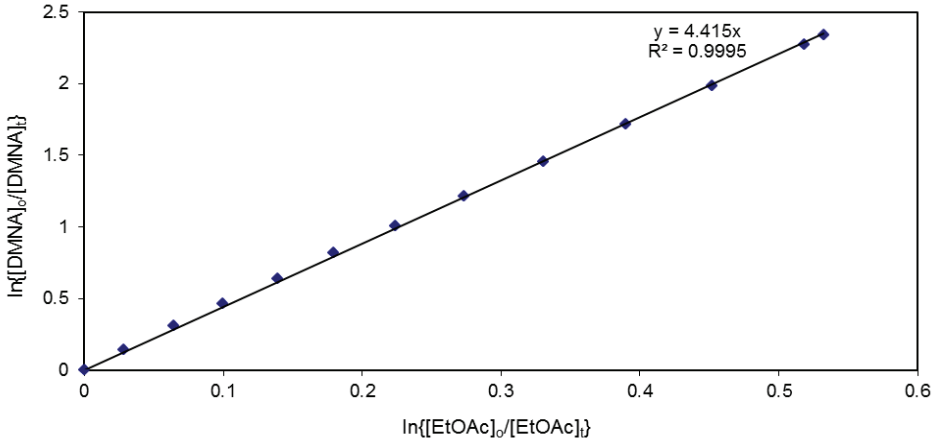

Experiment 1.

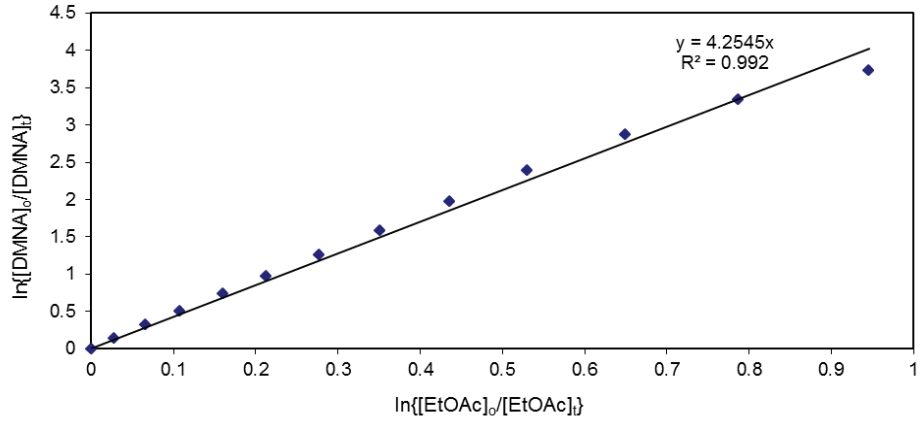

Experiment 2.

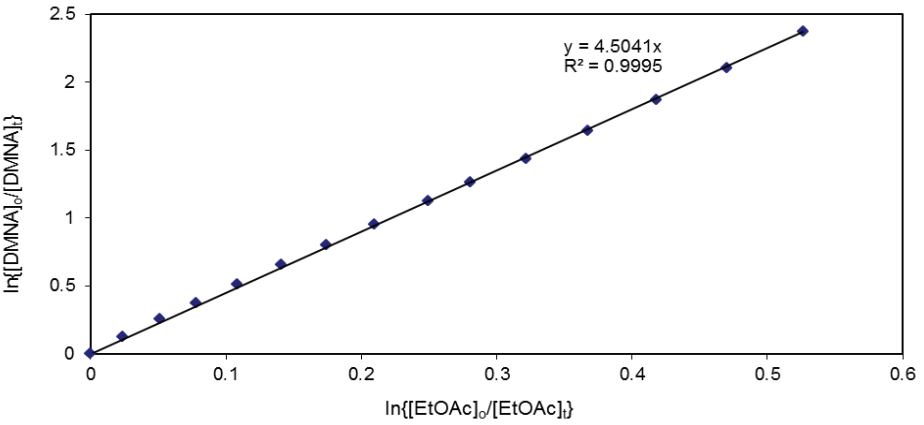

Experiment 3.

L. Relative rate plots showing the decays of Ethylnitramine and Methanol (CH_3OH) at 1013 hPa and 298 K in the presence of Cl atoms.

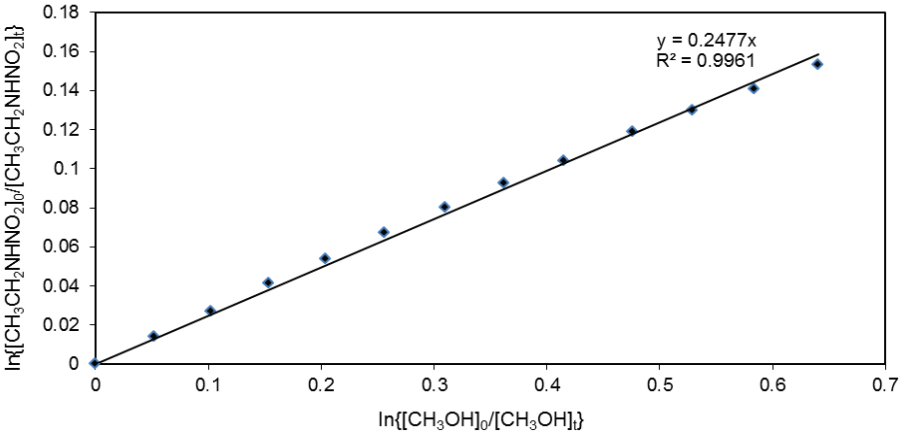

Experiment 1.

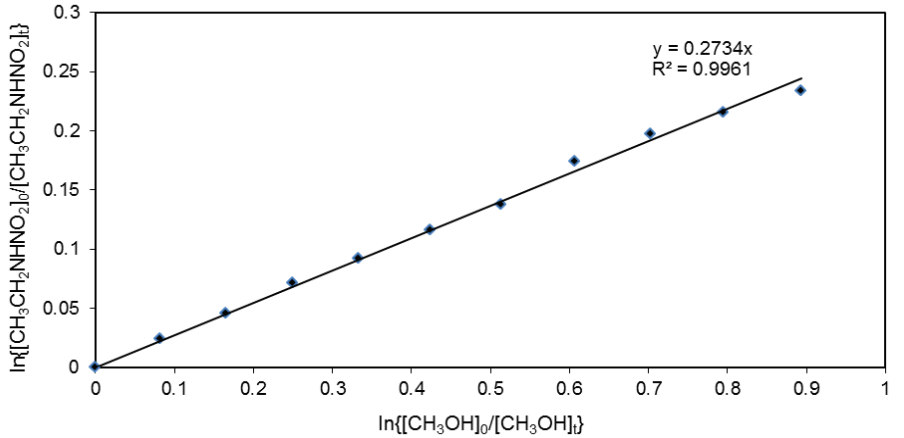

Experiment 2.

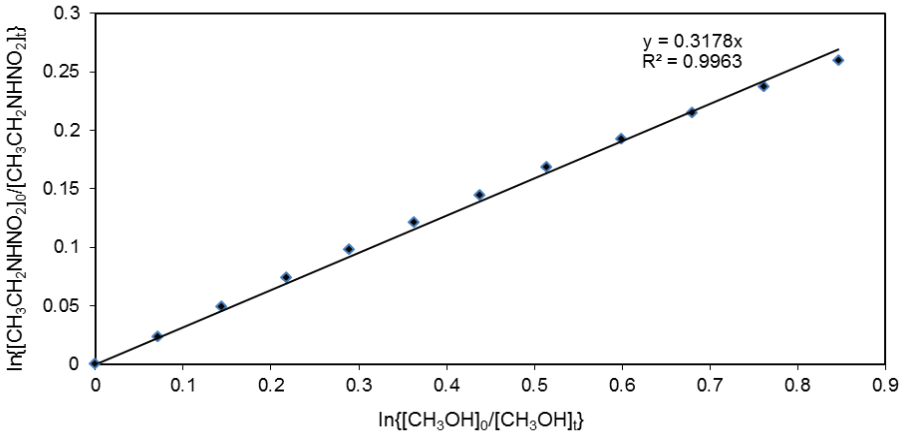

Experiment 3.

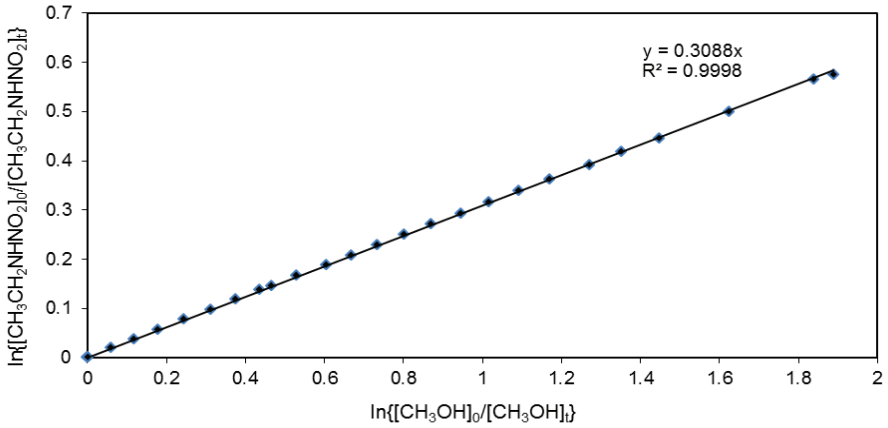

Experiment 4.

M. Relative rate plots showing the decays of Ethylnitramine and Ethylacetate (EtOAc) at 1013 hPa and 298 K in the presence of Cl atoms.

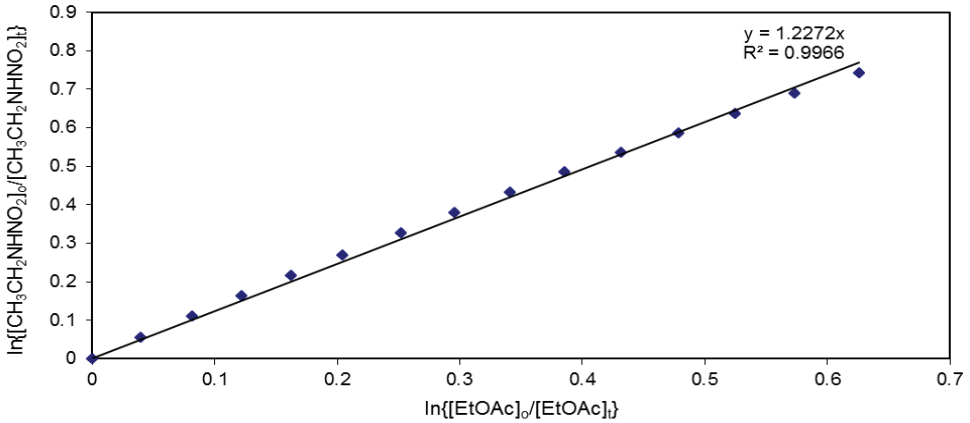

Experiment 1.

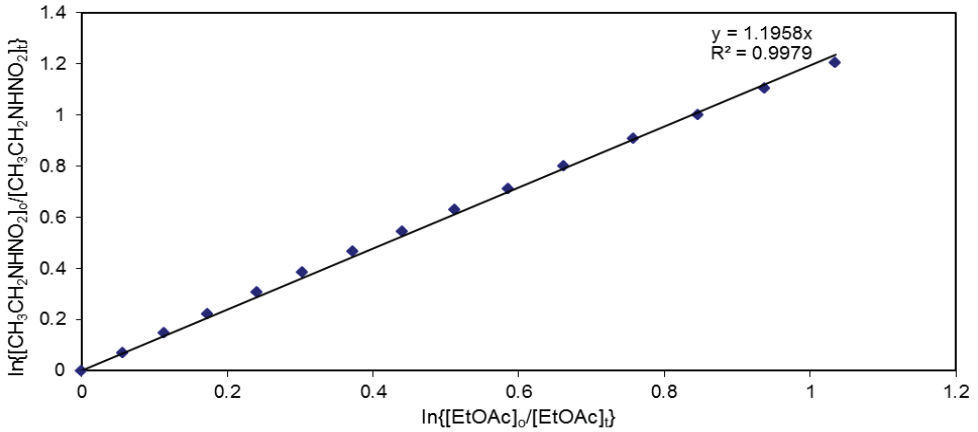

Experiment 2.

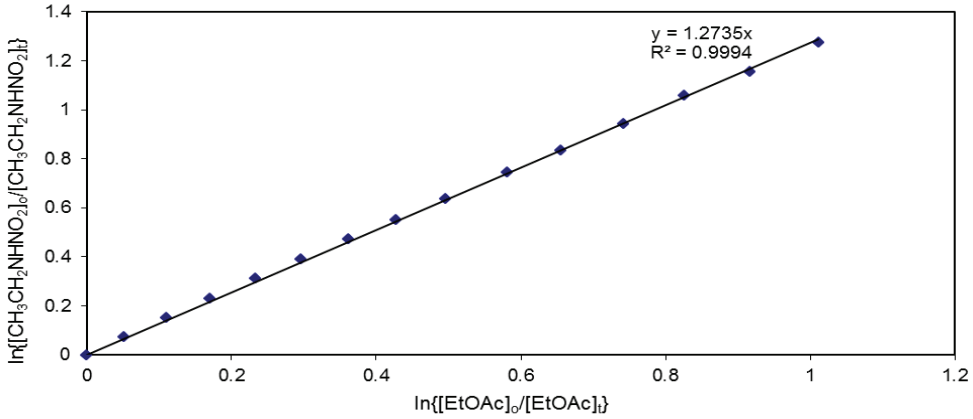

Experiment 3.

N. Relative rate plots showing the decays of Diethylnitramine and Methanol (CH_3OH) at 1013 hPa and 298 K in the presence of Cl atoms.

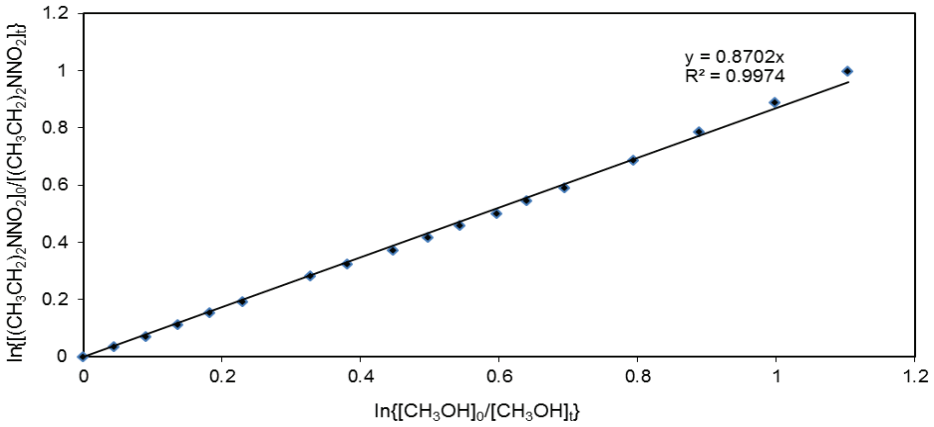

Experiment 1.

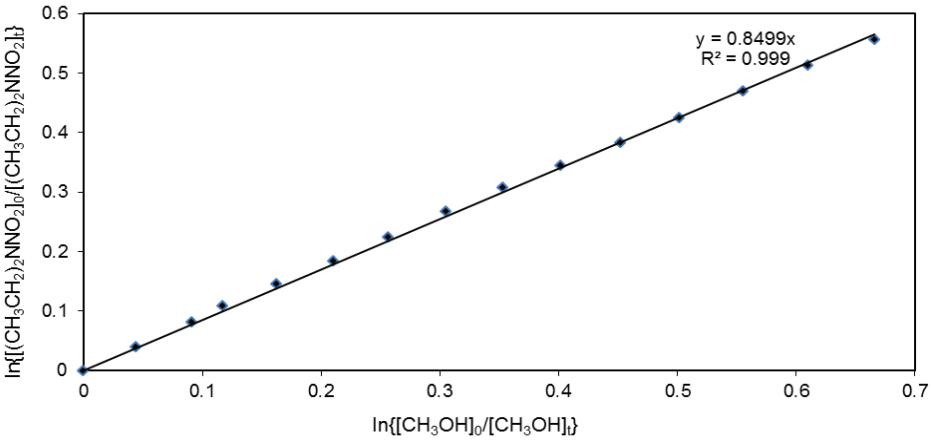

Experiment 2.

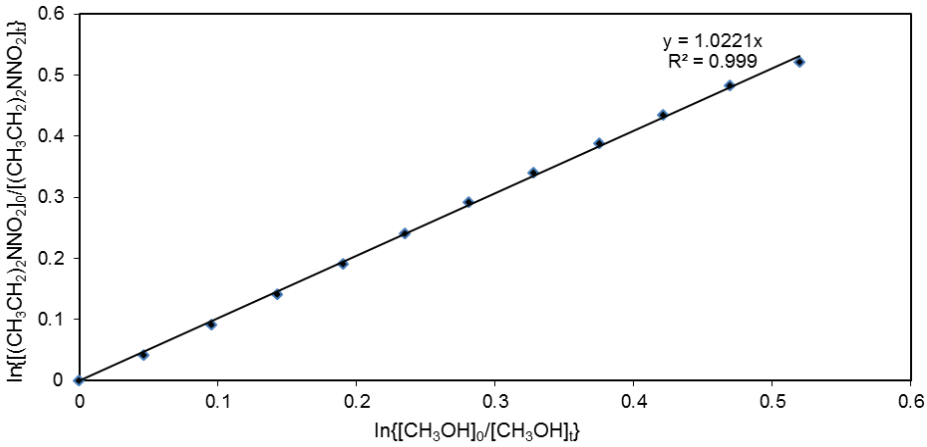

Experiment 3.

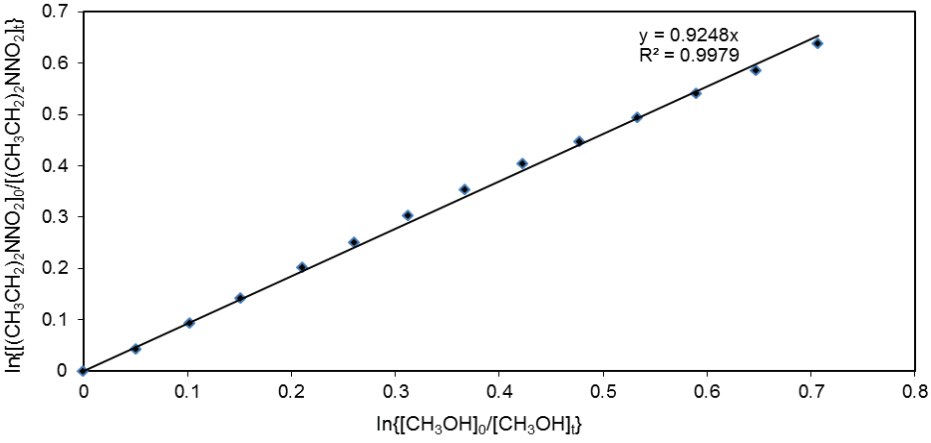

Experiment 4.

O. Relative rate plots showing the decays of Diethylnitramine and Ethylacetate (EtOAc) at 1013 hPa and 298 K in the presence of Cl atoms.

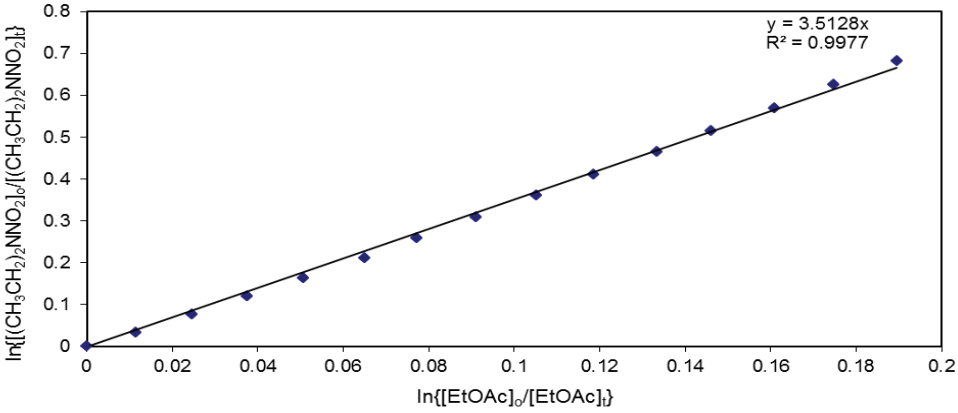

Experiment 1.

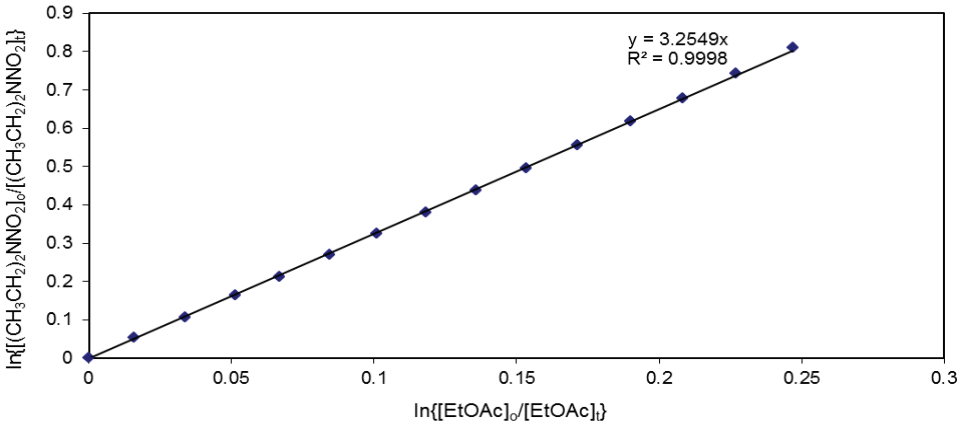

Experiment 2.

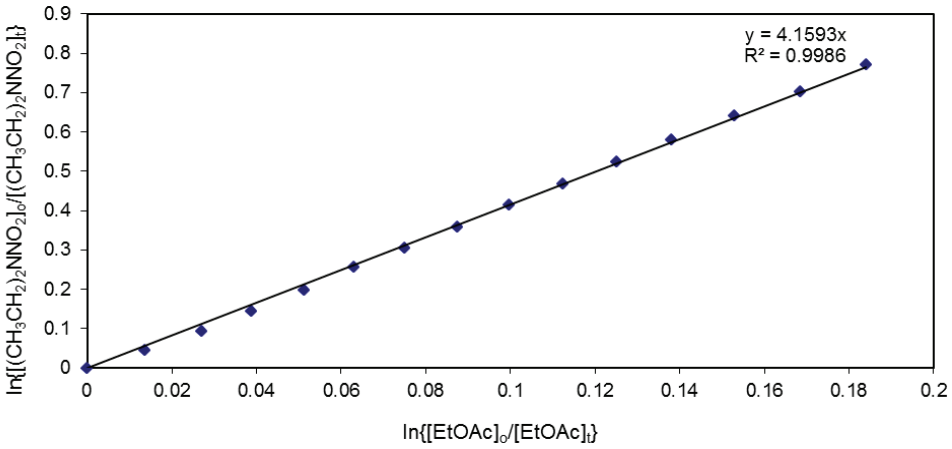

Experiment 3.

P. Relative rate plots showing the decays of Dimethylnitrosamine and Ethylene (CH_2=CH_2) at 1013 hPa and 298 K in the presence of Nitrate radicals (NO_3).

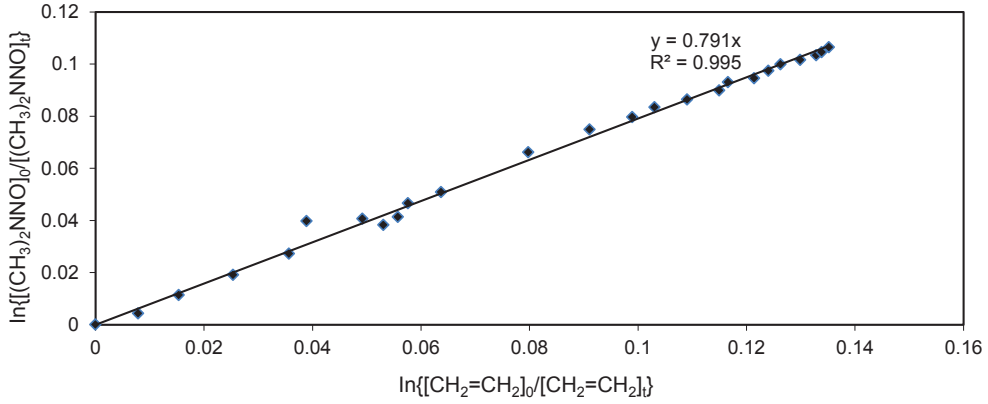

Experiment 1.

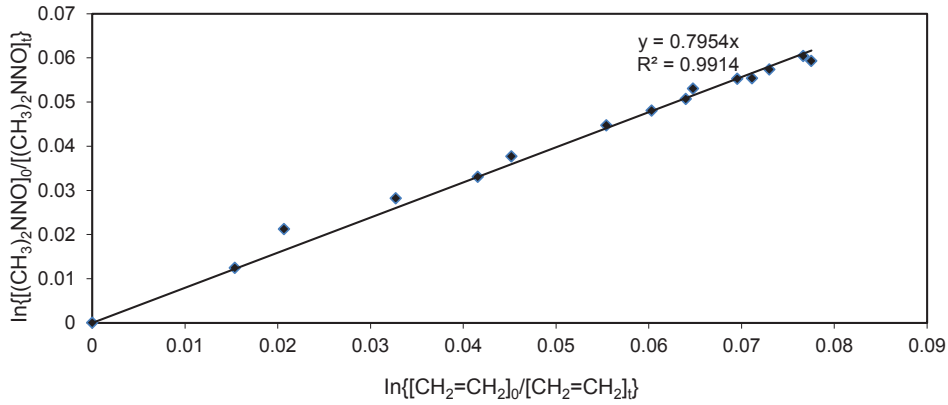

Experiment 2.

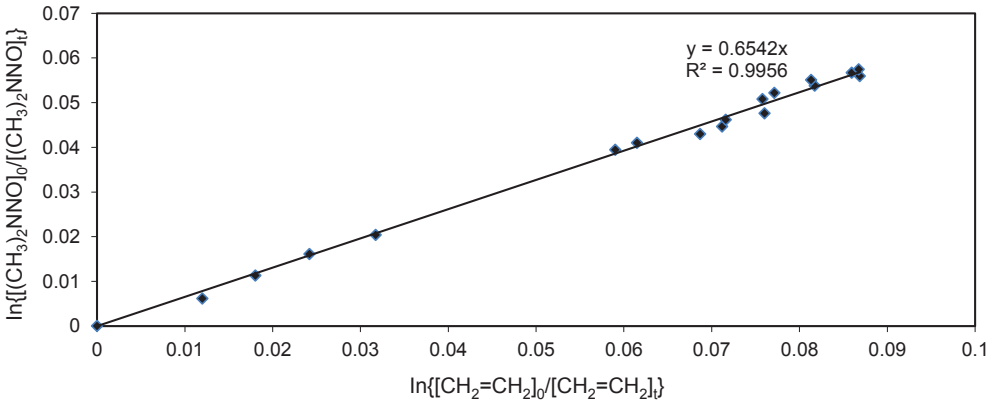

Experiment 3.

Q. Relative rate plots showing the decays of Dimethylnitrosamine and Formaldehyde (CH_2O) at 1013 hPa and 298 K in the presence of Nitrate radicals (NO_3).

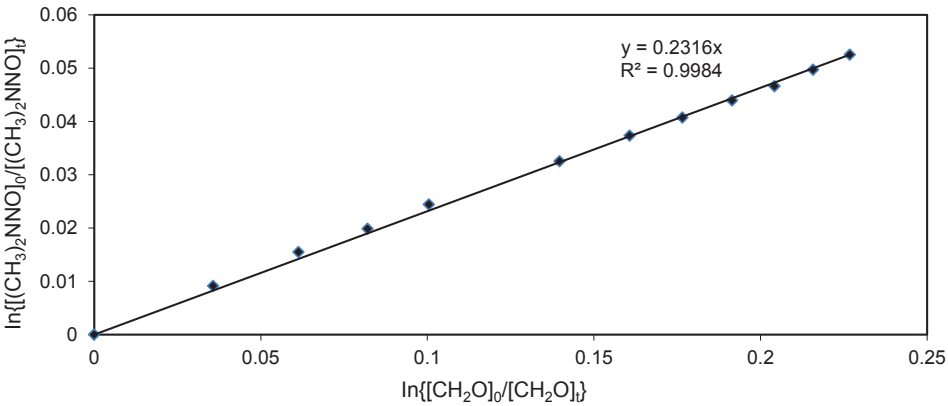

Experiment 1.

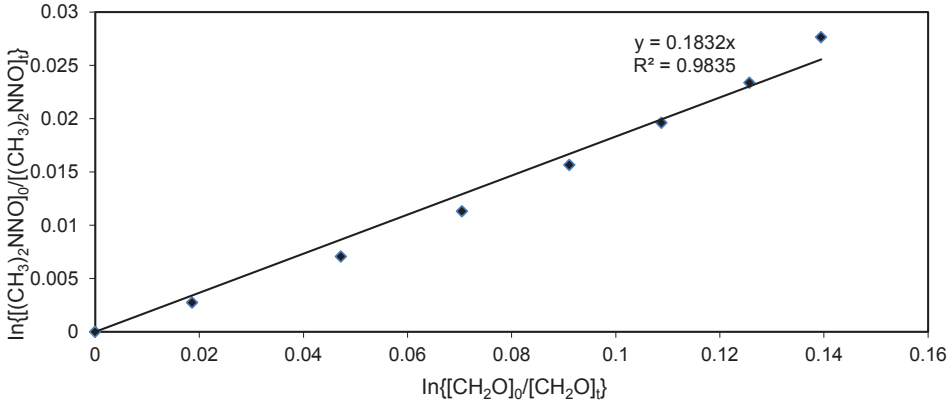

Experiment 2.

R. Relative rate plots showing the decays of Diethylnitrosamine (Et_2NNO) and Ethylene ($CH_2=CH_2$) at 1013 hPa and 298 K in the presence of Nitrate radicals (NO_3).

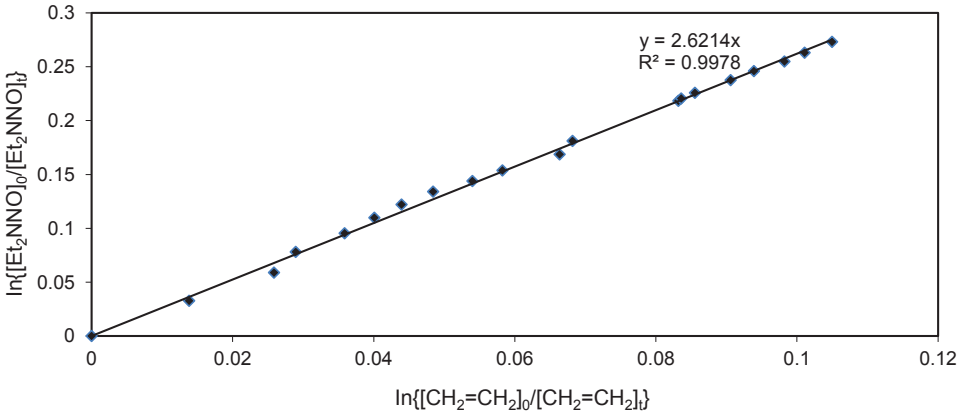

Experiment 1.

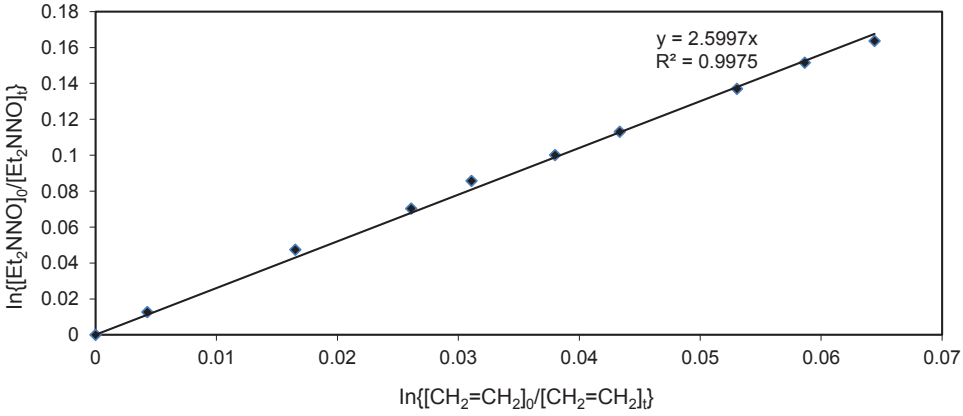

Experiment 2.

S. Relative rate plots showing the decays of Diethylnitrosamine and Fomaldehyde (CH_2O) at 1013 hPa and 298 K in the presence of Nitrate radicals (NO_3).

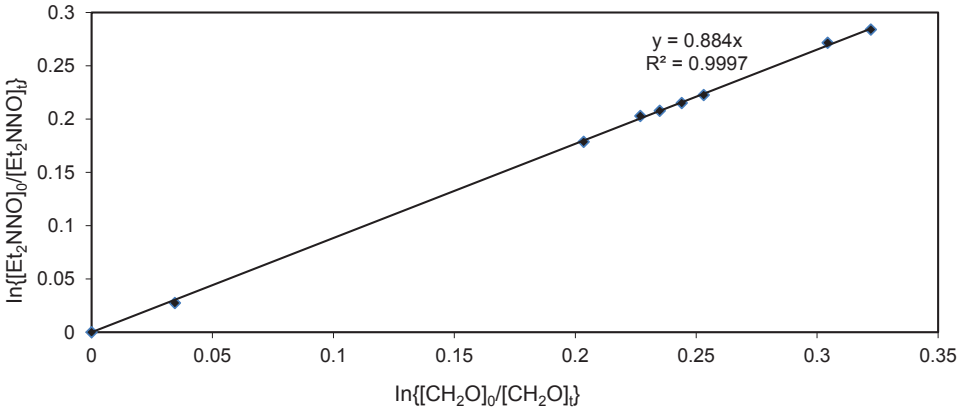

Experiment 1.

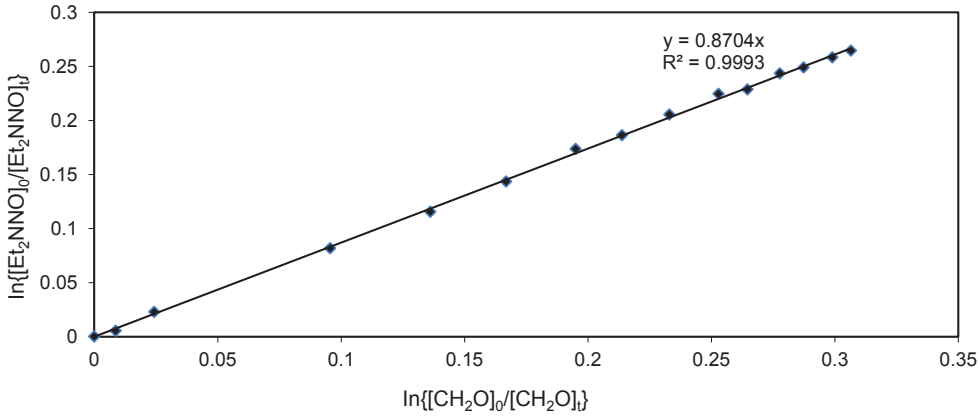

Experiment 2.

7.6 Appendix 6: Calibration curves for some of the compounds involved in the study ploted as: Average integral band intensities)*ln10 versus concentrations (mbars).

A. Methylamine (obtained using C-H stretch in the region 3150 – 2650 cm^{-1})

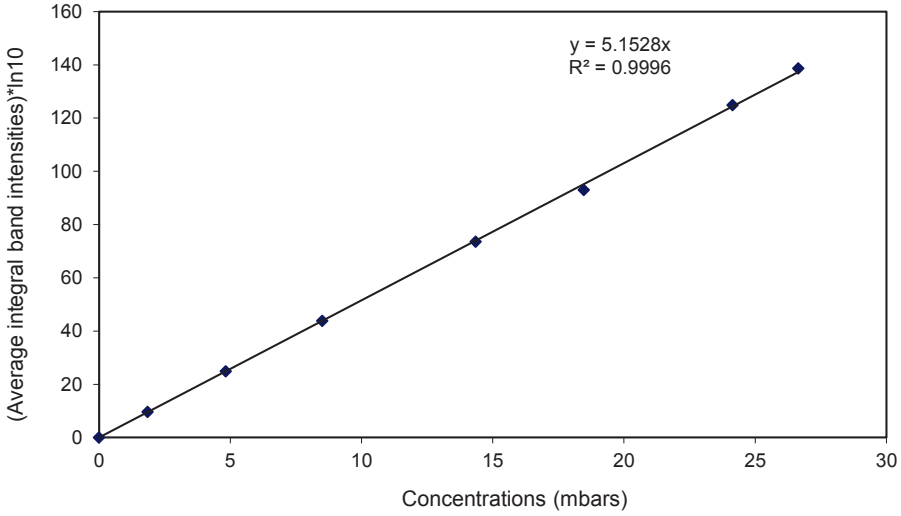

B. Dimethylamine (obtained using C-H stretch in the region 3050 – 2650 cm^{-1})

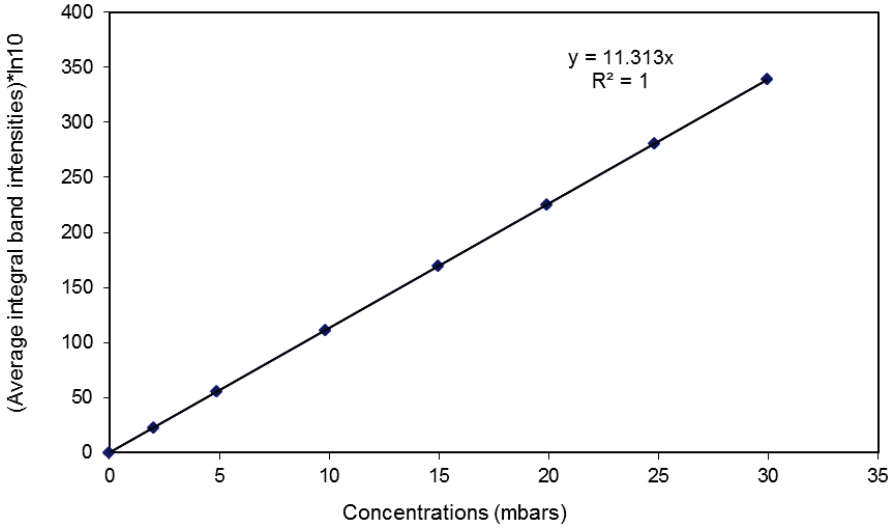

C. Trimethylamine (obtained using C-N stretch in the region 900 – 760 cm^{-1})

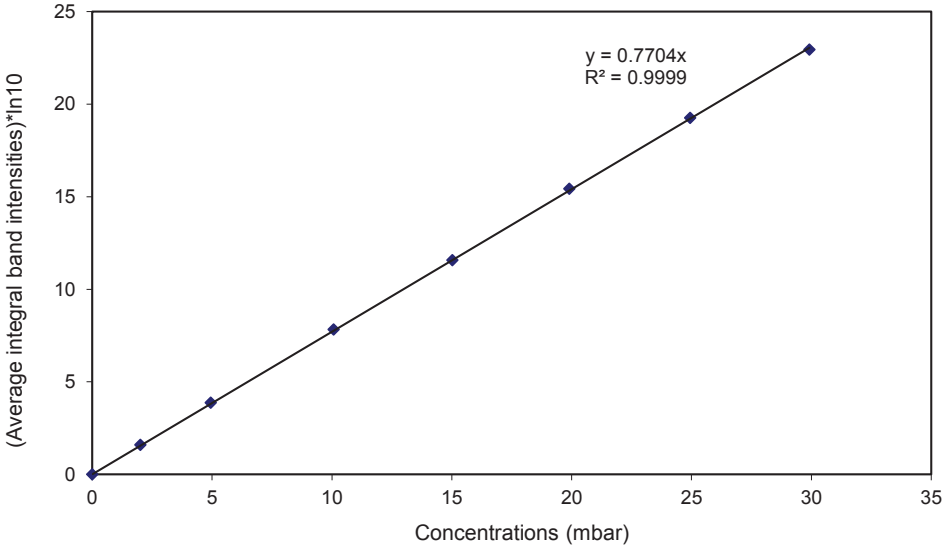

D. Deuterated methylamine (using C-D in the region 2350 – 1950 cm^{-1})

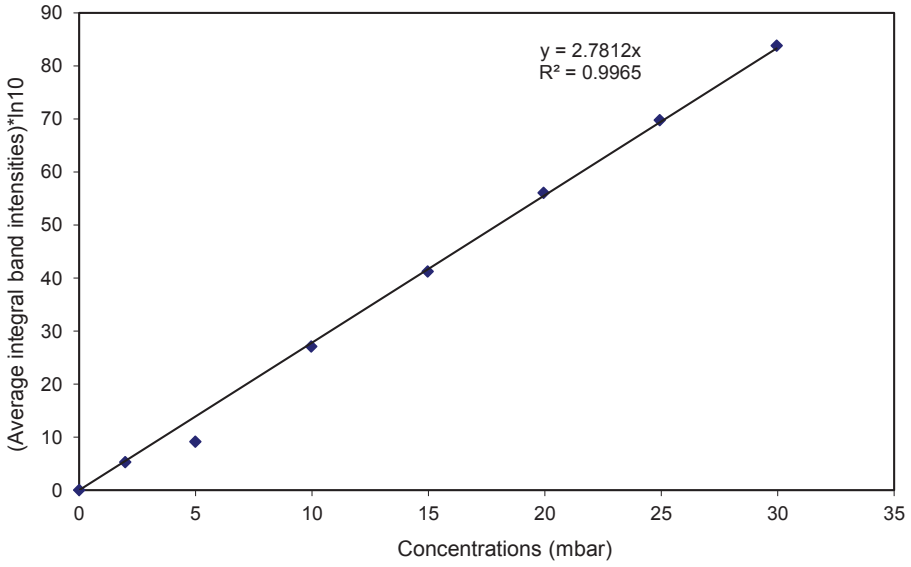

E. Dideutared methylamine (obtained using C-D stretch in the region 2375 – 1925 cm^{-1})

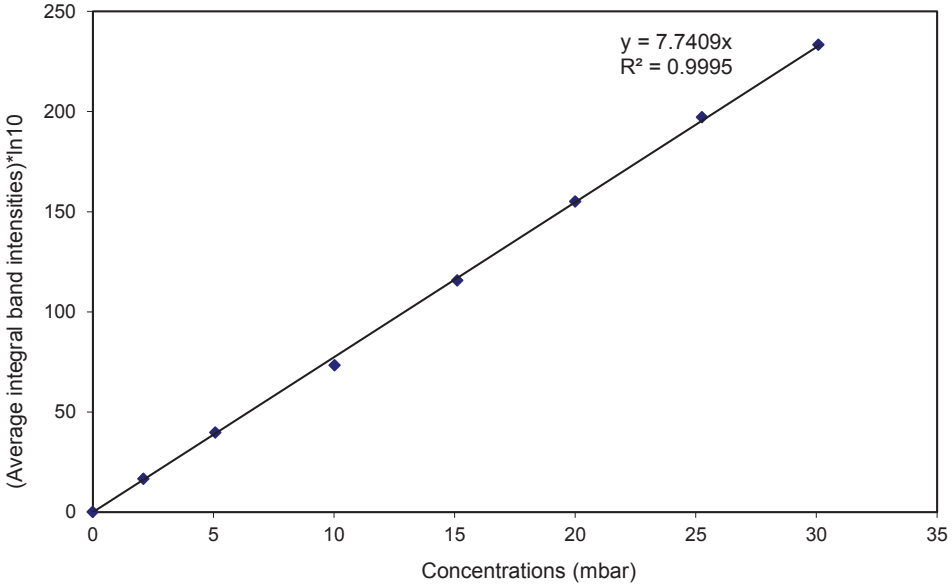

F. Trideuterated methylamine (obtained using C-D stretch in the region 2270 – 1980 cm^{-1})

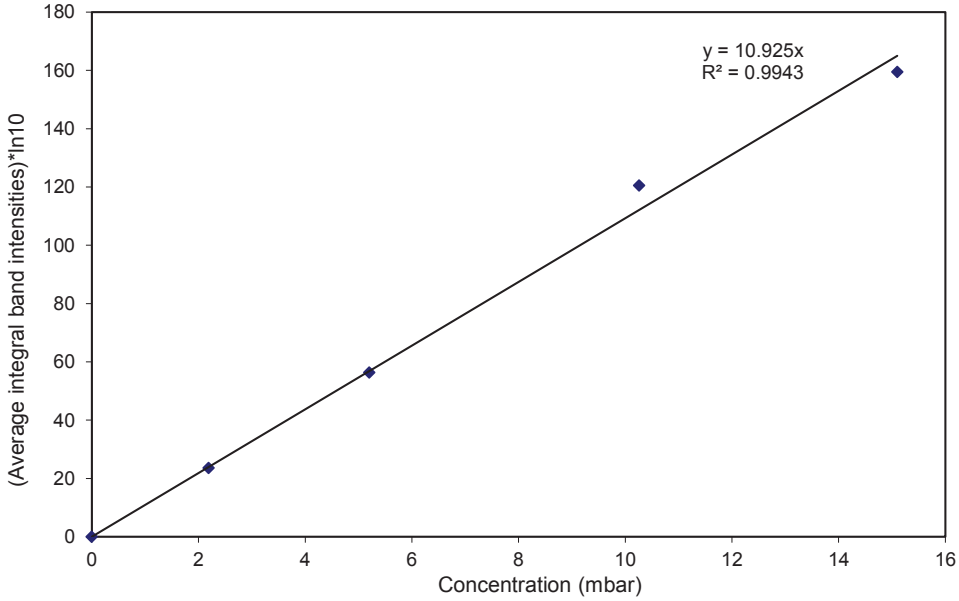

G. Isocyanic acid (obtained using the N-H stretch in the region 3800 – 3200 cm^{-1})

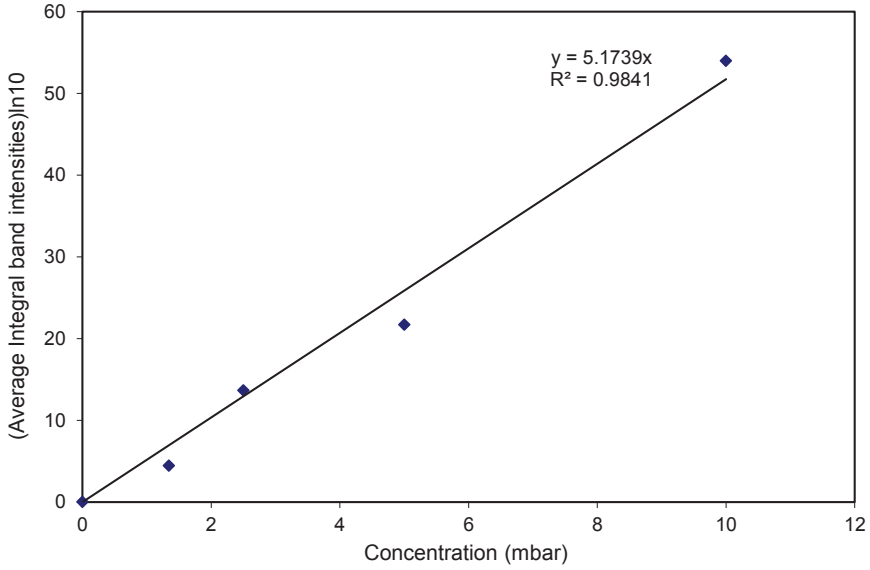

H. Acetonitrile (obtained using C-N stretch in the region 2350 – 2200 cm^{-1})

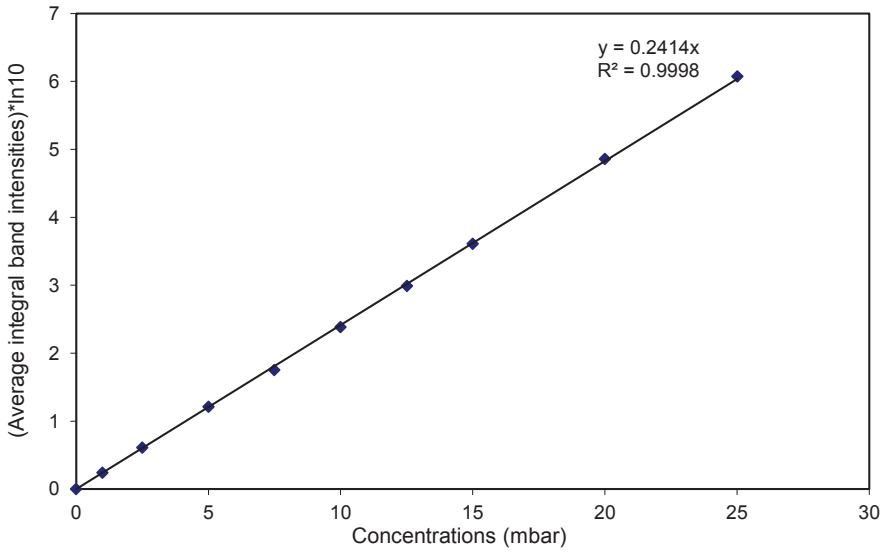

7.7 Appendix 7: Protocols for the experiments done at the Europen Photochemical Reactor (Euphore).

CHAMBER: B	**DATE:** 2008-10-01	**REF. NUM.:** 2464	
Responsaible Scientists: Nielsen, Cl.			
Coworkers: Borrás, Esther; Gómez Alvarez, Elena; Marqués, María; Muñoz, Amalia; Ródenas, Mila; Sánchez, Pilar; Vázquez, Mónica; Vera, Teresa			
Participating Institutions: CEAM Foundation; University of Oslo (UIO)			
Research Project: Atmospheric Degradation of Amines -ADA-		**Financial Support:** University of Oslo (UIO)	
Locator Protocol:			
Temperature (°C): 16.07	**Pressure (mbar):** 1002.81	**Humidity:** -38.88 °C (Dwp)	

Objective of the Experiment
CD3NH2/CH3NH2 + H2O2

Equipment	**Euph.**	**Remarks about the instrumentation**	**Operator**
Barometer AIR-DB-VOC	1		Vázquez, Mónica
CO Monitor TE48C	1	Range: 5 ppm	Vázquez, Mónica
GC-MS System Varian	1	DBwax0t0250c15_250	Gómez Alvarez, Elena; Muñoz, Amalia
Hygrometer Walz	1		Vázquez, Mónica
J(NO2) Filter Radiometer	1		Vázquez, Mónica
NO/NO2 Analyser CLD 770	1	Range: 10 ppb Int: 30 sec	Vázquez, Mónica
NOx Analyser API	1	Range: 500 ppb	Vázquez, Mónica
NOx Analyser ML 9841A	1	Range: 500 ppb Over Range: 1000 ppb	Vázquez, Mónica
Ozone Analyser ML9810	1	Range: 500 ppb Over Range: 1000 ppb	Vázquez, Mónica
Particle Size Distribution DMA 3081	1	Sheath flow at 2 lpm	Borrás, Esther
Spectral Radiantmeter Gigaherzt Optic	1	Wavelength: 290-510 nm	Vázquez, Mónica
TEOM	1		Borrás, Esther

Reactant	Amount Injected (quant. or concent.)	Method of Injection
H2O2	30 mL	sprayer
Methylamine	180 cm3 1 ppm	syringe
methylamine-D3	0.5044 g 1 ppm	synthesized + heating
SF6	5 mL	air stream

Time Table		Action and Remarks
06:24		Stop flushing
06:45	07:19	SPME background
06:54		FTIR BK (media vuelta). T=16.3°C
07:05		FTIR data collection (10')
07:27	07:37	Methylamine-D3 introduction
07:41	07:44	Methylamine injection
08:00		SF6 injection
08:01		TEOM = -234 SMPS= 2.6
09:03	09:05	H2O2 injection, SMSP around 6
09:47		chamber opened to sunlight. TEOM= -23.9, SMPS= 10, O3=127
09:55	10:26	SPME sample
11:04	11:34	SPME sample
11:59		FTIR Restarted. REL3x.spa
13:03		FTIR restarted. REL4X.SPA (G=4). Telesc. to initial position
15:00		Chamber closed
16:03		Experiment stops
16:03		FTIR optical bench alignment
16:05		Chamber flushing

CHAMBER: B	DATE: 2008-10-02	REF. NUM.: 2465	
Responsaible Scientists: Nielsen, Cl.			
Coworkers: Borrás, Esther; Gómez Alvarez, Elena; Ródenas, Mila; Vázquez, Mónica			
Participating Institutions: CEAM Foundation; University of Oslo (UIO)			
Research Project: Atmospheric Degradation of Amines -ADA-		**Financial Support:** University of Oslo (UIO)	
Locator Protocol:			

Temperature (°C): 17	Pressure (mbar): 1000.08	Humidity: -41.2

Objective of the Experiment
Relative reaction of dimethylamine and its deuterated

Equipment	Euph.	Remarks about the instrumentation	Operator
Barometer AIR-DB-VOC	1		Vázquez, Mónica
CO Monitor TE48C	1	Range: 5 ppm	Vázquez, Mónica
FTIR Nicoletet Magna 550	1	VM=7.5V, Vm=-6V, G=2, Res=0.5cm-1	Ródenas, Mila
GC-MS System Varian	1	PFBHA applied on SPME fibres	Gómez Alvarez, Elena
Hygrometer Walz	1		Vázquez, Mónica
J(NO2) Filter Radiometer	1		Vázquez, Mónica
NO/NO2 Analyser CLD 770	1	Range: 10 ppb Int: 30 sec	Vázquez, Mónica
NOx Analyser API	1	Range: 500 ppb	Vázquez, Mónica
NOx Analyser ML 9841A	1	Range: 500 ppb Over Range: 1000 ppb	Vázquez, Mónica
Ozone Analyser ML9810	1	Range: 500 ppb Over Range: 1000 ppb	Vázquez, Mónica
Particle Size Distribution DMA 3081	1	Sheath flow at 2 lpm	Borrás, Esther
Spectral Radiantmeter Gigaherzt Optic	1	Wavelength: 290-510 nm	Vázquez, Mónica
TEOM	1		Borrás, Esther

Reactant	Amount Injected (quant. or concent.)	Method of Injection
Dimethylamine	1ppm APROX	air stream
Dimethylamine-D3	1 ppm	heated air stream from reaction as previous days

Time Table		Action and Remarks
06:29		Stop chamber flushing
06:36		Start FTIR BK (340scans). T=17.0ºC
06:41		Start SMPS data collection, Filter TEOM changed
06:48		Start FTIR data collection (REL1x.spa). 10'
06:56		SPME background
07:16	07:23	Dimethylamine addition (100ml aprox)
07:54		Dimethylamine addition. 2nd addition (80ml)
08:06		SF6 added
08:11	08:18	Dimethylamine deuterated
08:21		SMPS: 1.60um/m2
09:25		SMPS: 0.65um/m2
09:26	09:27	H2O2 addition
10:00		Floor cooling on
10:00		Chamber opened
10:01		SMPS at 8.65 ug/m3; TEOM at 29 ug/m3
10:10	10:41	SPME sample
11:20		Too many Bad scans -->FTIR data collection (G=4)
11:35		FTIR Telescope aligned (1 vuelta horaria)
11:46	11:17	SPME sample
13:10		FTIR Restarted. REL3x.spa. Tel aligned (1/2 vuelta antihoraria)
15:00	15:00	Chamber closed
16:06		Start chamber flushing

CHAMBER: B	**DATE:** 2008-10-06	**REF. NUM.:** 2467	CEAM FUNDACIÓN CENTRO DE ESTUDIOS AMBIENTALES DEL MEDITERRANEO
Responsaible Scientists: Nielsen, Cl.			
Coworkers: Borrás, Esther; Gómez Alvarez, Elena; Vázquez, Mónica			
Participating Institutions: CEAM Foundation; University of Oslo (UIO)			
Research Project: Atmospheric Degradation of Amines -ADA-		**Financial Support:** University of Oslo (UIO)	
Locator Protocol:			

Temperature (°C): 15.16	**Pressure (mbar):** 1005.9	**Humidity:** -41.59

Objective of the Experiment
Realtive photoxidation of trimethylamime

Equipment	**Euph.**	**Remarks about the instrumentation**	**Operator**
Barometer AIR-DB-VOC	1		Vázquez, Mónica
CO Monitor TE48C	1	Range: 5 ppm	Vázquez, Mónica
GC-MS System Varian	1	PFBHA SPME	Gómez Alvarez, Elena
Hygrometer Walz	1		Vázquez, Mónica
J(NO2) Filter Radiometer	1		Vázquez, Mónica
NO/NO2 Analyser CLD 770	1	Range: 50 ppb Int:30 sec	Vázquez, Mónica
NOx Analyser API	1	Range: 500 ppb	Vázquez, Mónica
NOx Analyser ML 9841A	1	Range: 500 ppb Over Range: 1000 ppb	Vázquez, Mónica
Ozone Analyser ML9810	1	Range: 500 ppb Over Range: 1000 ppb	Vázquez, Mónica
Particle Size Distribution DMA 3081	1	Sheath flowat 2 lpm	Borrás, Esther
Spectral Radiantmeter Gigaherzt Optic	1	Wavelength: 290-510 nm	Vázquez, Mónica
TEOM	1		Borrás, Esther

Reactant	Amount Injected (quant. or concent.)	Method of Injection
H2O2	30 ml	sprayer
SF6	5 ml	air stream
Trimethylamine	180 cm3 1 ppm	syringe
Trimethylamine-D3	768.8 mg 1 ppm	synthesized

Time Table		Action and Remarks
06:30		Chamber flange opened to fix HONO monitor
07:32		Stop flushing
07:37		Start FTIR background
07:55		Start FTIR sampling collection
07:58	08:28	SPME background
08:07		trimethylamine 1st injection
08:10		trimethylamine 2nd injection
08:22	08:34	trimethylamine-D3 introduction
08:37		SF6 addition
09:41	09:45	H2O2 addition
10:19		Chamber opened to sunlight
10:19		NOx-API= 219.5 ppb, O3= 140 ppb, NO/NO2/NOy= 106/-14/92 ppb
10:22		SMPS= 4.74,TEOM= 19.4
10:27	10:59	SPME sample
11:04	11:34	SPME sample
13:03		FTIR restarted
15:07		Chamber closed
16:18		Start chamber flushing

CHAMBER: B	**DATE:** 2008-10-16	**REF. NUM.:** 2472	
Responsaible Scientists: Nielsen, Cl.			
Coworkers: Alacreu, Paco; Borrás, Esther; Ródenas, Mila; Vázquez, Mónica			
Participating Institutions: CEAM Foundation; University of Oslo (UIO)			
Research Project: Atmospheric Degradation of Amines -ADA-		**Financial Support:**	
Locator Protocol:			
Temperature (°C): 17.91	**Pressure (mbar):** 1005.29	**Humidity:** -39.67	

Objective of the Experiment
Relative photo-oxidation of dimethylmethylamine

Equipment	**Euph.**	**Remarks about the instrumentation**	**Operator**
Barometer AIR-DB-VOC	1		Vázquez, Mónica
CO Monitor TE48C	1	Range: 5 ppm	Vázquez, Mónica
FTIR Nicoletet Magna 550	1	0.5 cm-1 resolution, MAM.spa	Alacreu, Paco; Ródenas, Mila
Hygrometer Walz	1		Vázquez, Mónica
J(NO2) Filter Radiometer	1		Vázquez, Mónica
NO/NO2 Analyser CLD 770	1	Range: 50 ppb Int: 30 sec	Vázquez, Mónica
NOx Analyser API	1	Range: 500 ppb	Vázquez, Mónica
NOx Analyser ML 9841A	1	Range: 500 ppb Over Range: 1000 ppb	Vázquez, Mónica
Ozone Analyser ML9810	1	Range: 500 ppb Over Range: 1000 ppb	Vázquez, Mónica
Particle Size Distribution DMA 3081	1		Borrás, Esther
Spectral Radiantmeter Gigaherzt Optic	1	Wavelength: 290-510 nm	Vázquez, Mónica
TEOM	1		Borrás, Esther

Reactant	Amount Injected (quant. or concent.)	Method of Injection
Dimethylamine	90 cm3 0.5 ppm	syringe
Dimethylamine	90 cm3 0.5 ppm	syringe
Dimethylamine-D3	655.1 mg 1 ppm approx.	(CD3)2NH·HCl+NaOH(807 mg) (aq) + Heating
H2O2	30 ml	sprayer

Time Table		Action and Remarks
06:13		Stop flushing
06:15		Start FTIR background
06:28		Start FTIR data collection
07:06	07:17	Addition of deuterated dimethyl amine
07:31		1st addition of dimethyl amine gas
07:34	07:34	2nd additon of dimethyl amine
07:39		SF6 addition
08:39	08:42	H2O2 addition
09:17		Chamber opened to sunlight
09:34		Floor cooling on
11:46		FTIR collection restarted (MAM2x.spa). G=autogain.T=29.7°C, Ppanel=-0.10
13:08		FTIR collection restarted (MAM3x.spa). G=autogain.T=30.2°C, Ppanel=-0.10
14:30		Chamber closed
15:30		Chamber flushed

CHAMBER: B	**DATE:** 2009-02-23	**REF. NUM.:** 2482	
Responsaible Scientists: Nielsen, Cl.			
Coworkers: Borrás, Esther; Marqués, María; Muñoz, Amalia; Ródenas, Mila; Vázquez, Mónica			
Participating Institutions: CEAM Foundation; University of Oslo (UIO)			
Research Project: Atmospheric Degradation of Amines -ADA-		**Financial Support:** University of Oslo (UIO)	
Locator Protocol:			
Temperature (°C): 9.99	**Pressure (mbar):** 1004.72	**Humidity:** -41.80	

Objective of the Experiment
(CH3)3N/(CD3)3N + H2O2

Equipment	**Euph.**	**Remarks about the instrumentation**	**Operator**
Barometer AIR-DB-VOC	1		Vázquez, Mónica
CO Monitor TE48C	1	Range: 5 ppm	Vázquez, Mónica
FTIR Nicoletet Magna 550	1	VM=3.3, Vm=-2.3, G=1, Res=0.5cm-1	Ródenas, Mila
GC 8000 Fisons	1	80ºC	Marqués, María
GC-MS System Varian	1	Amines	Muñoz, Amalia
HCHO Monitor	1		Marqués, María
HONO Monitor	1		Marqués, María
Hygrometer Walz	1		Vázquez, Mónica
J(NO2) Filter Radiometer	1		Vázquez, Mónica
NO/NO2 Analyser CLD 770	1	Range: 50 ppb Int: 30 sec	Vázquez, Mónica
NOx Analyser API	1	Range: 500 ppb	Vázquez, Mónica
NOx Analyser ML 9841A	1	Range: 500 ppb Over Range: 1000 ppb	Vázquez, Mónica
Ozone Analyser ML9810	1	Range: 500 ppb Over Range: 1000 ppb	Vázquez, Mónica
PAN GC	1		Marqués, María
Particle Size Distribution DMA 3081	1	Sheath flow at 2lpm	Borrás, Esther
Spectral Radiantmeter Gigaherzt Optic	1	Wavelength: 290-510 nm	Vázquez, Mónica
TEOM	1		Borrás, Esther

Reactant	Amount Injected (quant. or concent.)	Method of Injection
H2O2	25 ml	sprayer
SF6	5 ml	air stream
Trimethylamine	180 cm3 1 ppm	syringe
Trimethylamine-D3	762.2 mg 1ppm	(0.9322 mg NaOH)+heating

Time Table		Action and Remarks
07:25		Stop chamber flushing
07:30		START FTIR BK
07:41		Pid T Changed from 160ºC to 80ºC
07:47		Start FTIR data collection (10') Samx.spa. Res=0.5 cm-1
08:03		SF6 addition
08:33	08:38	Trimethylamine injection
08:53	09:00	trimethylamine-D3 injection
10:15		H2O2 addition
10:48		Chamber cooling on
10:52		Chamber opened to sunlight
10:58		Air inlet ON to increase chamber pressure
16:31		Chamber closed
17:36		Start chamber flushing

CHAMBER: B	**DATE:** 2008-10-27	**REF. NUM.:** 2473	
Responsaible Scientists: Nielsen, Cl.			
Coworkers: Borrás, Esther; Marqués, María; Ródenas, Mila; Vázquez, Mónica			
Participating Institutions: CEAM Foundation; University of Oslo (UIO)			
Research Project: Atmospheric Degradation of Amines -ADA-		**Financial Support:** University of Oslo (UIO)	
Locator Protocol:			

Temperature (°C): 14	**Pressure (mbar):** 1004.25	**Humidity:** -41.51 °C (Dwp)

Objective of the Experiment
(CD3)NH2/(CH3)NH2 + H2O2

Equipment	**Euph.**	**Remarks about the instrumentation**	**Operator**
Barometer AIR-DB-VOC	1		Vázquez, Mónica
CO Monitor TE48C	1	Range: 5 ppm	Vázquez, Mónica
FTIR Nicoletet Magna 550	1	VM=6, Vm=-5V, G=2,App=17, Res=0.5cm-1	Ródenas, Mila
GC 8000 Fisons	1	80ºC	Marqués, María
HCHO Monitor	1		Marqués, María
Hygrometer Walz	1		Vázquez, Mónica
J(NO2) Filter Radiometer	1		Vázquez, Mónica
NO/NO2 Analyser CLD 770	1	Range: 10ppb Int: 30 sec	Vázquez, Mónica
NOx Analyser API	1	Range: 500 ppb	Vázquez, Mónica
NOx Analyser ML 9841A	1	Range:500 ppb Over Range: 1000 ppb	Vázquez, Mónica
Ozone Analyser ML9810	1	Range: 500 ppb Over Range: 1000 ppb	Vázquez, Mónica
PAN GC	1		Marqués, María
Particle Size Distribution DMA 3081	1		Borrás, Esther
Spectral Radiantmeter Gigaherzt Optic	1	Wavelength: 290-510 nm	Vázquez, Mónica
TEOM	1		Borrás, Esther

Reactant	Amount Injected (quant. or concent.)	Method of Injection
Methylamine	90 cm3	air stream
Methylamine	90 cm3	air stream
Methylamine	0.5150 g	Synthetised with 0.6465 g of NaOH
methylamine-D3	0.5027 g	Synthetised with 0.6150 g of NaOH

Time Table		Action and Remarks
07:15		Stop chamber flushing
07:20		Start FTIR BK (340 scans)
07:33		Start FTIR data collection (10')
07:50		SF6 addition
07:53		Methylamine 1st addition (90cm3)
07:56		Methylamine 2nd addition (90cm3)
08:07	08:17	Methylamine deuterated->ERROR: MAmine introduced instead of deuterated
09:21		Start chamber flushing to remove compound
10:12		Stop chamber flushing
10:17	10:19	Hygromter mirror cleaning
10:25	10:33	Methylamine deuterated
10:47		SF6 3ml added
11:32		Floor cooling on
11:41	11:43	H2O2 introduction
11:50		Open chamber
14:09		FTIR ADC saturated. G changed to G=2
16:04		Chamber closing
17:08		Start chamber flushing
17:09		Start flushing

7.8 Appendix 8: List of chemicals

Name	Formula	Structure	CAS No
2-(diethylamino) acetaldehyde	$C_6H_{13}NO$	$(CH_3CH_2)_2NCH_2CHO$	32314-21-9
2-(Ethylamino) acetaldehyde	C_4H_9NO	$CH_3CH_2NHCH_2CHO$	1262944-47-7
Acetaldehyde	C_2H_4O	CH_3CHO	75-07-0
Acetamide	C_2H_5NO	$H_2NC(O)CH_3$	60-35-5
Acetic acid	$C_2H_4O_2$	$CH_3C(O)OH$	64-19-7
Acetone	C_3H_3O	$CH_3C(O)CH_3$	67-64-1
Acetonitrile	C_2H_3N	CH_3CN	75-05-8
Aziridine	C_2H_5N		151-56-4
Diethylamine (or *N*-Ethyl ethanamine)	$C_4H_{11}N$	$(CH_3CH_2)_2NH$	109-89-7
Diethylanitramine (or *N*-ethyl-*N*-nitro ethanamine)	$C_4H_{10}N_2O_2$	$(CH_3CH_2)_2N\text{-}NO_2$	7119-92-8
Diethylnitrosamine (or *N*-ethyl-*N*-nitroso ethanamine)	$C_4H_{10}N_2O$	$(CH_3CH_2)_2N\text{-}NO$	55-18-5
Dimethylamine (or *N*-Methyl methanamine)	C_2H_7N	$(CH_3)_2NH$	124-40-3
Dimethylnitramine (or *N*-Methyl-*N*-nitro methanamine)	$C_2H_6N_2O_2$	$(CH_3)_2N\text{-}NO_2$	4164-28-7
Ethanamine (or Ethylamine)	C_2H_7N	$CH_3CH_2NH_2$	75-04-7
Ethanimine	C_2H_5N	$CH_3\text{-}CH{=}NH$	20729-41-3
Ethenamine	C_2H_5N	$CH_2{=}CH\text{-}NH_2$	593-67-9
Formaldehyde	CH_2O	$H_2C{=}O$	50-00-0

Formamide	CH_3NO	H_2NCHO	75-12-7
Formic acid	CH_2O_2	$HC(O)OH$	64-18-6
Isocyanic acid	CHNO	H-N=C=O	75-13-8
Isocyanato methane	C_2H_3NO	CH_3-N=C=O	624-83-9
Methanol	CH_4O	CH_3OH	67-56-1
Methylamine	CH_5N	CH_3NH_2	74-89-5
Methylnitramine (or *N*-Nitro methanamine	$CH_4N_2O_2$	CH_3NHNO_2	598-57-2
Monoethanolamine	C_2H_7NO	$HO\text{-}CH_2CH_2NH_2$	141-43-5
N-(2-Oxoethyl) acetamide	$C_4H_7NO_2$	$CH_3C(O)NHCH_2CHO$	64790-08-5
N,N-Diethyl acetamide	$C_6H_{13}NO$	$(CH_3CH_2)_2NC(O)CH_3$	685-91-6
N,N-Diethyl ethanamine	$C_6H_{15}N$	$(CH_3CH_2)_3N$	121-44-8
N,N-Diethylformamide	$C_5H_{11}NO$	$(CH_3CH_2)_2NCHO$	617-84-5
N-Acetyl acetamide	$C_4H_7NO_2$	$CH_3C(O)NHC(O)CH_3$	625-77-4
N-Ethyl acetamide	C_4H_9NO	$CH_3CH_2NHC(O)CH_3$	625-50-3
N-Ethylidene acetamide	C_4H_7NO	$CH_3C(O)\text{-}N=CHCH_3$	70603-39-3
N-Ethylidene ethanamine	C_4H_9N	$CH_3CH_2\text{-}N=CHCH_3$	1190-79-0
N-Ethylidene methanamine	C_4H_7N	$CH_3\text{-}N=CHCH_3$	6896-67-5
N-Ethyl-*N*-nitroethanamine	$C_4H_{10}N_2O_2$	$(CH_3CH_2)_2N\text{-}NO_2$	7119-92-8
N-Ethyl-*N*-nitroso ethanamine	$C_4H_{10}N_2O$	$(CH_3CH_2)_2N\text{-}NO$	55-18-5
N-Formyl acetamide	$C_3H_5NO_2$	$CH_3C(O)NHCHO$	21163-79-1
Nitromethane	CH_3NO_2	CH_3NO_2	75-52-5
N-Methyl acetamide	C_3H_7NO	$CH_3NHC(O)CH_3$	79-16-3
N-Methylene ethanamine	C_3H_7N	$CH_2=N\text{-}CH_2CH_3$	43729-97-1
N-Methylene formamide	C_2H_3NO	$CH_2=N\text{-}CHO$	83442-29-9

N-Methyl formamide	C_2H_5NO	CH_3NHCHO	123-39-7
N-Nitrosodimethylamine	$C_2H_6N_2O$	$(CH_3)_2N\text{-}NO$	571-61-9
Triethylamine	$C_6H_{15}N$	$(CH_3CH_2)_3N$	121-44-8
Trimethylamine	C_3H_9N	$(CH_3)_3N$	75-50-3

7.9 Appendix 9: Chemical synthesis

General:

Safety precautions: All reactions were done in an inert atmosphere (N_2) in a well ventilated fume hood. Usual precautions were implemented when working with these compounds, *i.e.* use of gloves, laboratory coat and safety goggles. Those compounds specially suspected to be cancer promoting or explosive were treated wet and destroyed according to standard laboratory practice. Work was performed behind safety shields. All chemical waste were sealed in special flasks and sent to authorized companies for destruction of such materials.

Methylnitramine, CH_3NHNO_2.

To 130 mL 70 % HNO_3 cooled to 5 °C 23 g (124 mmol; MW 185.24) *N*-methyl-p-toluenesulfonamide was added portion wise with stirring. When all the sulfonamide had dissolved the solution was cooled to 0 °C and 130 mL 100 % HNO_3 was added. The solution was stirred at this temperature for another 10 min. when this was poured carefully into a beaker with ice/water ≈200 mL. The precipitated nitrosulfonamide (MW 230.24) was filtered and recrystallized from ethanol (95 %). Yield: 23.8 g (83 %), Mp. 55-57 °C. ^{1}H NMR (300 MHz, $CDCl_3$): δ 2.44 (s, 3H), 3.68 (s, 3H), 7.35 (d, *J* 8.5 Hz, 2H), 7.87 (d, *J* 8.5 Hz, 2H); ^{13}C NMR (75 MHz, $CDCl_3$): δ 21.91 (CH_3), 35.76 (CH_3), 129.49 (CH x 2), 130.04 (CH x 2), 133.34 (C), 146.71 (C) ppm. To a solution of 40 mL 1M NaOH was added 4.6 g (20 mmol) *N*-nitro-*N*-methyl-p-toluolsulfonamide and the mixture was heated to reflux for 1h or till a clear solution resulted. The solution was acidified with 6M HCl (aq) by careful addition. Extraction with ether gave the methylnitramine (MW 76.05). Yield: 1.11g (73 %). Mp. 34-36 °C. ^{1}H NMR (300 MHz, $CDCl_3$): δ 3.16 (s, 3H), 9.27 (bs, 1H); ^{13}C NMR (75 MHz, $CDCl_3$): δ 32 ppm.

Dimethylnitramine; Me_2NNO_2

Trifluoroacetic anhydride (91.7 mL, 0.663 mol) was placed in a 250 mL three-necked round-bottom flask equipped with a magnetic stirring bar and under nitrogen. The reaction mixture was cooled to -5 to 0 °C using a dry ice-ethanol cooling bath. Next, fuming nitric acid (30.8 mL, 0.733 mol) was added slowly by means of a dropping funnel. After complete addition of the nitric acid, the reaction mixture was cooled to -30 °C and dimethylformamide (10.6 mL, 0.137 mol) was added drop wise using a dropping

funnel. After complete addition, the reaction was allowed to stand for 10 minutes before being concentrated to approximately half its volume in *vacuo*. Effervescence of brown gas was observed during this process. The resulting solution was poured on ice (~ 150 g) and made alkaline (~ pH 10) using 50% NaOH. The aqueous solution was extracted six times with ether and the combined organic phase was dried ($MgSO_4$), filtered and evaporated in *vacuo* to yield dimethylnitramine as a white solid. Recrystallization (diethyl ether) gave 8.75 g (71 %) dimethylnitramine as large, white crystals. Mp. 55-56 °C. ^{1}H NMR (300 MHz, $CDCl_3$): δ 3.04 (s, 3H), 3.76 (s, 3H); ^{13}C NMR (75 MHz, $CDCl_3$): δ 40.48 ppm.

Ethylnitramine; $CH_3CH_2NHNO_2$

To 130 mL 70% HNO_3 cooled to 5^{o}C 24.7 g (124 mmol; MW 199.27) N-ethyl-p-toluene-sulfonamide was added portionwise with stirring. When all the sulfonamide had dissolved the solution was cooled to 0^{o}C and 130 mL 100% HNO_3 was added. The solution was stirred at this temperature for another 10 min. when this was poured carefully into a beaker with ice/water ≈200 mL. The precipitated nitrosulfonamide (MW 244.27) was filtered and recrystallized from ethanol (95%). Yield: 28.3g (93%).

To a solution of 40 mL 1M NaOH (1.6 g in 40 mL) was added 4.9 g (20 mmol) N-nitro-N-ethyl-p-toluolsulfonamide and the mixture was heated to reflux for 1h or till a clear solution resulted. The solution was acidified with 6M HCl(aq) by careful addition. Extraction with ether gave the ethylnitramine (MW 90.08). Yield: 0.98g (54%).

Diethylnitramine; $(CH_3CH_2)_2NNO_2$

Trifluoroacetic anhydride (20 mL) was cooled to -5 to 0 °C. Absolute nitric acid (7.5 mL) was added by means of a dropping funnel over 20 min. After stirring for another 15 min. and diethylformamide (3 g, 0.030 mol, 1 equiv.) was added dropwise. After stirring for another 1.5 h all gas evolution ceased and the volume was decreased to ≈ ½ under slight vacuum and maintaining the temperature at 0 ^{o}C. The residue was carefully poured on ice (10-20 grams) and the pH was adjusted to basic (litmus) using 10M NaOH. Extraction with ether (4 x 20 mL), drying ($MgSO_4$) and evaporation gave an oil identified as pure diethylnitramine; Yield: 2.49 g (71%).

Dimethylnitrosamine; *$(CH_3)_2NNO$*

Dimethylamine hydrochloride (24.5 g, 0.302 mol, 1 equiv.) was dissolved in water (12 ml) and the reaction mixture was acidified with 2 M HCl (1 mL). The mixture was stirred

vigorously and heated to around 75 °C. Next, sodium nitrite (23.5 g, 0.341 mol, 1.08 equiv.) was dissolved in water (30 mL) and slowly added to the reaction mixture by means of a dropping funnel over a period of one hour. The reaction mixture was tested regularly with litmus paper and small volumes of 2 M HCl were added from time to time to ensure an acidic reaction environment. Following the complete addition of sodium nitrite, the reaction mixture was then stirred for two hours.

Next, the reaction mixture was distilled until essentially dry; after which 15 mL of water was added to the flask and the process repeated. The distillates were combined and potassium carbonate was added in order to "salt out" the dimethylnitrosoamine. The upper organic layer was separated and the water phase was extracted three times with ether.

The combined organic phases were dried (K_2CO_3) and distilled using a Claisen-Vigreux apparatus. Yield 21.0 g (94%) of a pale yellow oil. Bp 145 °C/760 mmHg. ^{1}H NMR (300 MHz, $CDCl_3$): d 3.04 (s, 3H), 3.76 (s, 3H); ^{13}C NMR (75 MHz, $CDCl_3$): d 32.84, 40.61 ppm

Diethylnitrosamine; $(CH_3CH_2)_2NNO$

Diethylamine hydrochloride (50.0 g, 0.456 mol, 1 equiv.) was dissolved in water (40 mL) and the reaction mixture was acidified with 2 M HCl (4 mL). The mixture was stirred vigorously under an nitrogen atmosphere for 5 minutes and then heated to 70-75 °C. Sodium nitrite (34.0 g, 0.493 mol, 1.1 equiv.) was dissolved in water (50 mL) and slowly added to the reaction mixture by means of a dropping funnel over a period of one hour. The reaction mixture was tested regularly with litmus paper and small volumes of 2 M HCl were added from time to time to ensure an acidic reaction environment. The reaction mixture was then stirred for an additional two hours, and then allowed cooled to ambient temperature. Two distinct phases were then observed, with a faint yellow organic layer being on top. The reaction mixture was saturated with NaCl and the contents were poured into a separatory funnel. The organic layer was separated, and the aqueous phase extracted with diethyl ether (3 x 50 mL). The combined organic phase was dried (K_2CO_3 + $MgSO_4$). Concentration in vacuo and distillation of the yellow residue using an ordinary Claise-Vigreux set up gave 30.9 g (68%) of the product as a pale yellow oil. Bp. 55-58 ^{o}C/10-13 mmHg. ^{1}H NMR (300 MHz, $CDCl_3$): d 1.06 (t, 3H, *J* 7.5 Hz), 1.36 (t, 3H, *J* 6.9 Hz), 3.56 (q, 2H, *J* 7.5 Hz), 4.09 (q, 2H, *J* 7.5 Hz); ^{13}C NMR (75 MHz, $CDCl_3$): d 11.11, 13.95, 38.60, 47.15 ppm.